



HAL
open science

Contribution to fault tolerant flight control under actuator failures

Lunlong Zhong

► **To cite this version:**

Lunlong Zhong. Contribution to fault tolerant flight control under actuator failures. Embedded Systems. INSA de Toulouse, 2014. English. NNT : 2014ISAT0001 . tel-01073618

HAL Id: tel-01073618

<https://theses.hal.science/tel-01073618>

Submitted on 10 Oct 2014

HAL is a multi-disciplinary open access archive for the deposit and dissemination of scientific research documents, whether they are published or not. The documents may come from teaching and research institutions in France or abroad, or from public or private research centers.

L'archive ouverte pluridisciplinaire **HAL**, est destinée au dépôt et à la diffusion de documents scientifiques de niveau recherche, publiés ou non, émanant des établissements d'enseignement et de recherche français ou étrangers, des laboratoires publics ou privés.



Université
de Toulouse

THÈSE

En vue de l'obtention du
DOCTORAT DE L'UNIVERSITÉ DE TOULOUSE

Délivré par :
Institut National des Sciences Appliquées de Toulouse (INSA Toulouse)

Discipline ou spécialité :
Automatique

Présentée et soutenue par :
Lunlong ZHONG

le : lundi 27 janvier 2014

Titre :

Contribution to Fault Tolerant Flight Control under Actuator Failures

JURY

Shaoping WANG
Alexandre Carlos BRANDAO RAMOS
Andrei DONCESCU
Thierry MIQUEL

Ecole doctorale :
Systèmes (EDSYS)

Unité de recherche :
MAIAA/ENAC

Directeur(s) de Thèse :

Félix MORA-CAMINO

Rapporteurs :

Houcine CHAFOUK
Daniel CHOUKROUN

Acknowledgements

This doctoral research was carried out within MAIAA (Laboratoire de Mathématiques Appliquées, Informatique, et Automatique pour l'Aérien) laboratory of Air Transport department at ENAC.

First of all, I would like to express my deepest gratitude to my thesis supervisor Professor Félix Mora-Camino for his continuous guidance and support throughout the research. His encouragement and advice led me to the right path and are greatly appreciated.

Secondly, I would like also to thank all the members of my jury for accepting to review my thesis.

My heartfelt appreciation also goes to the friends and colleagues at the Automation Research Group. They made my life at MAIAA an enjoyable and memorable experience.

I would also like to extend my deepest gratitude to everyone who, in one way or another, has helped me get through these years.

This work was sponsored by CSC (China Scholarship Council) and CAUC (Civil Aviation University of China).

Abstract

The objective of this thesis is to optimize the use of redundant actuators for a transportation aircraft once some actuators failure occurs during the flight. Here, the fault tolerant ability resulting from the redundant actuators is mainly considered. Different classical concepts and methods related to a fault tolerant flight control channel are first reviewed and new concepts useful for the required analysis are introduced. The problem which is tackled here is to develop a design methodology for fault tolerant flight control in the case of a partial actuator failure which will allow the aircraft to continue safely the intended maneuver. A two stages control approach is proposed and applied to both the remaining maneuverability evaluation and a fault tolerant control structure design. In the first case, an offline handling qualities assessment method based on Model Predictive Control is proposed. In the second case, a fault tolerant control structure based on Nonlinear Inverse Control and online actuator reassignment is developed. In both cases, a Linear Quadratic (LQ) programming problem is formulated and different failure cases are considered when an aircraft performs a classical maneuver. Three numerical solvers are studied and applied to the offline and online solutions of the resulting LQ problems.

Key words: fault tolerant control, flight control, actuator failure, linear quadratic programming problem, actuator reassignment

Résumé

L'objectif de cette thèse est d'optimiser l'utilisation d'actionneurs redondants pour un avion de transport lorsqu'une défaillance des actionneurs arrive en vol. La tolérance aux pannes résulte ici de la redondance des actionneurs présents sur l'avion. Différents concepts et méthodes classiques liés aux chaînes de commande de vol tolérantes aux pannes sont d'abord examinés et de nouveaux concepts utiles pour l'analyse requise sont introduits. Le problème qui est abordé ici est de développer une méthode de gestion des pannes des commandes de vol dans le cas d'une défaillance partielle des actionneurs, qui va permettre à l'avion de poursuivre en toute sécurité la manœuvre prévue. Une approche de commande en deux étapes est proposée et appliquée à la fois à l'évaluation de la manoeuvrabilité restante et à la conception de structures de commande tolérante aux pannes. Dans le premier cas, une méthode d'évaluation hors ligne des qualités de vol basée sur la commande prédictive est proposée. Dans le second cas, une structure de commande tolérante aux pannes basée sur la commande non linéaire inverse et la réaffectation des actionneurs en ligne est développée. Dans les deux cas, un problème de programmation linéaire quadratique (LQ) est formulé. Différents cas de pannes sont considérés lorsqu'un avion effectue une manoeuvre classique. Trois solveurs numériques sont appliqués aux solutions en ligne et hors ligne des problèmes LQ qui en résultent.

Mots clé: commande tolérante aux pannes, conduite automatique du vol, panne d'actionneur, problème LQ, réaffectation des actionneurs

Contents

GENERAL INTRODUCTION	1
General Considerations	3
Some Aviation Accident Examples Related to Actuator Failure	6
General Objectives of the Thesis.....	9
Thesis Organization.....	11
CHAPTER 1 FLIGHT CONTROL CHANNELS	13
1.1 Introduction	15
1.2 Composition and Organization of Flight Control Channels	15
1.2.1 Fast and slow flight control channels.....	15
1.2.2 Flight control channel solutions.....	16
1.3 Failures Related to Flight Control Channel.....	18
1.3.1 An overview of flight control actuator failures.....	20
1.3.2 An overview of sensors failures.....	24
1.3.3 Failures of the controlled process	27
1.4 Airworthiness Regulations	28
1.5 Conclusion.....	29
CHAPTER 2 TRANSPORT AIRCRAFT FLIGHT QUALITIES.....	31
2.1 Introduction	33
2.2 Flight Domain.....	33
2.2.1 Flight envelopes	33
2.2.2 Flight maneuvers.....	35
2.2.3 Effects of failures on flight domain	37
2.3 Flight Qualities	38
2.3.1 Definitions.....	38
2.3.2 Classical approach to the analysis of flight qualities	39
2.3.3 Modern approach to flight qualities analysis	40

2.4	Transportation Aircraft Flying Qualities	45
2.4.1	Longitudinal Flying Qualities	45
2.4.2	Lateral Flying Qualities	47
2.5	Effects of Actuator Failures on Handling Qualities.....	50
2.5.1	Residual controllability.....	50
2.5.2	Case studies.....	51
2.6	Conclusion.....	53
CHAPTER 3 FAULT TOLERANT FLIGHT CONTROL		55
3.1	Introduction	57
3.2	Physical and Analytical Redundancies.....	57
3.3	Fault Detection and Identification.....	59
3.4	Fault Tolerance Actuation Based on Redundancy.....	62
3.4.1	Definitions.....	63
3.4.2	Limitations	64
3.5	Fault Tolerant FBW aircraft.....	65
3.5.1	General features of FBW flight control channels	65
3.5.2	The Case of Airbus A330/A340.....	67
3.6	Fault Tolerant Control	70
3.7	Conclusion.....	73
CHAPTER 4 FORMULATION OF THE ACTUATOR ASSIGNMENT AND REASSIGNMENT PROBLEM		75
4.1	Introduction	77
4.2	General Representation of Actuator Redundant Systems.....	77
4.2.1	Representation of the dynamics and constraints.....	77
4.2.2	Illustration with a transportation aircraft	79
4.3	Output Based State Representation and Virtual Inputs	80
4.4	A Two stages Control Approach.....	81
4.5	The Actuator Assignment Problem (AAP).....	83
4.6	The Actuator Reassignment Problem (ARP).....	86
4.7	Direct Methods to Solve the Instant AAP and ARP	88
4.7.1	The explicit ganging method.....	88

4.7.2	The direct allocation method.....	89
4.7.3	The daisy chain method	90
4.8	Conclusion.....	91
CHAPTER 5 FAST SOLUTION APPROACHES FOR LQ OPTIMIZATION PROBLEMS		
		93
5.1	Introduction	95
5.2	Convex Optimization.....	95
5.3	Linear Quadratic Optimization Problem	96
5.4	Active Set Methods	99
5.5	Interior Point Approaches.....	101
5.6	Neural Networks Approaches.....	105
5.6.1	The development of neural network solvers for LQ problems	105
5.6.2	Classification of LQ neural network solvers.....	106
5.6.3	Example of a primal-dual LQ neural network solver	107
5.7	Conclusion.....	108
CHAPTER 6 ASSESSMENT OF HANDLING QUALITIES AFTER ACTUATOR FAILURE		
		111
6.1	Introduction	113
6.2	Aircraft Fast Dynamics and Effectiveness of Aerodynamic Actuators	114
6.2.1	Aircraft rotation dynamics	114
6.2.2	Multiplicity aerodynamic actuators for transportation aircraft	115
6.2.3	A reference model for rotational maneuver	116
6.3	Actuators Constraints and Limitations	117
6.3.1	Actuators Position and Speed Limitations	117
6.3.2	Global Constraints.....	117
6.4	Formulation of the Off-line Model Following Control Problem.....	118
6.4.1	The adopted predictive models	119
6.4.2	Formulation of the recurrent optimization problem.....	121
6.5	The Proposed Neural Network Solver.....	122
6.5.1	General formulation of the recurrent LQ problem.....	122
6.5.2	Fast neural solution for the LQ problem.....	123

6.6	Numerical Results for the Proposed Approach	124
6.7	Conclusion.....	127
CHAPTER 7 ONLINE ACTUATOR REASSIGNMENT FOR FAULT TOLERANT MANEUVERS		129
7.1	Introduction	131
7.2	Virtual Inputs for a General Maneuver.....	131
7.2.1	Virtual inputs for differential flat systems	131
7.2.2	Virtual inputs for aircraft maneuvers	133
7.3	The Case of an Equilibrated Turn Maneuver	134
7.3.1	Equilibrated turn maneuver.....	134
7.3.2	Nonlinear inverse control approach to determine the levels of the virtual inputs	136
7.4	Formulation of Actuator Reassignment Problem	137
7.5	Comparative Application of the Three Solvers to the Actuators Reassignment Problem	139
7.5.1	Soft fault scenario	140
7.5.2	Hard fault scenario	146
7.6	Conclusion.....	151
CHAPTER 8 GENERAL CONCLUSIONS.....		153
8.1	Achievements	155
8.2	Perspectives for Further Research.....	156
ANNEX A FLIGHT DYNAMICS		159
A.1	Introduction	161
A.1.1	Reference frame	161
A.1.2	Rotation matrices between different reference frames.....	162
A.2	Equations of Flight Mechanics.....	163
A.2.1	Forces and moments.....	163
A.2.2	Equations of motion.....	166
ANNEX B FAULT TOLERANT CONTROL TECHNIQUES		169
B.1	Fault Tolerant Control	171

B.2	Passive and Active Approaches	171
B.3	Active Fault Tolerant Control Approaches	174
B.3.1	Multi-model control	174
B.3.2	Adaptive control.....	176
B.4	Methods of Control Laws Synthesis.....	179
B.4.1	Model following control	179
B.4.2	Model predictive control.....	180
ANNEX C	RECCURENT NEURAL NETWORKS FOR LQ PROBLEM.....	183
ANNEX D	PARAMETERS FOR THE MPC PROBLEM.....	189
ANNEX E	NONLINEAR INVERSE CONTROL TECHNIQUE	193
E.1	Introduction	195
E.2	Affine nonlinear system.....	195
E.2.1	Relative degree.....	196
E.2.2	Normal form.....	197
E.3	Introduction to nonlinear inverse control	198
BIBLIOGRAPHY	201
RÉSUMÉ	213

List of Figures

0.1	Departures, flight Hours, and jet airplanes in service (from [Boeing Commercial Airplanes, 2013]).....	4
0.2	Accident rates and onboard fatalities by year (from [Boeing Commercial Airplanes, 2013])	5
0.3	Fatalities by aviation occurrence categories (from [Boeing Commercial Airplanes, 2013]) ..	5
1.1	Various control surfaces on an A330/A340 aircraft.....	16
1.2	General view of a mechanical flight control channel (source: Airbus)	17
1.3	General view of a fly-by-wire control channel (source: Airbus)	18
1.4	General architecture scheme of flight control system.....	20
1.5	Illustration of stuck failure.....	21
1.6	Illustration of hard-over failure.....	21
1.7	Illustration of float failure.....	22
1.8	Illustration of loss of effectiveness failure.....	22
1.9	Stuck aileron on B-767 in flight.....	23
1.10	Hardover rudder on Airbus Skylink (by Mick Ward)	24
1.11	Illustration of bias failure.....	25
1.12	Illustration of drift failure	26
1.13	Illustration of loss of accuracy failure	26
1.14	Illustration of freezing failure	26
1.15	Illustration of calibration error failure	27
2.1	Flight domain and limits (source: IENAC Flight Operations Manual, ENAC)	34
2.2	Detail of flight envelope ceiling	35
2.3	Automatic maneuver protections	36
2.4	Static and dynamic stability cases.....	40
2.5	Graphical criteria for dynamic stability and oscillations	44
2.6	Graphical condition for dynamic and static stability	45
2.7	Natural and augmented short period parameters	47
2.8	Natural and augmented response to a step input.....	47

2.9	Natural and controlled Dutch roll parameters.....	49
2.10	Natural and augmented perturbed sideslip dynamics	49
2.11	Natural and augmented short period parameters under fault-free or failure cases	52
2.12	Pitch angle response of controlled system to a step input under fault-free and failure case 4	52
2.13	Natural and controlled Dutch roll parameters under fault-free or failure cases	53
2.14	Natural and augmented perturbed sideslip dynamics fault-free and failure case 4	53
3.1	Main physical redundancy in A300 roll control channel.....	58
3.2	General view of a fault tolerant flight control system	59
3.3	Fault localization in physical processes.....	60
3.4	FDI based on residuals analysis.....	61
3.5	General Architecture of a FDI system	62
3.6	Redundant control surfaces and actuators for A330/A340 (source: Airbus).....	68
3.7	A330/A340 hydraulic power distribution and coverage (source: Airbus).....	68
3.8	Flight domain levels of protection	70
3.9	General scheme of a fault tolerant control system.....	72
3.10	Possible fail modes for a fault tolerant control structure	73
4.1	Maximum deflection of rudder versus airspeed A320.....	79
4.2	Example of configuration parameters on a wing.....	80
4.3	General scheme of a control structure with actuator assignment for redundant system control	82
4.4	A simple illustration of the four different assignment cases.....	84
4.5	Selection of the closest feasible solution	84
4.6	Adaptation of configuration to control objectives	85
4.7	Comparing fault free and faulty assignment cases	88
5.1	Architecture of adopted neural networks model.....	108
6.1	Example of Wing Actuators (A340)	116
6.2	Standard roll input and reference output.....	125
6.3	Case a: computed output and reference output.....	126
6.4	Case b: computed output and reference output.....	126
6.5	Case c: computed output and reference output.....	126

7.1	Illustration of the global flatness property of aircraft dynamics.....	133
7.2	Aircraft attitude during an equilibrated turn maneuver	135
7.3	Time evolution of command and desired maneuver (only display roll angular rate, pitch and yaw rates remain at zeros).....	141
7.4	Evolution of ailerons commands under soft fault scenario.....	142
7.5	Number of iterations and computation time for interior point and active set under soft fault scenario	143
7.6	Convergent behavior of the neural network solver (0.01ms)	143
7.7	The real and desired angular rates under soft fault scenario.....	144
7.8	Command rates for the right outer aileron under soft fault scenario	145
7.9	Evolution of actuators commands under hard fault scenario.....	147
7.10	Number of iterations and computation time for interior point and active set under hard fault scenario	148
7.11	Convergent behavior of the neural network solver (0.01ms)	148
7.12	The real and desired angular rates under hard fault scenario.....	149
7.13	Command rates for the right outer aileron under hard fault scenario	150
7.14	Fault tolerant control structure with actuator reassignment.....	152
A.1	Illustration of Earth frame and body-fixed frame	162
A.2	Illustration of aerodynamic frame and body-fixed frame	162
A.3	External forces applied on the aircraft	164
B.1	Main approaches of fault tolerant control.....	174
B.2	Block diagram of actuator allocation system.....	178
B.3	Scheme of model following control.....	180
C.1	Two-layer structure of the neural network model (source: [xia, 2000])	185

List of Tables

1.1	Some examples of actuator failures	23
1.2	Some examples of component failures	28
1.3	Classification of failures in the Aeronautics	28
5.1	An example of active set algorithm	101
5.2	An example of interior point algorithm	104
6.1	Parameters of actuators under nominal condition.....	124
B.1	Examples of FTC applications.....	171

GENERAL INTRODUCTION

General Considerations

The safety of air transport is an important issue for aeronautics especially for commercial aviation. World air transportation traffic has known a sustained increase over the last decades leading to airspace near saturation in large areas of developed and emerging countries. According to 2013 Boeing report [Boeing Commercial Airplanes, 2013] which summarizes commercial jet airplane accidents that occurred worldwide between 1959 and 2012 involving aircraft that are heavier than 30 tons maximum gross weight, it can be seen from Figure 0.1 that during the last ten years, annual flight hours has been more than doubled, departures and jet airplanes has almost been doubled. Fortunately, Researches, technical developments and implementation of effective procedures for operation and maintenance of aircraft have had remarkable achievements. From Figure 0.2, it is clear that although the total annual flight hours has more than doubled during the period 1993-2012, the number of accident rates has remained at the same level. It is also clear that during the early 60's, the number of fatal accidents has fallen sharply. All these achievements are contributed from many factors such as stringent safety measures imposed on the industry, the implementation of high safety technologies and increasingly extensive training for all aviation employees.

Figure 0.3 shows aircraft LOC (Loss Of Control) is the leading fatal accident category, with 18 accidents occurring during the period 1993-2012 that resulted in 1,648 fatalities. The 2013 report on worldwide fatal accidents by United Kingdom Civil Aviation Authority [Civil Aviation Authority, 2013] has revealed LOC to be the most prevalent type of accident involving large commercial jet and turboprop airplanes. "LOC in flight following technical failure" featured in the 5th most frequently assigned consequences.

In [Belcastro & Foster, 2010], Belcastro reviewed and analyzed 126 LOC accidents predominantly including large transports and smaller regional carriers from Part 121, those accidents occurred between 1979 and 2009 (30 years) and result in 6087 fatalities. The author grouped causal and contributing factors into three categories: adverse onboard conditions, vehicle upsets, and external hazards and disturbances. 119 LOC accidents are related to adverse onboard conditions, 57 of them were considered to be caused by system faults / failures / errors. 42 LOC

sequences were initiated by system failures. The initiating events for these accidents included: engine and engine control failures (17 accidents), flight control system and component design errors and failures (15 accidents), flight control sensors and instrumentation failures and malfunctions (9 accidents), and flight deck warning system failures (1 accident).

The accident reports published by NTSB (National Transportation Safety Board) have revealed that most LOC in-flight accidents were triggered by faults including subsystem/component failures, external hazards, and human errors [Chang et al., 2008]. In the following we focus on the causes and consequences of some accidents related to component failure, especially actuator failure.

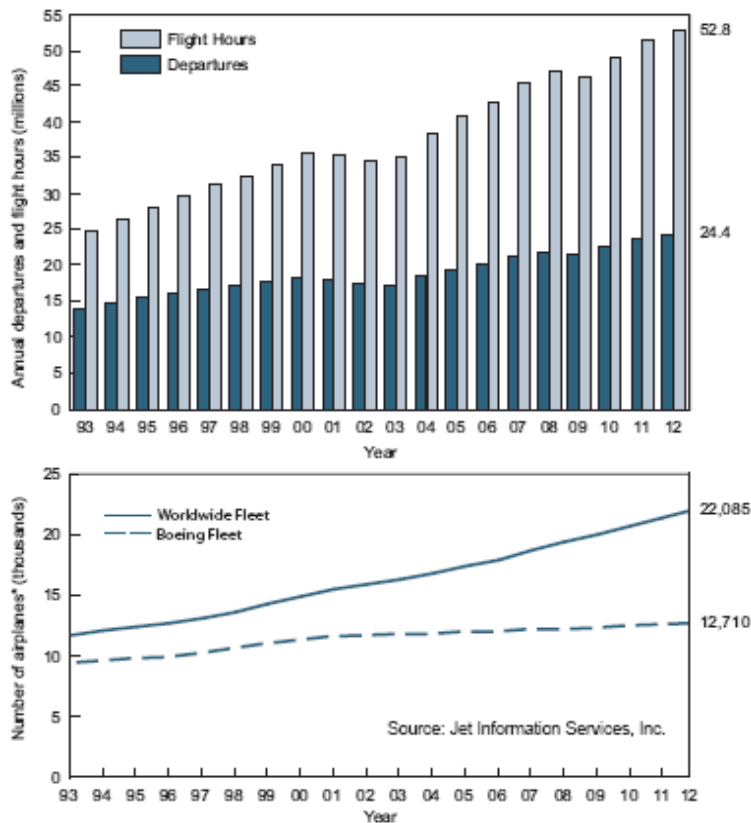


Figure 0.1 Departures, flight Hours, and jet airplanes in service (from [Boeing Commercial Airplanes, 2013])

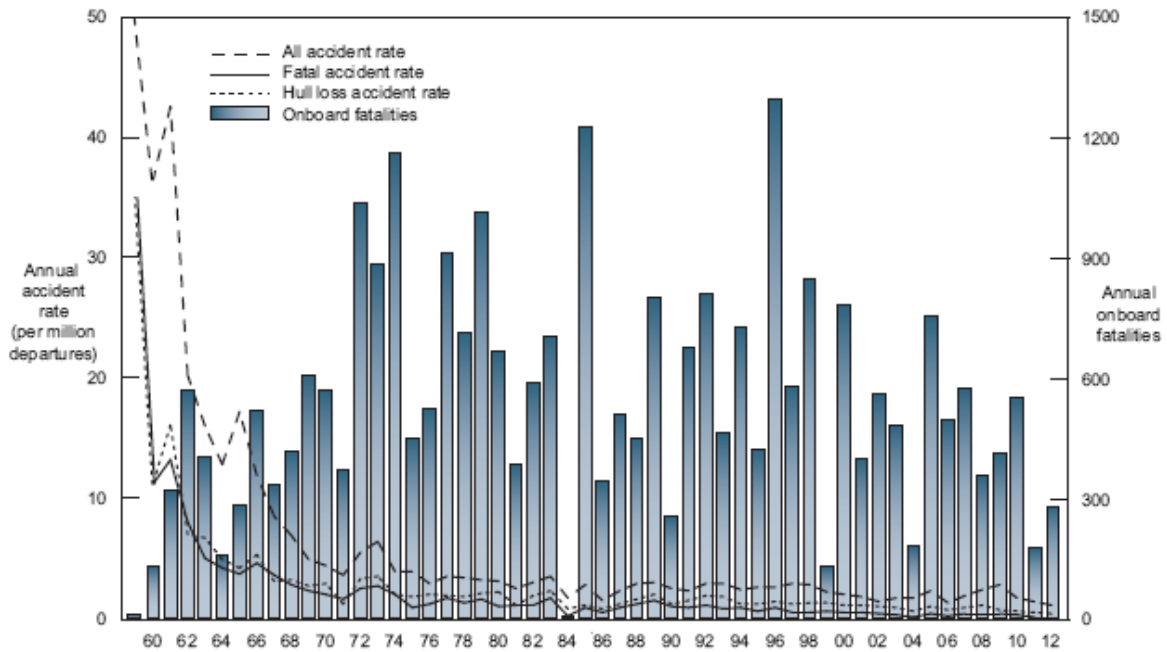


Figure 0.2 Accident rates and onboard fatalities by year (from [Boeing Commercial Airplanes, 2013])

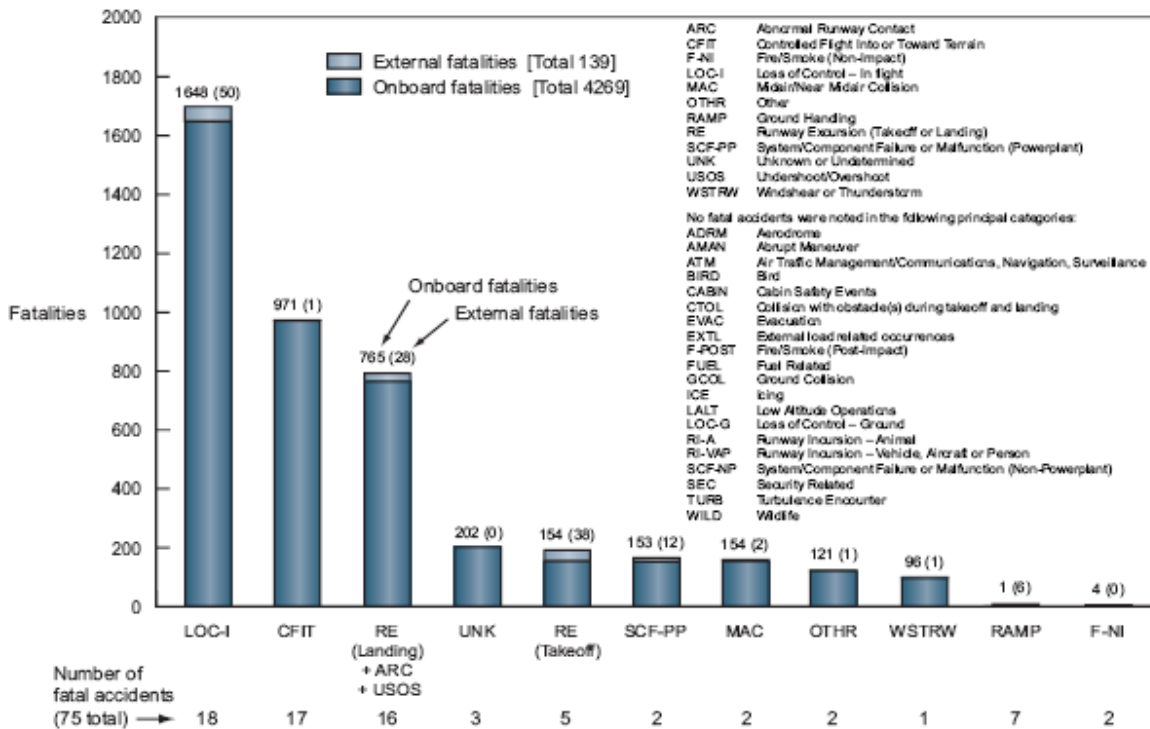


Figure 0.3 Fatalities by aviation occurrence categories (from [Boeing Commercial Airplanes, 2013])

Some Aviation Accident Examples Related to Actuator Failure

L-1011, April 12th, 1977, USA

On April 12th, 1977, Lockheed L-1011 trijet, Delta Airlines Flight 1080, left elevator jammed at the full trailing edge-up position before departure out of San Diego, California at night [Frank W. Burcham et al., 1997; McMahan, 1978]. This failure was not indicated to the pilots and it resulted in a large nose-up pitching and rolling moment that almost exceeded the capability of the flight controls. The airplane was just about to stall in the clouds, when the captain, using amazing insight, increased trust on the center engine and reduced the trust on the outboard ones. This action allowed him to regain enough control to maintain flight. The crew learned rapidly how to use the throttles to supplement the remaining flight controls, moved passengers forward to reduce the pitch-up tendency, and completed a safe landing. A crew with less knowledge about the actuation redundancy in the L-1011 aircraft would likely have not been able to save this airplane.

Boeing 747, August 12th, 1985, Japan

On August 12, 1985, JA8119 had completed four domestic flights when it landed at Tokyo-Haneda (HND) at 17:17. The next flight was to be Flight 123 to Osaka (ITM). A decompression had occurred and the crew got indications of problems with the R5 door. In fact, the rear pressure bulkhead had ruptured, causing serious damage to the rear of the plane. A portion of its vertical fin, measuring 5 m together with the section of the tailcone containing the auxiliary power unit (APU) were ripped off the plane. Due to the damage, the hydraulic pressure dropped and all ailerons, elevators and yaw damper became inoperative. Controlling the plane was very difficult as the airplane experienced Dutch roll and Phugoïd oscillations (unusual movement in which altitude and speed change significantly in a 20-100 seconds cycle without change of angle of attack). The aircraft started to descend to 6600 feet while the crew tried to control the aircraft by using engine thrust. Upon reaching 6600 feet the airspeed had dropped to 108 knots. The aircraft then climbed with a 39 degree angle of attack to a maximum of approximated 13400 feet and started to descend again. At 18:56 JAL123 finally brushed against a tree covered ridge, continued and struck the Osutaka Ridge, bursting into flames.

Boeing 737-200, March 3, 1991, USA

On March 3, 1991, a Boeing 737-200 operated by United Airlines, Flight 585, was on a scheduled passenger flight from Denver, Colorado, to Colorado Springs, Colorado. Shortly after completing its turn onto the final approach course to runway 35 at Colorado Springs Municipal Airport, the aircraft rolled steadily to the right and pitched nose down until it reached a nearly vertical attitude. The pilot tried to initiate a go-around by requesting 15 degrees of flaps in combine with increased thrust. Despite this crew effort, the altitude continued decreasing rapidly and the normal acceleration increased to over 4 g, before crashed into nearby Widefield Park, less than four miles from the runway threshold. The aircraft was destroyed completely by the impact forces and post-crash fire, and the 2 flight crew-members, 3 flight attendants and 20 passengers aboard were fatally injured.

The NTSB reopened the UAL 585 case after the crash of another 737, USAir Flight 427, which occurred three and a half years later. It was eventually determined that both crashes were the result of a sudden malfunction of the rudder power control unit. The pilots lost control of the airplane because "The rudder surface most likely deflected in a direction opposite to that commanded by the pilots as a result of a jam of the main rudder power control unit servo valve secondary slide to the servo valve housing offset from its neutral position and overtravel of the primary slide." [National Transportation Safety Board, 2001]

Boeing 747-200F, October 4th, 1992, Netherlands

On October 4th, 1992, a Boeing 747-200F freighter aircraft operated by Israel's national airline, EL AL Flight 1862, departed from Amsterdam Schiphol Airport towards Tel Aviv. Unfortunately, both right-wing engines were lost due to mechanical problem [Smaili et al., 2008]. In an attempt to return to the airport for an emergency landing, the aircraft flew several right-hand circuits in order to lose altitude and to line up with the runway as intended by the crew. During the second line-up, the crew lost control of the aircraft. As a result, the aircraft crashed, 13 km east of the airport, into an eleven-floor apartment building in the Bijlmermeer, a suburb of Amsterdam. Results of the accident investigation, conducted by several organizations including the Netherlands Accident Investigation Bureau and the aircraft manufacturer, were hampered by the fact that the actual extent of the structural damage to the right-wing, due to the loss of both

engines, was unknown. The analysis from this investigation concluded that given the performance and controllability of the aircraft after the separation of the engines, a successful landing was highly improbable. However, later study [Maciejowski & Jones, 2003] shows that the fatal crash of EL AL Flight 1862 could have been avoided by the help of fault tolerant control.

McDonnell Douglas MD-83, January 31th, 2000, USA

On January 31th, 2000, a McDonnell Douglas MD-83 operated by Alaska Airlines, Flight 261, crashed into the Pacific Ocean about 60 miles west of Los Angeles because of a jammed horizontal stabilizer. The 2 pilots, 3 cabin crewmembers, and 83 passengers on board were killed, and the airplane was destroyed by impact forces. The jam was later determined to be a direct result of the in-flight failure of the acme nut threads in the horizontal stabilizer trim system jackscrew assembly. The first fault the Flight 261 crew members encountered was a horizontal stabilizer jam at 0.4° , which was near the trim condition. This fault was not severe and the pilots were able to keep the aircraft aloft at 31,050 feet preparing for an emergency landing. But about twenty minutes later, the horizontal stabilizer was moved by an excessive force with huge noise from 0.4° to a new jam position, 2.5° airplane nose down, and the airplane began to pitch nose down, starting a dive. Things got worse after that – pilots lost control of the pitch axis, and the aircraft crashed into the ocean 11 minutes and 37 seconds later [Chang et al., 2008].

Beechcraft 1900D, January 8, 2003, USA

On January 8, 2003, a Beechcraft 1900D, Air Midwest Flight 5481, was a flight from Charlotte/Douglas International Airport in Charlotte, North Carolina, United States to Greenville-Spartanburg International Airport near the cities of Greenville, South Carolina and Spartanburg, South Carolina. The aircraft stalled after take-off, crashed into a US Airways hangar and burst into flames after leaving Charlotte/Douglas International Airport. All 19 passengers and 2 pilots aboard died in the accident, and 1 person on the ground received minor injuries. Investigation report revealed that the accident cause is an improper maintenance action of turnbuckles controlling tension on the cables to the elevators resulting in insufficient elevator travel, leading to the pilots not having sufficient pitch control [National Transportation Safety Board, 2004].

Airbus A300, November 22th, 2003, Iraq

On November 22th, 2003, an Airbus A300 cargo plane owned by European Air Transport and operated on behalf of DHL, was hit by a SAM-7 surface-to-air missile while climbing through 8000 feet shortly after departure from Baghdad. The missile struck the left wing and penetrated the no. 1A fuel tank. Fuel ignited, burning away a large portion of the wing. To make things worse, the plane lost all hydraulics and the pilots had to attempt a landing back at Baghdad Airport. After a missed approach they were forced to circle the field until they finally landed heavily on runway 33L, 16 minutes later. The aircraft ran off the left side of the runway and traveled about 600 meters through soft sand, struck a razor wire fence [Aviation Safety Network].

General Objectives of the Thesis

Automation has become increasingly important in ensuring the safety of flight operations. Today two main research domains are emerging in the control field applied to Aeronautics:

- One research domain concerns the design of embedded automatic systems helping to maintain flight safety against the occurrence of system failures in flight control of the aircraft (failure of components and subsystems of power circuits, actuator channels, control channels, etc.): leading to the design of fault-tolerant control schemes which are generally adaptive and nonlinear to assist the management of critical failure situations [Andrei, 2010; Edwards et al., 2010; R. J. Patton, 1997; Steinberg, 2005; Y. Zhang & Jiang, 2008].

- Another research domain concerns the design of automatic systems that contribute to air traffic management. Indeed, during the last several decades, it is successful to manage the finite airspace capacity and to minimize the collision risks between aircrafts in air transport when a more critically new problem resulting from increasing air traffic. Now automation offers a significant contribution to the efficiency of air traffic control [Billings, 1997; Hunt & Zellweger, 1987; Menon et al., 2004; Tomlin et al., 1998; Wickens, 1998].

Today, some airborne automatic systems such as the Airborne Collision Avoidance System (ACAS) are essential parts of the air traffic control system [ICAO, 2007] set by national and international authorities in charge of air traffic management and control.

This thesis focuses on the first research domain and tries to contribute to the flight safety of commercial aviation by developing new automatic control techniques to better manage hardware failures situations. Statistics shows that Loss Of Control (LOC) remains one of the largest contributors to fatal aircraft accidents worldwide, and system failure is the first contributing factor to LOC [Belcastro, 2011]. By ‘intelligent’ utilization of the control authority of the remaining control effectors in all axes consisting of the control surfaces and engines or a combination of both, fault tolerant flight control must allow improved survivability and recovery from adverse flight conditions induced by faults, damage and associated upsets. The main objective of these control strategies is to restore stability and maneuverability of the vehicle for recovery and continued safe operation.

Aerodynamic actuator failure is one of the critical failures for aircraft. Thanks to the onboard redundancy, this failure may be compensated taking into account the redundancy of actuators in terms of their effects on the dynamics of flight. At the same time, structural integrity should be considered by taking into account the possibility of excessive loads generated by failed actuators. Thus this situation can be dealt as safely as possible with the reassignment of the remaining operational actuators in order to perform either the required maneuver or an alternate maneuver while maintaining the structural integrity of the aircraft.

In fact it is supposed in this thesis that fault detection and identification (FDI) techniques allow to detect and identify timely actuator failures so that immediate reconfiguration can be pursued. Many studies in these fields have been already produced, leading to effective online actuator fault detection and identification techniques [Han et al., 2012; Hwang et al., 2010; Rolf Isermann, 2005, 2006; N. Zhang, 2010].

In this thesis first are analyzed for the case of modern transportation aircraft, the structure of their flight control channels and the failure modes of their main components. The flight qualities of modern transportation aircraft are revisited while the consequences of actuator failures on them are also discussed. Then general fault tolerance techniques are considered while adopted solutions on modern transportation aircraft are displayed and discussed.

Different useful concepts to analyze fault tolerance are introduced formally in this thesis, such as: degree of multiplicity of actuators, full input redundancy, total input redundancy, virtual

inputs, distribution and mixing matrices.

When some actuators failure occurs, an immediate reconfiguration should lead to the reassignment of the remaining operational actuators. This reassignment problem has been formulated as a Linear Quadratic (LQ) problem where different cases can be distinguished when considering the existence and multiplicity of solutions. During this research, three Linear Quadratic programming solvers have been studied, programmed and applied to different actuator reassignment situations.

The first considered situation, tackled offline, aims at characterizing the remaining flight qualities and handling qualities when a particular actuators failure scenario occurs. This problem has been tackled by adopting a Model Predictive Control (MPC) approach, leading effectively to a LQ problem.

In the other considered situation, where it is already known that the current fault case should not impair to perform a particular intended maneuver, the online solution of a LQ problem provides the necessary reassignment of the operational actuators. In that case, the required values for the virtual inputs to perform the intended maneuver are computed through nonlinear inversion of the output dynamics.

Thesis Organization

In Chapter 1, the organization of the control channels of modern transportation aircraft is displayed and analyzed, while an overview of flight control failure types is presented, showing the diversity of the failure situations to be coped with.

In Chapter 2, is discussed the effects of aerodynamic actuators failures on the flight qualities and the flight domain resulting in drastic limitations and showing the necessity to enforce minimum performances for the failed aircraft by introducing fault tolerant schemes based at this stage of the control channel on physical redundancy.

In Chapter 3, the use of physical and analytical redundancy to perform fault tolerance in general complex dynamical systems is discussed. Then solutions adopted for the control channels

of modern transportation aircraft are analyzed.

In Chapter 4, a two stages control approach to cope with actuators failures situations is proposed where first virtual inputs are computed from an appropriate control law and then the contribution of the remaining effective actuators is established by the solution of a LQ problem. This approach has considered that, depending on the current configuration of the aircraft, the consequences of actuators failures may be rather different, allowing or not.

In Chapter 5, fast solution methods to solve LQ optimization problem, i.e., the active set method, the interior point method and a neural networks based method, are introduced and analyzed. These numerical techniques are used further in this thesis.

In Chapter 6, a method is proposed for the assessment of the remaining handling qualities of an aircraft under partial actuators failure. The proposed approach leads to make use of an MPC technique resulting in the formulation of an LQ problem. In the case study considered, angular rate handling capability, this LQ problem is solved using a neural networks solver.

In Chapter 7, a method is proposed for the reassignment of the remaining effective actuators to perform an intended maneuver. It is shown that in the case of flight dynamics, which possess the differential flatness property, the two stages approach proposed in Chapter 4 is applicable. The chosen case study refers to a classical maneuver, the equilibrated turn. It appears that the three considered LQ solvers of Chapter 5 are able to provide online reassignment solutions to the resulting LQ problem.

Finally in the conclusion, the main results of this thesis are gathered to emphasize the methodological contribution of this thesis, and then further research perspectives are discussed.

Five Annexes are also provided to give more ground to the different concepts and methods used in the above chapters.

CHAPTER 1

FLIGHT CONTROL CHANNELS

1.1 Introduction

This first chapter is devoted to flight control channels, making a distinction between the slow control channels dedicated to fix the aircraft configuration and the fast control channels dedicated to flight argumentation and piloting functions. With respect to fast control channels, the current technical solution, fly-by-wire, is discussed. Then, an overview of failure types for the main components of flight control channels (sensors, processes and actuators) is performed.

1.2 Composition and Organization of Flight Control Channels

1.2.1 Fast and slow flight control channels

To make effective flight control transportation aircraft are equipped with different flight control channels. A distinction can be made between fast control channels involved with attitude dynamics and slow control channels involved with guidance dynamics. Then, to each main axis of an aircraft is attached a fast control channel responsible for generating a torque, allowing the pilot or the autopilot to master the rotational speed of the aircraft while slow control channels are in charge of the aerodynamic configuration of the aircraft and of the thrust delivered by the aero engines. A conventional fast control channel for a fixed-wing aircraft consists of cockpit controls, computers, connecting mechanical and electronic devices, several aerodynamic movable surfaces and the necessary power sources.

The type, the size and the number of aerodynamic surfaces to be controlled will be changed according to aircraft category. Figure 1.1 shows the classic layout for a big transport aircraft with its controlled aerodynamic surfaces: those surfaces indicated in red (elevators, ailerons and rudders) are called the primary flight control, they are in charge of the fast aircraft dynamics (pitch, roll and yaw movements) of the aircraft. The others surfaces indicated in blue form the secondary flight control are in charge of the overall aerodynamic configuration of the aircraft and of its slow dynamics through the control of the position of the flaps, slats, spoilers and of the trimmable horizontal stabilizer (THS). The smooth adaptation of this configuration provides the pilot with a finer control capability as well as eases his workload.

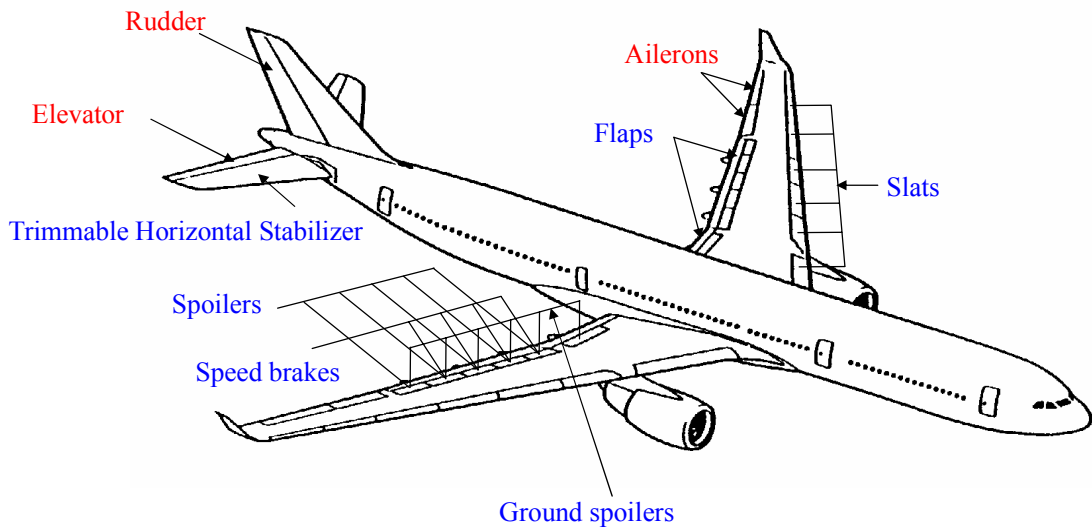


Figure 1.1 Various control surfaces on an A330/A340 aircraft

1.2.2 Flight control channel solutions

Two main flight control channels technology are encountered today on commercial aircraft: mechanical flight control channels and fly-by-wire control channels. Figure 1.2 displays the composition of a mechanically operated flight control channel. It can be found on small aircraft where the aerodynamic forces are not excessive. The involved technology has been available for a long time and employs cables and other mechanical devices to link the pilot levers to the servo controls of the hydraulic actuators attached to the movable aerodynamic surfaces. These cables run along the airframe from the cockpit area to the surfaces to be controlled. This type of system, while providing full airplane control over the entire flight regime with a rather simple and robust solution, has some important drawbacks such as:

- The necessary long cable runs, pulleys, brackets, and supports, all of these components bring an important weight penalty.

- Periodic costly maintenance is required for such mechanical systems, involving lubrication and adjustments operations.

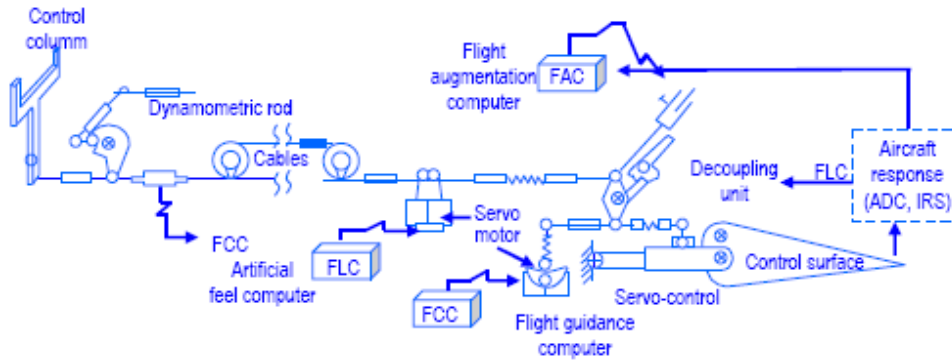


Figure 1.2 General view of a mechanical flight control channel (source: Airbus)

Electrical Flight Control Systems (EFCS, also known as Fly-By-Wire (FBW)) shown in Figure 1.3 include a computer in the corresponding control channels. This solution was first introduced in Civil Aviation in the 1960s by Aerospatiale and its installation in the Concorde aircraft was realized with analog computers. This solution allows replacing complex mechanical subsystems of the flight control channels by electronic ones. Sampled pilot's input signals and autopilot control signals are now integrated by software on these computers which generate the resulting signal sent to the servo controls of the actuators at each aerodynamic surface. Moreover, these computers can perform the necessary computation to realize the stability augmentation function of the aircraft and perform other tasks without attentions of the pilot. In this case the control signals towards the aerodynamic surfaces are transmitted by a redundant electrical wiring (hence the FBW term). Using the FBW solution has many benefits such as:

- Improved piloting ease when the inputs from the pilot are piloting targets (n_{zd} , p_d) submitted to a computer which determines, considering the current point in the flight domain and the actual aircraft configuration, the necessary deflections of the aerodynamic actuators.
- Integrating of the main automatic flight envelope protection functions within the control

channels.

This results in an improved flight safety and a reduction of the pilot's workload while other advantages for the aircraft operator are:

- Weight saving.
- Maintenance activities are largely reduced when compared with conventional mechanical flight control channels.

However, this solution relies heavily on electrical power sources and can be subject to external electromagnetic interferences, mainly when composite materials are used to build the aircraft frame. In the recent years many progress has been done in the field of airborne electric sources while light countermeasures have been introduced to avoid electromagnetic interferences.

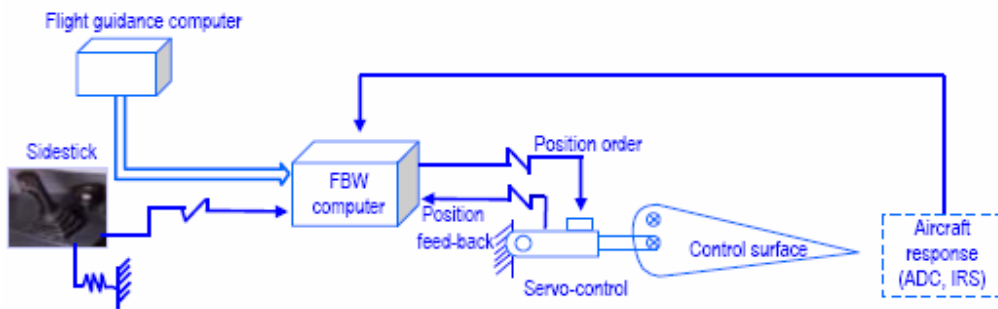


Figure 1.3 General view of a fly-by-wire control channel (source: Airbus)

1.3 Failures Related to Flight Control Channel

Before to consider the possible faults occurring in a flight control channel, detailed definitions of the main terms used in fault management are introduced. To identify accurately the various concepts appearing in fault tolerant systems, organizations such as the IFAC-Technical Committee SAFEPROCESS have made efforts to standardize the definitions related to fault tolerant systems [Rolf Isermann, 2006].

Fault: “A fault is an un-permitted deviation of at least one characteristic property (feature) of

the system from the acceptable, usual, standard condition.” That is to say, a fault is an abnormal condition which may not affect the correct functioning of the system but may eventually lead to a failure (term defined below). Moreover, faults may be *small* or *hidden*, and they may be difficult to be detected.

Example of fault: a loss of effectiveness of an actuator which traduces by a maximum positive slew rate of aileron changing from 25°/s to 15°/s, is a fault case. In that case, the actuator is still usable.

Since artificial systems are designed to perform one or several functions (measurement, actuation, transmission, computation, etc.), the following definition of failure has been proposed.

Failure: “*A failure is a permanent interruption of the ability of a system to perform a required function under specified operating conditions.*” Then a failure is a much more severe situation than a fault. When a failure occurs, the functional unit does not perform the required function any more. For example, when an aileron is stuck at a fixed position, this is a failure situation and the actuator does not work any more.

In the AMC 25.1309 certification requirements for large aircraft, *failure* is defined as “*An occurrence, which affects the operation of a component, part, or element such that it can no longer function as intended, (this includes both loss of function and malfunction)*” [European Aviation Safety Agency, 2007].

In the present study, faults and failures occurring in the flight control channels will be considered with the risk to degrade the flight qualities and the maneuverability of the aircraft. In the next chapters, faults and failures will not be strictly distinguished. A general view of a flight control system is displayed in Figure 1.4.

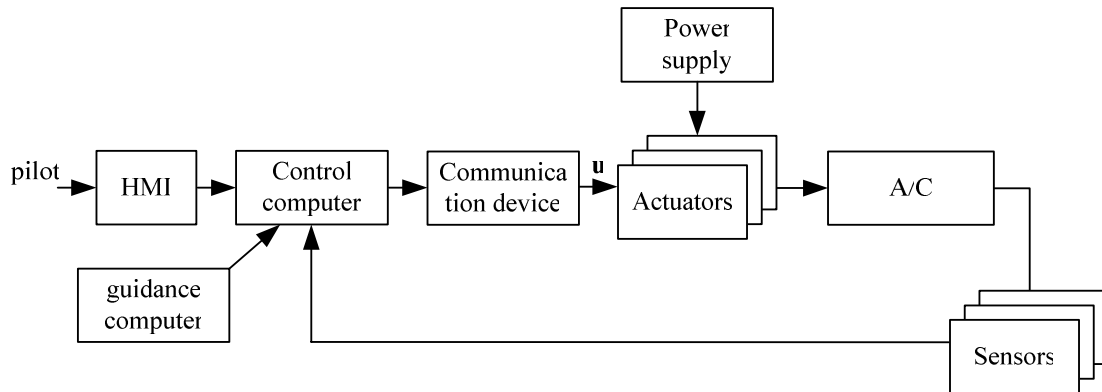


Figure 1.4 General architecture scheme of flight control system

Failure can occur in any subsystem or element of a flight control channel. Here are only considered failures that may happen at actuators, sensors or at the controlled process itself.

1.3.1 An overview of flight control actuator failures

Physically, the flight control actuator failures can be broadly divided into two categories:

- failures that result in a total loss of effectiveness of the control actuator, which includes lock in place, hard-over and float,
- failures that cause partial loss of effectiveness and are referred to as loss of effectiveness failures.

These common types of actuator failures for flight control channels are respectively shown in Figure 1.5-1.8 [Alwi, 2008; Jovan D. Boskovic & Mehra, 1999]. Some views of real actuator failures are shown in Figure 1.9, 1.10.

Lock in place failure, also called *stuck failure*, occurs when the actuator freezes at a particular position and does not respond to subsequent control signals. This might be caused by a mechanical jam, due to lack of lubrication for example. This type of failure not only reduces the number of available actuators, but also may cause a persistent disturbance to the system. This type of failure has been specially considered in [Bajpai et al., 2002; Chang et al., 2008; Jiang & Zhao, 2000; Pashilkar et al., 2006; Shin et al., 2005; Tang et al., 2007].

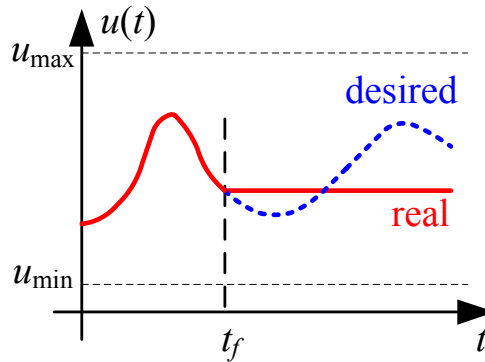


Figure 1.5 Illustration of stuck failure

Hard-over failure (*runaway failure*), is characterized by the actuator moving to and remaining at its upper or lower limits at maximum rate, regardless of the control signal. From the viewpoint of structural load and aircraft controllability, it is regarded as the most catastrophic types of failure. A rudder runaway can occur as the result of an electronic component failure which causes a (wrong) large signal which is sent to the actuators causing the rudder to be deflected at its maximum rate towards its maximum deflection. This type of failure is considered in [Burken et al., 2001; Kale & Chipperfield, 2002; Lombaerts et al., 2011].

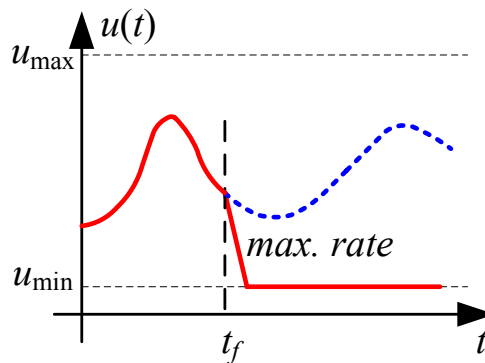


Figure 1.6 Illustration of hard-over failure

Float failure, also called *free-play failure*, occurs when the actuator floats with zero moment and does not contribute to the control effects. An example of a float failure is the loss of hydraulic fluid in the actuator of an elevator causing it to move freely to adopt the direction of the local angle of attack. Then it cannot produce any effective moment along the pitch axis. This type

of failure has been studied in [J. D. Boskovic & Mehra, 1998; Yang et al., 1999].

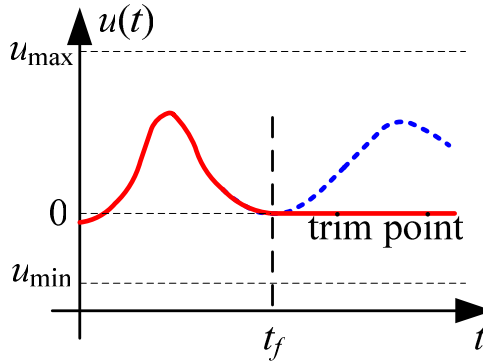


Figure 1.7 Illustration of float failure

Loss of effectiveness is characterized by actuators responding to control signals in an abnormal way (lower action level, saturation, lower response time, etc.). For example, the presence of a leaking cylinder could cause a power loss and degrade the response time of an actuator. Usually a lack of power supply will contribute to an incomplete response of actuator to a control signal. [Li et al., 2007; Totah, 1996] considered this type of failure.

Air transportation accident statistics demonstrate that actuator failures contribute significantly to the fatality accidents.

Table 1.1 lists some accidents whose original causes were actuator failures.

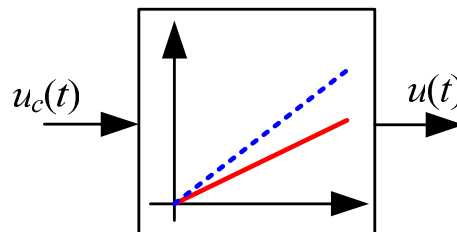


Figure 1.8 Illustration of loss of effectiveness failure

Table 1.1 Some examples of actuator failures

Actuator failures	examples
Stuck failure	1977, Flight 1080, Lockheed L-1011, left elevator was jammed at the full trailing edge-up position, landed safely
	2000, Flight 261, MD-83, crashed because of jammed horizontal stabilizer, 88 killed
	1972, Flight 96, DC-10, the rudder jammed with an offset, 11 persons injured
Hard over failure	2002, Flight 85, B-747, airplane rolled excessively caused by a lower rudder runaway to full left deflection, emergency landing and no injured
	1994, Flight 427, B-737, suffered from a rudder runaway to its blowdown limits, aircraft crashed and 132 killed
	1991, Flight 585, B-737, suffered a rudder hardover, lost control and crashed immediately, 25 killed
Float failure	1985, Flight 123, B-747, experienced a total hydraulic system loss as a result of a failure in an aft cabin pressure bulkhead. Most of the vertical fin was also lost, 520 killed
	2003, DHL A-300B4, all actuator didn't work due to a total loss of hydraulics occurred, landed safely
Loss of effectiveness	2000, a Cessna 210E made a hard landing maybe due to loss of elevator effectiveness



Figure 1.9 Stuck aileron on B-767 in flight



Figure 1.10 Hardover rudder on Airbus Skylink (by Mick Ward)

1.3.2 An overview of sensors failures

Importance of sensor failure for flight safety

Sensor failures may be as critical as actuator failures since they can result in a wrong control signal sent to the actuators. So it is important to avoid sensors failures, to detect them when they happen and to provide in that case alternate data. Sensor failures can occur due to malfunctions of some component of the measurement system itself, to the installation status of the measuring devices (loose mounting or wrong position) or to wear or tear leading to a loss of accuracy or no signal at all.

A failed sensor produces a signal more or less relevant and therefore results in variable error between the displayed value and the real value, thus the control system that receives this incorrect information may be driven to generate control signals completely inadequate to perform a certain function and may risk the system's survival.

Statistics provide many examples of accidents whose primary cause is a sensor failure:

- On Aug. 1, 2005, a serious incident involving Flight 124, a B-777 aircraft experienced un-commanded maneuvers by acting on false indications. The ATSB report said that it was

probable that a latent software error allowed Air Data Inertial Reference Unit (ADIRU) to use data from a failed accelerometer [Australian Transport Safety Bureau, 2007].

- On June 1, 2009, the Airbus A330-203 airliner serving the flight AF 447 crashed into the Atlantic Ocean, killing all 216 passengers and all 12 crew members. The final report from Bureau d'Enquêtes et d'Analyses [Bureau d'Enquetes et d'Analyses, 2012] pointed out that this accident was originated from temporary inconsistency between the measured speeds, likely as a result of the obstruction of the pitot tubes by ice crystals, causing autopilot disconnection and reconfiguration to “alternate law”.

A sensor failure classification

According to the matching of measurement and real value, sensor failures can be classified into five types which are shown in Figure 1.11-1.15:

Bias: when there is a constant offset between real signal and measured signal of sensor, it is called *Bias*.

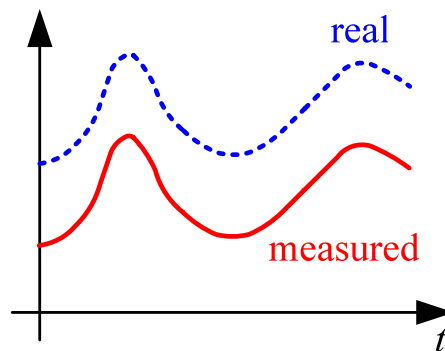


Figure 1.11 Illustration of bias failure

Drift: Sometimes the measured signal diverges slowly from the real signal goes more and more far away, it is called *drift*.

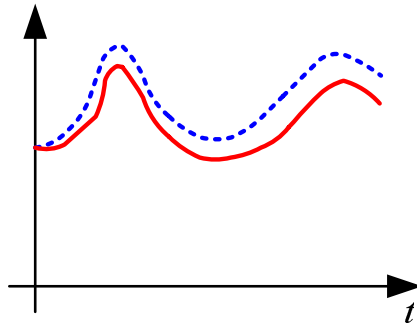


Figure 1.12 Illustration of drift failure

Loss of accuracy: When the measurements never reflect the true values of the states, a *loss of accuracy* occurs.

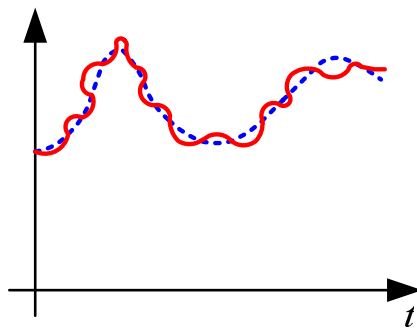


Figure 1.13 Illustration of loss of accuracy failure

Freezing: *Freezing* of a sensor signal indicates that the sensor provides a constant value regardless of the real value.

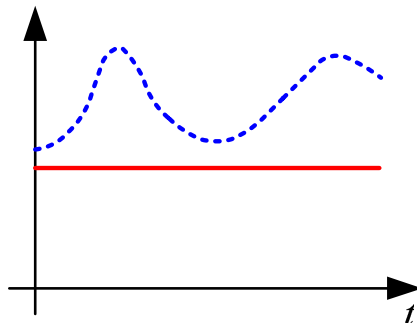


Figure 1.14 Illustration of freezing failure

Calibration error: a *calibration error* is a wrong representation of the actual physical meaning of the states from the electrical or electronic signals that come out from the sensor unit itself which can be seen as a transducer.

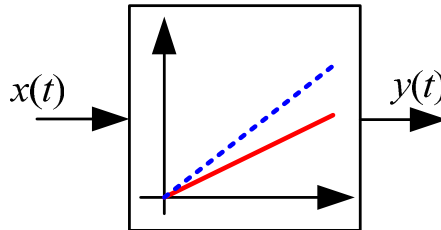


Figure 1.15 Illustration of calibration error failure

Many techniques have been developed to detect sensor failures and to eliminate their effect. In general these techniques integrate physical redundancy of sensors as well as measurements from other sensors through analytic redundancy [Hwang et al., 2010; R. Isermann & Balle, 1997; Rolf Isermann, 2005; Y. Zhang & Jiang, 2008].

1.3.3 Failures of the controlled process

This type of failure affects the controlled process itself or the auxiliary systems providing to him power and control signals. Often failures that are not failure of sensors or actuators are classified in this category. However, it can be worth to make a distinction. A component failure may be the result of a rupture or an alteration of some components of the controlled process, or a physical damage to a hydraulic or electrical system, or a breakdown of a computing or a communication device. This will reduce the capability of the flight control channel to perform its tasks in a standard way. In practice, this leads to a change in the characteristics of the system itself (deformation of a surface, altered bearing, fouling...). The occurrence of a failure in an auxiliary system of the flight control channels of a transport aircraft can lead to catastrophic situations.

Many examples of component failure can be found, some of them are shown in Table 1.2.

Table 1.2 Some examples of component failures

component failures	examples
detachment of control surfaces or structure	1985, Flight 123, B-747, detachments of some body parts of the aircraft e.g. the vertical fin/stabilizer, 520 killed
	2001, Flight 587, A-300, New York, 2001, 265 killed
engine	2009, Flight 1549, A-320, damage to both engines due to impact with flock of gees, ditched in the river and no life loss
	2008, B-777, Engines failed to respond to command from auto-throttle and from flight crew, aircraft entered an uncontrolled descent
computer	2005, B-737, because autopilot failure, aircraft driven into an upset condition by autopilot
	2000, Flight 179, B-747, possible autopilot anomaly resulting from an inappropriate maintenance action

1.4 Airworthiness Regulations

In order to enforce safety progress in air transportation, stringent airworthiness regulations have been established by national and international civil aviation authorities.

Classification of failure severity

In the field of Aeronautics, the classification of failures according to the criticality of their consequences and the allowed probability of occurrence plays an important role in aircraft design and safety performance evaluation processes. Table 1.3 shows the qualitative classification of failures built by airworthiness regulation AMC 25.1309 [European Aviation Safety Agency, 2007]. It is clear that the most disastrous event is required to occur with the lowest probability.

Table 1.3 Classification of failures in the Aeronautics

Failure Classification	Minor	Major	Hazardous	Catastrophic
Probability	$>10^{-5}/h$ Probable	$10^{-7}/h < p < 10^{-5}/h$ Remote	$10^{-9}/h < p < 10^{-7}/h$ Extremely remote	$p < 10^{-9}/h$ Extremely improbable
Effects	No apparent effect	- Reduction of safety margins - Increase in crew workload - Some minor injuries	- Significant reduction in safety margins - Difficulty for the crew to control the situation - Serious or fatal injury	- Multiple deaths with generally loss of Aeronef

The airworthiness regulations impose to aircraft manufacturers high safety objectives with respect to the loss of aircraft maneuvering capability through flight control channel partial or overall failure. This has led aircraft manufacturers such as Airbus, to adopt flight control channel architectures designed to protect against it.

For example, the loss of pitch control, the permanent loss of THS, the rudder loss or runaway and the loss of roll control are made extremely improbable (probability per flight hour $<10^{-9}$) while the loss of the elevators is extremely remote (probability per flight hour $< 10^{-7}$) [Airbus, 2000].

To obtain these safety objectives, different fault tolerant techniques have been adopted by the aircraft manufacturer [Briere et al., 2001; Traverse et al., 2006; Yeh, 1998].

1.5 Conclusion

This chapter has displayed the complexity of flight control channels for modern transportation aircraft as well as the diversity of failure situations. These failure situations, when having important (major, hazardous, catastrophic) consequences on the flight must be made as improbable as possible by adopting fail-safe solutions. In the next chapter, the consequences of actuator failures on the flight domain and the flight qualities of a transportation aircraft will be introduced.

CHAPTER 2

TRANSPORT AIRCRAFT FLIGHT

QUALITIES

2.1 Introduction

In this chapter, the classical characteristics of the flight domain and the flight qualities of a transportation aircraft are introduced. A modern approach to describe and analyze the flight qualities, based on a state representation, is adopted (the equations describing the flight dynamics of an aircraft are presented in Annex A). Then, the consequences of actuator failures on the flight domain as well as on augmented flight qualities are discussed. In the second case, different failure scenarios are considered with respect to the longitudinal and the lateral dynamics of an aircraft.

2.2 Flight Domain

A transportation aircraft is designed to operate within a flight domain which allows it to perform its air transport activity in safe conditions. The flight domain is composed of different flight envelopes and allowed maneuvers.

2.2.1 Flight envelopes

A flight envelope is defined as a range of airspeeds and flight levels where an aircraft can safely operate. Different concepts of flight envelopes must be distinguished when considering flight safety:

- **The operational flight envelope**, or normal flight envelope, is the flight domain in which the aircraft is able to operate safely in order to accomplish its operational mission. In this domain, no flight protection is activated and a stick released or running autopilot will not fly beyond this limit. In Figure 2.1, **MMO** denotes Maximum Operating Mach number, **VMO** denotes Maximum Operating Velocity, **CAS** denotes Calibrated Air Speed, **TAS** denotes True Air Speed.
- **The peripheral flight envelope** limits the normal flight envelope. There low and high speed protections are active. For the aircraft to follow a given flight plan will suppose many often to fly near the limits of the normal flight envelope with the risk of entering the

peripheral flight envelope.

- **The service flight envelope** goes up to the structural and performance limits of the aircraft. The service flight envelope is composed of the normal envelope and of the peripheral flight envelope.
- **The permissible flight envelope** covers the flight domain where it is still possible to return to the service flight envelope without exceptional pilot skill or technique while downgraded flight handling qualities may appear. Here maneuvering and speed protections are deactivated and full pilot's authority is restored.

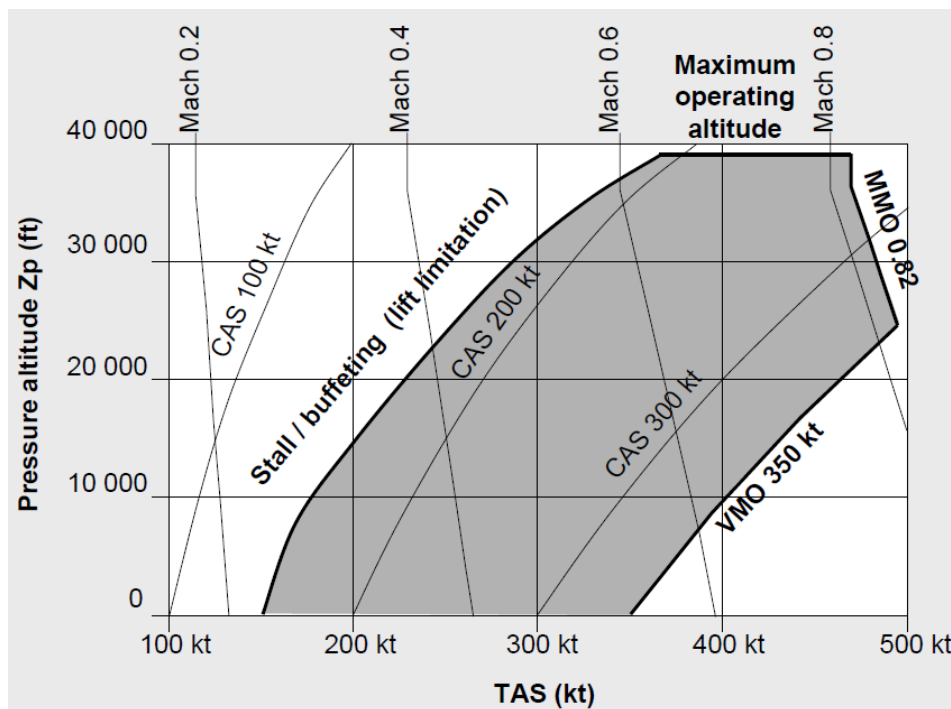


Figure 2.1 Flight domain and limits (source: IENAC Flight Operations Manual, ENAC)

In Figure 2.2 is represented in detail the upper limit of the flight envelope which is defined as the intersection of several domains considering buffeting, climb capability, maneuverability, maximum Mach number and propulsion limits.

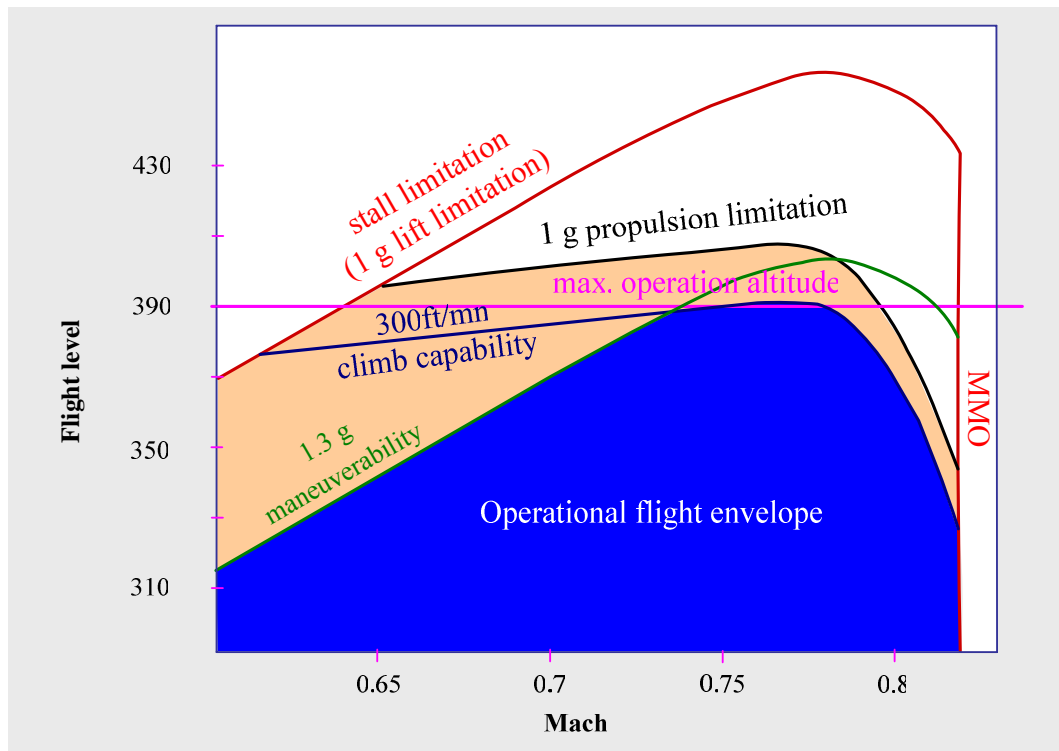


Figure 2.2 Detail of flight envelope ceiling

2.2.2 Flight maneuvers

All flight plans performed by a transportation aircraft are built from four fundamental basic flight situations: climbs, straight-and-level flight, turns and descents. These controlled flight situations are the consequence of the aircraft being able to perform basic maneuvers along its main axis. In the flight test program of an unpaired transportation aircraft, it must be proven that the aircraft can safely execute besides structure related maneuvers, a number of such maneuvers.

- **Longitudinal maneuvers:** As far as longitudinal maneuvers are concerned, the test program must include:
 - Quasi-steady maneuvers in which the load factor to be demonstrated (resource or dive maneuvers) is reached relatively slowly. In this maneuver the pitching velocity is low and is proportional to the load factor achieved. Since the elevator presents a very slow displacement rate the pitching acceleration is almost zero.

- Pitching maneuvers, where the longitudinal cockpit control displacement is a triangular or trapezoidal function of time.
- **Rolling maneuvers:** It should be made sure that any rolling maneuvers to be performed in flight testing do not lead to structural overloading and/or controllability problems.
- **Yawing maneuvers:** These maneuvers are not limited by the lateral load factor n_y or the yaw rate r , however they may be limited by sideslip angle β . The critical sideslip angle may be related to structural loading, engine/inlet compatibility, or dynamic stability at high angles of attack or high airspeeds. Often, these yawing conditions are critical for stressing the vertical tail plane and the rear fuselage.

In Figure 2.3 the main manoeuvring protections available within the service flight envelope of a modern transportation aircraft are displayed.

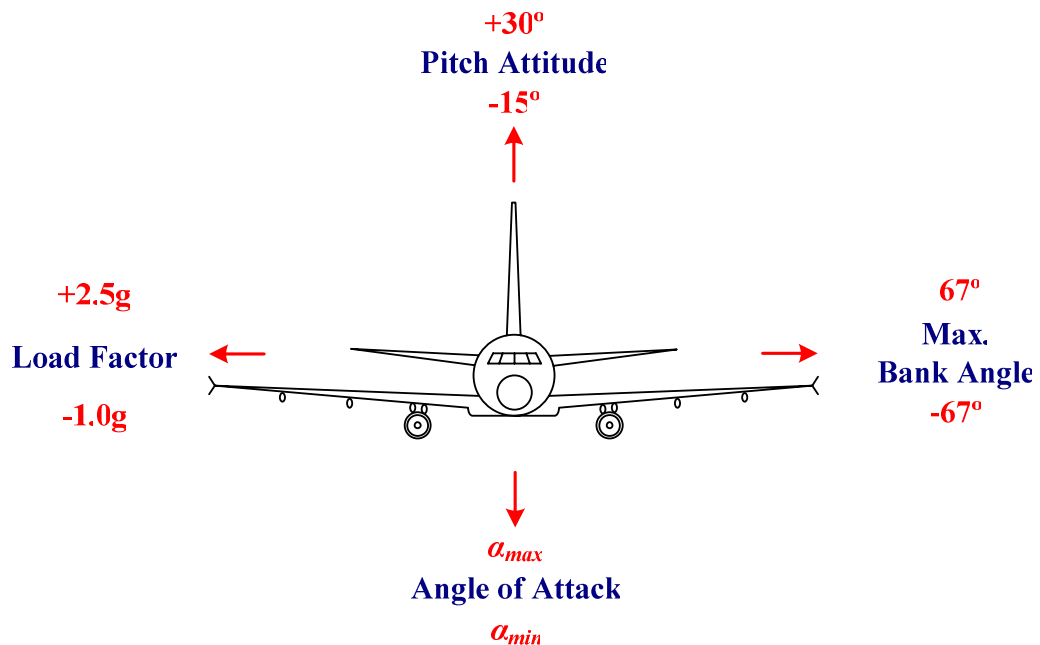


Figure 2.3 Automatic maneuver protections

2.2.3 Effects of failures on flight domain

The consequences of the occurrence of a flight control channel failure are to limit the effectiveness of these basic maneuvers and to restrict the different flight envelopes. These failures will impair the use of automatic flight protections.

For example in the case of the A320, if the flight control monitoring system detects one of the following faults:

- Trimmable Horizontal Stabilizer (THS) not available because it is blocked, or because its position is unknown following a failure of the corresponding sensor,
- failure of one of the elevators, or failure of the servo control of the yaw damper,
- failure of the shutters, or failure of the slats position sensor.

then the following automatic protections will be lost:

- turbulence damping protection,
- pitch angle limitation at piloting,
- low energy protection and high speed protection at guiding.

This constitutes the Alternate 1 flight control mode of A320.

With one of the following failures:

- the two engines,
- the failure of all spoilers, or the failure of all inner ailerons,
- the loss of information about pedal force.

This leads to the A320 Alternate 2 flight control mode where the only remaining manoeuvring protections are the load factor protection and angle of attack protection, while the bank angle limitation protection is lost.

2.3 Flight Qualities

2.3.1 Definitions

Flight qualities refer to the reaction of an aircraft to an external disturbance (wind gust in general) or to the variation of the deflections of some control surfaces. Acceptable flight qualities are an essential part of airworthiness requirements for a transportation aircraft. Flight qualities are subdivided into flying qualities and handling qualities. While the main issue considered in **flying qualities** studies is the ability of the aircraft to maintain an initial state of balance or to reach a new one through its natural reaction when initially moved away by some perturbation, the main issue treated in **handling qualities** studies is the ability of the aircraft to modify the initial state of balance: maneuverability (controllability/governability) through control surface.

Flying and handling qualities are the result of the aircraft design: overall sizing, position and shape (wing, tail and main body) as well as the sizing, position and shape of control surfaces and stabilizers. They contribute to flight safety and flight envelopes limits. Flying qualities can be also subdivided in natural flying qualities and augmented flying qualities. In the first case, flying qualities refer to the natural reaction of an aircraft with frozen control surfaces at their trim values, while in the second case automatic stabilization schemes have been introduced permanently to improve these natural flying qualities. In general, for transportation aircraft, handling qualities are considered for an aircraft with augmented flying qualities.

Flight qualities regulations:

The overall objective of the FAR / JAR 25 is to ensure that, all over the flight envelope, to maintain a trajectory does not imply an unacceptable workload for the pilot.

For the A300/A310 generation aircraft, regulation reflected this goal by specifying a positive static stability (see next paragraph) characterized by:

- a pitch down (up) control should result in a speed reduction (increase),
- after releasing the stick, the aircraft should naturally return to its equilibrium speed.

Some additional elements could be required to satisfy this condition throughout the operational flight envelope.

For A320/A340 generation aircraft, the overall objective of the regulation is directly satisfied by the normal load factor n_z with an operating auto-trim, although the positive static stability criteria is no more satisfied in all circumstances (flight domain and aircraft configuration).

2.3.2 Classical approach to the analysis of flight qualities

Static and Dynamical Stability

An aircraft is said to be **statically stable** if it automatically produces forces and moments which tend either to initially reduce the effect of a disturbance on the aircraft or to make the aircraft react initially to a control input towards its final state [Mora-Camino, 2013].

In static control situation, the control force required to operate the aircraft in a given flight situation should be in the capability of a nominal pilot. The stick force should be zero near the desired cruise speed, while the speed increases immediately by pushing on the stick or decreases immediately by pulling on it.

An aircraft is said **dynamically stable** if after a perturbation, it returns over time to the original steady flight condition (asymptotic stability) or to another near one (non-asymptotic stability). Dynamic stability is also related with the tendency to oscillate during the return phase towards steady flight conditions.

Figure 2.4 displays different cases of static and dynamic stability, introducing also the intermediate situations of neutral static stability and neutral dynamic stability.

Although aircraft can be statically and dynamically unstable and still be flown safely providing the controls are sufficiently effective and the pilot is enough experienced, static and dynamical stability are required for transportation aircraft.

Classical flight qualities analysis

The classical flying qualities evaluation considers the values of the aerodynamic derivatives:

$\left(\frac{\partial \dot{x}_i}{\partial x_j}\right)$ (where x_j is a flight parameter). The variation and the sign of these derivatives according to the aircraft configuration, flight level and Mach number is of particular importance.

The classical handling qualities evaluation considers the study of aerodynamic derivatives: $\left(\frac{\partial \dot{x}_i}{\partial u_k}\right)$ where u_k is a flight control parameter such as the variation of the position of a control surface (ailerons, elevator, and rudder) or engines with respect to its trim position for a given position of the secondary surfaces.

These aerodynamic derivatives are directly related with the design characteristics of the aircraft: overall size and shape parameters of the aircraft, wings parameters (sweep angle, dihedral angle, wings position), THS size and position and finally engine position.

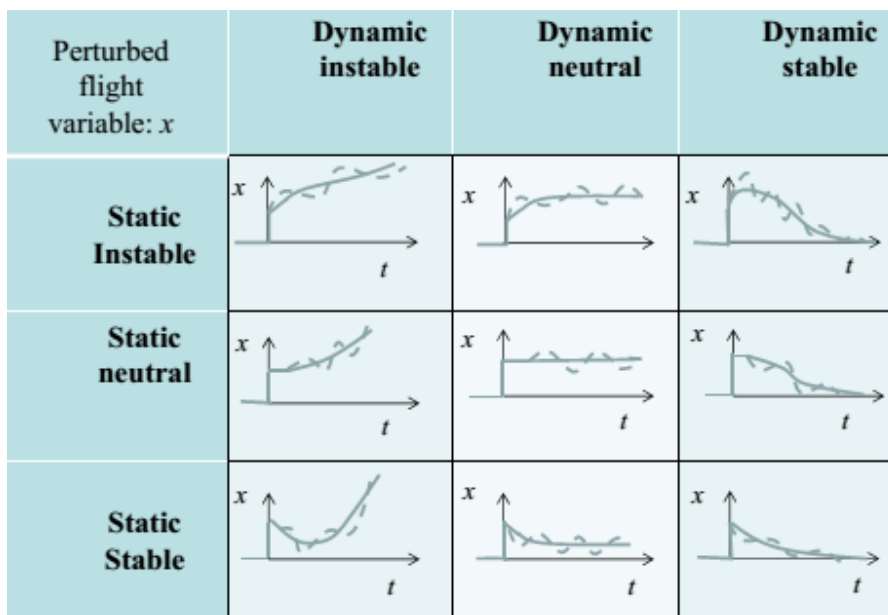


Figure 2.4 Static and dynamic stability cases

2.3.3 Modern approach to flight qualities analysis

Transportation aircraft operates during the major part of a commercial flight near flight

equilibrium conditions or near flight conditions with some fixed flight parameters (airspeed, path angle, heading angle or bank angle), then the study of the flight qualities around these trimmed flight situations is essential in this operational perspective.

Trim conditions

A general 11th order nonlinear representation of the flight dynamics of an aircraft (see Annex A) such as:

$$\dot{\underline{x}} = f(\underline{x}, \underline{u}, \underline{c}) \quad \underline{x} \in R^n, \underline{u} \in R^m, \underline{c} \in R^s, f \in C^\infty \quad (2.1)$$

$$\underline{y} = h(\underline{x}, \underline{u}) \quad \underline{y} \in R^p, h \in C^\infty \quad (2.2)$$

$$\text{with } \underline{x} = (u, v, w, \phi, \theta, \psi, p, q, r, z, T)' \text{ and } \underline{u} = (\delta_p, \delta_q, \delta_r, \delta_T)'$$

where u , v and w are the body referenced inertia speed components of the aircraft, ϕ is the bank angle, θ is the pitch angle, ψ is the heading angle, p , q and r are respectively the body referenced roll, pitch and yaw rates, z is the flight altitude and T is the total engine thrust. When navigation problems are considered, this state vector may be complemented by the horizontal position of the aircraft. Here δ_p , δ_q and δ_r are respectively the equivalent deflection of ailerons, elevator and rudder surfaces while δ_T is the common setting of the thrust levers. Here \underline{c} is a vector giving the position of the secondary actuators which characterize the aerodynamic configuration of the aircraft.

Then the set of equilibrium points and the set of equilibrium states can be introduced:

- the set $E(f)$ of equilibrium points in R^{n+m} is such as:

$$E(f) = \{(\underline{x}_0, \underline{u}_0, \underline{c}_0) \in R^n \times R^m \times R^s \mid f(\underline{x}_0, \underline{u}_0, \underline{c}_0) = \underline{0}\} \quad (2.3)$$

- the set $e(f)$ of equilibrium states (trim) in R^n is such as:

$$e(f) = \{\underline{x}_0 \in R^n \mid \exists (\underline{u}_0, \underline{c}_0) \in R^m \times R^s, f(\underline{x}_0, \underline{u}_0, \underline{c}_0) = \underline{0}\} \quad (2.4)$$

where the projection of $E(f)$ on R^n is equal to $e(f)$.

The trim problem consists in determining the values of \underline{u}_0 and \underline{c}_0 for a given $\underline{x}_0 \in e(f)$.

Flight dynamics linearization

Then around an equilibrium point representative of a sustained flight situation, the flight dynamics model (equations (2.1) and (2.2)) is linearized to provide a first order approximation of the dynamics of the small variations of the flight variables \underline{x} with respect to the control variable \underline{u} for a given configuration of the aircraft \underline{c}_0 around that equilibrium point. This results in a linear state representation of the flight dynamics near this equilibrium point:

$$\dot{\underline{X}} = A \underline{X} + B \underline{U} \quad \text{and} \quad \underline{Y} = C \underline{X} + D \underline{U} \quad (2.5)$$

where

$$A = \left. \frac{\partial f}{\partial x} \right|_{x_0, u_0, c_0} \quad B = \left. \frac{\partial f}{\partial u} \right|_{x_0, u_0, c_0} \quad C = \left. \frac{\partial h}{\partial x} \right|_{x_0, u_0, c_0} \quad D = \left. \frac{\partial h}{\partial u} \right|_{x_0, u_0, c_0} \quad (2.6)$$

with

$$\underline{X} = \underline{x} - \underline{x}_0 \quad \text{and} \quad \underline{U} = \underline{u} - \underline{u}_0 \quad (2.7)$$

● Analysis of the linearized flight equations

The resulting full linearized flight dynamic model is in general composed of two slightly coupled subsystems relative to longitudinal flight dynamics:

$$\begin{bmatrix} \dot{u} \\ \dot{\alpha} \\ \dot{q} \\ \dot{\theta} \\ \dot{z} \\ \dot{T} \end{bmatrix} = \begin{bmatrix} * & * & 0 & * & 0 & * \\ * & * & * & * & 0 & 0 \\ 0 & * & * & * & 0 & * \\ 0 & 0 & * & 0 & 0 & 0 \\ * & * & 0 & * & 0 & 0 \\ 0 & 0 & 0 & 0 & 0 & * \end{bmatrix} \begin{bmatrix} u \\ \alpha \\ q \\ \theta \\ z \\ T \end{bmatrix} + \begin{bmatrix} 0 & 0 \\ 0 & * \\ 0 & * \\ 0 & 0 \\ 0 & 0 \\ * & 0 \end{bmatrix} \begin{bmatrix} \delta_T \\ \delta_q \end{bmatrix} \quad (2.8a)$$

and to the lateral flight dynamics:

$$\begin{bmatrix} \dot{\beta} \\ \dot{p} \\ \dot{r} \\ \dot{\phi} \\ \dot{\psi} \end{bmatrix} = \begin{bmatrix} * & * & * & * & 0 \\ * & * & * & 0 & 0 \\ * & * & * & * & 0 \\ 0 & * & 0 & 0 & 0 \\ 0 & 0 & * & 0 & 0 \end{bmatrix} \begin{bmatrix} \beta \\ p \\ r \\ \phi \\ \psi \end{bmatrix} + \begin{bmatrix} 0 & * \\ * & 0 \\ * & * \\ 0 & 0 \\ 0 & 0 \end{bmatrix} \begin{bmatrix} \delta_p \\ \delta_r \end{bmatrix} \quad (2.8b)$$

The longitudinal as well as the lateral flight dynamics of an aircraft are based on two time

scales:

- one which is related to the aircraft attitude (with respect to Earth with pitch θ and bank ϕ angles, with respect to the air with angle of attack α and side slip β angles), the piloting dynamics,
- one which is related with the trajectory followed by the aircraft between or towards trimmed situations, the guidance dynamics, where the piloting dynamics can be considered to be causal for the guidance dynamics.

A very important point for the design of robust flight control laws through gain scheduling techniques [Nichols et al., 1993; Rugh, 1991; Shamma & Athans, 1992] is to observe that the values of the nonzero coefficients of matrices A , B , C and D varies very slowly according to the considered point in the flight envelope.

● Stability criteria

The flying and handling qualities of an aircraft are related with the characteristics of the linearized models of the piloting dynamics. Then the stability of these dynamics around a reference equilibrium point can be analyzed using algebraic criteria applied to their linearized models. For that, let $\Lambda = \{\lambda_1, \lambda_2, \dots, \lambda_n\}$ be the spectra of a state matrix A , solution of the characteristic equation:

$$|\lambda I - A| = 0 \quad \text{or} \quad \prod_{i=1}^n (\lambda - \lambda_i) = 0 \quad (2.9)$$

Here dynamic stability covers two cases: asymptotic stability and non asymptotic stability. A necessary and sufficient condition for asymptotic stability is: $\text{Re}(\lambda_i) < 0 \quad \forall i \in \{1, \dots, n\}$ while a sufficient condition for non asymptotic stability (SC) is: $\exists ! \lambda_i = 0 \quad \forall j \neq i \quad \text{Re}(\lambda_j) < 0$. This results in the graphical criteria displayed in Figure 2.5.

Here static stability is related with the initial reaction of a component of the state of the system to return or not to the initial equilibrium point when a perturbation is applied instantaneously on this state component.

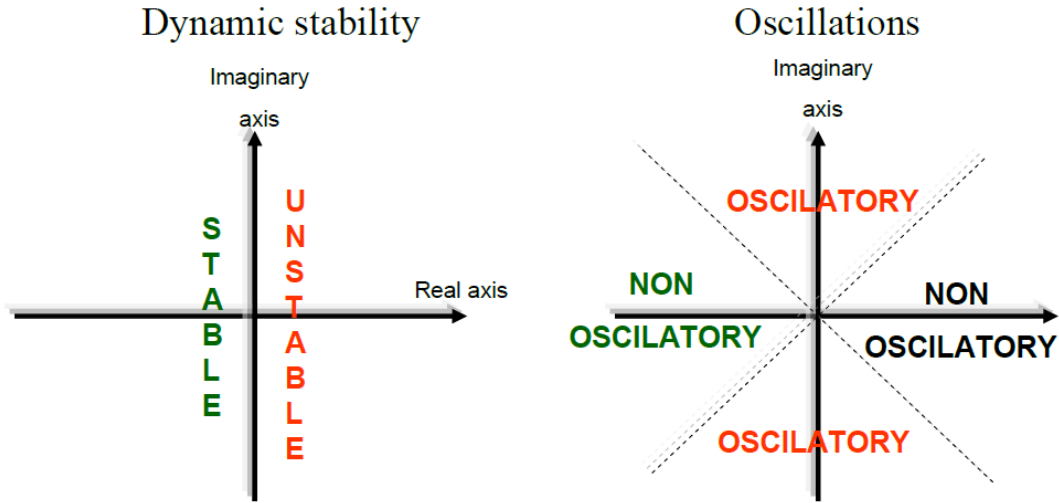


Figure 2.5 Graphical criteria for dynamic stability and oscillations

Let the initial variation of the state vector be given by $\underline{x}(0) = [0 \ \dots \ 0 \ x_j(0) \ 0 \ \dots \ 0]^T$, then according to the linear state equation, the Laplace transform of this state component is given by:

$$x_j(s) = C_j (sI - A)^{-1} C_j' \cdot x_j(0) \quad (2.10)$$

$$\text{with } C_j = [0 \ \dots \ 0 \ 1 \ 0 \ \dots \ 0]$$

or

$$x_j(s) = H_{jj}(s) \cdot x_j(0) \quad (2.11)$$

$$\text{where } H_{jj}(s) = C_j (sI - A)^{-1} C_j' = \frac{N_{jj}(s)}{D_{jj}(s)} = \frac{\prod_{h=1}^{m_j} (s - z_h)}{\prod_{k=1}^{n_j} (s - p_k)} \quad (2.12)$$

$$\text{with } \{p_1, p_2, \dots, p_{n_j}\} \subset \{\lambda_1, \lambda_2, \dots, \lambda_n\}$$

Then a sufficient condition for static stability is that all the zeros of the above transfer function are stable. The resulting graphical criteria for static and dynamic stability are displayed in Figure 2.6.

Observe that since no control term appears in the above expressions, natural stability, either static or dynamic will not be impaired by actuator failures. On the contrary, handling qualities which are related with the characteristics of the transfer functions between the control inputs and

the piloting variables:

$$\underline{x}(s) = F(s) \cdot \underline{u}(s) \tag{2.13}$$

$$\text{where } F(s) = (sI - A)^{-1} B \tag{2.14}$$

will be directly affected by actuator failures.

A necessary and sufficient condition for local controllability is derived from Caley-Hamilton theorem and is given by the following condition on the controllability matrix:

$$\text{rank} \left(\begin{bmatrix} B & AB & A^2B & \dots & A^{n-1}B \end{bmatrix} \right) = n \quad \text{with } n = \dim(\underline{x}) \tag{2.15}$$

Of course linear flight dynamics of an unpaired aircraft fulfill this condition.

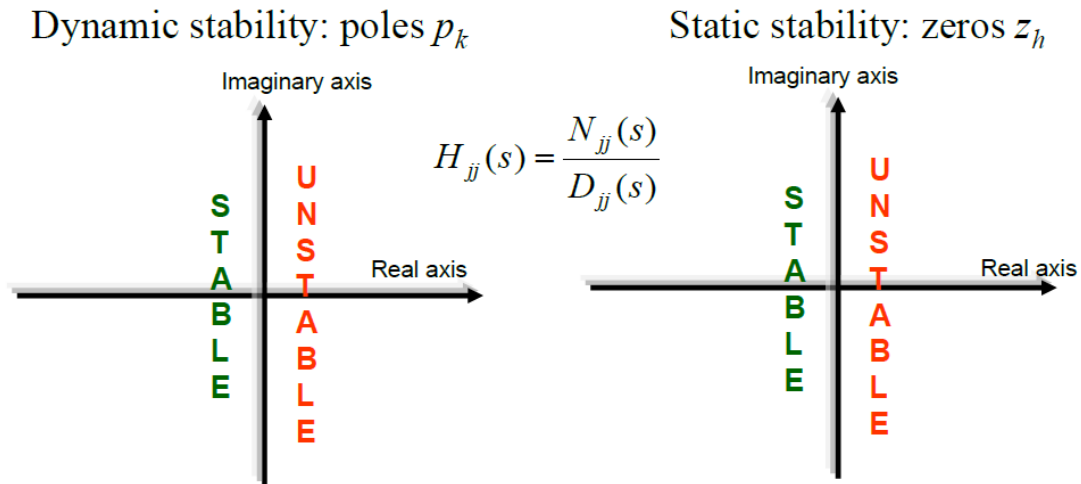


Figure 2.6 Graphical condition for dynamic and static stability

2.4 Transportation Aircraft Flying Qualities

As said before, the flight qualities of an aircraft can be subdivided into longitudinal and lateral flying qualities.

2.4.1 Longitudinal Flying Qualities

When considered the linearized equation (2.8a), it appears that the current thrust T plays the role of an input parameter submitted to a first order dynamics while the flight altitude z plays the

role of an output variable. In both cases there are no noticeable interactions with the other longitudinal variables. Then in general the longitudinal dynamics of an aircraft are considered to be represented by the evolution of the set of variables $\{u, \alpha, q, \theta\}$ (where $\alpha \approx w/V_0$ with $V_0 = \sqrt{u_0^2 + v_0^2 + w_0^2}$), which constitutes a fourth order dynamic system. This fourth order dynamic system is composed of two second order dynamic modes:

- one which is related with the pitch motion (fast dynamics), termed *short period oscillation*,
- one which is related with the motion of the center of gravity in the vertical pale (slow dynamics), termed *phugoid*.

All these modes are naturally dynamically stable even if they can be the source of longitudinal oscillatory motions.

Numerical Example: For a large transportation aircraft flying around 2000 m with an airspeed of 150 m/s, the linearized equations of motion for longitudinal flight dynamics are as follows:

$$\begin{bmatrix} \dot{u} \\ \dot{\alpha} \\ \dot{q} \\ \dot{\theta} \end{bmatrix} = \begin{bmatrix} -0.0088 & 3.9128 & 0.018 & -9.81 \\ -0.0009 & -0.8192 & 1.0025 & 0 \\ 0 & -1.9958 & -0.6617 & 0 \\ 0 & 0 & 1 & 0 \end{bmatrix} \begin{bmatrix} u \\ \alpha \\ q \\ \theta \end{bmatrix} + \begin{bmatrix} -0.5079 \\ -0.0711 \\ -2.923 \\ 0 \end{bmatrix} \delta_q \quad (2.16)$$

The conjugate eigenvalues of the uncontrolled short period mode are $-0.7405+1.4123 j$ and $-0.7405-1.4123 j$ corresponding to a damping factor of 0.48 with a natural frequency of 1.6 rad/s. To satisfy one of the flying quality requirements attached to pitch motion, the damping factor should be about 1 with a natural frequency of 2.18 rad/s. This can be achieved by the stability augmentation system by considered a pitch rate feedback in the elevator control law such as:

$$\delta_q = 0.984 q + \delta_q^e \quad (2.17)$$

where δ_q is the deflection signal sent to the elevator while δ_q^e is an independent input related with the performed attitude control function. The dynamics of the elevator is not considered here because in a fault-free situation its time response is very short with respect to the pitch time response. When introducing the pitch rate feedback in the elevator control law, relation (2.17),

the eigenvalues of the stabilized dynamics change to $-2.1789 + 0.1202 j$ and $-2.1789 - 0.1202 j$, while the required damping factor and natural frequency are achieved.

In Figure 2.7 are displayed the parameters associated to the natural and controlled short period dynamics, while in Figure 2.8 the pitch time responses of the aircraft to a step input is displayed in both situations.

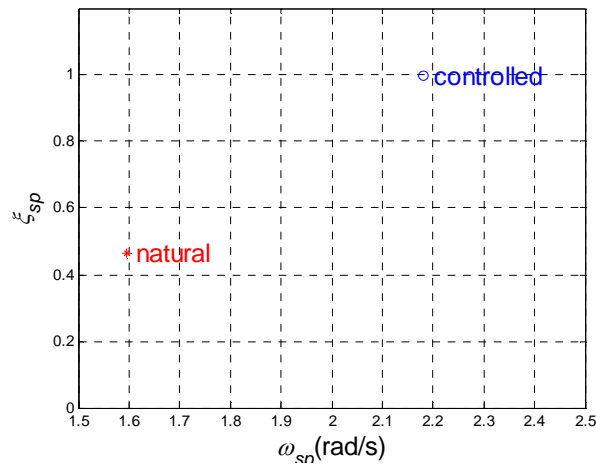


Figure 2.7 Natural and augmented short period parameters

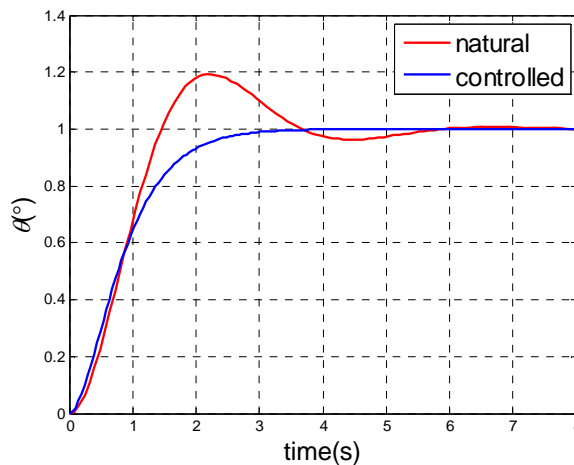


Figure 2.8 Natural and augmented response to a step input

2.4.2 Lateral Flying Qualities

When considered the linearized equation (2.8b), it appears that the heading parameter ψ plays the role of an output variable since there is no noticeable interaction with the other lateral variables.

Then in general the lateral dynamics of an aircraft are considered to be represented by the evolution of the set of variables $\{\beta, p, r, \phi\}$ where $\beta \approx v/V_0$, which constitutes here also a fourth order dynamic system. This fourth order dynamic system is composed of a second order and two first order dynamic modes:

- The second order dynamic mode corresponds to a fast coupled motion around the roll and yaw axis, the *Dutch roll*,
- one of the first order mode corresponds to the fast damping of the roll motion of an aircraft, the *roll mode*.
- The other first order dynamic mode corresponds to the slow return of the wings to horizontality, this is the *spiral mode*.

Here also, according to airworthiness requirements for transportation aircraft, these three modes must be naturally dynamically stable even if they can be the source of lateral oscillatory motions. While the natural roll mode is not a problem in conventional aircraft, the natural Dutch roll appears insufficiently damped and a yaw damping function must be performed by the flight augmentation system.

Numerical example: When considering a large transportation aircraft flying around 12000 m with an airspeed of 230m/s, the linearized equations of motion for the lateral flight dynamics are as follows [MathWorks, 2009]:

$$\begin{bmatrix} \dot{\beta} \\ \dot{r} \\ \dot{\phi} \\ \dot{p} \end{bmatrix} = \begin{bmatrix} -0.056 & -0.997 & 0.080 & 0.042 \\ 0.598 & -0.115 & -0.032 & 0 \\ 0 & 0.805 & 1 & 0 \\ -3.05 & 0.388 & -0.465 & 0 \end{bmatrix} \begin{bmatrix} \beta \\ r \\ \phi \\ p \end{bmatrix} + \begin{bmatrix} 0.007 & 0 \\ -0.475 & 0.008 \\ 0 & 0 \\ 0.153 & 0.143 \end{bmatrix} \begin{bmatrix} \delta_r \\ \delta_a \end{bmatrix} \quad (2.18)$$

The four eigenvalues of this system are respectively $-0.0329 + 0.9467i$, $-0.0329 - 0.9467i$, -0.5627 , -0.0073 resulting in a damping factor of 0.035 for the natural Dutch roll mode. Adopting a control law such as:

$$\delta_r = 2.85r - 0.93\beta \quad (2.19)$$

where δ_r is the deflection of the rudder when, like in the case of longitudinal control, the dynamics of the actuators are taken as instantaneous.

Figure 2.9 displays the parameters attached to the Dutch roll for a fault-free rudder control channel in the natural and the controlled situations.

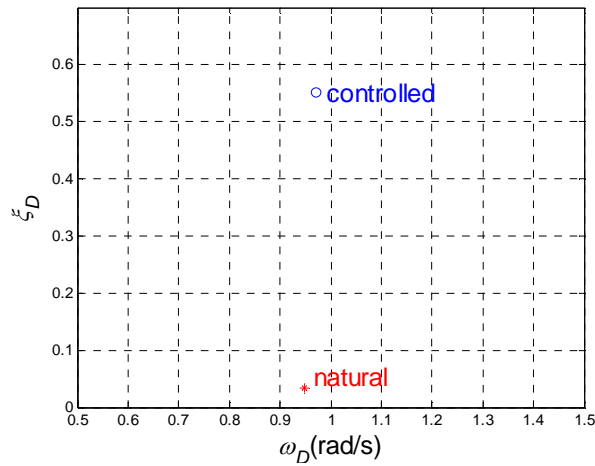


Figure 2.9 Natural and controlled Dutch roll parameters

Figure 2.10 displays the evolution of different sideslip responses to a disturbance of 1° in both situations.

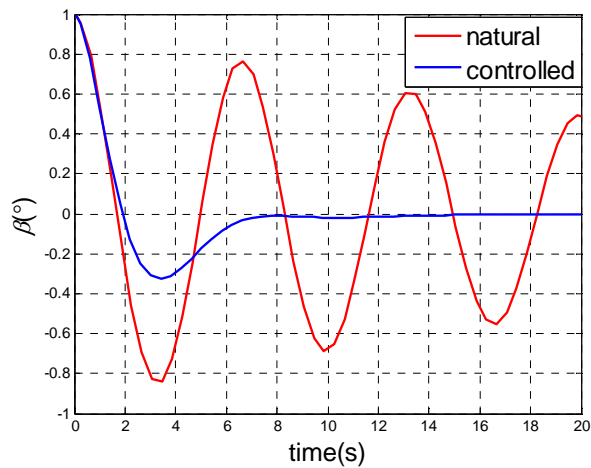


Figure 2.10 Natural and augmented perturbed sideslip dynamics

2.5 Effects of Actuator Failures on Handling Qualities

2.5.1 Residual controllability

To make apparent the contribution of each input to the flight dynamics around a trim situation, relation (2.13) can be rewritten as:

$$\underline{x}(s) = (sI - A)^{-1} \left(\sum_{j=1}^m \underline{b}_j u_j(s) \right) \quad \text{with } m = \dim(\underline{u}) \quad (2.20)$$

where \underline{b}_j is the j^{th} column of matrix B . Then when the k^{th} control input becomes ineffective there is no contribution of the k^{th} input. In the case in which the k^{th} control input is stuck to a non zero value u_k^0 , the linearized dynamics become:

$$\underline{x}(s) = (sI - A)^{-1} \left(\sum_{j=1, j \neq k}^m \underline{b}_j u_j(s) + \underline{b}_k u_k^0 / s \right) \quad \text{with } m = \dim(\underline{u}) \quad (2.21)$$

where the failed actuator acts like a permanent external perturbation.

Now one important issue is to consider the controllability of the pair (A, B) when B has lost its k^{th} column.

In the case of the lateral dynamics of a classical transportation aircraft where roll and yaw motions are controlled by the deflection of the ailerons and of the rudders, it happens that in general the determinant of the controllability matrix (here a square matrix) attached to a sole rudder is much larger than the one of the controllability matrix attached to a sole pair of ailerons which is close to zero. Then it appears of interest to assign to the rudder control channel backups to cover the failure of this channel. This is the case with the fly by wire rudder control channel of the recent Airbus family where a mechanical backup is present in the rudder control channel while there is no mechanical backup to control roll.

Stability augmentation of natural flight dynamics is obtained in general through feedback of tendency information, so that the stability augmented flight dynamics are written as:

$$\underline{x}(s) = (sI - (A - BG))^{-1} B H \underline{v}(s) \quad \text{with } \underline{u}(s) = -G \underline{x}(s) + H \underline{v}(s) \quad (2.22)$$

where G is the feedback gain and H is the feedforward gain applied to the independent input \underline{v} .

Many techniques [McLean, 1990; Pratt, 2000; Stevens & Lewis, 1992] are available to compute matrices G and H so that the eigenvalues of matrix $A-BG$ remain within a target domain in the complex plan (see Figure 2.4 and 2.5) and the eigenvectors allows to satisfy dynamic decoupling conditions [Balasubramanian, 1989; Q. Wang, 2003].

2.5.2 Case studies

Failure in the pitch control channel

When considering the longitudinal equations of (2.16), the following failure cases for the elevator control channel are considered here:

- Failure case 1: Full failure with one elevator, which is stuck or hardover
- Failure case 2: Full failure with floating elevator,
- Failure case 3: Loss of deflection effectiveness of elevator,
- Failure case 4: Loss of rate of deflection effectiveness of elevator

These failure cases can be modeled as a degraded control effectiveness parameter. Substituting this changed parameter into (2.16), degraded handling qualities can be deduced. Figure 2.11 displays the short period parameters under fault-free or examples of above failure cases and Figure 2.12 displays the response of controlled system under fault-free and failure case 4. It is easy to see that all failure cases will impact the handling qualities of the aircraft. In detail, failure cases 1 to 3 impact the position of poles and then damping ratios and natural frequency. Failure case 4 causes latency to the response. All these failures impact the augmented flying and handling qualities of the aircraft.

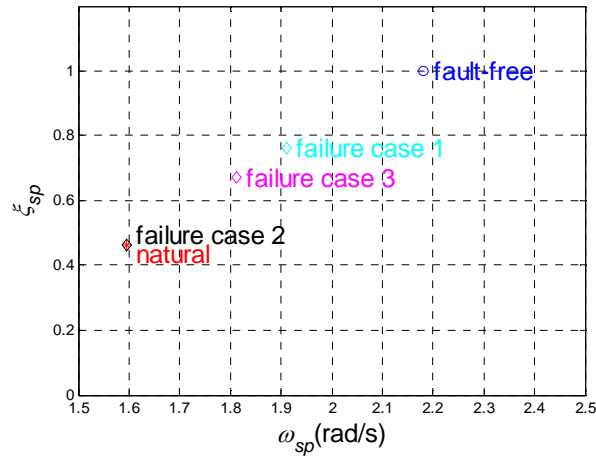


Figure 2.11 Natural and augmented short period parameters under fault-free or failure cases

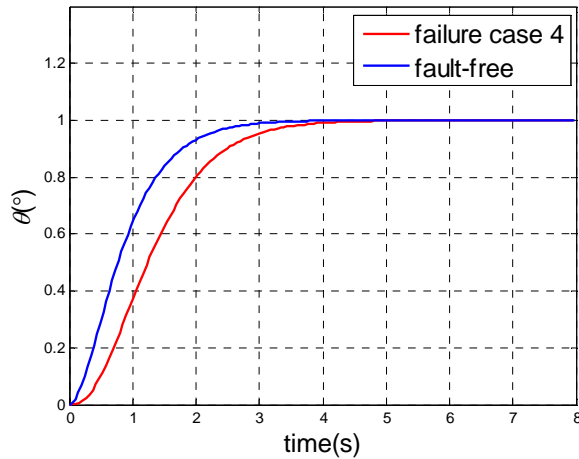


Figure 2.12 Pitch angle response of controlled system to a step input under fault-free and failure case 4

Failure in the yaw control channel

For the lateral equations of (2.18), the same failure cases as above are considered for the rudder control channels.

The resulting performances with respect to the Dutch roll are displayed in the parameter space (Figure 2.13) as well as in the time reference by considering the response of the aircraft to a sideslip disturbance (Figure 2.14). A similar conclusion as in the longitudinal case can be made that all failure cases will impact the lateral augmented flying and handling qualities of the aircraft. In detail, failure cases 1 to 3 impact the position of poles and then damping ratios and natural

frequency. From Figure 2.14, although failure case 4 does not modify the eigenvalues of the system matrix but also cause an oscillating response.

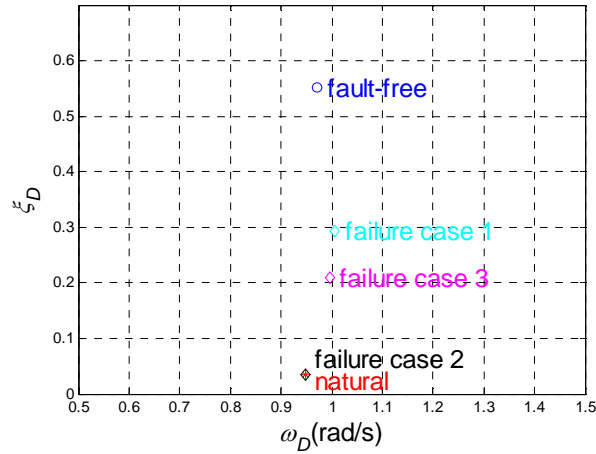


Figure 2.13 Natural and controlled Dutch roll parameters under fault-free or failure cases

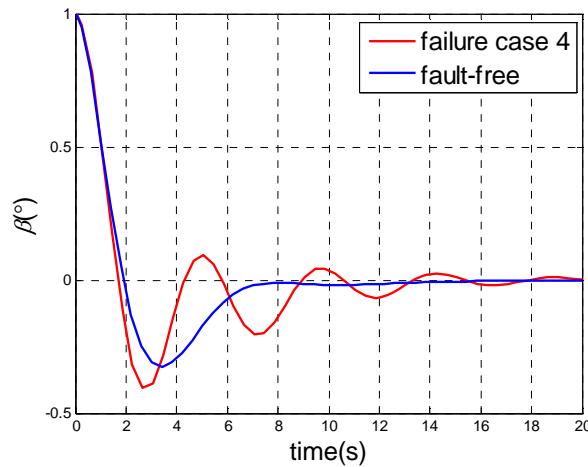


Figure 2.14 Natural and augmented perturbed sideslip dynamics fault-free and failure case 4

2.6 Conclusion

From the above analysis, it appears that natural flight qualities must be enhanced by stability augmentation systems. These systems are special to generate fast control signals to the actuators and when some actuators failure occurs, the resulting flying and handling qualities are at stake.

To avoid these situations, different fault tolerant schemes must be adopted where a difficult trade-off between flight safety and flight efficiency must be solved. The issue of fault tolerant flight is introduced in the next chapter.

CHAPTER 3

FAULT TOLERANT FLIGHT CONTROL

3.1 Introduction

In this chapter an overview of techniques leading to a fault tolerant flight control system is performed. Physical and analytical redundancies are the main basis for fault detection and identification as well as for fault tolerance actuation. While the study of FDI technique has remained at a general level in this thesis, a large emphasis has been given to fault tolerant control based on physical redundancy. Annex B is devoted to the design of fault tolerant control laws. In this chapter the case of fly-by-wire (FBW) control channels is analyzed, showing the two level strategy adopted by aircraft manufacturers.

3.2 Physical and Analytical Redundancies

For systems whose failure involves human life and high economic costs, such as transportation aircraft, highly reliable architectures must be adopted for their control.

Physical redundancy: This technique consists in disposing in parallel of identical subsystems or components to diminish the probability of their overall failure. Redundant actuators will allow to continue to act on a process while redundant sensors will allow to detect the failure of one of them and adopt the correct signal. High order physical redundancy can be of interest for critical components. Then subsystems which develop a critical function whose failure should be proven to be extremely improbable may present a duplex, triplex or even quadruplex architecture. Figure 3.1 displays main redundancies in the roll control channel of past generation transportation aircraft (A300).

Analytical redundancy: The concept of analytical redundancy is based on the use of a mathematical model of the controlled system which displays analytical relationships between different physical parameters. Then the measure of some physical parameters provides indirect information about others which may be no more accessible to measurement when the sensors in charge of their direct measure fail. Analytical redundancy is mainly used for fault detection and identification. There residuals can be computed from the comparison of measurements with expected values from mathematical models, leading when threshold levels are exceeded to detect possible faults.

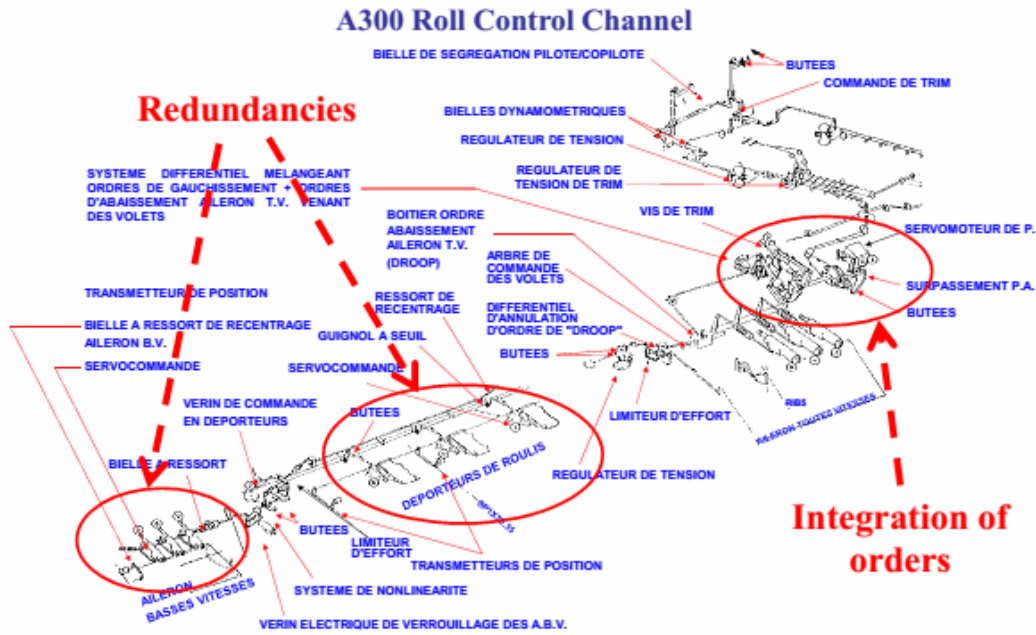


Figure 3.1 Main physical redundancy in A300 roll control channel

For example, roll, pitch and yaw rates of an aircraft can be either estimated from attitude angles measures through the Euler equations (See Annex A) or measured directly with gyrometers. Since modern transportation aircraft make use of three gyro lasers, the failure of one of them will be detected by majority voting and the triplex redundancy will be maintained by replacing the measure of the failed gyro laser by the estimation from the Euler equations and the attitude measurements. This can be done simultaneously for the three body axis. Also, to feed the longitudinal normal law of modern transportation aircraft, Airbus uses analytical redundancy to validate the pitch rate information when provided by a single inertial reference unit. The load factor is estimated through the pitch rate information and compared to the available accelerometric measurements in order to validate the Inertial Reference System (IRS) data [Briere et al., 2001].

The adoption of analytical redundancy techniques can also to reduce the overall weight of the resulting fault tolerant critical system and to limit its maintenance needs. In many situations, it appears that a combination of the two forms of redundancy provides better solutions [R. J. Patton, 1997].

The general structure of a fault tolerant flight control system is shown in Figure 3.2 where physical redundancies of actuators, sensors and control computers are colored in red. Of course, the circuits between actuators, sensors and control computers present also an adequate degree of physical redundancy. Observe that since the failure of actuators or sensors may break critical control loops, redundancy is commonly introduced at their level. In Figure 3.2, information flows resulting from analytical redundancy are colored in blue.

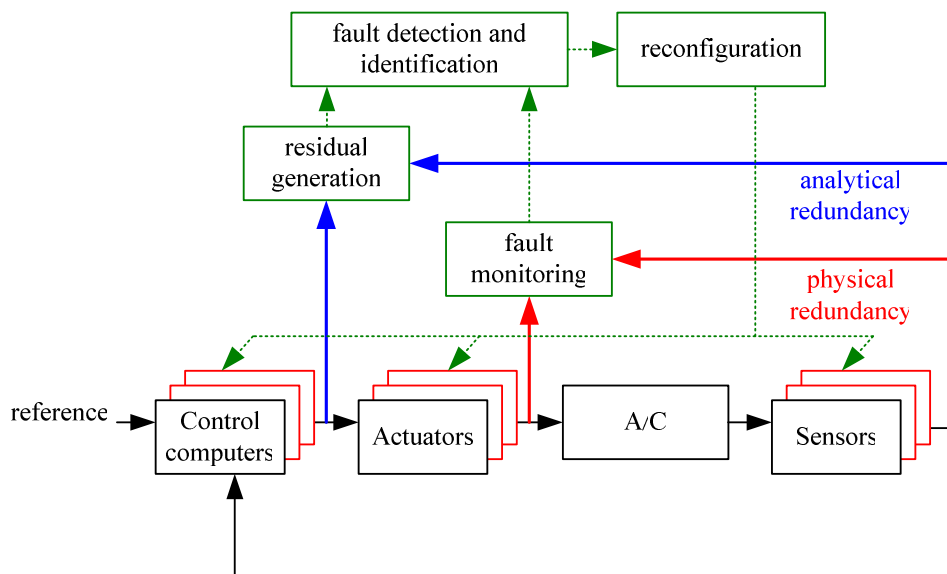


Figure 3.2 General view of a fault tolerant flight control system

3.3 Fault Detection and Identification

Faults leading to failures of a controlled physical process can appear either at the level of the control channels, at the level of the controlled process itself or at the level of the data channels (see Figure 3.3). An efficient fault detection and identification (FDI) scheme is essential to guarantee safety of a critical system by allowing the activation of automatic protections and reconfiguration mechanisms resulting in fault tolerance.

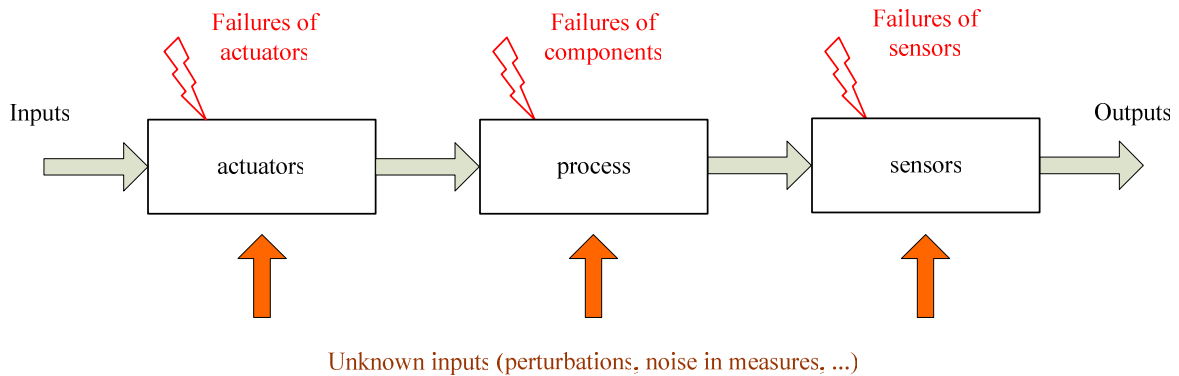


Figure 3.3 Fault localization in physical processes

Fault detection and identification is composed of three main activities:

- Detection: a fault is detected in the system [Gertler, 1988]. If there is a nominal model of the fault free system, a fault will be characterized by the existing distance of the process parameters to those of the nominal model.
- Location: it allows to trace the origin of the fault when a fault has been detected [Frank, 1991]. In general an original fault may generate a sequence of failures in a system and these cascading failures may mask their real cause.
- Identification: it determines the time the fault occurred, its duration and its amplitude.

The main technical performance criteria for fault detection and identification are: detectability, isolability, sensibility and robustness.

- The detectability is the ability of the diagnostic system to detect the presence of a failure in the process. It is closely related to the notion of fault indicators (residuals): the residual generator must, somehow, be sensitive to the failure to be detected. It will actually set a compromise between the false alarm rate and the non-detection.
- The isolability is the ability of the diagnostic system to directly trace back the origin of the fault. Failure often causes a sequence of cascading alarms and it can be difficult to trace the original faulty component. The degree of fault isolation is related to the structure of the

generated residuals and to the detection technique.

- The sensitivity is characterized by the ability of the FDI system to detect faults of a certain amplitude. It depends not only on the structure of the residuals but also of the relationship between the measuring noise and the fault.
- The robustness characterizes the ability of the FDI system to detect faults regardless of modeling errors (sensitivity to residual faults and insensitivity to disturbances).

Most studies about the development of new fault detection and identification devices have concentrated on the generation of residuals based on analytical redundancy which allow probabilistic tests to decide about the presence of a fault or not [Edwards et al., 2010]. Figure 3.4 displays the data processing sequence in a model based FDI technique.

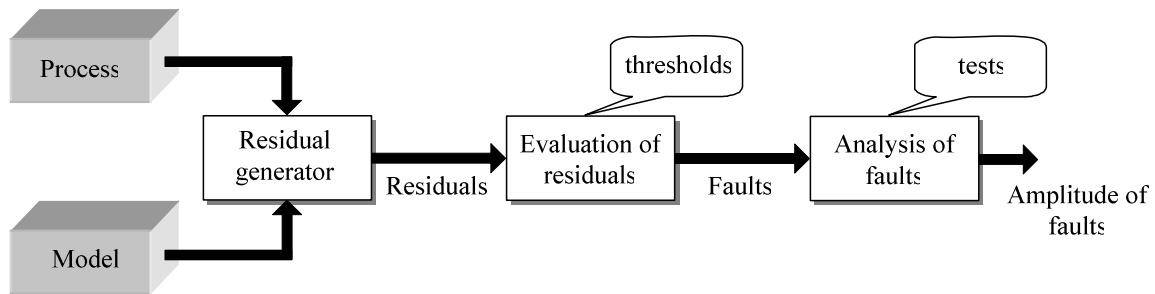


Figure 3.4 FDI based on residuals analysis

To have an overview of FDI techniques including advanced methods based on mathematical properties of flight dynamics models (differential flatness [Michel Fliess et al., 1995; W Lu et al., 2005]) which allows to perform FDI on highly nonlinear systems, see [N. Zhang, 2010]. Figure 3.5 displays the general architecture of a FDI system for a physical process.

Going back to transportation aircraft, multiple air and inertia data channels (ADIRUs) are used to provide online redundant data for the flight control system. Voting schemes ensure that the transmitted signal is correct while faulty sensors can be detected [Goupil, 2011]. Fault detection is mainly performed by cross checks, consistency tests, voting mechanisms and built-in test

techniques of varying sophistication [Edwards et al., 2010]. For example, threshold logics are often used for actuator and sensor monitoring. If a measurement signal exceeds a given limit threshold, then the failure of this measurement unit is declared. Besides these classical fault detection techniques, modern fault detection and identification approaches start to be used onboard aircraft. For example, analytical redundancy techniques are already used on A340 and A380, though it is not used widely.

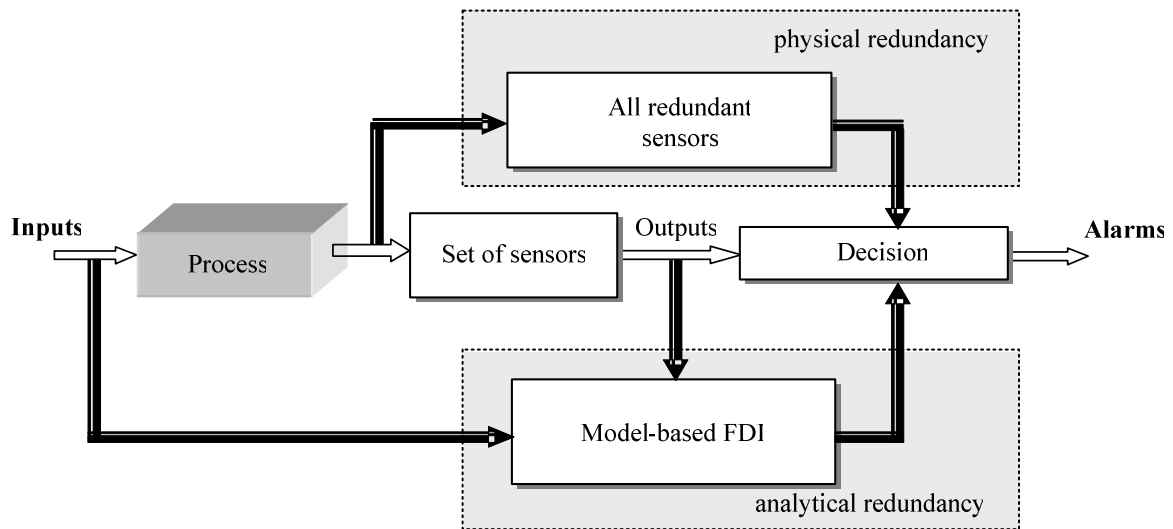


Figure 3.5 General architecture of a FDI system

3.4 Fault Tolerance Actuation Based on Redundancy

As seen before, at the stage of flight control system design, the most basic way to achieve fault tolerance is through physical redundancy in the control channels including actuators, sensors, computers and power supplies.

When flight dynamics are linearized around an equilibrium point, a linear state space representation can be found as discussed in Section 2.3.3 and the effectiveness of the inputs is expressed by the control matrix whose elements are stability derivatives associated with the inputs or equivalent control surfaces. These stability derivatives play no part in governing the stability

properties of an uncontrolled aircraft, but they are important for achieving stability augmentation for a controlled aircraft. Therefore, an actuator failure will change flight qualities, maneuverability, flight domain, safety operation range and finally may threat the survival of aircraft. Then, fault tolerance is especially important for flight control channels. To satisfy the stringent airworthiness and safety requirements, physical redundancy is often introduced in flight control channels, including actuators.

Different concepts related to redundancy can be introduced to characterize the effects of redundancy. For example, the longitudinal or lateral linearized flight dynamics around a trim condition can be described by a multi-input linear system such as:

$$\begin{aligned}\dot{\underline{x}} &= A\underline{x} + B\underline{u} \\ \underline{y} &= C\underline{x}\end{aligned}\quad (3.1)$$

here vectors $\underline{x} \in R^n$, $\underline{y} \in R^p$ are respectively the system state and the output. The state matrix, $A \in R^{n \times n}$ and the output matrices, $C \in R^{p \times n}$. The control matrix $B \in R^{n \times m}$, to see clearly the contribution from different actuators, it can be rewritten with its columns $B = [\underline{b}_1 \quad \underline{b}_2 \quad \cdots \quad \underline{b}_m]$ with $\underline{b}_i \in R^n$, $1 \leq i \leq m$.

3.4.1 Definitions

Definition: Degree of multiplicity of actuators

The components of the input vector are associated to redundant actuators (surfaces) such as:

$$u_i = \sum_{j \in a_i} \mu_j^i \delta_j^i \quad \text{with} \quad \sum_{j \in a_i} \mu_j^i = 1, \quad i \in \{1, \dots, m\} \quad (3.2)$$

Here a_i is the set of actuators contributing to input i , while δ_j^i is the deflection of the j^{th} actuator of input i and μ_j^i is its relative effectiveness.

Then, $m_i = |a_i|$ is the *degree of multiplicity of actuators* for input i , where $|\cdot|$ is the dimension of a vector.

For example, on a transportation aircraft, ailerons, spoilers, rudders, all of them have respectively a redundant system. On the contrary, the deflections of these three surfaces contribute to the generation of roll moment, so the degree of multiplicity of actuators for the input of roll moment is to sum up the numbers of redundant actuators for these three surfaces.

In general each input has a major effect on some state variable, but the couplings between the state variables make that the state variables are indirectly controllable from other inputs. This leads to the concept of input redundancy.

Definition: full input redundancy

The system (3.1) is said to have *full input redundancy*, if the pair (A, \underline{b}_i) is completely controllable, $\forall i (1 \leq i \leq m)$

Definition: total input redundancy

The system (3.1) is said to have *total input redundancy*, if the pair (A, B^i) where B^i is the B matrix without its i^{th} column, is completely controllable, $\forall i (1 \leq i \leq m)$

Definition: Fault tolerance to a failure

Let the occurrence of a failure k in a subsystem of the control channel of a process affects the actuators so that the set of effective actuators of input i is changed from a_i to d_i^k with $d_i^k \subseteq a_i$, $i \in \{1, \dots, m\}$. Then if the system:

$$\dot{\underline{x}} = A \underline{x} + \sum_{i, d_i^k \neq \emptyset} \underline{b}_i u_i \quad (3.3)$$

is completely controllable, the original process is said *fault tolerant to failure k* .

3.4.2 Limitations

Considering aircraft itself is a complex nonlinear system, the above approach and definitions have some important limitations which should be noticed:

- First of all, flight dynamics are nonlinear and this feature appears any time the aircraft is performing a transition maneuver to follow its flight plan. These transient situations are in general characterized by the activation of the secondary actuators and the adoption of new thrust settings for the engines while they are not taken into account in the above trim based approach.
- Observe that controllability is an algebraic concept providing a global property for an abstract linear dynamical system while for nonlinear dynamical systems, controllability is a local concept.
- Another limitation of this approach is that the controllability criterion does not take into account time scales and do not distinguish between slow and fast actuation.
- Finally, actuator limitation (position and rate limitations) are not taken into account when considering controllability.

All these limitations make that the above definitions should remain local concepts when they are applied near trim conditions.

3.5 Fault Tolerant FBW aircraft

In this paragraph are described the main characteristic of redundant FBW flight control channels for a modern transportation aircraft.

3.5.1 General features of FBW flight control channels

The longitudinal maneuvers are mainly achieved by controlling the deflections of elevators while new longitudinal trim conditions are achieved automatically by THS slow positioning. Different hydraulic servo-controls drive the elevator surfaces. Each servo-control has three operating modes:

- Active: the servo is electrically controlled,
- Damped: the servo operates as a hydraulic damper on the surface,

- Centered: the servo is maintained hydraulically at neutral position.

In normal operation a servo is in active mode while the others are in damped mode. Some large maneuvers can cause the activation of damped actuators. In case of failure of the active servo-control, a damped servo-control becomes active, and the failed servo adopts the centered mode. If all the servo-controls fail, they adopt the centered mode. In case of total failure of the actuators of an elevator surface, the deflection of the remaining elevator surface is limited to avoid excessive unbalanced loads on the THS or to tail of the aircraft. When the elevator control channel fails, the pilots can still control manually through the trim wheel the positioning of the THS, providing a slow maneuvering capability. In normal operation the elevator and THS are controlled by a FBW computer and the left and right elevators are actuated respectively by two different hydraulic systems while the THS hydraulic motors are actuated by an electric motor. In case of failure of the FBW computer, of one of the two hydraulic servo-controls, the elevator control is automatically realized with a second FBW computer and a third hydraulic servo-control is activated while the THS hydraulic motors are now actuated by a second electric motor. In the case of failure of the second FBW computer, a configuration computer ensures elevator control. A third electrical motor is available to actuate the THS hydraulic motors. The wheel control of the THS can be used at any time provided that one of its hydraulic motors is operative, it overrides its FBW computer control.

Lateral maneuvers on large transportation aircraft are mainly achieved by controlling multiple surface ailerons and rudders while secondary flight control surfaces such as spoilers and engines can be used to produce additional yaw and roll torques. So when an elementary lateral surface is no more controllable, the aircraft can still perform lateral maneuvers by using other control surfaces.

The roll actuation is provided by one or two ailerons and different spoilers on each wing. In normal operation, the ailerons are controlled by a dedicated FBW computer. In case of failure of that computer, the aileron control is automatically transferred to a second dedicated FBW computer. Each aileron is actuated by different hydraulic servo-controls where only one is active, the other being in damped mode. In case of failure of the two dedicated FBW computers, all ailerons servo-controls enter the damped mode. The control of the different spoilers is realized by different

configuration computers so that under their partial failure, some spoilers remain operative. In the case of a failure of a configuration computer, its controlled spoilers retract automatically.

The rudder is actuated by different independent hydraulic actuators working in parallel. These actuators are either electrically controlled by the FBW computers under different modes (turn coordination, flight augmentation) or by a mechanical wired rudder from the pilots' pedals.

3.5.2 The Case of Airbus A330/A340

Various control surfaces of an A330/A340 aircraft have been shown in Figure 1.1. Here, Figure 3.6 displays logically the control surfaces redundancies for the flight control channels of the A330/A340 aircraft:

- Aileron redundancy with a pair of inboard and outboard ailerons.
- Spoilers redundancy with six pairs of them.
- Elevator redundancy with two of them.

Figure 3.6 displays also the distribution of hydraulic power from three independent hydraulic systems (Y, B, G) to the different elementary control surfaces. It appears that only a complete failure of the three hydraulic power systems will imply a loss of efficient control along the three body axis, impairing from the remaining mechanical backups (wheel controlled THS and pedals controlled rudder) to maintain flight augmentation and to perform fast maneuvers.

Also on Figure 3.6 is given the assignment sequence of FBW computers (PRIMARY and SECONDARY computers) to the different control surface according to their fail state.

Figure 3.7 displays also the distribution of hydraulic power in A330/A340 to different control surfaces as well as to perform different functions (pitch trim, yaw damping and ground braking).

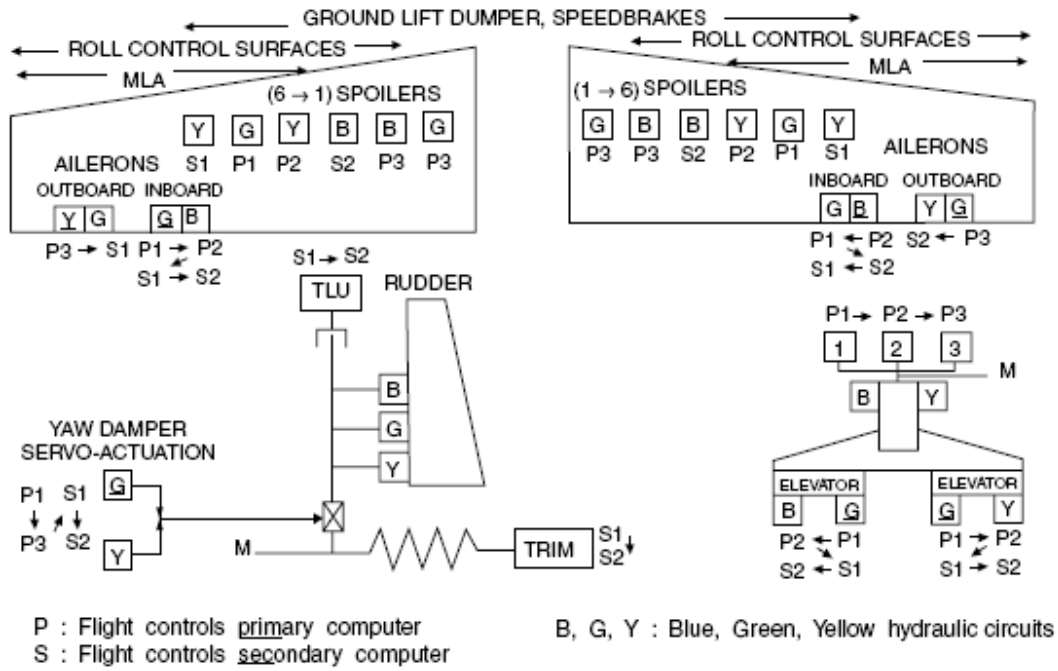


Figure 3.6 Redundant control surfaces and actuators for A330/A340 (source: Airbus)

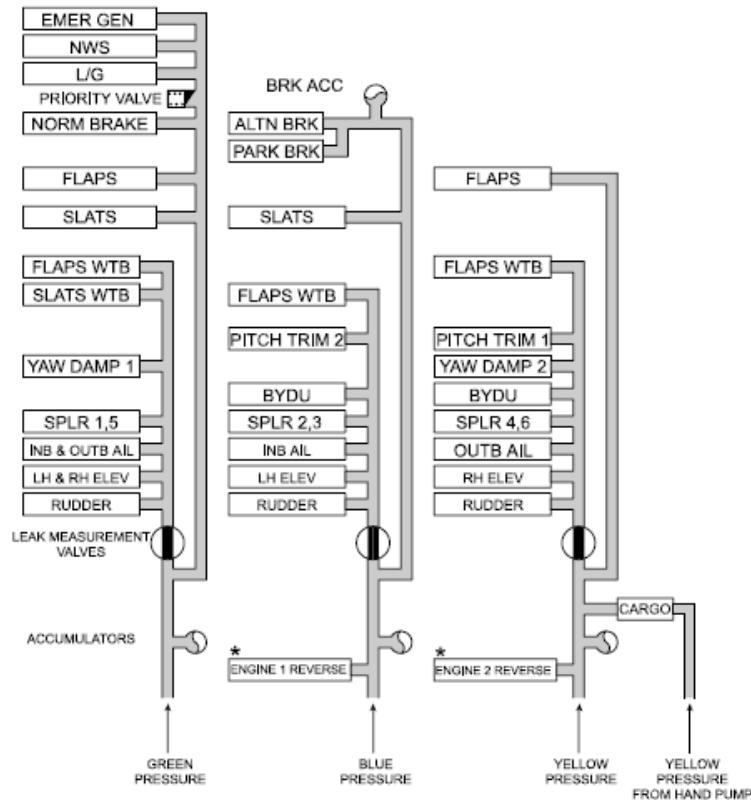


Figure 3.7 A330/A340 hydraulic power distribution and coverage (source: Airbus)

It appears that the automatic control of the rudder deflection is lost only when all three hydraulic power systems are out.

It appears that Airbus has adopted a two levels strategy for the reconfiguration of the flight control system [Goupil, 2011]:

The first level takes care of the system reconfiguration by replacing active faulty components (control surfaces, hydraulic power supply systems and FBW computers) by fault free ones. For example, considering in Figure 3. 6 the reconfiguration of the roll control channel, the actuator of the inboard left wing aileron is driven by the green hydraulic circuit is in active mode and is controlled by computer P1. The other actuator is driven by the blue hydraulic circuit which follows the movement of the active actuator. This second actuator is in passive mode and is controlled by computer P2. If the active actuator is detected failed, then it changes to passive state while the previously passive control surface becomes active. Also a switch of function is performed between the original active computer P1 and the stand-by computer P2.

The second level of configuration is relative to the flight control mode reconfiguration. According to the importance of the flight control or data channel failure case, the flight control mode may change from the “normal law” mode to the “alternate law” mode or to the “direct law” mode. In the first case the aircraft operates in the normal flight envelope (in yellow in Figure 3.8) with the availability of all the automatic flight protections which provide a full flight protection. In the case of the “alternate law” mode, the level of automatic flight protections is reduced and the pilot can even engage without protection the aircraft into the peripheral flight envelope shown in orange in Figure 3.8. In the case of the “direct law” mode the aircraft will not be impeded from leaving the permissible flight envelope of the aircraft since no automatic flight protection is active.

These **two levels** of reconfiguration contribute to the fault tolerance capability of the flight control system.

There are, however, catastrophic events that can disrupt entire systems so that the inherent reconfiguration strategies are no longer applicable but manual reconfiguration or other control schemes may work well. For example, in the case of mentioned accident, Delta Flight 1080 on

April 12, 1977, the elevator became jammed and the pilot had been given no indication of this malfunction. Fortunately, the pilot successfully reconfigured the available control elements and landed the aircraft safely, based on his experience and knowledge about the actuation redundancy on the aircraft. On the other hand, only with pilot skill is not enough. In another accident involving American Airlines Flight 191, DC-10, crash in Chicago (May 25, 1979), only 15 s left for the pilot to react before the aircraft crashed [R. J. Patton, 1997]. Studies show that with a fault tolerant control system, the accident of Flight 191 and other several accidents could have been avoided. Flight 191 could be avoided if restructurable control was used [Y. Zhang & Jiang, 2008]. Maciejowski argued that the fatal crash of El Al Flight 1862 with structural damage and aerodynamic change might have been avoided by using fault-tolerant control [Maciejowski & Jones, 2003]. All of these show that there is a need to develop a fault tolerant flight control system which has the ability to reconfigure and/or restructure the control law automatically in case of control and/or sensor element failures.

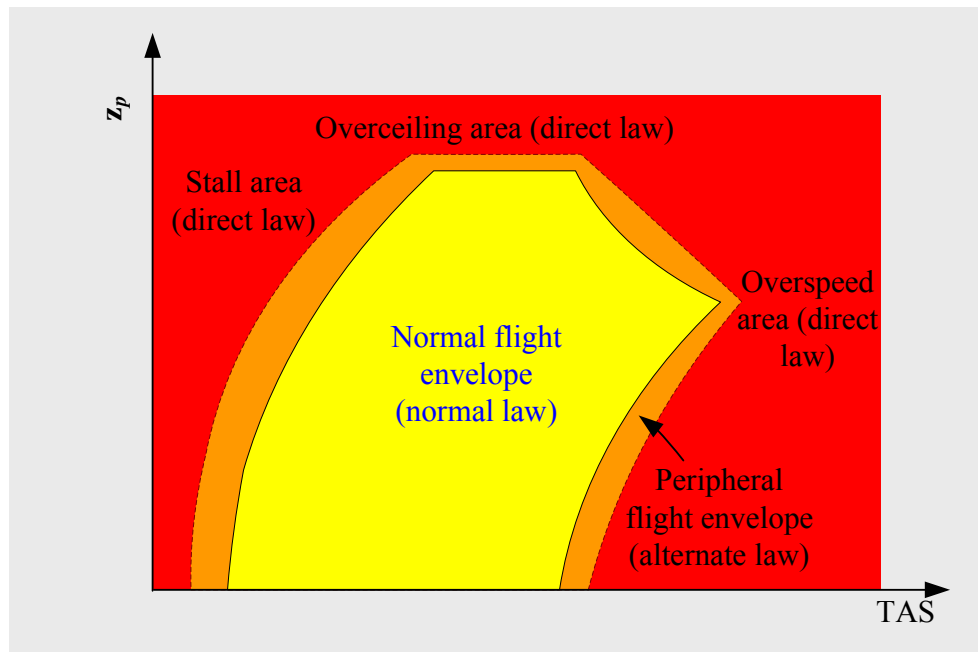


Figure 3.8 Flight domain levels of protection

3.6 Fault Tolerant Control

As stated above, to meet the stringent requirement of airworthiness regulations, flight control

systems are extremely redundant, resulting in safe fault tolerant systems. However, increased physical redundancy not only supposes higher production and maintenance costs, but also is the cause of larger weight. Moreover, even with this redundancy level it seems that the performance of conventional control techniques is hardly able to tackle efficiently unexpected or novel failure situations. So, new control laws are being developed to maintain system performance and stability in the event of failure. Fault tolerant control laws are expected to help to reduce the redundancy degree of the control system while improving its safety level. It has been argued that several air transportation accidents could have been avoided if fault tolerant control techniques have been in use [Alwi, 2008].

A fault tolerant control system has the ability to deal with its faults automatically so that it is able to achieve its control objectives.

In general, the fault tolerant control system must guarantee at least stability and/or acceptable degraded performance in the presence of major failures (failures of sensors and actuators, physical changes of the controlled process).

Over the last three decades, the growing demand for safety, reliability, maintainability, and survivability in safety-critical systems has motivated significant research in fault tolerant control [Jiang & Yu, 2012]. Annex B presents a survey about fault tolerant control-FTC. FTC approaches can be divided into passive and active FTC approaches. Both classes of FTC approaches integrate the FDI capability while the active FTC techniques include also fault accommodation and control system reconfiguration capabilities [Huzmezan & Maciejowski, 1997; Marcos et al., 2003; R. Patton, 1997; Y. Zhang & Jiang, 2008]. The main ideas related to the design and development of a reconfigurable control system were initially proposed by Blanke [Z. Yang & Blanke, 2000a, 2000b] and Patton [Patton et al., 2000]. An efficient implementation of a reconfigurable fault tolerant control system will depend on the ability of the FDI subsystem to identify the fault timely and accurately [Patton et al., 2000; Polycarpou & Vemuri, 1995; Q. Zhang, 1999; Q. Zhang et al., 1997].

Figure 3.9 displays the general structure of a fault tolerant flight control system implementing automatic reconfiguration.

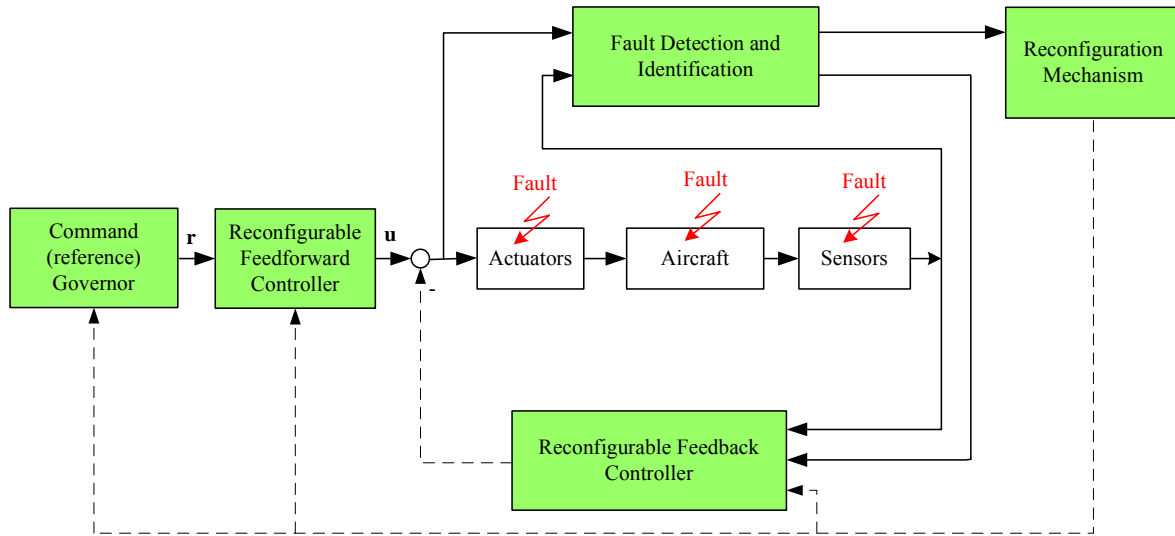
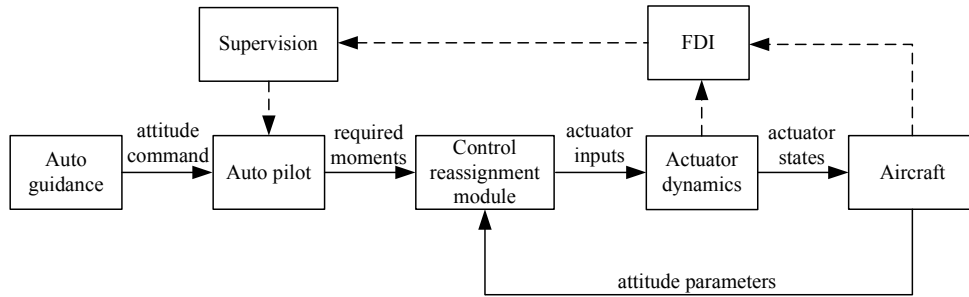


Figure 3.9 General scheme of a fault tolerant control system

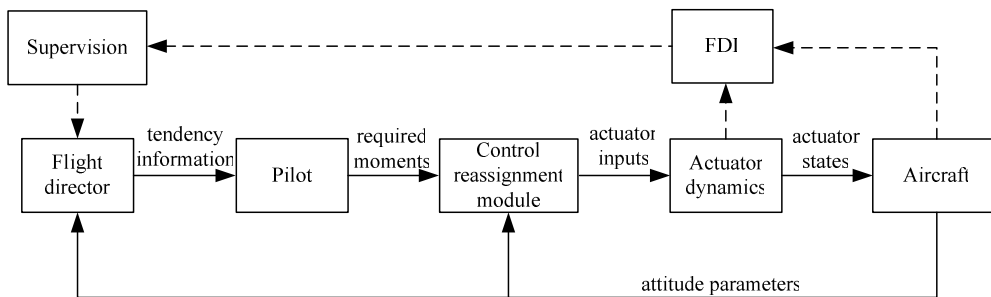
It consists of a fault detection and identification module, a reconfigurable control module designed to activate fault free redundant components and a flight control law reconfiguration module to adapt the control law to the new control situation (active actuators and sensors, operational state of the controlled process). There, the solid lines represent the main signals (control, instructions, estimates, measures) while the dotted lines represent adaptation (adjusting, programming, reconfiguration or restructuring).

It appears opportune to include in a fault tolerant control structure, next to an FDI module, a supervision module associated to the knowledge base and whose main function is to decide if the fault situation can be managed as a fail-operational or a fail-passive situation. In the first case, through an actuator reassignment module, see [Zhong & Mora-Camino, 2012, 2013; Zhong et al., 2011], the current flight condition (manual or auto flight modes) at the occurrence of the fault will be maintained as well as the nominal handling performances of the aircraft, since the remaining active actuators are found able to produce timely the required moments to perform nominal maneuvers [Zhong & Mora-Camino, 2014]. Figure 3.10 (a) displays the fail-operational case with a running autopilot. Otherwise, Figure 3.10 (b), to insure a fail-passive situation, flight control will return to manual mode through the actuator reassignment module and with the help of a flight director. The flight director modes which provide tendency information to the pilot will take into account the identified downgraded handling capability of the aircraft under the

current actuator failure situation.



(a) fail-operational mode



(b) fail-passive mode

Figure 3.10 Possible fail modes for a fault tolerant control structure

3.7 Conclusion

From the above analysis, it appears that regards the flight control field, despite many academic publications, many numerical simulation results and some tests performed on actual prototypes, the application of fault tolerant control is still very limited in this area. Thus physical redundancy techniques continue to play a critical role in ensuring flight safety. This has led to the introduction of different concepts to assess the consequences of physical redundancy, such as full input redundancy and total input redundancy while a definition of fault tolerance to a failure for a controlled system is proposed. The two level strategy adopted by aircraft manufacturers lead, according to the importance of the failed elements in the flight control channels, to suppress

function such as automatic protections for the flight domain excursions. A way to limit this degradation of these functions is to make the best use of the remaining effective actuators. This issue is discussed in the next chapter where the actuators reassignment problem is introduced and analyzed.

CHAPTER 4

FORMULATION OF THE ACTUATOR

ASSIGNMENT AND REASSIGNMENT

PROBLEM

4.1 Introduction

The aim of this chapter is to formulate the actuator reassignment problem (ARP) which should in general be solved in case of a fast actuator failure situation. Since the effectiveness of fast actuators is closely related with the current aircraft aerodynamical configuration, a parameterized state representation of the flight dynamics is proposed. Then the main limitations of the fast and slow actuators are considered while position and rate constraints are introduced. To better formulate ARP problem, the notion of virtual inputs whose values are related to the intended maneuver by a chosen control law, are introduced. Then, taking into account the multiplicity of contributors, among the actuators, to the virtual inputs, the actuator reassignment problem is formulated as a linear quadratic (LQ) program. The existence and uniqueness of optimal solution as well as of approximate solution for this problem is discussed.

4.2 General Representation of Actuator Redundant Systems

Some dynamical systems, especially safety-critical systems, adopt in their design a multiplicity of actuators, which contribute in a supplementary or a complementary way to the realization of the necessary control functions.

4.2.1 Representation of the dynamics and constraints

To express such problem mathematically, a rather general state space representation, termed *parameter affine*, is adopted to describe the dynamics of smooth nonlinear systems:

$$\dot{\underline{x}} = f(\underline{x}, \underline{c}) + g(\underline{x}, \underline{c}) \cdot \underline{u} \quad \text{with} \quad \underline{x} \in R^n, \underline{u} \in R^m \quad (4.1)$$

$$\dot{\underline{c}} \approx \underline{0} \quad \text{with} \quad \underline{c} \in R^s \quad (4.2)$$

$$\text{and } \underline{y} = h(\underline{x}) \quad \text{with} \quad \underline{y} \in R^p \quad (4.3)$$

where $f(\underline{x})$, $g(\underline{x})$ and $h(\underline{x})$ are smooth vector fields of \underline{x} .

Here \underline{x} is the state vector representing the dynamics of the system, \underline{c} is a configuration parameter vector, \underline{u} are fast varying controls and \underline{y} is the chosen output of the system related with the adopted control objectives with respect to the evolution of this system.

Relation (4.1) which represents through a general nonlinear state equation the dynamics of the considered system remains representative if the state \underline{x} remains in a nominal domain X .

Relation (4.2) expresses either that the values of the configuration parameters \underline{c} can be changed very slowly or that they can take constant values chosen among a discrete set. Then they satisfy either the following constraints:

$$\tau_j \dot{c}_j + c_j = c_j^e \quad \text{with } j \in S_c \subset N \quad (4.4)$$

$$\text{or } c_j^{\min}(\underline{x}) \leq c_j \leq c_j^{\max}(\underline{x}) \quad \text{and } |\dot{c}_j| \leq \dot{c}_j^{\max} \quad j \in S_l \subset N \quad (4.5)$$

$$\text{or } c_j \in C_j \quad j \in S_D \subset N \quad (4.6)$$

$$\text{with } S_c \oplus S_l \oplus S_D = \{1, \dots, s\} \quad (4.7)$$

In relation (4.4), it is assumed that some configuration parameters (set S_c) modify their values according to a first order dynamics where τ_j is a long time constant and c_j^e is the current reference value for c_j which should also satisfy the position constraint of (4.5). Relation (4.5) corresponds to the configuration parameters (set S_l) which can be changed arbitrarily while satisfying extreme position and rate constraints. Relation (4.7) considers the configuration parameters (set S_D) whose values belong to a discrete set and whose shift from one value to another is considered instantaneous.

The fast inputs $u_j, j = 1$ to m , are also submitted to position and rate limits or constraints. The limits are the consequence of the adopted technology (hydro/mechanical/electrical) for their realizations, while the constraints can be related with structural limits of their support. These constraints may be expressed in general as:

$$u_j^{\min}(\underline{x}) \leq u_j \leq u_j^{\max}(\underline{x}) \quad \text{and} \quad \dot{u}_j^{\min}(\underline{x}) \leq \dot{u}_j \leq \dot{u}_j^{\max}(\underline{x}) \quad j = 1 \text{ to } m \quad (4.8)$$

It is also supposed that at fault free trim conditions these fast inputs are equal to zero, so that trim conditions are then written:

$$f(\underline{x}, \underline{c}^e) = \underline{0} \quad \text{with} \quad \underline{c}_{\min}(\underline{x}) \leq \underline{c}^e \leq \underline{c}_{\max}(\underline{x}) \quad (4.9)$$

4.2.2 Illustration with a transportation aircraft

When considering the problem of vertical guidance of an aircraft, the state vector can be composed of the pitch rate q , the pitch-angle θ , the normal load factor n_z , the angle of attack α , the altitude z , the longitudinal airspeed u , as well as the total thrust T . There the output vector may be composed of the airspeed and the altitude. The nominal domain X here is the nominal flight envelope of the aircraft with its high and low speed limitations, its high (ceiling) and low (ground) altitudes, as well as its load factor, angle of attack, pitch angle and pitch rate limitations.

Here the configuration vector is composed of the position of the trimmable horizontal stabilizer (THS) ($\in S_I$), the position of the flaps ($\in S_I$) and of the speed brakes ($\in S_D$) and the reference value of the total thrust ($\in S_C$). An example of constraints (4.5) is the limitations of flap deflection with airspeed.

In this case, the fast inputs are either the angular deflection or the rate of deflection of elevator surfaces and the variation of the thrust around its reference value.

Figure 4.1 shows a lateral example of fast input position constraint is the maximum deflection accepted Airbus for the rudder of A320 aircraft. Figure 4.2 shows an example of configuration parameters.

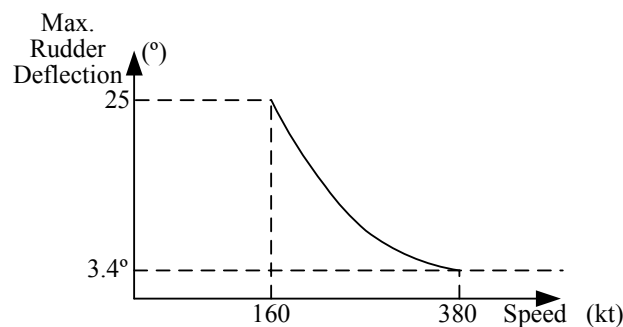


Figure 4.1 Maximum deflection of rudder versus airspeed A320

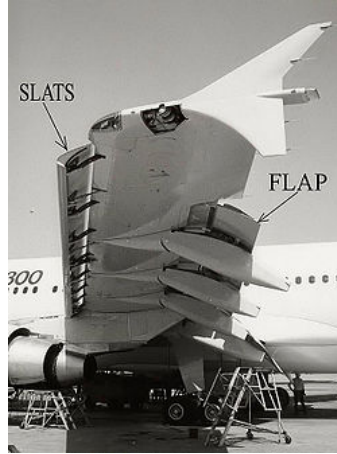


Figure 4.2 Example of configuration parameters on a wing

4.3 Output Based State Representation and Virtual Inputs

When considering trajectory tracking problems, an output based state representation can be adopted:

$$\underline{X} = \left(y_1 \quad \dot{y}_1 \quad \cdots \quad y_1^{(r_1-1)} \quad \cdots \quad y_p \quad \dot{y}_p \quad \cdots \quad y_p^{(r_p-1)} \quad z_1 \quad \cdots \quad z_q \right)' \quad \text{with} \quad \sum_{j=1}^p r_j + q = n \quad (4.10)$$

where r_j is the relative degree of output j [Isidori, 1983; Slotine & Li, 1991] and q is the dimension of the inner dynamics of the output based state representation given by:

$$\dot{\underline{X}} = F(\underline{X}, \underline{c}) + G(\underline{X}, \underline{c})\underline{u} \quad (4.11)$$

where $G \in R^{n \times m}$, is a matrix with p non zero rows at positions:

$$p_1 = r_1, \cdots, p_j = \sum_{k=1}^j r_k, \cdots, p_p = \sum_{k=1}^p r_k \quad (4.12)$$

Let P be the set of these rows, $P = \{p_1, p_2, \cdots, p_p\}$, then this state representation can be rewritten:

$$\dot{\underline{X}} = F(\underline{X}, \underline{c}) + H \underline{v} \quad \text{with} \quad \underline{v} \in R^p \quad (4.13)$$

where

$$H \in R^{n \times p} \quad \text{and} \quad h_{ij} = 0 \text{ if } i \notin P \text{ or } j \neq i, \text{ otherwise, } h_{p_k p_k} = 1 \text{ for } k = 1 \text{ to } p \quad (4.14)$$

Then it is interesting to define the p virtual inputs v_j , $j=1$ to p , associated to the chosen p

independent outputs.

Definition: The p virtual inputs associated with the chosen output in (4.3) are given by:

$$v_i = \sum_{j=1}^m G_{p,j}(\underline{X}, \underline{c}) \cdot u_j \quad i = 1 \text{ to } p \quad (4.15)$$

or

$$\underline{v} = \tilde{G}(\underline{X}, \underline{c}) \cdot \underline{u} \quad (4.16)$$

Then the matrix $\tilde{G} \in R^{p \times m}$, will be called the *mixing matrix*.

When considering evolutions around a trim situation characterized by:

$$F(\underline{X}, \underline{c}) = \underline{0} \quad \text{with} \quad \underline{c}_{\min} \leq \underline{c} \leq \underline{c}_{\max} \quad (4.17)$$

The linearized dynamics are such as:

$$\Delta \dot{\underline{X}} = \frac{\partial F}{\partial \underline{X}}(\underline{X}_0, \underline{c}) \cdot \Delta \underline{X} + H \tilde{G}(\underline{X}_0, \underline{c}) \cdot \underline{u} \quad (4.18)$$

$$\text{or} \quad \Delta \dot{\underline{X}} = \frac{\partial F}{\partial \underline{X}}(\underline{X}_0, \underline{c}) \cdot \Delta \underline{X} + H \cdot \underline{v} \quad (4.19)$$

Then, from relation (4.18) it will be possible to check the local controllability and actuator fault tolerance properties of the dynamics (see Section 3.4.1) with respect to the virtual inputs, while relation (4.16) will allow to do the same with respect to each elementary input. It is then easy to check that the controllability properties as well as the tolerance to actuator faults will be the same if and only if matrix $\tilde{G}(\underline{X}_0, \underline{c})$ of $R^{p \times m}$ is full rank.

4.4 A Two stages Control Approach

In general, to solve a control problem, either in an offline context to find reference trajectories or in an online context to achieve trajectory tracking or regulation, many different control techniques are available to design an unconstrained control law which computes the ideal values for the inputs to achieve the control objective.

When actuator redundancy is present, the complete solution of the control problem includes the further assignment of the control effects of each virtual input to the actuators. When some of

these actuators are declared faulty, a reassignment of the necessary control effects to the remaining fault free actuators becomes necessary to maintain the control function.

A general scheme of the control system resulting from this two stages approach is represented in Figure 4.3.

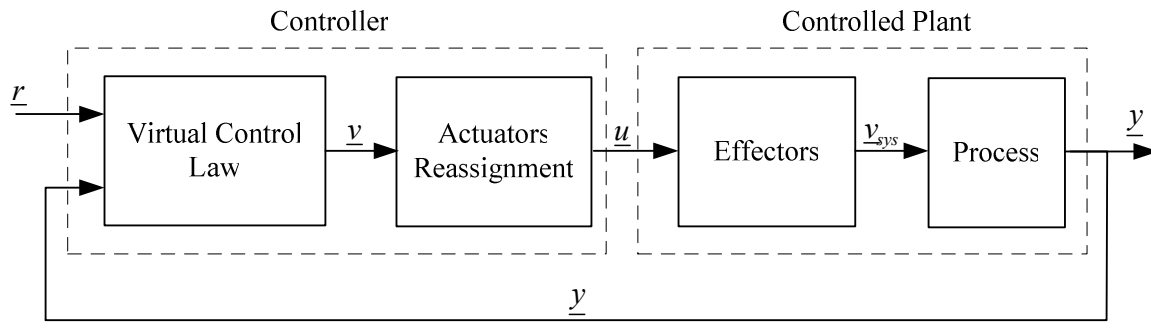


Figure 4.3 General scheme of a control structure with actuator assignment for redundant system control

The main benefits resulting from splitting the control signal definition problem in two stages are:

- When solving the control problem with virtual inputs, it is not necessary to take into account the physical constraints attached to each actuator. This is fortunate since few control techniques are able to take explicitly into account input constraints.
- The actuator constraints as well as other operational limitations can be taken more easily into account at the assignment stage.
- Additional objectives can be taken into account at the assignment stage. Examples of additional objectives are:
 - In the field of robot control are minimum-effort motion planning as, minimum-energy / torque-optimization, drift-free motion planning [Y. Zhang, 2005].
 - In the field of ship control: minimizing the total necessary thrust [Tor A. Johansen & Fossen, 2013].
 - In the field of flight control: minimum wing loading, minimum control surface deflection, minimum radar signature, minimum drag, maximum lift, rapid

reconfiguration for fault tolerance [Buffington, 1999], respecting a priority between actuators.

4.5 The Actuator Assignment Problem (AAP)

Most of existing methods for actuators assignment propose an online solution to equation (4.16) while taking into account the actuators constraints and limitations. In general the controller works with sampled signals at some short period Δt . Then the online actuator assignment problem consists in mathematical terms in finding a solution \underline{u}_t^* in R^m to the constrained set of equations:

$$\underline{v}_t = \tilde{G}(\underline{X}_t, \underline{c}_t) \cdot \underline{u}_t \quad (4.20)$$

$$\text{with } \max \left\{ \underline{u}^{\min}(\underline{X}_t), \underline{u}_{t-1}^* + \underline{\dot{u}}^{\min}(\underline{X}_t) \cdot \Delta t \right\} \leq \underline{u}_t \leq \min \left\{ \underline{u}^{\max}(\underline{X}_t), \underline{u}_{t-1}^* + \underline{\dot{u}}^{\max}(\underline{X}_t) \cdot \Delta t \right\} \quad (4.21)$$

This actuator assignment problem can be rewritten more shortly as:

$$\text{Find } \underline{u}_t \in R^p: \quad \underline{v}_t = G_t \cdot \underline{u}_t \quad (4.22)$$

$$\text{with } L_t \underline{u}_t \leq \underline{l}_t \quad (4.23)$$

$$\text{where } G_t \in R^{p \times m}, L_t \in R^{2m \times m} \text{ and } \underline{l}_t \in R^{2m} \quad (4.24)$$

Since G_t is supposed full rank with $p < m$, equation (4.22) has an infinity of solutions Σ_t . Points in R^m satisfying constraints (4.23) constitute a feasible convex region Ω_t . Then four cases can be considered:

- The interior of $\Sigma_t \cap \Omega_t$ is not empty and there is multiplicity of solutions.
- The set $\Sigma_t \cap \Omega_t$ is empty but there is multiplicity of solutions on its border.
- The set $\Sigma_t \cap \Omega_t$ is reduced to a unique point and there is a unique solution.
- The set $\Sigma_t \cap \Omega_t$ is empty and there is not even a feasible solution.

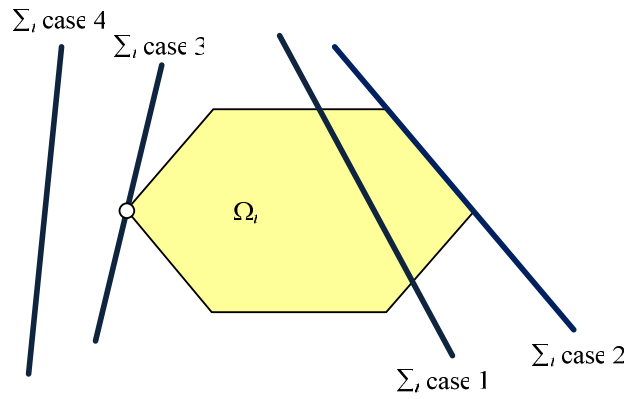


Figure 4.4 A simple illustration of the four different assignment cases

In the first two cases, only one solution must be selected. One simple way to select a solution is to consider in $\Sigma_t \cap \Omega_t$ the solution which is closest to the previous solution (see Figure 4.5).

Then, \underline{u}_t^* is solution of:

$$\underline{u}_t^* = \arg \min \left\{ \|\underline{u}_t - \underline{u}_{t-1}^*\|_m^2, \underline{u}_t \in \Sigma_t \cap \Omega_t \right\} \quad (4.25)$$

where $\|\cdot\|_m$ is an Euclidian distance over R^m .

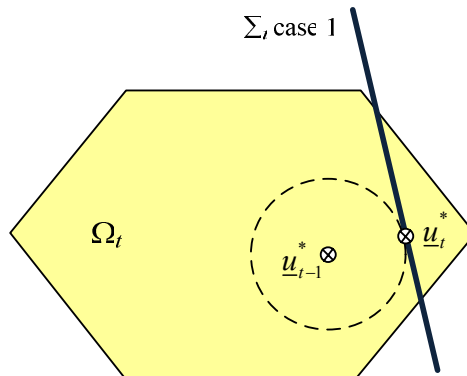


Figure 4.5 Selection of the closest feasible solution

Another approach could be to adopt an auxiliary criterion and search for an optimal solution

over the set $\Sigma_t \cap \Omega_t$.

In the case in which $\Sigma_t \cap \Omega_t$ is empty, that means that the control objective is not reachable at time t . Two cases can be considered here:

- In the case in which the configuration parameters can be changed, modify them such as $\Sigma_t' \cap \Omega_t' \neq \emptyset$ (see Figure 4.6) and solve the problem according to the previous steps.

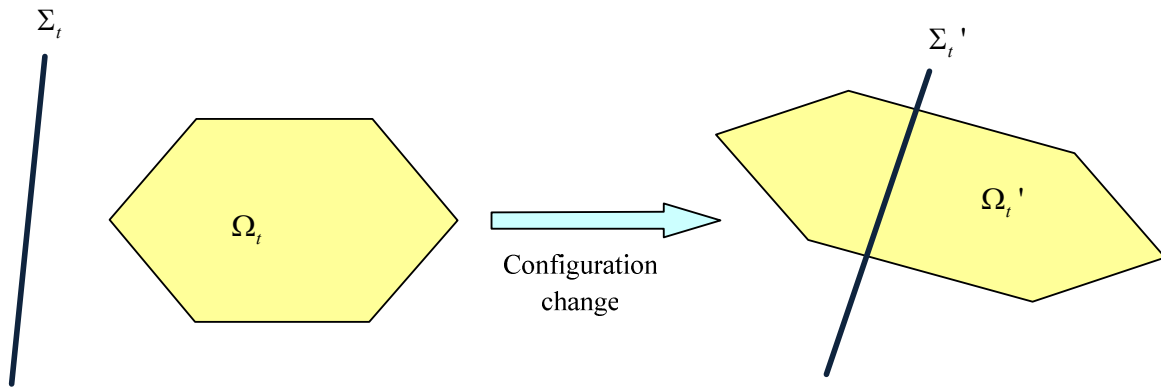


Figure 4.6 Adaptation of configuration to control objectives

- In the case in which the configuration has not to be changed, two approaches can be considered:

- ◆ Either choose \underline{u}_t^* such as:

$$\underline{u}_t^* = \arg \min \left\{ \|\underline{v}_t - G_t \underline{u}_t\|_m^2, \underline{u}_t \in \Omega_t \right\} \quad (4.26)$$

which is a small scale linear quadratic (LQ) optimization problem, and in general is easy to solve.

- ◆ or choose \underline{u}_t^* as the first solution element of the following linear quadratic programming problem over a time span $K \Delta t$:

$$\min_{\underline{u}_{t+k-1}} \sum_{k=1}^K \|\underline{v}_{t+k-1} - G_{t+k-1} \underline{u}_{t+k-1}\|_m^2 \quad \text{with} \quad \underline{u}_{t+k-1} \in \Omega_{t+k-1}, \quad k=1, \dots, K \quad (4.27)$$

when \underline{v}_{t+k-1} , G_{t+k-1} and Ω_{t+k-1} , $k=1, \dots, K$, can be computed or estimated in advance. In that case, the instant satisfaction of the control objective is shifted to an overall satisfaction over the period from t to $t+(K-1)\Delta t$ and the resulting LQ problem is no more so small.

When considering other types of constraints such as structural constraints, the feasible set Ω_t must be redefined by using these constraints.

4.6 The Actuator Reassignment Problem (ARP)

Here is first considered the case in which actuator faults produce a total loss of effectiveness (stuck, runaway, float faults).

Let the occurrence of fault k in a control channel lead to a reduced fault free set of actuators d^k of dimension D_k . Let h^k be the set of runaway or stuck fault actuators resulting from this fault (float fault does not impact on aerodynamics, so it is not considered here). Then the p virtual inputs associated to the remaining fault free actuators are now defined as:

$$v_i = \sum_{j \in d^k} G_{p,j}(\underline{X}, \underline{c}) \cdot u_j + \sum_{j \in h^k} G_{p,j}(\underline{X}, \underline{c}) \cdot u_j^0 \quad i = 1 \text{ to } p \quad (4.28)$$

where u_j^0 is the actual position of a runaway or stuck fault actuator j .

Relation (4.28) can be rewritten as:

$$\underline{v}_t = \tilde{G}(\underline{X}_t, \underline{c}_t, k) \cdot \underline{u}_t^k + \tilde{G}^0(\underline{X}_t, \underline{c}_t, k) \cdot \underline{u}_t^0 \quad (4.29)$$

where \underline{u}_t^k is deduced from \underline{u}_t by deleting the faulty entries. \underline{u}_t^0 is the inputs vector resulting from actuators with runaway or stuck faults.

Now the actuator constraints (4.21) are rewritten:

$$\max \left\{ \underline{u}_{\min}^k(\underline{X}_t), \underline{u}_{t-1}^{k*} + \dot{\underline{u}}_{\min}^k(\underline{X}_t) \cdot \Delta t \right\} \leq \underline{u}_t^k \leq \min \left\{ \underline{u}_{\max}^k(\underline{X}_t), \underline{u}_{t-1}^{k*} + \dot{\underline{u}}_{\max}^k(\underline{X}_t) \cdot \Delta t \right\} \quad (4.30)$$

The actuator reassignment problem ARP consists now in finding $\underline{u}_t^k \in R^{D_k}$ such that (4.29) and (4.30) are satisfied.

The actuator reassignment problem can be rewritten in that case more shortly as:

$$\text{Find } \underline{u}_t^k \in R^{D_k} : \quad \underline{v}_t = G_t^k \cdot \underline{u}_t^k + H_t^k \quad (4.31)$$

$$\text{with} \quad L_t^k \underline{u}_t^k \leq \underline{l}_t^k \quad (4.32)$$

$$\text{where } G_t^k \in R^{p \times D_k}, \quad L_t^k \in R^{2D_k \times D_k} \quad \text{and} \quad \underline{l}_t^k \in R^{2D_k} \quad (4.33)$$

Expressions for G_t^k , H_t^k , L_t^k and \underline{l}_t^k can be deduced easily from (4.29) and (4.30).

In the case of the occurrence of a partial loss of effectiveness for a failed actuator j which remains operative, the above formulation can be maintained by taking into account the current effectiveness of that actuator in the flight dynamics. This will lead to some changes in the analytical expression of $G_{p,j}$ in relations (4.28), (4.29) and (4.31).

Among the many actuator failure cases which can be considered, the actuator reassignment problem remains of interest only when there is still possibility to perform the intended maneuver represented by the virtual inputs. This will be only the case if matrix G_t^k remains full rank.

In general, according to the architecture of the control channels of modern transportation aircraft where, even if high redundancy is implemented, some resources are shared by different actuators, then it can be expected that the number of actuator faulty cases to be considered at the global aircraft level is much less than $2^m - 1$. So it appears feasible to check for every of these actuator faulty cases, the rank of the resulting mixing matrix.

In the case in which the mixing matrix is no more full rank after the occurrence of the actuator failure, the control objectives must be redefined according with the residual controllability to maintain when possible, some flight safety level.

Figure 4.7 illustrates the actuator reassignment situation where Σ_t^k and Ω_t^k represent the resulting Σ_t and Ω_t after failure k . The positions of optimal solution at previous and current instant which are denoted by \underline{u}_{t-1}^{k*} and \underline{u}_t^{k*} in Figure 4.7 will also change. For the reason of simplicity, only case 1 is considered here.

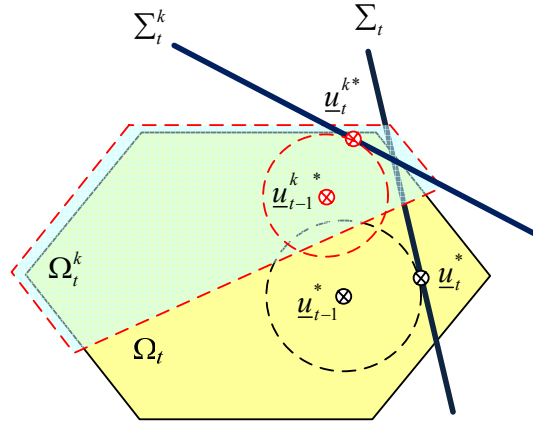


Figure 4.7 Comparing fault free and faulty assignment cases

In the case in which $\Sigma_t^k \cap \Omega_t^k$ is empty, the ARP can be reformulated as a LQ minimization problem such as:

$$\underline{u}_t^{k*} = \arg \min \left\{ \left\| \underline{y}_t - G_t^k \underline{u}_t^k \right\|_{D_k}^2, \underline{u}_t^k \in \Omega_t^k, L_t^k \underline{u}_t^k \leq \underline{l}_t^k \right\} \quad (4.34)$$

where $\| \cdot \|_{D_k}$ is an Euclidian distance over R^{D_k} .

Here also, considering other types of constraints, such as structural constraints, the feasible set Ω_t^k must be redefined by using these constraints.

4.7 Direct Methods to Solve the Instant AAP and ARP

Different direct methods have been developed with the objective of solving simply the actuator assignment and reassignment problems. Since the mathematical formulation for AAP and ARP are very close, adopting the same solution approaches, and for the sake of notation simplicity, the direct methods discussed in this section are illustrated only in the case of AAP.

4.7.1 The explicit ganging method

When it is obvious how to combine redundant actuators, the explicit ganging method can be used. The method distributes the control effort to each actuator according to its contribution to the virtual input [HONEYWELL & Lockheed Martin, 1996; Oppenheimer et al., 2006]. In other

words, a *distribution matrix* $K_t \in R^{m \times p}$ must be chosen such as:

$$\underline{u}_t = K_t \underline{v}_t \quad (4.35)$$

Considering relation (4.22), this distribution matrix is such that:

$$G_t \cdot K_t = I_p \quad (4.36)$$

where I_p is the identity matrix of size p . Then considering that G_t is assumed to be full rank, the general solution is such that:

$$K_t = \left(G_t' (G_t \cdot G_t')^{-1} + M_t \right) \quad (4.37)$$

where M_t is a $m \times p$ matrix such as $G_t \cdot M_t = 0$. This matrix must be chosen such as the actuator constraints and limitations (relation (4.23)) are satisfied. When it is possible to take $M_t = 0$, K_t is merely the right pseudo inverse of G_t .

4.7.2 The direct allocation method

A similar approach has been proposed by [Durham, 1994] for the AAP where virtual inputs are three moments. A scaling factor ρ_t is computed by considering the feasible maximum Euclidian norm of the virtual inputs $\|\underline{v}_t^*\|$ which is such as:

$$\underline{v}_t^* = G_t \underline{u}_t^* \quad (4.38)$$

where \underline{u}_t^* is the solution of the problem:

$$\underline{u}_t^* = \arg \max \left\{ \|G_t \underline{u}_t\|_p, \underline{u}_t \in R^m, L_t \underline{u}_t \leq l_t, \exists \rho_t \in R^+ : G_t \underline{u}_t = \rho_t \underline{v}_t \right\} \quad (4.39)$$

where $\|\cdot\|_p$ is an Euclidian distance over R^p .

Then the scaling factor ρ_t is given by:

$$\rho_t = \|\underline{v}_t\| / \|\underline{v}_t^*\| \quad (4.40)$$

and the direct allocation method computes the control inputs according to:

$$\underline{u}_t = \underline{u}_t^* \quad \text{if } \rho_t > 1 \quad \text{or} \quad \underline{u}_t = \underline{u}_t^* / \rho_t \quad \text{if } \rho_t < 1 \quad (4.41)$$

On one hand, this method preserves the direction of the current virtual input and on the other hand, unlike the explicit ganging methods, bound limits are now guaranteed. The disadvantages of the methods are that the origin ($\underline{u}_t = \underline{0}$) should be included in the bound limits [Bodson, 2002] and that the choice of \underline{u}_t^* is not always unique [Durham, 1994].

4.7.3 The daisy chain method

The daisy chain [Buffington & Enns, 1996] is a straightforward idea which assumes a hierarchy of actuators. This can be achieved with the multiple control surfaces of large transportation aircraft. There, when an actuator, or a group of actuators, saturates, the daisy chain method will then make use of additional non solicited actuators to produce the required amount of virtual input. For example, the m control inputs have been grouped into m_g groups of actuators and the mixing matrix is partitioned into the corresponding m_g sub-matrices:

$$\underline{u}_t = [\underline{u}_1^t \quad \underline{u}_2^t \quad \cdots \quad \underline{u}_{m_g}^t]^t \quad \text{and} \quad G_t = [G_1^t \quad G_2^t \quad \cdots \quad G_{m_g}^t] \quad (4.42)$$

where subscript i corresponds to the i^{th} group of actuators. Assuming that:

$$\text{rank}(G_i^t) = \dim(\underline{v}_t) = p \quad i = 1, \dots, m_g \quad (4.43)$$

Let K_i^t be the right inverse of G_i^t which can be computed using (4.37), then the daisy chain procedure can be stated as: repeat computation of (4.44) until all actuators has been distributed or no actuator saturation at some iteration:

$$\underline{u}_i^* = \text{sat}_{\underline{u}_i^t} \left[K_i^t \left(\underline{v}_t - \sum_{l=1}^{i-1} G_l^t \underline{u}_l^* \right) \right] \quad (4.44)$$

where function $\underline{u}^* = \text{sat}_{\underline{u}}(\tilde{\underline{u}})$ is a component-wise linear piecewise function (4.45), i.e., for the h^{th} component of \underline{u} :

$$u_h^* = \text{sat}_{u_h}(\tilde{u}_h) = \begin{cases} u_h^{\max}, & \text{if } \tilde{u}_h > u_h^{\max} \\ \tilde{u}_h, & \text{if } u_h^{\min} \leq \tilde{u}_h \leq u_h^{\max} \\ u_h^{\min}, & \text{if } \tilde{u}_h < u_h^{\min} \end{cases} \quad (4.45)$$

This method may fail to produce some virtual inputs which are indeed feasible while the grouping of actuators has a significant effect on the result of the daisy chain procedure. Once

again, like the direct allocation method, this method cannot face more complex inequality constraints.

4.8 Conclusion

In this chapter, the actuator assignment problem which should be part of a two stages control approach to get some degree of fault tolerance has been formulated as a general LQ problem and the existence and uniqueness of its solution has been discussed. According with the chosen control objective, this problem must be solved online or not. Some direct and rather intuitive methods have been designed to solve this problem. However, since these direct methods fail very often to provide the exact solution, exact solution methods for the LQ problem have been studied and are discussed in Chapter 5.

CHAPTER 5

FAST SOLUTION APPROACHES FOR

LQ OPTIMIZATION PROBLEMS

5.1 Introduction

In this chapter the mathematical problem which must be solved to achieve actuator reassignment is considered. The general as well as the particular (LQ problem) necessary optimization conditions for this problem are introduced (the KKT conditions) which are also sufficient for convex problem such as the ARP in the adopted formulation. Among the many solution methods and resulting algorithms to solve this problem or equivalently (in the LQ case) the KKT conditions, three solution approaches have been studied more accurately. Two of these methods (the interior point methods and the active set methods) have been chosen when considering the large amount of constraints and the necessity to have at hand at each iteration a feasible solution. The active set method has been also considered for its efficiency to cope with box constraints. Also a neural networks based direct method, which solves directly the optimality conditions, has been introduced. In that case, the optimality conditions are reached at the equilibrium state of the resulting dynamical system. The convergence of this process is discussed in Annex C.

5.2 Convex Optimization

Many decision problems in Engineering can be formulated as an optimization problem such as:

$$\min_{\underline{u}} f(\underline{u}) \quad (5.1)$$

$$\text{s.t. } g_i(\underline{u}) \leq 0 \quad i = 1, 2, \dots, q \quad (5.2a)$$

$$h_j(\underline{u}) = 0 \quad j = 1, 2, \dots, p \quad (5.2b)$$

$$\text{with } \underline{u} \in R^m \quad (5.2c)$$

here \underline{u} is a vector of decision variables, and the functions f , g_i , h_j are respectively objective function (performance index), inequality constraints, equality constraints supposed to be of C^∞ . The feasible set Ω of this problem is composed of the point of R^m satisfying its constraints (5.2a, 5.2b).

When the objective function f is a convex function and when the feasible set Ω is a convex

set [Boyd & Vandenberghe, 2004; Luenberger & Ye, 2008], the above optimization problem is said to be a *convex optimization* problem.

General necessary optimality conditions for this optimization problem are given by the *Karush-Kuhn-Tucker (KKT)* conditions [Kuhn & Tucker, 1951]:

$$\nabla f(\underline{u}^*) + \sum_{i=1}^q \lambda_i^* \nabla g_i(\underline{u}^*) + \sum_{i=1}^p \mu_i^* \nabla h_i(\underline{u}^*) = \underline{0} \quad (5.3a)$$

$$g_i(\underline{u}^*) \leq 0 \quad i = 1, 2, \dots, q \quad (5.3b)$$

$$h_j(\underline{u}^*) = 0 \quad j = 1, 2, \dots, p \quad (5.3c)$$

$$\lambda_i^* \geq 0 \quad i = 1, 2, \dots, q \quad (5.3d)$$

$$\lambda_i^* g_i(\underline{u}^*) = 0 \quad i = 1, 2, \dots, q \quad (5.3e)$$

where prefix ∇ denotes a gradient of function related to a vector, superscript $*$ denotes the minimum point. Here $\underline{\lambda}$ and $\underline{\mu}$ are vectors of Lagrange multipliers [Bertsekas, 1982] associated respectively to inequality constraints (5.2a) and equality constraints (5.2b). Vectors \underline{u} is also called *primary variables* while $\underline{\lambda}$ and $\underline{\mu}$ are termed *dual variables*. A solution satisfying such conditions maybe either a local solution or a global one.

In the case of a convex optimization problem, the satisfaction of the KKT conditions is a necessary and sufficient to get a global optimum of this problem [Boyd & Vandenberghe, 2004; Luenberger & Ye, 2008].

Many algorithms have been designed to solve convex as well as nonconvex optimization problems [Luenberger & Ye, 2008; Nocedal & Wright, 1999]: gradient projection methods, reduced gradient methods, penalty methods, barrier methods, cutting-plane methods, etc.

5.3 Linear Quadratic Optimization Problem

A special case of convex optimization is termed linear quadratic (LQ) optimization problem, where f is a quadratic function while the g_i and h_j functions are affine. In that case, the optimization problem can be such as:

$$\min_{\underline{u}} f(\underline{u}) = \frac{1}{2} \underline{u}^T Q \underline{u} + \underline{c}^T \underline{u} \quad (5.4)$$

$$\text{s.t. } g(\underline{u}) = A \underline{u} - \underline{b} \leq \underline{0} \quad (5.5a)$$

$$h(\underline{u}) = E \underline{u} - \underline{d} = \underline{0} \quad (5.5b)$$

$$\text{with } \underline{u} \in R^m \quad (5.5c)$$

here $Q \in R^{m \times m}$ is a positive semidefinite symmetric matrix, $\underline{c} \in R^m$, $A \in R^{q \times m}$, $\underline{b} \in R^q$, $E \in R^{p \times m}$, $\underline{d} \in R^q$, $\underline{\xi}^- \in R^m$, $\underline{\xi}^+ \in R^m$, $\underline{0}$ with the appropriate dimension.

In this case the KKT conditions (5.3) become:

$$Q \underline{u}^* + \underline{c} + A^T \underline{\lambda}^* + E \underline{\mu}^* = \underline{0} \quad (5.6a)$$

$$A \underline{u}^* - \underline{b} \leq \underline{0} \quad (5.6b)$$

$$E \underline{u}^* - \underline{d} = \underline{0} \quad (5.6c)$$

$$\underline{\lambda}^* \geq \underline{0} \quad (5.6d)$$

$$(A \underline{u}^* - \underline{b})^T \underline{\lambda}^* = 0 \quad (5.6e)$$

Different formulation of the actuator assignment or reassignment problem in Chapter 4 can be written as a LQ optimization problem:

$$\min_{\underline{u}} f(\underline{u}) = \frac{1}{2} \underline{u}^T Q \underline{u} + \underline{c}^T \underline{u} \quad (5.7)$$

$$\text{s.t. } g(\underline{u}) = A \underline{u} - \underline{b} \leq \underline{0} \quad (5.8a)$$

$$\underline{\xi}^- \leq \underline{u} \leq \underline{\xi}^+ \quad (5.8b)$$

$$\text{with } \underline{u} \in R^m \quad (5.8c)$$

where Q is a positive definite matrix, there is no equality constraint and a part of the inequality constraints are expressed as box/bound constraints (5.8c). For the AAP or the ARP problems, in this formulation, the equality constraints resulting from the control objectives expressed through required levels for the virtual inputs are imbedded in the quadratic objective function (5.7) while (5.8a) represents level inequality constraints and (5.8b) represents interval (box) constraints related to physical actuators.

A large variety of algorithms exist to solve LQ optimization problems. Among these three solution approaches have mainly developed:

- direct methods: which solve directly the KKT conditions. They include the null-space method [Bjorck, 1996; S. Wright, 1988], the range-space method [P.E. Gill et al., 1982; Nocedal & Wright, 1999], the conjugate gradient method [Gould et al., 2001; O'Leary, 1980], the gradient projection method [Philip E. Gill & Murray, 1978; He & Hubland, 1992], as well as the Newton's method [Broyden & Attia, 1988; Dennis & Schnabel, 1996]. These techniques are mainly used to solve simple equality constrained and/or bound constrained LQ problems, and they maybe found embedded in other solution approaches [Nocedal & Wright, 1999]. Many of these methods have been implanted in general solvers for KKT conditions.

More recently, specialized neural networks have been designed to solve directly the KKT conditions for LQ problems with inequality constraints. The idea is to design a special nonlinear dynamical system whose equilibrium point approximates or corresponds exactly to the satisfaction of the KKT conditions. This research has got recently an increasing attention when considering parallel and distributed computing characteristics of neural networks, with a potential for faster convergence to the solution [Bouzerdoum & Pattison, 1993; Kamel & Xia, 2009; Liu & Wang, 2011; Maa & Shanblatt, 1992; Xia, 1996; Y. Zhang, 2005; Y. Zhang et al., 2004; Y. Zhang & Wang, 2002].

- active set methods: at each iteration, an equality constrained problem is solved. These methods are often recommended to solve small to medium-scale LQ programming problems because of their efficiency in coping with box constraints [Bjorck, 1996; Nocedal & Wright, 1999; Wong, 2011].
- interior point methods: the current solution at each iteration is in the interior of the feasible set rather than on its boundary, and in general progresses continuously towards the optimal solution. They limit the difficulties associated with determining which constraints will be active at the solution [Gondzio, 2012; Hindi, 2006; Nocedal & Wright, 1999; S. J. Wright, 1997].

5.4 Active Set Methods

The name *Active set* is given to methods used to solve optimization problems with a relatively large number of interval (or box) constraints. The idea underlying the active set methods is to generate successive partitions of the inequality constraints set into two groups: one where the constraints are to be treated as active constraints and one where the constraints are to be treated as inactive constraints (and be ignored somehow at a given stage of the solution process). At each iteration, the active inequality constraints will be treated as equality ones and will constitute the working set. Through the successive partitions of the inequality constraints set, the method reduces the constrained problem to a sequence of equality constrained sub-problems where the inactive constraints are temporarily ignored, while an updating process modifies the working set at each stage of the search process towards the solution.

In this situation, problem (5.7, 5.8) is rewritten in a form presenting only level inequality constraints:

$$\min_{\underline{u}} f(\underline{u}) = \frac{1}{2} \underline{u}^T Q \underline{u} + \underline{c}^T \underline{u} \quad (5.9)$$

$$\text{s.t. } g(\underline{u}) = \tilde{A} \underline{u} - \tilde{\underline{b}} \leq \underline{0} \quad (5.10)$$

where $\tilde{A} = \begin{bmatrix} A \\ I_d \\ -I_d \end{bmatrix}$, $\tilde{\underline{b}} = \begin{bmatrix} \underline{b} \\ \underline{\xi}^+ \\ -\underline{\xi}^- \end{bmatrix}$ and I_d is an identity matrix of size $m \times m$.

At each iteration, the active set method solves a sub-problem (equality constrained LQ problem) which is written as:

$$\min_{\underline{u}} f_w(\underline{u}) = \frac{1}{2} \underline{u}^T Q \underline{u} + \underline{c}^T \underline{u} \quad (5.11)$$

$$\text{with } \tilde{A}_w \underline{u} - \tilde{\underline{b}}_w = \underline{0} \quad (5.12)$$

The subscript w denotes the working set index. Let the solution at the k^{th} iteration be written \underline{u}_k and let \underline{p}_{k+1} be a possible search direction. Then the following problem is considered at iteration $k+1$:

$$\min_{\underline{p}_{k+1}} f_w(\underline{p}_{k+1}) = \frac{1}{2} \underline{p}_{k+1}^T Q \underline{p}_{k+1} + \underline{p}_{k+1}^T (Q \underline{u}_k + \underline{c}) \quad (5.13)$$

$$\text{with } \tilde{A}_w \underline{p}_{k+1} = \underline{0} \quad (5.14)$$

Consider the KKT conditions of problem (5.13, 5.14).

$$\begin{bmatrix} Q & \tilde{A}_w^T \\ \tilde{A}_w & 0 \end{bmatrix} \begin{Bmatrix} \underline{p}_{k+1} \\ \underline{\lambda}_{k+1} \end{Bmatrix} = \begin{Bmatrix} -(Q \underline{u}_k + \underline{c}) \\ \underline{0} \end{Bmatrix} \quad (5.15)$$

As long as \tilde{A}_w is full row-rank, and since Q is here a positive definite matrix, the coefficient matrix in (5.15) termed as KKT matrix is nonsingular [Boyd & Vandenberghe, 2004]. Then Solving (5.15) is straightforward and a new search direction \underline{p}_{k+1} and the associated Lagrange multipliers $\underline{\lambda}_{k+1}$ are obtained. If the length of \underline{p}_{k+1} is very small and the KKT conditions are satisfied (all elements of $\underline{\lambda}_{k+1}$ are nonnegative), then optimal solution is reached, or else the current solution and working set should be updated according to the values of \underline{p}_{k+1} and $\underline{\lambda}_{k+1}$.

When the current solution needs to be updated, a line search process along search direction \underline{p}_{k+1} is performed:

$$\underline{u}_{k+1} = \underline{u}_k + \alpha_{k+1} \underline{p}_{k+1} \quad (5.16)$$

where α_{k+1} is a scale factor computed at each iteration. There, to make sure that \underline{u}_{k+1} is feasible, it is only necessary to consider the constraints that are not in the working set and such as $\tilde{A}_i \underline{p}_{k+1} > 0$, while α_{k+1} must be as large as possible within $[0,1]$. So α_{k+1} can be given by:

$$\alpha_{k+1} = \min \left\{ 1, \min_{i \in W_k, \tilde{A}_i \underline{p}_{k+1} > 0} \left(\frac{\tilde{b}_i - \tilde{A}_i \underline{u}_k}{\tilde{A}_i \underline{p}_{k+1}} \right) \right\} \quad (5.17)$$

If there are only bound constraints and no other inequality constraints, problem (5.13, 5.14) can be reformulated as an unconstrained least square problem [Harkegard, 2002] and the computation of its solution becomes easier. When considering the presence of inequality constraints such as structural integrity constraints in the AAP or the ARP problems, methods considering the compute KKT matrix (5.15) should be used.

Table 5.1 displays an example of active set algorithm [Nocedal & Wright, 1999].

Table 5.1 An example of active set algorithm

Compute or take the previous solution as a feasible starting point \underline{u}_0 ;
 Let W_0 be the working set corresponding to \underline{u}_0 ;
for $k = 0, 1, 2, \dots$
 solve (5.15) to find \underline{p}_{k+1} and $\underline{\lambda}_{k+1}$;
 if $\|\underline{p}_{k+1}\| = 0$
 if $\underline{\lambda}_{k+1} \geq 0$
 STOP with solution $\underline{u}^* = \underline{u}_k$;
 else
 set $j = \arg \min \underline{\lambda}_k$
 $\underline{u}_{k+1} = \underline{u}_k$; $W_{k+1} = W_k - \{j\}$
 else ($\|\underline{p}_{k+1}\| \neq 0$)
 compute α_{k+1} from (5.17)
 $\underline{u}_{k+1} = \underline{u}_k + \alpha_{k+1} \underline{p}_{k+1}$;
 if there are new active constraints
 add one of them to W_{k+1} ;
 else
 $W_{k+1} = W_k$
end (for)

It has been already proved that the active set method converges to the solution of problems such as (5.9, 5.10) after a rather small number of iterations [Luenberger & Ye, 2008].

5.5 Interior Point Approaches

The idea supporting *interior point* methods is to approach the solution of the KKT equations by successive descent steps. Each descent step is a Newton-like step and is obtained by solving a system of linear equations. The main advantage of interior point methods over active set method is their scalability [Lau et al., 2009; Petersen & Bodson, 2005].

To turn problem (5.7, 5.8) into a standard form for interior point methods, let

$$\underline{u} = \underline{x} + \underline{\xi}^- \tag{5.18}$$

which makes apparent the gap between \underline{u} and its lower limits.

Substituting (5.18) into (5.7) and (5.8), and omitting the constant term in the objective function which will not impact the final solution, the original problem is equivalent to the following problem:

$$\min_{\underline{x}} f(\underline{x}) = \frac{1}{2} \underline{x}^T Q \underline{x} + \underline{x}^T \tilde{\underline{c}} \tag{5.19}$$

$$\text{s.t.} \quad \underline{g}(\underline{x}) = A \underline{x} + \tilde{\underline{b}} \leq \underline{0} \tag{5.20a}$$

$$\underline{0} \leq \underline{x} \leq \underline{x}^+ \quad (5.20b)$$

where $\underline{\tilde{c}} = Q\underline{\xi}^- + \underline{c}$, $\underline{\tilde{b}} = A\underline{\xi}^- - \underline{b}$ and $\underline{x}^+ = \underline{\xi}^+ - \underline{\xi}^-$.

Adding slack variables \underline{y} , \underline{z} to turn inequalities into equalities, the following formulation is obtained:

$$\min_{\underline{x}} \frac{1}{2} \underline{x}^T Q \underline{x} + \underline{x}^T \underline{\tilde{c}} \quad (5.21)$$

$$\text{s.t.} \quad A \underline{x} + \underline{\tilde{b}} + \underline{y} = \underline{0}, \quad \underline{x} + \underline{z} = \underline{x}^+ \quad (5.22a)$$

$$\underline{x} \geq \underline{0}, \underline{y} \geq \underline{0}, \underline{z} \geq \underline{0} \quad (5.22b)$$

One of the basic ideas behind the interior point methods is to use barrier functions to force the satisfaction of the bound constraints. Then a modified Lagrangian for problem (5.21, 5.22) is expressed as:

$$\begin{aligned} L = & \frac{1}{2} \underline{x}^T Q \underline{x} + \underline{x}^T \underline{\tilde{c}} - \tau \sum_{i=1}^m \log(x_i) - \tau \sum_{i=1}^q \log(y_i) \\ & - \tau \sum_{i=1}^m \log(z_i) + \underline{\mu}^T (A \underline{x} + \underline{\tilde{b}} + \underline{y}) + \underline{\varphi}^T (\underline{x} + \underline{z} - \underline{x}^+) \end{aligned} \quad (5.23)$$

where $\tau > 0$ is the barrier parameter and is used to guide the solution along a trajectory called the *central path*. Equation (5.23) approximates the Lagrangian of problem (5.21, 5.22) more and more closely as τ goes to zero [Boyd & Vandenberghe, 2004; Luenberger & Ye, 2008]. Here $\underline{\mu}$, $\underline{\varphi}$ are dual variables associated to equality constraints (5.22a). Adopting the modified Lagrangian function (5.23), the necessary and sufficient conditions for the global minimum of convex problem (5.23), i.e. the KKT conditions, can be written:

$$\nabla_{\underline{x}} L = Q \underline{x} + \underline{\tilde{c}} - \underline{\lambda} + A^T \underline{\mu} + \underline{\varphi} = \underline{0} \quad (5.24a)$$

$$\nabla_{\underline{y}} L = Y \underline{\mu} - \tau \underline{e} = \underline{0} \quad (5.24b)$$

$$\nabla_{\underline{z}} L = Z \underline{\varphi} - \tau \underline{e} = \underline{0} \quad (5.24c)$$

$$X \underline{\lambda} - \tau \underline{e} = \underline{0} \quad (5.24d)$$

$$\nabla_{\underline{\mu}} L = A \underline{x} + \underline{\tilde{b}} + \underline{y} = \underline{0} \quad (5.24e)$$

$$\nabla_{\underline{\varphi}} L = \underline{x} + \underline{z} - \underline{x}^+ = \underline{0} \quad (5.24f)$$

$$\underline{x} > \underline{0}, \underline{y} > \underline{0}, \underline{z} > \underline{0}, \underline{\lambda} > \underline{0}, \underline{\mu} > \underline{0}, \underline{\varphi} > \underline{0} \quad (5.24g)$$

where X , Y , and Z are diagonal matrices whose diagonal elements are \underline{x} , \underline{y} , \underline{z} respectively, \underline{e} is a vector whose components are all equal to unity. Here $\underline{\lambda}$ is another dual variable. The quantity $\underline{x}^T \underline{\lambda} + \underline{y}^T \underline{\mu} + \underline{z}^T \underline{\varphi}$ is termed a *duality gap* [Boyd & Vandenberghe, 2004; Luenberger & Ye, 2008].

Applying Newton's method to the system of equations (5.24), we obtain the linear system to be solved:

$$\begin{bmatrix} Q & 0 & 0 & -I_{d1} & A^T & I_{d1} \\ 0 & M & 0 & 0 & Y & 0 \\ 0 & 0 & \Phi & 0 & 0 & Z \\ \Lambda & 0 & 0 & X & 0 & 0 \\ A & I_{d2} & 0 & 0 & 0 & 0 \\ I_{d1} & 0 & I_{d1} & 0 & 0 & 0 \end{bmatrix} \begin{bmatrix} \Delta \underline{x} \\ \Delta \underline{y} \\ \Delta \underline{z} \\ \Delta \underline{\lambda} \\ \Delta \underline{\mu} \\ \Delta \underline{\varphi} \end{bmatrix} = - \begin{bmatrix} \underline{r}_x \\ \underline{r}_y \\ \underline{r}_z \\ \underline{r}_\lambda \\ \underline{r}_\mu \\ \underline{r}_\varphi \end{bmatrix} \quad (5.25)$$

where Λ , M and Φ are diagonal matrices whose diagonal elements are $\underline{\lambda}$, $\underline{\mu}$ and $\underline{\varphi}$, respectively. The I_d matrices are identity matrices with appropriate dimensions. The right hand side \underline{r} are defined as:

$$\begin{aligned} \underline{r}_x &= Q\underline{x} + \tilde{\underline{c}} - \underline{\lambda} + A^T \underline{\mu} + \underline{\varphi}, & \underline{r}_y &= Y\underline{\mu} - \tau \underline{e}, & \underline{r}_z &= Z\underline{\varphi} - \tau \underline{e}, \\ \underline{r}_\lambda &= X\underline{\lambda} - \tau \underline{e}, & \underline{r}_\mu &= A\underline{x} + \tilde{\underline{b}} + \underline{y}, & \underline{r}_\varphi &= \underline{x} + \underline{z} - \underline{x}^+ \end{aligned} \quad (5.26)$$

Equation (5.25) can be solved sequentially as:

$$\begin{aligned} \Delta \underline{x} &= -H^{-1} \underline{r}_x, & \Delta \underline{y} &= -(\underline{r}_y + A \Delta \underline{x}), & \Delta \underline{z} &= -(\underline{r}_z + \Delta \underline{x}), \\ \Delta \underline{\lambda} &= -X^{-1}(\underline{r}_\lambda + \Lambda \Delta \underline{x}), & \Delta \underline{\mu} &= -Y^{-1}(\underline{r}_y + M \Delta \underline{y}), \\ \Delta \underline{\varphi} &= -Z^{-1}(\underline{r}_z + \Phi \Delta \underline{z}) \end{aligned} \quad (5.27a)$$

where

$$H = Q + X^{-1} \Lambda + A^T Y^{-1} M A + Z^{-1} \Phi \quad (5.27b)$$

$$\underline{r}_x = \underline{r}_x - A^T Y^{-1} \underline{r}_y - Z^{-1} \underline{r}_z + X^{-1} \underline{r}_\lambda + A^T Y^{-1} M \underline{r}_\mu + Z^{-1} \Phi \underline{r}_\varphi \quad (5.27c)$$

Since Q is positive definite, A is full row rank and during iteration, \underline{x} , \underline{y} , \underline{z} , $\underline{\lambda}$, $\underline{\mu}$, $\underline{\varphi}$ remain greater than zero, H is an invertible matrix.

Different numerical algorithms can be derived from this approach depending on whether solving the primal or the dual variables and on the choice of the initial point \underline{x}_0 . Following [Petersen & Bodson, 2005], the values of $\underline{x}_0, \underline{z}_0, \underline{\lambda}_0, \underline{\mu}_0, \underline{\varphi}_0$ can be chosen such that $r_x=0$ and $r_\varphi=0$. In the AAP and ARP cases, \underline{x}_0 may be chosen as the vector of the mean values of the upper and lower bounds or the values at the previous instant. Then, the values of $\underline{z}_0, \underline{\lambda}_0, \underline{\mu}_0, \underline{\varphi}_0$ are chosen based on the values of \underline{x}_0 . Moreover, under normal situation, (5.22a) can be strictly satisfied with a positive vector \underline{y}_0 and \underline{z}_0 .

Based on [Antonious & Lu, 2007], a feasible-initialization primal-dual path-following algorithm can be proposed as shown in Table 5.2.

Table 5.2 An example of interior point algorithm

Step 0 Initialization

Set index $k = 0$, initialize the parameters $\sigma_1, \sigma_2, \sigma_3$ and the tolerance level ε . Choose the values of $\underline{x}_0, \underline{y}_0, \underline{z}_0, \underline{\lambda}_0, \underline{\mu}_0, \underline{\varphi}_0$ such that $\underline{x}_0 > \underline{0}, \underline{y}_0 > \underline{0}, \underline{z}_0 > \underline{0}, \underline{\lambda}_0 > \underline{0}, \underline{\mu}_0 > \underline{0}, \underline{\varphi}_0 > \underline{0}$ and the equations $r_x=0, r_\varphi=0$ and $r_\mu=0$ are satisfied.

Step 1 Compute the duality gap,

Compute $d_k = \underline{x}_k^T \underline{\lambda}_k + \underline{y}_k^T \underline{\mu}_k + \underline{z}_k^T \underline{\varphi}_k$, if $d_k \leq \varepsilon$, the optimal solution is given by $\underline{u}_k = \underline{x}_k + \underline{\xi}^-$ and stop, otherwise continue to step 2.

Step 2 Update the barrier parameter τ_k and the search direction according to:

Compute $\tau_k = \min\{\sigma_1, \sigma_2, \sigma_3\} \cdot \rho_k$ where $\rho_k = d_k / (2m + q)$. Compute residuals using (5.26) and update search directions using (5.27).

Step 3 Define the step size α_k and update the variables.

Compute α_k using relation (a, b, c), and update the primal and dual variables using (d)

$$\alpha_k = \sigma_3 \alpha_{\min} \quad (a)$$

$$\text{where } \alpha_{\min} = \min(\alpha_x, \alpha_y, \alpha_z, \alpha_\lambda, \alpha_\mu, \alpha_\varphi) \quad (b)$$

$$\text{with } \begin{cases} \alpha_\Omega = \min_{i \text{ with } (\Delta\Omega)_i < 0} [-(\Omega)_i / (\Delta\Omega)_i], \\ \Omega \in \{ \underline{x}, \underline{y}, \underline{z}, \underline{\lambda}, \underline{\mu}, \underline{\varphi} \} \\ \Delta\Omega \in \{ \Delta\underline{x}, \Delta\underline{y}, \Delta\underline{z}, \Delta\underline{\lambda}, \Delta\underline{\mu}, \Delta\underline{\varphi} \} \end{cases} \quad (c)$$

and update variables according to equations:

$$\begin{aligned} \underline{x}_{k+1} &= \underline{x}_k + \alpha_k \Delta\underline{x}, \underline{y}_{k+1} = \underline{y}_k + \alpha_k \Delta\underline{y}, \underline{z}_{k+1} = \underline{z}_k + \alpha_k \Delta\underline{z} \\ \underline{\lambda}_{k+1} &= \underline{\lambda}_k + \alpha_k \Delta\underline{\lambda}, \underline{\mu}_{k+1} = \underline{\mu}_k + \alpha_k \Delta\underline{\mu}, \underline{\varphi}_{k+1} = \underline{\varphi}_k + \alpha_k \Delta\underline{\varphi} \end{aligned} \quad (d)$$

Set $k = k + 1$, and repeat step 1.

5.6 Neural Networks Approaches

In many applications including fault tolerant flight control, a real time solution for LQ programming problems is desired. However, traditional techniques such as the mentioned active set and interior point solvers for LQ problems are computationally too time consuming. One possible and very promising approach to real-time optimization is to adopt specialized artificial neural networks. Because of the inherent nature of parallel and distributed information processing in neural networks, and it can be implemented physically in designated hardware such as specific integrated circuits where optimization is carried out in a truly parallel and distributed manner. Nowadays, Neural networks are considered to be promising computational models for solving in real time large-scale optimization problems [Xia & Wang, 2001].

5.6.1 The development of neural network solvers for LQ problems

An early attempt to develop analog circuits for solving linear programming problems was done by Pyne in 1956 [Pyne, 1956]. Soon after, some other circuits were proposed for solving various optimization problems. In 1986, Tank and Hopfield [Tank & Hopfield, 1986] introduced a linear programming neural network using an analog circuit which should be well suited for applications that require on-line optimization. Their pioneer work has inspired many researchers to investigate alternative neural networks for solving LQ programming problems. Many optimization neural networks have been developed, see [Ghasabi-Oskoei & Mahdavi-Amiri, 2006; Kennedy & Chua, 1988; Liu & Wang, 2008a, 2008b; Tank & Hopfield, 1986; Tao et al., 2001; J. Wang, 1993; Wu et al., 1996; Xia, 1996; Xia & Wang, 1995; Y. Zhang, 2005; Y. Zhang & Wang, 2002; Y. Zhang et al., 2003]. From the optimization point of view, most of the methods employed by these existing neural networks belong to either the penalty function method or the Lagrangian method. For more discussion on the advantages and disadvantages of these models and their variants, see Cichocki and Unbehauen [Cichocki & Unbehauen, 1993]. Using the gradient and projection methods Bouzerdoum and Pattison [Bouzerdoum & Pattison, 1993] presented a neural network for solving LQ optimization problems with bounded variables. This network has good computational performances but was not able to solve general LQ programming problems. By considering duality and projection methods, Xia and Zhang [Xia,

1996; Y. Zhang et al., 2003] developed neural networks capable of solving general LQ programming problems.

To formulate an optimization problem in terms of a neural network, there are two types of methods [Xia & Wang, 2001]. One approach commonly used in developing an optimizing neural network is to convert the original constrained optimization problem into an associated unconstrained optimization problem at first, and then design a neural network that solves the unconstrained problem with gradient methods. Another approach is to construct a set of differential equations such that their equilibrium points correspond to the desired solutions and then find an appropriate Lyapunov function such that all trajectories of the system converge to some equilibrium point.

5.6.2 Classification of LQ neural network solvers

According to the architecture of the network, the existing neural networks for solving LQ programming problems can be divided into primal network, dual network and primal-dual network [Y. Zhang & Wang, 2002].

- a) In a primal network such as proposed in [Kennedy & Chua, 1988; Tank & Hopfield, 1986; J. Wang, 1993], only the variables of the original problem appear explicitly. In general they are based on the use of a penalty function method where a penalty item of constraints is added to the objective function to convert a constrained problem into an unconstrained one, then a gradient descent method is used to solve the unconstrained problem. One of the advantages of this kind of network is that the solution is forced to satisfy the constraints during the entire optimization process, though a tolerance that depends on the penalty parameter. This last issue is the most critical one for primal networks, because it affects also the quality of the solution: in fact, the exact solution may be found only when the penalty parameter is infinite, which is impossible to achieve in practice. Also, it may generate infeasible solutions which are unacceptable for some applications.
- b) A dual network solves the problem using only the dual decision variables. Nowadays, some dual neural network models such as [Liu & Wang, 2008a, 2008b; Y. Zhang & Wang, 2002; Y. Zhang et al., 2003] have been developed for LQ programming problems

which subject to equality constraint, inequality constraints and box constraints. This network has been mainly developed for strictly convex LQ programming problems and it needs a computation of the inverse of a matrix.

- c) The main idea of primal-dual methods is to map both the primal and the dual optimization problem on a dynamical system such that its equilibrium point satisfies the KKT conditions and therefore is also a solution of the LQ programming problem. The main advantage of the primal-dual approach is that the exact solution is reached without any need of parameter tuning (e.g. the penalty parameter). There are, however, some disadvantages: the first one is the increased size of the network due to the introduction of the dual variables; the second one is that the primal variables satisfy the constraints only at the equilibrium point, therefore, during the evolution of the network, the solution can be infeasible and this could be unacceptable for some applications.

5.6.3 Example of a primal-dual LQ neural network solver

Aimed to solve LQ problems online, a primal-dual neural network solver based on linear variational inequalities (LVI) has been proposed by Zhang which has proven its global convergence [Y. Zhang, 2005]. Based on the KKT conditions of problem (5.7, 5.8), the original problem can be turned equivalent to the following set of LVIs:

$$(\underline{s} - \underline{s}^*)^T (N\underline{s}^* + \underline{\rho}) \geq 0 \quad \forall \underline{s} \in \Omega \quad (5.28)$$

with the primal-dual variables $\underline{s} = [\underline{u}^T \quad \underline{\lambda}^T]^T$, $\underline{\lambda}$ is the dual variable vector corresponding to inequality constraint (5.8a). Then the problem is to find a solution vector \underline{s}^* where its feasible set Ω and its lower/upper limits are given by:

$$\Omega := \{ \underline{s} \mid \underline{\zeta}^- \leq \underline{s} \leq \underline{\zeta}^+ \}, \underline{\zeta}^- = [\underline{\xi}^- \quad \underline{0}]^T, \underline{\zeta}^+ = [\underline{\xi}^+ \quad \underline{\omega}^+]^T \quad (5.29)$$

Here $\underline{\omega}^+$ is considered with the appropriate dimension and each of its entries is sufficiently large to replace numerically $+\infty$. The coefficients are defined as:

$$\underline{\rho} = [\underline{c}^T \quad \underline{b}^T]^T \quad N = \begin{bmatrix} Q & A^T \\ -A & 0 \end{bmatrix} \quad (5.30)$$

Then the neural network model which solves problem (5.7, 5.8) is given by:

$$\frac{ds}{dt} = \eta(I_{d3} + N^T) \{ P_{\Omega}(s - (Ns + \rho)) - s \} \tag{5.31}$$

where η is a positive learning parameter which can be used to adjust the convergence speed of the network, I_{d3} is an identity matrix, $P_{\Omega}[\cdot]$ is a piecewise-linear function defined as:

$$P_{\Omega}[s_i] = \begin{cases} \zeta_i^-, & \text{if } s_i \leq \zeta_i^- \\ \zeta_i^+, & \text{if } s_i \geq \zeta_i^+ \\ s_i, & \text{otherwise} \end{cases} \tag{5.32}$$

Figure 5.1 displays the architecture of the Neural Networks model. Through the feedback of primal-dual variables, a recurrent neural network is realized and equilibrium point of the network will correspond to optimal point.

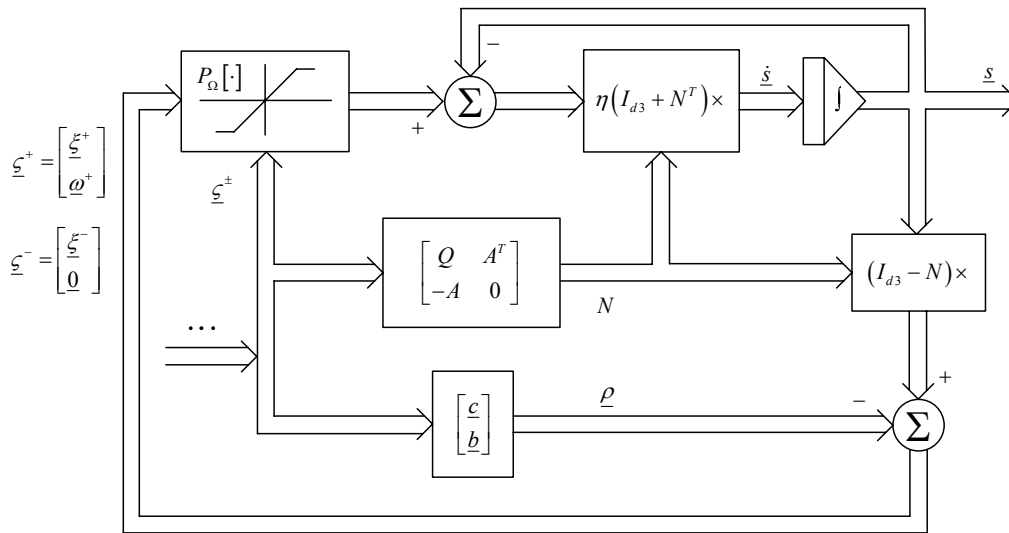


Figure 5.1 Architecture of adopted neural networks model

For clear, a simplified block diagram and convergent proof are given in Annex C.

5.7 Conclusion

From the performed analysis, as well as from the numerical applications which are displayed in the following chapters, it appears that the three types of algorithms can be considered as good

candidates to solve the LQ problem resulting from the actuator assignment problem. It will be shown that these solution techniques can be either used to solve large off-line LQ problems or be embedded in an online fault tolerant control scheme.

CHAPTER 6

ASSESSMENT OF HANDLING

QUALITIES AFTER ACTUATOR

FAILURE

6.1 Introduction

The objective of this chapter is, to contribute to the evaluation of the remaining maneuverability of a transportation aircraft in the situation in which some aerodynamic actuators have failed while actuator redundancy management is effective.

The solution approach adopted here is to perform at first an off-line study using a realistic flight simulation model of the aircraft to design a controller for the deflection of the remaining actuators with the objective of performing reference maneuvers in a nominal way. When considering a particular maneuver which can be no more performed nominally, the adoption of this control approach will turn possible to assess feasible downgraded maneuvers. The off-line controller design approach adopted at this step of the study with the above objective and which is described in this chapter follows the main steps of classical MPC control using as test bed a realistic flight simulation model of the considered aircraft. This approach lead to the formulation of an off-line linear quadratic problem as defined in (4.27). Then, by performing a systematic generation of possible actuators failure scenarios where some effectiveness over each axis remains, a full panorama of the handling qualities of an aircraft with actuator reassignment capability can be built and structured as a knowledge base.

The maneuverability issue here is concentrated on the control of the three rotations along the main axis of a transportation aircraft, since they are basic for stabilization, attitude control and further maneuvers. These rotations are mainly the result of the aerodynamic moments created by the deflection of the primary and secondary aerodynamic actuators. Since it is considered that in fault free conditions, targets values for the angular rates should be reached according to nominal linear dynamics, the question is to know if this will be still possible, or if these target values will be achieved with additional delay or if these target values will remain out of range.

6.2 Aircraft Fast Dynamics and Effectiveness of Aerodynamic Actuators

6.2.1 Aircraft rotation dynamics

The equation for the rotational movement of a rigid aircraft in the body reference frame (see Annex A) can be expressed as:

$$\underline{M} = I_m \underline{\dot{\omega}} + \underline{\omega} \times (I_m \underline{\omega}) \quad (6.1)$$

where $\underline{M} = (L \ M \ N)'$, L , M , N are respectively the roll, pitch, and yaw aerodynamic torques, I_m is the matrix of inertial moments, $\underline{\omega}$ is the inertial rotational velocity written in the body reference $(p, q, r)'$ where p is the roll rate, q is the pitch rate and r is the yaw rate, $\underline{\dot{\omega}}$ is the inertial rotational acceleration in the body-fixed axis system, \times is the cross product operator.

The aerodynamic moments along each body axis are given by:

$$L = \frac{1}{2} \rho V^2 S l C_l, \quad M = \frac{1}{2} \rho V^2 S l C_m, \quad N = \frac{1}{2} \rho V^2 S l C_n \quad (6.2)$$

where C_l , C_m and C_n are respectively the roll, pitch and yaw dimensionless aerodynamic coefficients. Here V is the airspeed, ρ is the density of air, S and l are respectively reference area and length specific to the considered aircraft.

The dimensionless coefficients of the main axis aerodynamic torques can in general be expressed such as:

$$C_m = C_{m0} + C_{m\alpha} \cdot \alpha + C_{mq} \cdot ql/V + C_{m\delta_{hs}} \cdot \delta_{hs} + \underline{C}_{m\delta_q}' \cdot \underline{\delta}_q \quad (6.3a)$$

$$C_l = C_{l0} + C_{l\beta} \cdot \beta + C_{lp} \cdot pl/V + C_{lr} \cdot rl/V + \underline{C}_{l\delta_p}' \cdot \underline{\delta}_p + \underline{C}_{l\delta_r}' \cdot \underline{\delta}_r \quad (6.3b)$$

$$C_n = C_{n0} + C_{n\beta} \cdot \beta + C_{np} \cdot pl/V + C_{nr} \cdot rl/V + \underline{C}_{n\delta_p}' \cdot \underline{\delta}_p + \underline{C}_{n\delta_r}' \cdot \underline{\delta}_r \quad (6.3c)$$

where α is the angle of attack, β is the side slip angle, $\underline{\delta}_p$, $\underline{\delta}_q$, $\underline{\delta}_r$ are respectively the aileron, elevator and rudder deflections while δ_{hs} is the deflection of the trimmable horizontal stabilizer, if any.

6.2.2 Multiplicity aerodynamic actuators for transportation aircraft

As seen from Chapter 3, considering mainly the size of modern transportation aircraft as well as the reliability issue, the aircraft present in general a multiplicity of actuators to generate contributions to the roll, pitch and yaw moments. The effectiveness of these control surfaces appears through the contributions of their angular deflections to these moments through dimensionless coefficients as in relations (6.3a), (6.3b) and (6.3c). According to the relationship between aerodynamic derivatives and aerodynamic torque, the expressions of the different aerodynamic torques generated by these control surfaces can be approximated by affine forms with respect to the corresponding deflections of the different aerodynamic actuators, so that equations related to torques and deflections can be expressed as:

$$L(t) = L^0(t) + \sum_{i \in I^L} C_i^L(t) \delta_i(t) \quad (6.4a)$$

$$M(t) = M^0(t) + \sum_{i \in I^M} C_i^M(t) \delta_i(t) \quad (6.4b)$$

$$N(t) = N^0(t) + \sum_{i \in I^N} C_i^N(t) \delta_i(t) \quad (6.4c)$$

with $I = I^L \cup I^M \cup I^N$, where I^L is the set of actuators generating some roll moment, I^N is the set of actuators generating some yaw torque, while I^M is the set of actuators generating pitch moments. Here the current values $L^0(t)$, $M^0(t)$ and $N^0(t)$ as well as $C_i^L(t)$, $C_i^M(t)$ and $C_i^N(t)$ depend on the airspeed V , the flight level and on the values of α , β , p , q and r . Global aerodynamic torques generated by aircraft aerodynamic actuators can be rewritten in a global affine form as:

$$\underline{M} = \underline{M}^0 + C \cdot \underline{\delta} \quad \text{with} \quad \underline{\delta} \in R^{|I|} \quad \text{and} \quad C \in R^{3 \times |I|} \quad (6.5)$$

To illustrate the multiplicity of actuators on transportation aircraft, Figure 6.1 displays a simplified version of Figure 1.1, where the different aerodynamic surfaces on A340's wing which contribute mainly to the roll moment are shown.

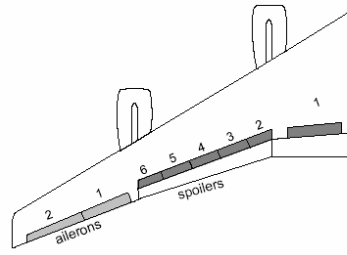


Figure 6.1 Example of Wing Actuators (A340)

6.2.3 A reference model for rotational maneuver

To make apparent the effects of the deflections of the fast actuators on the rotational accelerations, substituting torques expression (6.5) into (6.1). Then the dynamics of rotational accelerations can be written as:

$$\dot{\underline{\omega}} = I_m^{-1} \left(\underline{M}^0 + C \cdot \underline{\delta} - \underline{\omega} \times (I_m \underline{\omega}) \right) \quad (6.6)$$

For the actuators whose deflection is present in the above relation, it is in general assumed that they present a linear domain in which they obey to first order dynamics such as:

$$\dot{\underline{\delta}} = \Lambda (\underline{\delta}_c - \underline{\delta}) \quad (6.7)$$

where $\underline{\delta}_c$ is the control signal and Λ is a constant diagonal matrix whose elements λ_i are the reciprocals of time constants of each actuator ($\lambda_i = 1/\tau_i$). Current values for τ_i in transportation aircrafts are down to 1/30 s.

Considering relations (6.6) and (6.7), the rotation vector $\underline{\omega}$ is related to the control signal $\underline{\delta}_c$ by a rather complex nonlinear second order differential relation. Then it appears opportune to consider that the expected nominal rotational dynamics have to follow second order linear dynamics with adequate damping ratios, natural frequencies and constant time responses. So a reference model can be given by:

$$\ddot{\underline{\omega}} + 2Z_\omega W_\omega \dot{\underline{\omega}} + W_\omega^2 (\underline{\omega} - \underline{\omega}_c) = 0 \quad (6.8)$$

where $\underline{\omega}$ is nominal rotation rates vector and $\underline{\omega}_c$ is the desired rotational rates vector taken as

input signal for this reference model. Here Z_ω , W_ω are respectively the damping ratios and natural frequencies organized in 3×3 diagonal matrices. Let the resulting overall response time for these dynamics to step inputs along each axis be given by $T_R = \max\{T_p, T_q, T_r\}$. Here it is expected for feasibility reasons that the chosen time responses T_i are many times the value of the time responses of the involved actuators in a fault free situation. When the remaining handling qualities do not allow an acceptable behaviour during the realization of the intended standard maneuver, the feasibility of downgraded reference maneuvers can be investigated.

6.3 Actuators Constraints and Limitations

The deflection of each aerodynamic surface is subject to minimum and maximum bounds while its deflection rates are limited by the adopted actuator technology. This should limit somehow the capability of the aircraft to perform extreme maneuvers relying on large deflection angles or on very fast angular rates for the actuators. Also, global physical constraints must be taken into account to ensure aircraft integrity especially when some actuators fail. These limitations are taken into consideration explicitly here as they should be considered by any efficient fault tolerant control system.

6.3.1 Actuators Position and Speed Limitations

In general, the linear dynamics given in (6.7) are limited by position and rate constraints such as:

$$\delta_i^{\min} \leq \delta_i \leq \delta_i^{\max} \quad i \in I \quad (6.9a)$$

$$\dot{\delta}_i^{\min} \leq \dot{\delta}_i \leq \dot{\delta}_i^{\max} \quad i \in I \quad (6.9b)$$

where δ_i^{\min} , δ_i^{\max} , $\dot{\delta}_i^{\min}$ and $\dot{\delta}_i^{\max}$ are respectively the low and upper bounds of deflection position and deflection speed values.

6.3.2 Global Constraints

Global constraints are in general related with structural considerations. It has been shown that

total wing bending and torsion moments during maneuver can be written in an affine form [Roux, 2006]:

$$M_{bend}(t) = A_{bend}(t) + \sum_{i \in I^{wing}} Y_{bend}^i(t) \delta_i(t) \quad (6.10a)$$

and

$$M_{tors}(t) = A_{tors}(t) + \sum_{i \in I^{wing}} Y_{tors}^i(t) \delta_i(t) \quad (6.10b)$$

with $I^{wing} \subset I$ is the set of wing actuators contributing to the bending and the torsion moments, where A_{bend} , Y_{bend}^i , A_{tors} and Y_{tors}^i depend on the long run on the flight envelope parameters (airspeed and flight level) and on the short run on the current attitude parameters such as the angle of attack α , the sideslip angle β , pitch and bank angles θ and ϕ and the roll, pitch and yaw rates p , q and r .

To take into account the structural integrity of the aircraft, global constraints considering the maximum wing bending and torsion moments can be introduced:

$$A_{bend}(t) + \sum_{i \in I^{wing}} Y_{bend}^i(t) \delta_i(t) \leq M_{bend}^{max} \quad (6.11a)$$

and

$$A_{tors}(t) + \sum_{i \in I^{wing}} Y_{tors}^i(t) \delta_i(t) \leq M_{tors}^{max} \quad (6.11b)$$

where M_{bend}^{max} and M_{tors}^{max} are maximum acceptable bending and torsion moments at the wing root. Here it is supposed that the satisfaction of these global constraints implies the satisfaction of local bending and torsion moment constraints.

6.4 Formulation of the Off-line Model Following Control Problem

Model predictive control (MPC) is widely used today in control because of its ability to cope with hard constraints on controls and states as well as with modeling errors for the dynamics of the controlled process [Mayne et al., 2000]. In the flight control field, since actuator failures can result in new constraints, some authors have tried during the last decade to apply the MPC approach to design fault tolerant flight control systems. For example, in [Maciejowski & Jones, 2003] a MPC based controller was proposed to tackle with the fault situation found in the

accident of flight El Al 1862. In [Gaulocher et al., 2007; Lafourcade et al., 2010], actuator assignment has been considered for aircraft flight control using MPC without taking into account the actuator dynamics, while in [Luo et al., 2004] a MPC based dynamic control allocation algorithm considering actuator dynamics has been developed for a re-entry vehicle. However, MPC has proven most successful when controlling slow processes in the industrial field. In fact, the MPC approach implies at each time step the recurrent solution of an optimization problem whose size is roughly proportional to the size of the control horizon. Even if the resulting problem can be formulated as a standard LQ optimization problem and with the current development of on-board computer capabilities, the direct adoption of this approach to perform flight dynamics on-line control, may appear rather questionable. If one of the resulting issues risen by MPC adoption is relative to possible numerical problems, another one is the quality of the resulting control performances which is not guaranteed, specially in the presence of fault, either successfully identified or not. However, to perform the present off-line study, these characteristics of the MPC approach are not limitative while its capability to take explicitly into account actuator constraints appears decisive.

6.4.1 The adopted predictive models

Equations (6.6) and (6.7) represent the complete rotation dynamics of the aircraft and their discretization according to Euler's method, provides the discrete expressions:

$$\underline{\omega}(k+1) = \underline{\omega}(k) + I_m^{-1}T \left[\underline{M}^0 + C \cdot \underline{\delta}(k) - \underline{\omega}(k) \times (I_m \underline{\omega}(k)) \right] \quad (6.12)$$

$$\underline{\delta}(k+1) = \underline{\delta}(k) + \Lambda T \left[\underline{\delta}_c(k) - \underline{\delta}(k) \right] \quad (6.13)$$

where T is the sampling period.

Since when considering longitudinal or lateral maneuvers for a transportation aircraft, the cross product of relation (6.12) remains in general very small, so the following approximate linear model for the rotational dynamics is adopted:

$$\underline{\omega}(k+1) = \underline{\omega}(k) + I_m^{-1}T \left[\underline{M}^0 + C \cdot \underline{\delta}(k) \right] \quad (6.14)$$

This simplification allows to avoid coping, within the MPC approach, with a recurrent non convex optimization problem, whose resolution may face numerical difficulties such as local non

optimal minima. Then, combining relations (6.13) and (6.14), the following model which is a rough linear approximation of the discrete rotation dynamics is obtained:

$$\underline{\omega}(k+1) = \underline{\omega}(k) + I_m^{-1}T \left[\underline{M}^0 + C(I_\delta - T\Lambda)\underline{\delta}(k-1) + CT\Lambda\underline{\delta}_c(k-1) \right] \quad (6.15)$$

where I_δ is an identity matrix with size $|I| \times |I|$.

When considering the Model Predictive Approach the above discrete linear model will be used to predict the behaviour of the rotational dynamics over the receding control horizon T_R . Then at current time k , the prediction of the rotation vectors $\underline{\omega}^p(k+i|k)$ $i=1$ to K , where K is the prediction horizon, given here by $K = \lceil T_R / T \rceil$, are such as:

$$\underline{\omega}^p(k+1|k) = \underline{\omega}(k) + I_m^{-1}T \left[\underline{M}^0 + C \cdot \underline{\delta}(k) \right] \quad (6.16a)$$

and

$$\underline{\omega}^p(k+i|k) = \underline{\omega}^p(k+i-1|k) + I_m^{-1}T \left[\underline{M}^0 + C \cdot \underline{\delta}^p(k+i-1|k) \right] \quad i=2 \text{ to } K \quad (6.16b)$$

with the predicted deflections of actuators at time k given by:

$$\underline{\delta}^p(k+i|k) = \underline{\delta}^p(k+i-1|k) + \Lambda T \left[\underline{\delta}_c(k+i-1|k) - \underline{\delta}^p(k+i-1|k) \right] \quad i=1 \text{ to } K-1 \quad (6.16c)$$

Here at time k , $\underline{\delta}^p(k|k) = \underline{\delta}(k)$, $\underline{\delta}^p(k+i|k)$, $i=1$ to $K-1$, is the predicted deflection value predicted at time k for time $k+i$, $\underline{\delta}_c(k+i|k)$, $i=0$ to $K-2$, is the computed input solution for the recurrent optimization problem used by the MPC method, while $\underline{\delta}_c^*(k) = \underline{\delta}_c(k|k)$ is the adopted input solution for period k .

To proceed with the comparison of this predicted behaviour with the reference behaviour, the reference model of relation (6.8) must be also discretized. Let:

$$\begin{aligned} \underline{x}_1(k) &= \underline{\omega}(k) \\ \underline{x}_2(k) &= \underline{\dot{\omega}}(k) \end{aligned}$$

Then, according to Euler's method, the first order derivative and the second one of the reference signal can be expressed as:

$$\begin{aligned} \underline{\dot{\omega}}(k) &= \left[\underline{x}_1(k+1) - \underline{x}_1(k) \right] / T \\ \underline{\ddot{\omega}}(k) &= \left[\underline{x}_2(k+1) - \underline{x}_2(k) \right] / T \end{aligned} \quad (6.17a)$$

Substituting (6.17a) into (6.8), a state space can be found:

$$\begin{bmatrix} \underline{x}_1(k+1) \\ \underline{x}_2(k+1) \end{bmatrix} = \begin{bmatrix} I_\omega & TI_\omega \\ -TW_\omega^2 & (I_\omega - 2TZ_\omega W_\omega) \end{bmatrix} \begin{bmatrix} \underline{x}_1(k) \\ \underline{x}_2(k) \end{bmatrix} + \begin{bmatrix} 0 \\ TW_\omega^2 \end{bmatrix} \tilde{\omega}_c(k) \quad (6.17b)$$

where I_ω is an identity matrix with size 3×3 .

Since only step responses starting at steady conditions are considered, the predicted trajectory for the reference rotation vector is given at time k by:

$$\tilde{\omega}(k+i) = \begin{bmatrix} I_\omega & 0 \end{bmatrix} \left\{ \begin{bmatrix} I_\omega & TI_\omega \\ -TW_\omega^2 & (I_\omega - 2TZ_\omega W_\omega) \end{bmatrix} \begin{bmatrix} \underline{x}_1(k+i-1) \\ \underline{x}_2(k+i-1) \end{bmatrix} + \begin{bmatrix} 0 \\ TW_\omega^2 \end{bmatrix} \tilde{\omega}_c \right\} \quad i = 1 \text{ to } K \quad (6.17c)$$

with

$$\underline{x}_1(k) = \underline{x}_2(k) = \underline{0}, \tilde{\omega}_c(k+i) = \tilde{\omega}_c \quad i = 0 \text{ to } K-1 \quad (6.17d)$$

6.4.2 Formulation of the recurrent optimization problem

According to the considered problem and following the MPC technique, an objective function can be formulated at time k such as:

$$J(k) = \sum_{i=1}^K \left\| \tilde{\omega}(k+i) - \omega^p(k+i|k) \right\|^2 \quad (6.18)$$

where $\|\cdot\|$ is the Euclidian norm. This function will be minimized with respect to the control inputs $\underline{\delta}_c(k+i|k)$, $i = 0$ to $K-1$, while the predicted actuator deflections should satisfy positions and rates constraints. It is worth to observe that in the adopted formulation of the objective function, there is no need to introduce explicitly a penalty relative to control deviations since they are taken into account directly by the actuator constraints. Also, no differentiated weightings are needed in the penalty relative to the deviation of the output from its nominal behaviour if no priority is introduced between elementary aircraft rotations when considering the maneuverability. Then, the problem of the choice of the quadratic weightings of the objective function which has to be faced with classical MPC is not an issue here.

The necessary discretization of constraints (6.9a) and (6.9b) leads to:

$$\underline{\delta}^{\min} \leq \underline{\delta}^p(k+i|k) \leq \underline{\delta}^{\max} \quad i = 1 \text{ to } K-1 \quad (6.19a)$$

$$T \underline{\delta}^{\min} \leq \underline{\delta}^p(k+i|k) - \underline{\delta}^p(k+i-1|k) \leq T \underline{\delta}^{\max} \quad i = 2 \text{ to } K-1 \quad (6.19b)$$

Also the predicted actuator deflections should satisfy structural constraints such as:

$$A_j + Y_j \underline{\delta}^p(k+i|k) \leq M_j^{\max} \quad i = 1 \text{ to } K \quad j \in \{bend, tors\} \quad (6.20)$$

while it is considered that the control input must also satisfy the extreme deflection constraints:

$$\underline{\delta}^{\min} \leq \underline{\delta}_c(k+i|k) \leq \underline{\delta}^{\max} \quad i = 0 \text{ to } K-2 \quad (6.21)$$

Considering the predictive model of relation (6.16c), when introducing the input parameters $\underline{\delta}_c$, these inequalities (6.19a), (6.19b), (6.20) can be transformed into affine inequalities with respect to these input parameters.

6.5 The Proposed Neural Network Solver

As seen from above, an optimization problem resulting from the MPC approach to solve the model following problem is introduced. This problem has been reformulated as a recurrent LQ optimization problem. In Chapter 5, different LQ optimization solvers have been displayed and discussed. Among them, specialized neural networks provide fast convergence which is of interest with the necessity to solve repeatedly this problem at each new sampled time. Then, a dynamic neural network solver, as discussed in Chapter 5 has been adopted to solve the current problem.

6.5.1 General formulation of the recurrent LQ problem

The minimization of objective function $J(k)$ at time k under constraints (6.19a), (6.19b), (6.20) and (6.21) leads to the resolution of a LQ problem which can takes the form:

$$\min_{\underline{\delta}_c(k)} \underline{\delta}_c(k)^T R(k) \underline{\delta}_c(k) + \underline{s}(k)^T \underline{\delta}_c(k) \quad (6.22)$$

$$\text{s.t.} \quad A(k) \underline{\delta}_c(k) + \underline{b}(k) \leq \underline{0} \quad (6.23)$$

$$\underline{\delta}_c^{\min} \leq \underline{\delta}_c(k) \leq \underline{\delta}_c^{\max} \quad (6.24)$$

where

$$\underline{\underline{\delta}}_c(k) = \begin{bmatrix} \underline{\delta}_c(k|k) \\ \underline{\delta}_c(k+1|k) \\ \vdots \\ \underline{\delta}_c(k+K-2|k) \end{bmatrix} \in R^{l \times (K-1)} \quad (6.25)$$

In Annex D the expressions of the current parameters $R(k)$, $\underline{s}(k)$, $A(k)$, $\underline{b}(k)$, $\underline{\delta}^{\min}$ and $\underline{\delta}^{\max}$ of the LQ optimization problem considered at stage k are given. There it can be checked that matrix $R(k)$ is positive semidefinite.

6.5.2 Fast neural solution for the LQ problem

As seen from Chapter 5, many mathematical programming techniques are today available to solve convex optimization problems which adopt the general LQ formulation displayed in (6.22), (6.23) and (6.24). Among them, solvers based on dynamic neural networks whose convergence speed is not compromised by the size of the problem have been proposed to solve the considered problem in the context of signal processing, robot control where real-time solving is desired [Xia & Wang, 2001; Zhong & Mora-Camino, 2012]. Thanks to the unchanged convergent speed, dynamic neural networks is a promising way to solve the allocation problem when the size of the problem is large, as it should be the case when adopting the MPC approach.

For using the neural networks model discussed in Chapter 5, at first the state of the corresponding dynamic neural network is defined as:

$$\underline{x} = \begin{bmatrix} \underline{\delta}^T & \underline{u}^T \end{bmatrix}^T \quad (6.26)$$

where \underline{u} is the dual variable vector associated to the inequality constraints (6.23) and its dynamics obeys to the piecewise differential equation as in (5.31), rewritten here:

$$\frac{d\underline{x}}{dt} = \eta \left(I_{d3} + N^T \right) \left\{ P_{\Omega} \left(\underline{x} - (N\underline{x} + \underline{\rho}) \right) - \underline{x} \right\} \quad (6.27)$$

where η is a positive parameter, I_{d3} is an identity matrix, N and $\underline{\rho}$ are defined by:

$$N = \begin{bmatrix} R & A^T \\ -A & 0 \end{bmatrix} \quad \underline{\rho} = \begin{bmatrix} \underline{s}^T & -\underline{b}^T \end{bmatrix}^T \quad (6.28)$$

Here Ω is the primal-dual feasible set defined by:

$$\Omega = \{ \underline{x} \mid \underline{\mu}^- \leq \underline{x} \leq \underline{\mu}^+ \} \quad \text{with} \quad \underline{\mu}^- = \left[\left(\underline{\delta}^{\min} \right)^T \underline{0}^T \right]^T \quad \text{and} \quad \underline{\mu}^+ = \left[\left(\underline{\delta}^{\max} \right)^T \underline{\Delta}^T \right]^T \quad (6.29)$$

where $\underline{\Delta}$ is a vector whose elements are all a very large positive number and P_{Ω} is a projection operator over Ω such as:

$$P_{\Omega} [x_i] = \begin{cases} \mu_i^- & \text{if } x_i \leq \mu_i^- \\ x_i & \text{if } \mu_i^- < x_i < \mu_i^+ \\ \mu_i^+ & \text{if } x_i \geq \mu_i^+ \end{cases} \quad (6.30)$$

Since the MPC approach is incremental over a receding time window, the initial state of the dynamic neural network at step $k+1$ has been taken equal to the solution of the LQ problem of step k .

6.6 Numerical Results for the Proposed Approach

Here a large transport aircraft with a reference flight speed of 120m/s has been considered. This aircraft has multiple actuators which provide some redundancy for performing the considered maneuver:

Two ailerons per wing, two elevators per side, and two rudders.

These actuators are supposed to follow first-order dynamics with position and rate limitations. The values of these limitations and of the time constants of the actuator dynamics have been adopted from [Lambrechts et al., 1997] and are displayed in Table 6.1. A flight dynamics simulator of this aircraft has been developed within the Simulink environment and used as test bed.

Table 6.1 Parameters of actuators under nominal condition

Actuator	No. of actuators	Position limits	Slew rate limits	Time constant
aileron	4	-25° ~ 25°	-25°/s ~ 25°/s	0.15s
elevator	4	-25° ~ 10°	-15°/s ~ 15°/s	0.15s
rudder	2	-30° ~ 30°	-25°/s ~ 25°/s	0.3s

The basic maneuver which has been considered here is a pure roll maneuver under different

actuator failure situations. Figure 6.2 displays the roll input (p_{std}) composed of two inverse steps and the output (p_{ref}) resulting from the second order linear model (damping ratio $z_p=0.8$ and natural frequency $w_{np}=2.5$ rad/s) chosen as reference.

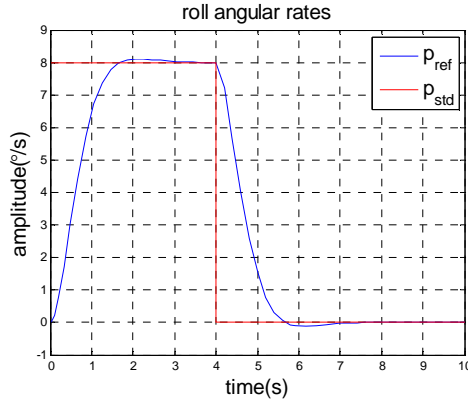


Figure 6.2 Standard roll input and reference output

The sampling period for discretization has been chosen equal to 0.05 s and since the response time of the reference maneuver is 2 seconds, the width of the sliding time window used in the MPC approach has been taken equal to $K=40$. The recurrent LQ problem associated to MPC is then composed of 160 variables with 320 constraints. The dynamic neural network solver when tuned properly (choice of the value of η) produced each solution after a computation time close to 0.01 s. This shows, that if the computation feasibility was the only criteria, MPC based flight control systems could be of interest.

The failure cases which are displayed here are relative to three situations:

- *case a*: the maximum deflection of the outer ailerons becomes limited to 10° .
- *case b*: the time constants of the outer ailerons become equal to 0.6 s.
- *case c*: the outer ailerons are stuck at neutral position and the maximum deflection of the inner ailerons is limited to 15° .

Figure 6.3, Figure 6.4 and Figure 6.5 display the output behaviour obtained through the MPC process in these three cases.

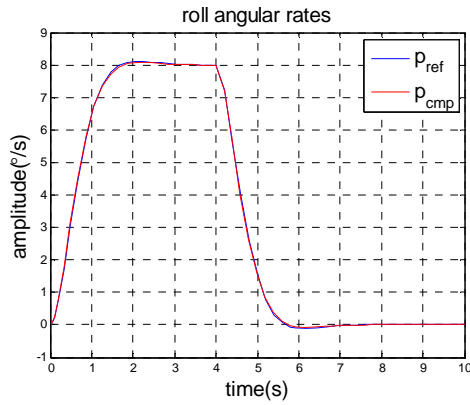


Figure 6.3 Case a: computed output and reference output

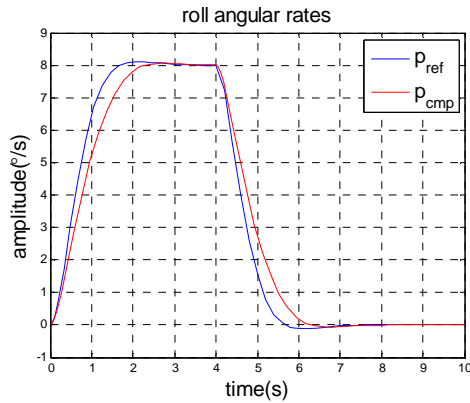


Figure 6.4 Case b: computed output and reference output

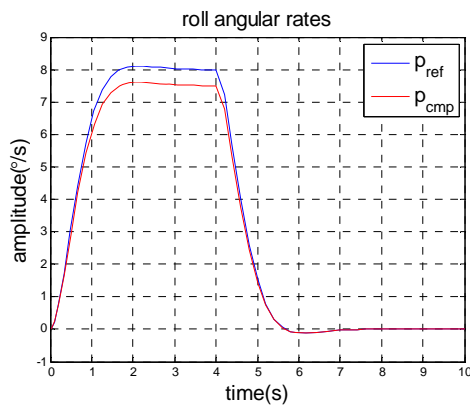


Figure 6.5 Case c: computed output and reference output

From the displayed results it appears that *case a* can be tackled as a fail-operational situation since the computed output is almost identical to the reference output while the other two cases should be tackled as fail-passive situations: in one case, *case b*, the response time of the basic roll

loop is increased by 25% while in the other case, *case c*, the roll rate is limited to 7.5 deg/s.

6.7 Conclusion

In this chapter, the proposed approach to evaluate the remaining handling qualities of a transportation aircraft in an aerodynamic actuator failure situation has been based on the off-line resolution of a model following problem using a MPC approach coupled with a dynamic neural network solver to get a solution to the associated LQ problem.

The maneuverability issue in the present study has been limited to the control of the three rotations along the main axis of a transportation aircraft, since they are basic for stabilization, attitude control and further maneuvers. The numerical results corresponding to three failure scenarios show the computational feasibility of the proposed approach.

The proposed approach can be applied to other maneuvers as well as to other types of actuators than those considered in this study, specially the engines. This provides a new tool to predict downgraded handling qualities resulting from actuator failures and then allows to build an exhaustive knowledge base which should be useful for the supervision of an efficient fault tolerant flight control system.

CHAPTER 7

ONLINE ACTUATOR REASSIGNMENT FOR FAULT TOLERANT MANEUVERS

7.1 Introduction

In this chapter is considered the case in which actuator reassignment is needed to continue to perform a feasible maneuver, even with some failed actuators. Considering the differential flatness property of flight dynamics [Wenchi Lu et al., 2004], it is shown that the proposed two stages approach (see Chapter 4) can be adopted when considering has virtual inputs the three external main moments as well as eventually the thrust. To illustrate the feasibility of this approach, the case of a lateral maneuver in which as aircraft goes from straight level flight to equilibrated turn is treated. The values of the corresponding virtual inputs are computed through a nonlinear inverse control technique while the actuator reassignment problem is formulated as a LQ problem to be solved online.

7.2 Virtual Inputs for a General Maneuver

Before considering a particular maneuver realized currently by transportation aircraft, here is first analyzed the case of a general maneuver performed by any vehicle or system, to display the generality of the proposed approach.

7.2.1 Virtual inputs for differential flat systems

For a given configuration, the dynamics of a physical system can be described by the general state equation:

$$\dot{\underline{x}} = f(\underline{x}, \underline{u}), \quad \underline{x} \in R^n, \underline{u} \in R^m \quad (7.1)$$

where \underline{x} is the state and \underline{u} is the vector of its elementary inputs, f is a smooth function.

Let us consider the problem of controlling p outputs of this system: $y_i, i = 1$ to p , with $p \leq m$ with:

$$\underline{y} = h(\underline{x}) \quad (7.2)$$

where h is a smooth function.

In general the inputs having some effects on these outputs can be combined into general effects,

or virtual inputs of the same dimension as the controlled outputs. For example, in the case of mechanical systems, these virtual inputs will be the components of the resultant forces or moments applied to the system. Then the state equation describing the behavior of the system can be rewritten as:

$$\dot{\underline{x}} = f_v(\underline{x}, \underline{v}), \quad \underline{x} \in R^n, \underline{v} \in R^p \quad (7.3)$$

where f_v is a smooth function and where :

$$\underline{v} = G(\underline{x}, \underline{u}) \quad (7.4)$$

The above system (7.2), (7.3) is said *differentially flat* [M Fliess et al., 1992; Michel Fliess et al., 1995] with respect to the p virtual inputs, if and only if, the state vector and the virtual inputs can be expressed as smooth functions of \underline{y} and a finite number of its derivatives:

$$\underline{x} = \phi_x(\underline{y}, \dot{\underline{y}}, \ddot{\underline{y}}, \dots, \underline{y}^{(q)}) \quad (7.5)$$

$$\underline{v} = \phi_v(\underline{y}, \dot{\underline{y}}, \ddot{\underline{y}}, \dots, \underline{y}^{(q+1)}) \quad (7.6)$$

In that case, the output \underline{y} is said to be a *flat output*.

In fact, many systems have proved to be differentially flat, providing ground to new control law designs [Wenchi Lu, 2005] as well as new fault detection and identification methods [N. Zhang, 2010].

From equation (7.6) it can be seen that to each trajectory followed by the flat output vector can be computed online the necessary values of the virtual input \underline{v} all along the trajectory.

When some failure k occurs, it results in the impediment of some of the elementary inputs so that the basic input vector \underline{u} can be such as:

$$\underline{u}_k = \begin{bmatrix} \underline{u}_{\bar{F}_k} \\ \underline{u}_{F_k} \end{bmatrix} \quad (7.7)$$

where \bar{F}_k is for fault free elementary inputs and F_k is for faulty ones.

Then, to pursue the planned maneuver, the fault free elementary inputs should be set online to values so that:

$$\underline{v} = G_k(\underline{x}, \underline{u}_{\bar{F}_k}) \quad (7.8)$$

where
$$G_k(\underline{x}, \underline{u}_{F_k}) = G(\underline{x}, \underline{u}_k) \tag{7.9}$$

which constitute an online reassignment problem for the fault free elementary inputs.

7.2.2 Virtual inputs for aircraft maneuvers

It has been shown in [Wenchi Lu, 2005] that the components of the position of the center of gravity of an aircraft, x, y, z and its heading angle ψ , whose time history define the trajectory of the aircraft are implicit flat outputs (see [Wenchi Lu et al., 2004]) with flat entries ϕ, θ, ψ and T , for the guidance dynamics of the aircraft. Here ϕ is its bank angle, θ is the pitch angle of the aircraft and T is the total engine thrust. As well it has been shown that the piloting dynamics of the aircraft are differentially flat with ϕ, θ and ψ as flat outputs while L, M and N as flat entries, where L, M and N are respectively the roll, pitch and yaw moments created by the aerodynamic actuators. This is shown in Figure 7.1 where the angles χ and γ are respectively the aerodynamic azimuth angle and flight path angle (or "slope"). The angle α, β and μ are respectively angle of attack, slid slip angle and the aerodynamic angle of roll. p, q and r denote respectively angular rates of roll, pitch and yaw. V is the airspeed.

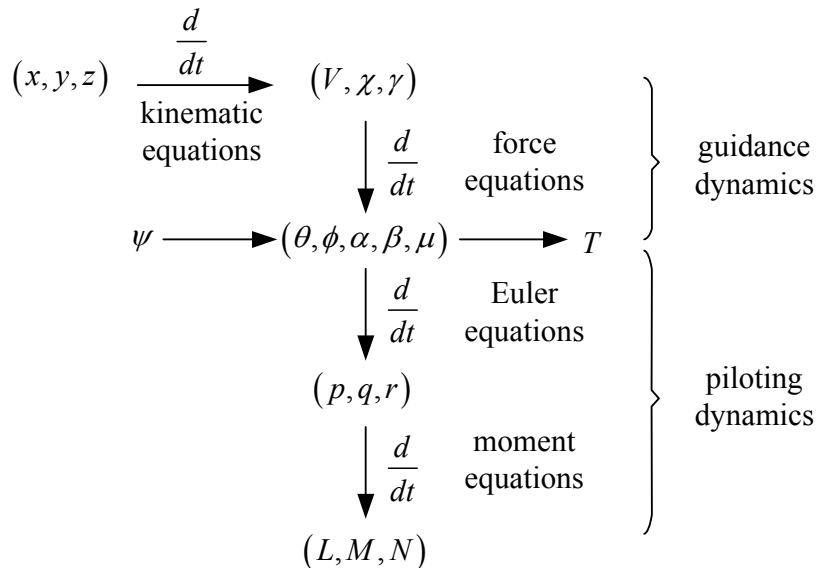


Figure 7.1 Illustration of the global flatness property of aircraft dynamics

Then, if L, M and N appear as natural virtual inputs for angular maneuvers, L, M, N and T appear to be virtual inputs for the guidance dynamics. Then, the effective realization of any piloting

tel-01073618, version 1 -

or guidance maneuver will result in the solution of an elementary actuators assignment problem to solve online equations such as (7.4) in the fault free case and (7.8) in a k^{th} fault case, where \underline{v} is computed online from the intended maneuver. Of course, actuators limitations as well as other structural constraints should be taken into account.

7.3 The Case of an Equilibrated Turn Maneuver

Transportation aircraft have to follow today flight plans composed of straight segments connected by curved segments. While flying these curved segments the aircraft is supposed to perform equilibrated turns so that lateral load factor remains small, insuring comfort to passengers, crew and freight.

7.3.1 Equilibrated turn maneuver

The condition for equilibrated turn (also termed as coordinated turn) is that the apparent weight of the aircraft remains in its vertical plane during a steady yaw maneuver at constant flight level and constant ground speed (see Figure 7.2). This implies different relations between the bank angle, the yaw rate, the pitch rate and the ground speed.

Here it is considered that $\phi = \phi_0$ (in general $-33^\circ \leq \phi_0 \leq +33^\circ$) and $\theta = \theta_0$ where θ_0 is a very small angle. Then the Euler equations provide different relations at equilibrium:

First the body angular rates can be expressed as a function of Euler angular rates:

From the Euler's yaw equation:

$$r = -\dot{\theta} \sin \phi + \dot{\psi} \cos \phi \cos \theta$$

leads to:

$$r = \dot{\psi} \cos \phi_0 \cos \theta_0 \quad (7.10a)$$

The Euler's roll equation:

$$p = \dot{\phi} - \dot{\psi} \sin \theta$$

leads to:

$$p = -r \tan \theta_0 / \cos \phi_0 \quad (7.10b)$$

The Euler's pitch equation:

$$q = \dot{\theta} \cos \phi + \dot{\psi} \sin \phi \cos \theta$$

leads to:

$$q = r \tan \phi_0 \quad (7.10c)$$

From Figure 7.2 it appears also that:

$$r = \cos \phi_0 \cdot \cos \theta_0 \cdot \Omega \quad \text{and} \quad \tan \phi_0 = V \Omega / g$$

where g denotes the gravity acceleration, m is the total mass of the aircraft.

Then:

$$r = \frac{g}{V} \cdot \sin \phi_0 \cdot \cos \theta_0 \quad (7.11a)$$

and the relations (7.10a), (7.10b), (7.10c) can be rewritten as:

$$\dot{\psi} = \Omega = \frac{g}{V} \cdot \tan \phi_0$$

$$p = -\frac{g}{V} \cdot \tan \phi_0 \sin \theta_0 \quad (7.11b)$$

$$q = \frac{g}{V} \cdot \frac{\sin^2 \phi_0}{\cos \phi_0} \cos \theta_0 \quad (7.11c)$$

Then it appears that the equilibrated turn is characterized by three angular rates which are parameterized by the chosen bank angle ϕ_0 .

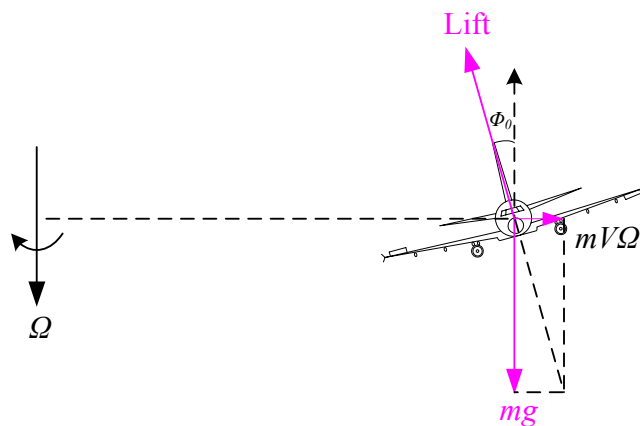


Figure 7.2 Aircraft attitude during an equilibrated turn maneuver

7.3.2 Nonlinear inverse control approach to determine the levels of the virtual inputs

The characteristic outputs for the equilibrated turn maneuver are the roll, pitch and yaw rates. They are given by the moment equations such as [Etkin & Reid, 1996]:

$$\dot{p} = \frac{I_{zz}}{\Delta} L + \frac{I_{xz}}{\Delta} N + \frac{(I_{xx} - I_{yy} + I_{zz})I_{xz}}{\Delta} pq + \frac{(I_{yy} - I_{zz})I_{zz} - I_{xz}^2}{\Delta} qr \quad (7.12a)$$

$$\dot{q} = \frac{1}{I_{yy}} M + \frac{I_{zz} - I_{xx}}{I_{yy}} pr - \frac{I_{xz}}{I_{yy}} (p^2 - r^2) \quad (7.12b)$$

$$\dot{r} = \frac{I_{xz}}{\Delta} L + \frac{I_{xx}}{\Delta} N + \frac{(I_{xx} - I_{yy})I_{xz} + I_{xz}^2}{\Delta} pq + \frac{(I_{yy} - I_{xx} - I_{zz})I_{xz}}{\Delta} qr \quad (7.12c)$$

where $\Delta = I_{xx}I_{zz} - I_{xz}^2$, I_{xx} , I_{yy} and I_{zz} are respectively inertial moments around the roll, pitch, and yaw axes, I_{xz} is the inertial moment on XZ plane of the aircraft.

Then, applying the nonlinear inverse control approach (NLI, see Annex E, also [Andrei, 2010; Isidori, 1983]), it appears that the relative degrees of outputs p , q and r are all equal to one with respect to the virtual inputs L , M and N . This leads to choose for the transient dynamics of these outputs towards they reference values (relations (7.11)) first order dynamics such as:

$$\tau_p \dot{p} + p = -(g/V) \cdot \tan \phi_0 \sin \theta_0 \quad (7.13a)$$

$$\tau_q \dot{q} + q = (g/V) \cdot \frac{\sin^2 \phi_0}{\cos \phi_0} \cos \theta_0 \quad (7.13b)$$

$$\tau_r \dot{r} + r = (g/V) \cdot \sin \phi_0 \cos \theta_0 \quad (7.13c)$$

where τ_p , τ_q and τ_r are respectively time constant of roll, pitch and yaw rate.

Considering the airspeed V is much larger that the gravity acceleration g and θ_0 is very small, so a simplified version of (7.13) can be written as:

$$\tau_p \dot{p} + p = 0 \quad (7.14a)$$

$$\tau_q \dot{q} + q = (g/V) \cdot \tan \phi_0 \sin \phi_0 \quad (7.14b)$$

$$\tau_r \dot{r} + r = (g/V) \cdot \sin \phi_0 \quad (7.14c)$$

Then, the online virtual input constraints can be established according to relations (7.12) and (7.14):

$$M = I_{yy} \left((g/V) \cdot \tan \phi \sin \phi - q \right) / \tau_q - I_{xz} r^2 \quad (7.15a)$$

and

$$\begin{bmatrix} L \\ N \end{bmatrix} = \begin{bmatrix} -I_{xz} \\ I_{zz} \end{bmatrix} \left((g/V) \sin \phi - r \right) / \tau_r + \begin{bmatrix} (I_{zz} - I_{yy})qr \\ I_{xz}qr \end{bmatrix} \quad (7.15b)$$

$$(7.15c)$$

where subscript 0 for ϕ_0 is deleted taking into account of time-varying property during transition.

7.4 Formulation of Actuator Reassignment Problem

Here it is considered that the situations where some failure k affects some of the commonly used actuators but the designed actuator redundancy still allows performing some maneuvers.

Depending on the remaining degree of redundancy between elementary actuators, it may be possible to find a solution matching the moment constraints (6.4) which are rewritten here again for convenient:

$$L(t) = L^0(t) + \sum_{i \in I_k^L} X_i^L(t) \tilde{\delta}_i(t) \quad (7.16a)$$

$$M(t) = M^0(t) + \sum_{i \in I_k^M} X_i^M(t) \tilde{\delta}_i(t) \quad (7.16b)$$

$$N(t) = N^0(t) + \sum_{i \in I_k^N} X_i^N(t) \tilde{\delta}_i(t) \quad (7.16c)$$

with $I_k = I_k^L \cup I_k^M \cup I_k^N$, where I_k^x denote the set of actuators generating the corresponding moments after failure k . $\tilde{\delta}$ denotes the deflection position of actuators after some failures happen.

In this case the maneuver will be performed still in a standard way, otherwise, an approximate maneuver will be performed. In order to get a feasible reassignment which avoids too fast or too large solicitations of the actuators which could activate some structural modes of the aircraft, solutions as close as possible to the solution adopted at the previous control period will be privileged. Also, it is admitted that when the standard maneuver can no more be performed, a

close maneuver, in fact a slightly degraded maneuver, will be retained as a running solution. So, instead of considering the pure satisfaction of the moment constraints (7.16a), (7.16b) and (7.16c), a measure $m(\underline{\tilde{\delta}}, L, M, N)$ of the degree of satisfaction of these constraints is introduced. In this study the following measure of satisfaction of the constraints has been adopted:

$$m(\underline{\tilde{\delta}}, L, M, N) = w_L \left(\sum_{i \in I_k^L} X_i^L(t) \tilde{\delta}_i(t) - L(t) + L^0(t) \right)^2 + w_M \left(\sum_{i \in I_k^M} X_i^M(t) \tilde{\delta}_i(t) - M(t) + M^0(t) \right)^2 + w_N \left(\sum_{i \in I_k^N} X_i^N(t) \tilde{\delta}_i(t) - N(t) + N^0(t) \right)^2 \quad (7.17)$$

where w_L , w_M and w_N are positive weights. Then a LQ optimization problem to be solved on-line is formulated. This problem considers the following objective function to be minimized:

$$J(\underline{\tilde{\delta}}) = \sum_{i \in I_k} \pi_i \cdot (\tilde{\delta}_i(t) - \tilde{\delta}_i(t-T))^2 + \gamma \cdot m(\underline{\tilde{\delta}}, L, M, N) \quad (7.18)$$

where the π_i , $i \in I_k$ and γ are positive weights.

The complete definition of this actuator reassignment problem is such as:

$$\min_{\underline{\tilde{\delta}}} J(\underline{\tilde{\delta}}) \quad (7.19)$$

with the following structural constraints:

$$A_{bend}(t) + \sum_{i \in I_k^{wing}} Y_{bend}^i(t) \delta_i(t) \leq M_{bend}^{max} \quad (7.20a)$$

$$A_{tors}(t) + \sum_{i \in I_k^{wing}} Y_{tors}^i(t) \delta_i(t) \leq M_{tors}^{max} \quad (7.20b)$$

here I_k^{wing} denotes the set of wing actuators contributing to the bending and the torsion moments after failure k .

and with the box constraints:

$$\max \left\{ \delta_i^{min}, \tilde{\delta}_i(t-T) + \dot{\delta}_i^{min} T \right\} \leq \tilde{\delta}_i(t) \leq \min \left\{ \delta_i^{max}, \tilde{\delta}_i(t-T) + \dot{\delta}_i^{max} T \right\} \quad i \in I_{\bar{F}_k} \quad (7.21a)$$

$$\max \left\{ \tilde{\delta}_i^{min}, \tilde{\delta}_i(t-T) + \dot{\delta}_i^{min} T \right\} \leq \tilde{\delta}_i(t) \leq \min \left\{ \tilde{\delta}_i^{max}, \tilde{\delta}_i(t-T) + \dot{\delta}_i^{max} T \right\} \quad i \in I_{FL_k} \quad (7.21b)$$

$$\max \left\{ \tilde{\delta}_i^{min}, \tilde{\delta}_i(t-T) + \dot{\delta}_i^{min} T \right\} \leq \tilde{\delta}_i(t) \leq \min \left\{ \tilde{\delta}_i^{max}, \tilde{\delta}_i(t-T) + \dot{\delta}_i^{max} T \right\} \quad i \in I_{FS_k} \quad (7.21c)$$

with

$$\tilde{\delta}_j = 0 \quad \text{if } i_j \in I_{FF_k}, j \in \{p, q, r, ths\} \quad (7.22a)$$

and

$$\tilde{\delta}_{i_j} = \bar{\delta}_{i_j} \quad \text{if } i_j \in I_{FP_k}, j \in \{p, q, r, ths\} \quad (7.22b)$$

with $I_k = I_{\bar{F}_k} \cup I_{FL_k} \cup I_{FS_k} \cup I_{FF_k} \cup I_{FP_k}$, where $I_{\bar{F}_k}$ is the set of fault free actuators, I_{FL_k} , I_{FS_k} are the set of loss of effectiveness and are respectively the set of actuators whose angular positions, angular speed are subject to additional limitations, I_{FF_k} is the set of float actuators which are not subject to a torque from their servo-control and with a zero deflection, I_{FP_k} is the set of stuck or runaway actuators which are froze at a known angular position. The positive parameters w_L, w_M and w_N are chosen in the case of a roll maneuver such as:

$$w_L \gg w_M \quad \text{and} \quad w_L \gg w_N \quad (7.23)$$

The above LQ problem can be solved using numerical solvers discussed in Chapter 5. Using the previous period value of the deflections of the actuators as initial values of current period, then in a few iterations the solution of this small size LQ problem should be obtained.

7.5 Comparative Application of the Three Solvers to the Actuators Reassignment Problem

Here the same large transport aircraft as in Chapter 6 is considered, with 120 tons, flight speed 120m/s, initial angle of attack is 4° . The corresponding parameters of the aircraft actuator have been given in Section 6.6. Considering the solutions established in Section 7.3.1, the desired roll maneuver leading to an equilibrated turn is defined by the following equations where p_c follows the time history displayed in Figure 7.3:

$$\tau_p \dot{p} + p = p_c \quad (7.24a)$$

$$\tau_q \dot{q} + q = 0 \quad (7.24b)$$

$$\tau_r \dot{r} + r = (g / V) \cdot \sin \phi \quad (7.24c)$$

The time constant in (7.24) are all chosen as 1/3s. Here mainly give the simulation results of the actuator reassignment problem (7.19, 7.21, 7.22). Due to the lack of modeling parameters, structural constraints are not considered. Actually, with the help of command governor such as the approach introduced in Chapter 6, it will not affect the demonstration because solutions to the

problem always exist.

To check the feasibility and performances of three solvers for on-line flight fault tolerant control, two fault scenarios have been considered: a soft one where only a deflection rate is affected by a fault and a hard one where a main actuator remains stuck. The command and desired coordinated maneuver to be performed is illustrated in Figure 7.3 where only roll rate is illustrated and pitch must maintained equal to zero, and yaw rate will change according to equation (7.24c). It is hoped that the final maneuver will be as closely as possible to the desired maneuver. From Figure 7.4 to Figure 7.13, the star symbol denotes the failure instant.

In the numerical application, the sampling time adopted by the digital control system of the different actuators is taken equal to 0.05s. The weights of the optimality criterion (7.18) are chosen as, $\gamma = 10^6$, the weighting parameters for various aerodynamic moments and actuators are all equal to one. The parameters for the neural network are chosen as 10^{10} to replace numerically $+\infty$ in (5.29) and $\eta = 10^7$.

7.5.1 Soft fault scenario

In this case it is assumed that all actuators are fault free except for the rate limits of the right outer aileron which changes to ± 5 deg/s at 1s.

The time evolution of ailerons command is shown in Figure 7.4 where smooth evolutions can be observed and the trajectory are only small different for three solvers. From Figure 7.5 (a) and (b), active set method appears to need much less iterations than the programmed interior point method because of the small size of the problem (the computation time is not accurate because it changes a lot between different run). Also, the whole convergence trajectory of the built neural network for different instant is shown in Figure 7.6 (a), which seems like a staircase because of the fast convergence at each instant and it takes about 0.01ms to convergent as shown in Figure 7.6 (b). Under these three methods, desired maneuver will be almost obtained from Figure 7.7 (a) to (c), the differences between real and desired maneuver mainly from the actuator dynamics. Figure 7.8 (a), (b) and (c) display the speed of the failed actuator which reaches at different stages its speed limit when using active set and neural network and the trajectory look the same under

these two solvers, however, it never reaches speed limit when using interior point due to the contour of objective function become very smooth and not enough iteration has been done for interior point. From them, it seems that the performance of active set method is the best because it will find the exact optimum at a fast speed, and the performance of neural network is almost the same as active set. It appears that these three methods can handle the soft failure situation satisfactory even if many realistic factors such as time lags caused by FDI and NDI are not considered.

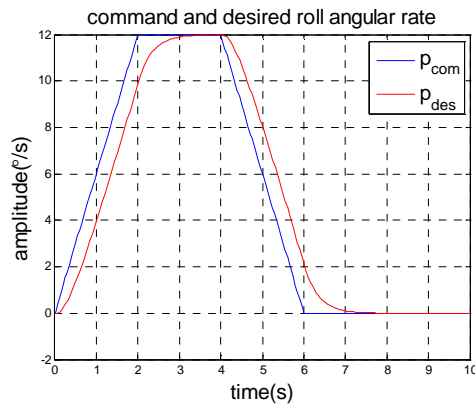
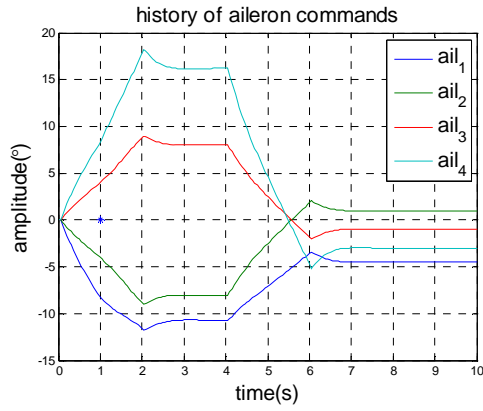
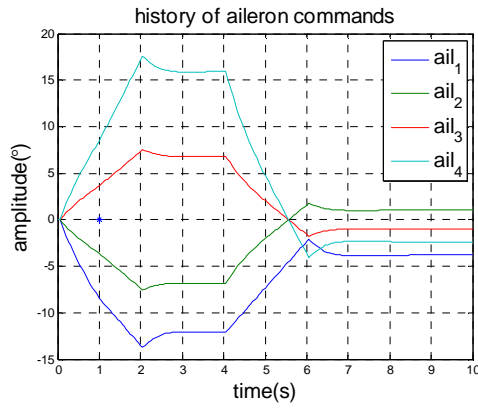


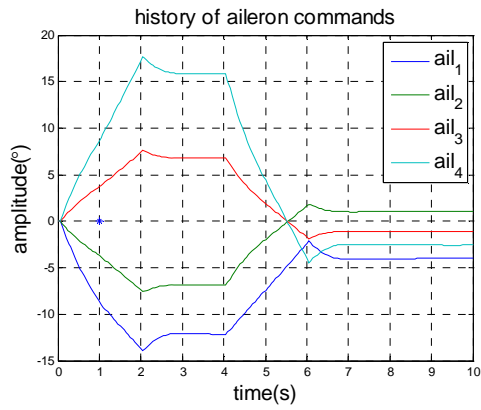
Figure 7.3 Time evolution of command and desired maneuver (only display roll angular rate, pitch and yaw rates remain at zeros)



(a) Result of interior point

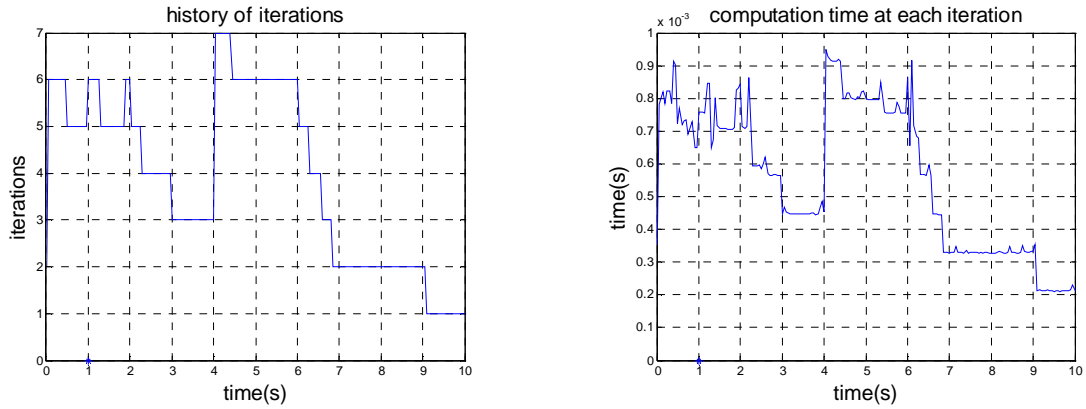


(b) Result of active set

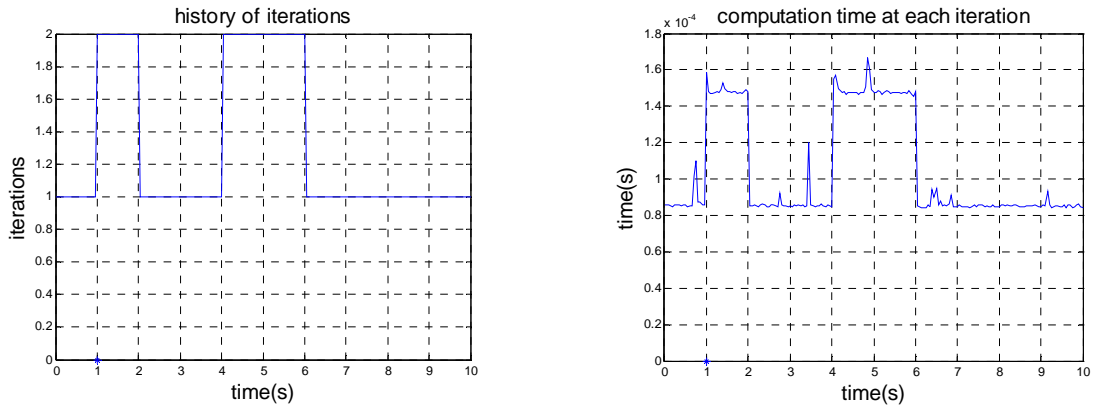


(c) Result of neural network

Figure 7.4 Evolution of ailerons commands under soft fault scenario

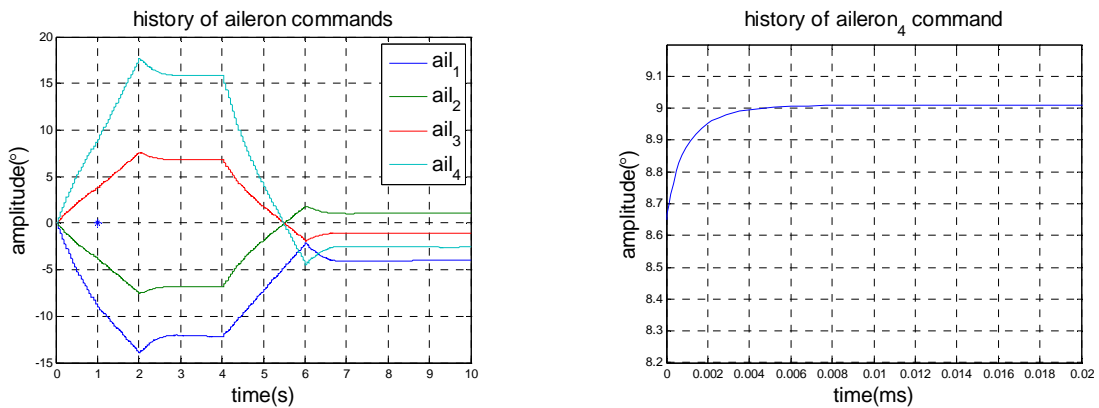


(a) Result of interior point



(b) Result of active set

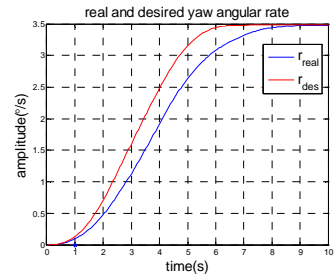
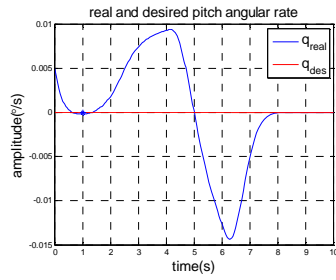
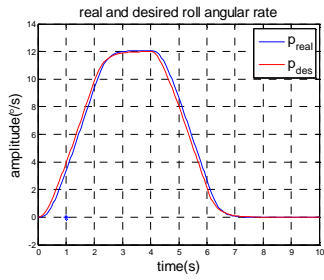
Figure 7.5 Number of iterations and computation time for interior point and active set under soft fault scenario



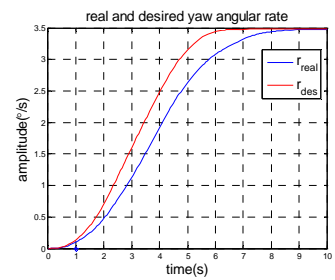
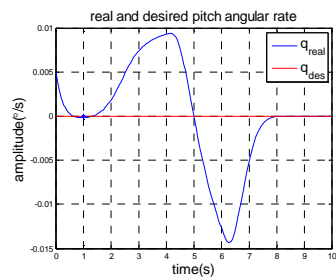
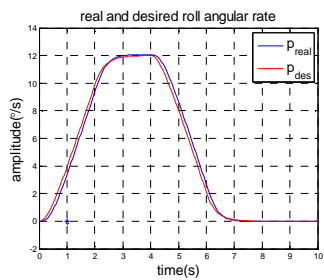
(a) Evolution of network outputs during the whole time-span

(b) zoomed picture to show the convergence speed of network

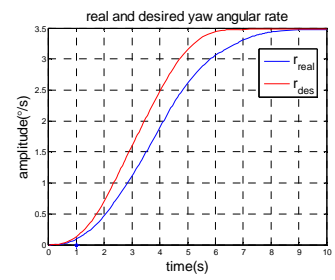
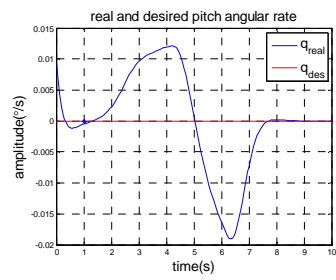
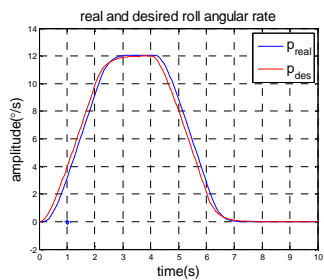
Figure 7.6 Convergent behavior of the neural network solver (0.01ms)



(a) Result of interior point

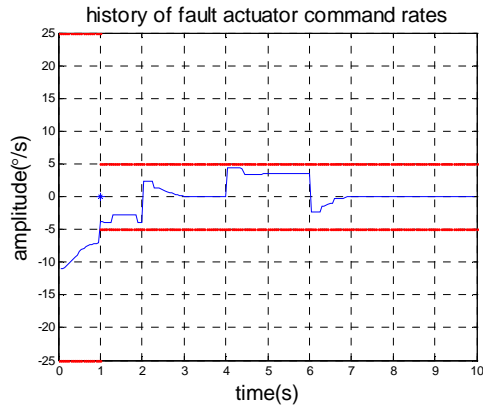


(b) Result of active set

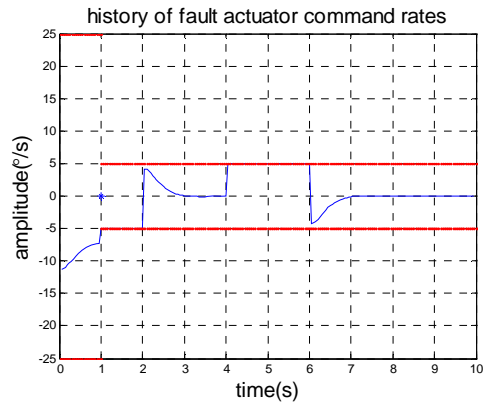


(c) Result of neural network

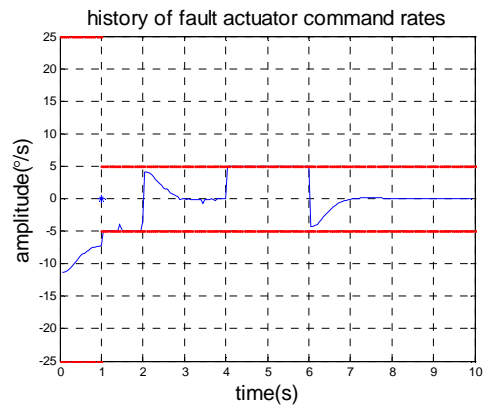
Figure 7.7 The real and desired angular rates under soft fault scenario



(a) result of interior point



(b) result of active set



(c) result of neural network

Figure 7.8 Command rates for the right outer aileron under soft fault scenario

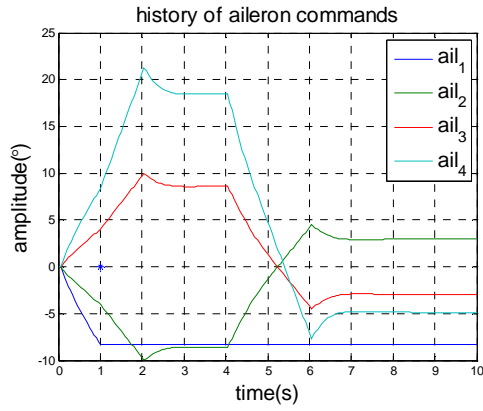
7.5.2 Hard fault scenario

A more serious failure case occurs when an actuator remains stuck at a non neutral position. Here, while the configuration of the neural network remains the same, since a box constraint is considered by the interior point algorithm and for the simplicity of the problem, the column corresponding to the stuck actuator must be deleted from the control effectiveness matrix and the virtual control input and limits should be changed accordingly under interior point and active set methods.

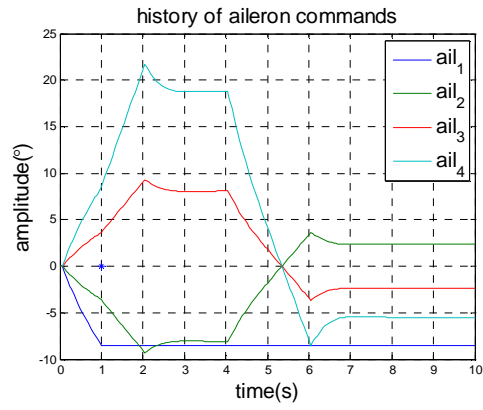
The case where the right outer aileron is stuck at its current position at 1s is simulated. Simulation parameters are the same as before. The corresponding results are displayed from Figure 7.9 to Figure 7.13.

Here again since angular dynamics, actuator deflections and speed are small different with the three techniques, they are displayed in Figure 7.9 and Figure 7.13. From Figure 7.9 and Figure 7.13, it can be concluded that in the considered case, the three methods achieve to deal effectively with the faulty actuator stuck at a fixed position.

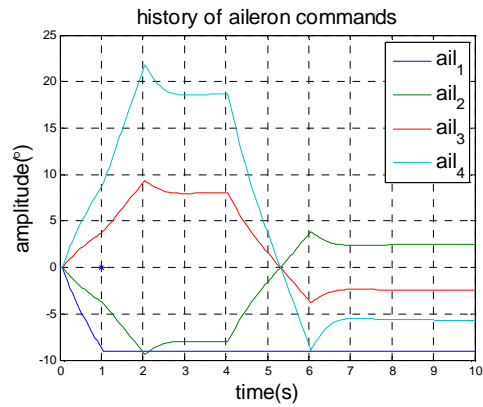
From Figure 7.10 (a) and (b), it also appears that the active set method needs less iterations than the interior point method may be because of the small size of the problem. It is maybe due to the same reason when compare Figure 7.5 (b) and Figure 7.10 (b). Here also, the neural network converges to the solution in 0.01 ms as shown in Figure 7.11. From Figure 7.12 (a), (b) and (c), it is noticed that for three methods, a downgraded maneuver is obtained. There is a constant deviation for roll rate as shown in Figure 7.12, it is because the actuator command consider in the optimal problem is different from the actual actuator position and cause a constant deviation in the final angular rate. This deviation also exists in yaw rate but it is less the deviation in pitch angular rate.



(a) result of interior point

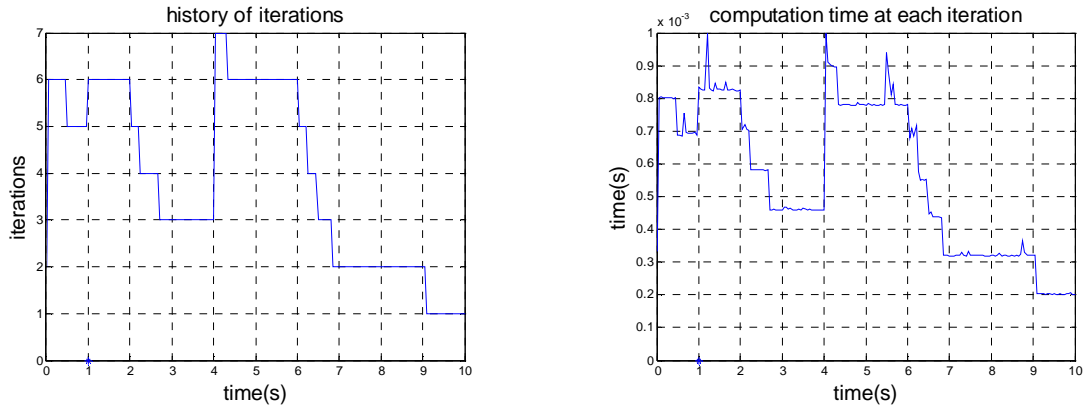


(b) result of active set

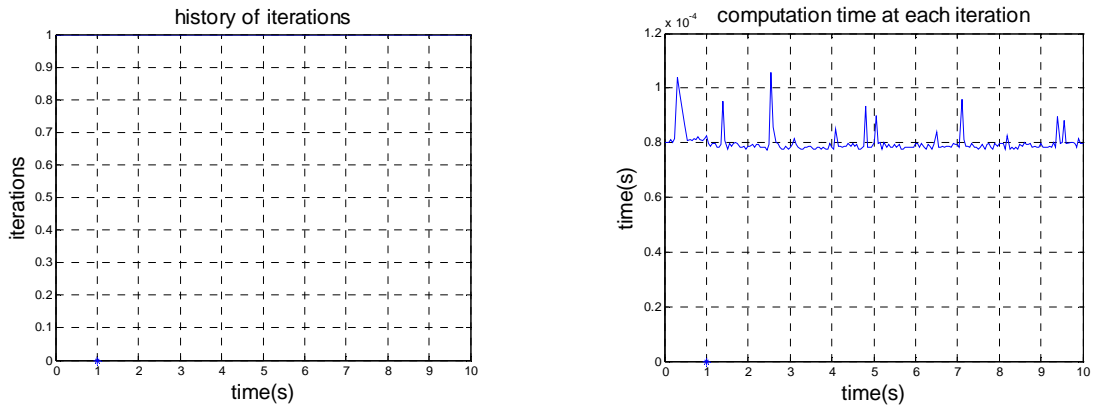


(c) result of neural network

Figure 7.9 Evolution of actuators commands under hard fault scenario

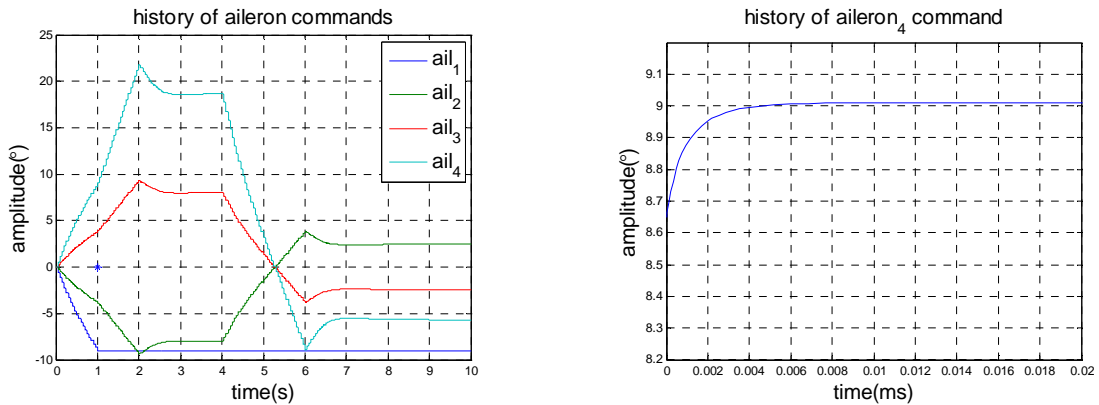


(a) Result of interior point



(b) Result of active set

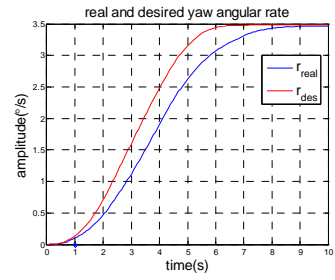
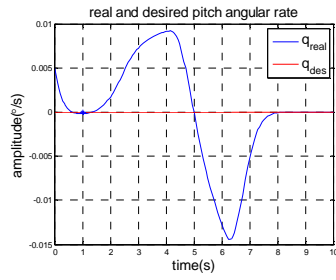
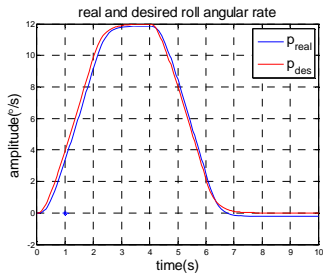
Figure 7.10 Number of iterations and computation time for interior point and active set under hard fault scenario



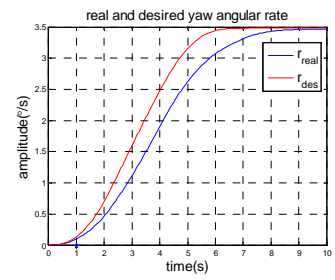
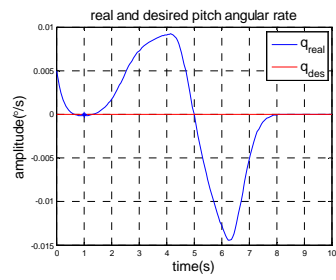
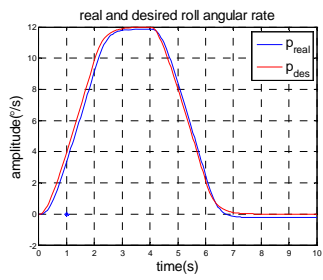
(a) Evolution of network outputs during the whole time-span

(b) zoomed picture to show the convergence speed of network

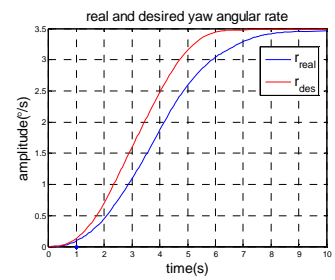
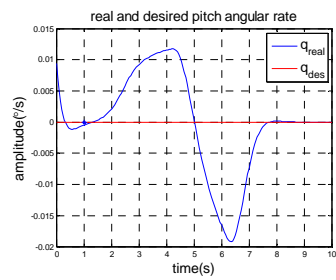
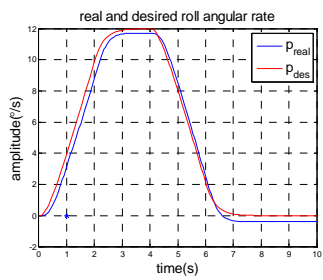
Figure 7.11 Convergent behavior of the neural network solver (0.01ms)



(a) Result of interior point

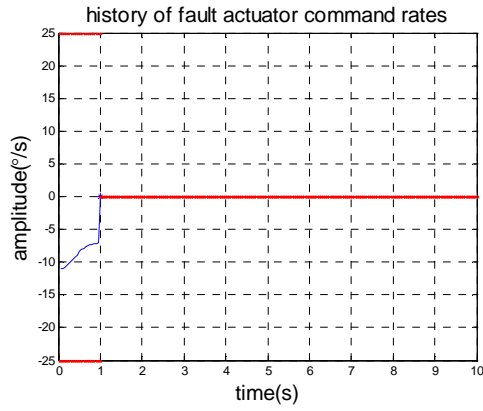


(b) Result of active set

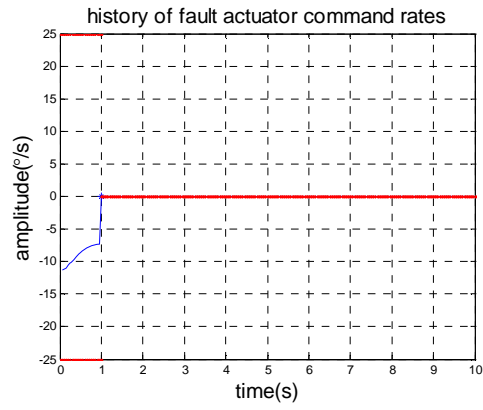


(c) Result of neural network

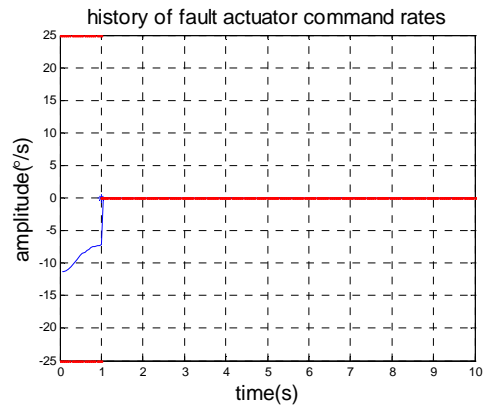
Figure 7.12 The real and desired angular rates under hard fault scenario



(a) Result of interior point



(b) Result of active set



(c) Result of neural network

Figure 7.13 Command rates for the right outer aileron under hard fault scenario

From the simulation results above, it appears that the three considered methods are able, for the two failure scenarios, to provide the optimal solution with an acceptable response time. The neural network method presents by far the best performance with respect to computation time (at most 0.01 ms to compare with a common actuator sampling time of 0.05 s) but feasibility of the solution is only guaranteed at convergence. The computation time performance of the active set method is a little bit better than the one of the interior point method, both being acceptable. Also these two methods provide at each step a feasible solution which can be adopted in the case of time-outs. The interior point method reaches the solution after a larger number of iterations than the active set method but it copes with a problem of larger dimensions (more variables and more constraints). From the point of view of algorithmic complexity, the active set method presents the lower complexity and when an actuator failure is detected and identified, the setting of the resulting optimization problem and solver appears easier than for the interior point method. In the case of the neural network solver, its structure is already fixed and some parameters will be changed according to the result of the FDI process.

7.6 Conclusion

In this chapter a general framework, based on the differential flatness property of aircraft flight dynamics, has been introduced. This gives support to the two stages approach proposed to cope with partial failures of aircraft actuators. When considering a classical maneuver performed by transportation aircraft, transition from straight flight to equilibrated turn, it has been shown that the resulting LQ problem can be solved online by any of the three solution methods studied previously (the interior point method, the active set method and neural networks). This proves the effectiveness of the proposed method. The resulting fault tolerant control structure is displayed by Figure 7.14.

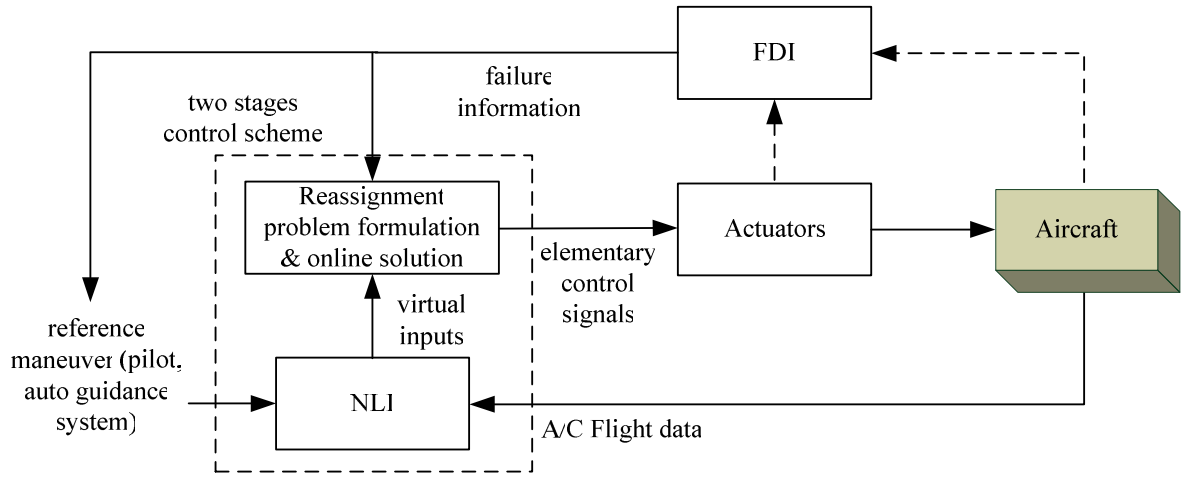


Figure 7.14 Fault tolerant control structure with actuator reassignment

CHAPTER 8

GENERAL CONCLUSIONS

8.1 Achievements

The main objective of this research has been to contribute to the design of flight fault tolerant structures for transportation aircraft by optimizing the use of redundant actuators.

However along the way towards this objective, different classical concepts have been revisited while new concepts, useful to perform the required analysis, have been introduced. It has been particularly important to distinguish between slow and fast actuators, allowing a more precise definition of different levels of redundancy as well as of fault tolerance. This has also led to propose a new view of flight dynamics for transportation aircraft where configuration changes associated with slow dynamics actuator settings have relevant consequences with respect to the efficiency of remaining fast actuators in a partial actuators failure situation. In the same way, when considering aircraft performance under a partial actuators failure, the performed analysis has distinguished between flying/handling qualities on one side and maneuver/flight domain limits on the other side, providing more insight in the choices performed by aircraft manufactures when defining nominal and downgraded levels of operations.

Also, to achieve this objective, different methods and techniques have been studied and when judged useful, developed and applied. It is the case with different advanced control design techniques such as Model Predictive Control (MPC) and Nonlinear Inverse Control (NLI). It is the case with different methods to solve a LQ problem associated with the actuator reassignment problem: Interior Point methods, Active Set methods, dedicated Neural Networks.

The proposed approach to tackle in the best way with actuators redundancy and partial failure situations is composed of two stages:

- One stage, where, according to the intended maneuver, the levels of the virtual inputs, as defined in this thesis, are established using an adequate control law synthesis method.
- One stage, where, the reassignment of the remaining operational actuators is performed to produce the required levels for the virtual inputs.

In the case of flight dynamics, it has been shown, that taking into consideration its differential

flatness property which can be tackled either at the guidance level or at the piloting level, natural virtual inputs appear.

In this thesis, the actuator reassignment problem has been formulated as a LQ problem, although different situations, fault scenarios and analysis objectives have been treated. Efficient solution methods for this problem have been developed and compared, showing their ability to treat either online problems, requiring very fast convergence to the solution, or offline problem with a large size.

The proposed approach has been applied with two different but complementary objectives:

- On one side, it has allowed to study the remaining flying/handling qualities under a given partial actuator failure scenario by formulating a reference trajectory tracking problem, solved offline using the MPC approach which has led to the solution of a LQ problem. As told in Chapter 6, this provides a tool to predict, for a given failure situation, possibility identified through the use of some FDI schemes, the resulting handling qualities.
- On the other side, the proposed approach has allowed to design a fault tolerant control structure to perform, when this is yet possible, standard maneuvers associated either with a flight plan or to ATC directives. The case study considered corresponds to a classical maneuver for transportation aircraft. It has made use of the NLI control technique to generate online the reference values for the corresponding virtual inputs and of dedicated solvers to get an online solution of the LQ problem resultant from the actuator reassignment problem.

8.2 Perspectives for Further Research

At this stage of the research, many points remain to be further studied, analyzed and developed.

Some of them can be still tackled in the academic area, these are points more theoretical, such as:

- The control of complex nonlinear systems through slow and fast controllers either with or

without actuators failures.

- The association of virtual inputs to control objective through differential flatness or other mathematical properties of flight dynamics.
- The integration of FDI function with actuator management function to provide more efficient fault tolerant structures for flight control.

Some other points should be tackled in the industry area, these are more practical points such as:

- Building from failure analysis of the flight control system of a given aircraft, a quite exhaustive list of actuator failure scenarios and assessing the resulting flying and handling qualities of the aircraft.
- Build a supervision system which, based on results from an FDI for the flight control channels, will perform diagnosis and allow or not some maneuvers, limit or not some of them and provide to pilot a clear view of the remaining capabilities of the aircraft.

Improving the safety of air transportation is an endless task and it is hoped that this thesis contributes with a small step towards this objective.

ANNEX A

FLIGHT DYNAMICS

A.1 Introduction

This annex presents the main equations related to the flight mechanics of the aircraft and is used as the basis for modifications in flight dynamics used in this study. Here, automatic control the aircraft is interested, and some assumptions are made: the aircraft is a rigid body and any structural flexibility will be neglected; earth is considered flat and is regarded as an inertial system so that Newtonian laws of motion can be applied; atmosphere is considered standard. These assumptions lead to express the equation of motion in the form of reduced nonlinear differential equations.

A.1.1 Reference frame

To represent and analyze atmospheric flight dynamics, the rotations (angle and angular rate) are usually applied at the center of gravity of the aircraft in different reference frames:

- Earth reference frame $G_E (X_E, Y_E, Z_E)$: The origin of this reference frame coincides with the center of gravity of the aircraft. X_E axis is directed along a reference azimuth (true north and magnetic north in general). Z_E axis is oriented in the direction of the center of the earth. The Y_E axis is perpendicular to the X_E-Z_E plane and is oriented to the east.
- Body-fixed reference frame $G_B (X_B, Y_B, Z_B)$: This reference frame is the study basis for the movement of the aircraft relative to another reference frame. The X_B -axis is from the original O_B and points towards the nose of the aircraft. It is the longitudinal axis of the aircraft, usually close to its principal inertial axis. Y_B -axis is perpendicular to the symmetry plane of the aircraft and points to the right. The X_B-Z_B plane coincides with the symmetry plane of the aircraft. Z_B axis is perpendicular to the X_B-Y_B horizontal plane and points downward.

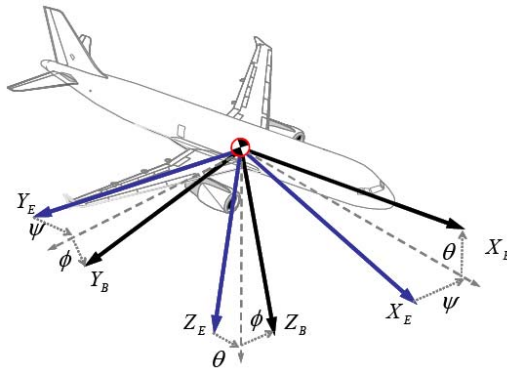


Figure A.1 Illustration of Earth frame and body-fixed frame

- Aerodynamic or wind reference frame $G_W (X_W, Y_W, Z_W)$ X_W axis is oriented along the direction of the air velocity vector. The Z_W axis is perpendicular to X_W axis and points downward. The Y_W axis is perpendicular to the X_W - Z_W plane and points to the right.

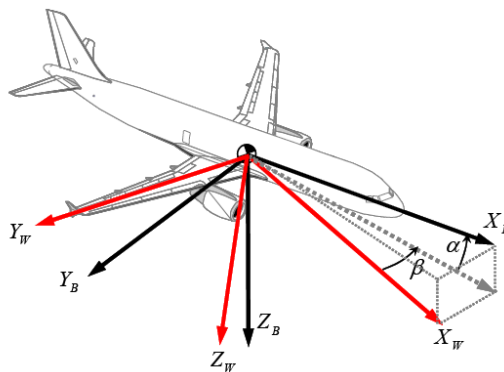


Figure A.2 Illustration of aerodynamic frame and body-fixed frame

A.1.2 Rotation matrices between different reference frames

The variables of the flight dynamics of an aircraft can be expressed more clearly following a particular reference frame. It may be necessary to change from one representation to another by a rotation process around the center of gravity of the aircraft. The transform matrices associated with these rotations are:

- Transform from the aerodynamic frame to body-fixed frame: The rotation matrix of the aerodynamic frame to the body-fixed frame (a β rotation and then a α rotation) is given by:

$$L_{W \rightarrow B} = \begin{bmatrix} \cos \alpha \cos \beta & -\cos \alpha \sin \beta & -\sin \alpha \\ \sin \beta & \cos \beta & 0 \\ \sin \alpha \cos \beta & -\sin \alpha \sin \beta & \cos \alpha \end{bmatrix} \quad (\text{A.1})$$

• Transform from the Earth frame to body-fixed frame: The rotation matrix corresponding to follow three rotations ($\psi \rightarrow \theta \rightarrow \phi$) from the Earth frame to body-fixed frame:

$$L_{E \rightarrow B} = \begin{bmatrix} \cos \psi \cos \theta & \sin \psi \cos \theta & -\sin \theta \\ \cos \psi \sin \theta \sin \phi - \sin \psi \cos \phi & \sin \psi \sin \theta \sin \phi + \cos \psi \cos \phi & \cos \theta \sin \phi \\ \cos \psi \sin \theta \cos \phi + \sin \psi \sin \phi & \sin \psi \sin \theta \cos \phi - \cos \psi \sin \phi & \cos \theta \cos \phi \end{bmatrix} \quad (\text{A.2})$$

where the three angles ϕ , θ and ψ are the Euler angles (bank, pitch, heading or yaw angle).

• Transform from the aerodynamic frame to Earth frame: Following the successive rotations ($\chi \rightarrow \gamma \rightarrow \mu$) the aerodynamic frame will be changed to the Earth frame. The corresponding rotation matrix is written as:

$$L_{W \rightarrow E} = \begin{bmatrix} \cos \chi \cos \gamma & \cos \chi \sin \gamma \sin \mu - \sin \chi \cos \mu & \cos \chi \sin \gamma \cos \mu + \sin \chi \sin \mu \\ \sin \chi \cos \gamma & \sin \chi \sin \gamma \sin \mu + \cos \chi \cos \mu & \sin \chi \sin \gamma \cos \mu - \cos \chi \sin \mu \\ -\sin \gamma & \cos \gamma \sin \mu & \cos \gamma \cos \mu \end{bmatrix} \quad (\text{A.3})$$

where the angles χ and γ are respectively the aerodynamic azimuth angle and flight path angle (or "slope"). The angle μ is the aerodynamic angle of roll.

A.2 Equations of Flight Mechanics

The equations governing the dynamic behavior of a conventional aircraft which is assumed as a constant mass rigid body are based on Newtonian mechanics. Forces and moments acting on the aircraft are generally expressed in different frames and finally are expressed in the body frame following rotations between different frames and the body-fixed frame.

A.1.3 Forces and moments

An aircraft flying in the atmosphere is subject to external forces and moments mainly associated with the thrust of the engine, gravity and aerodynamic effects (see Figure A.3) that can

be expressed in the body-fixed frame such that:

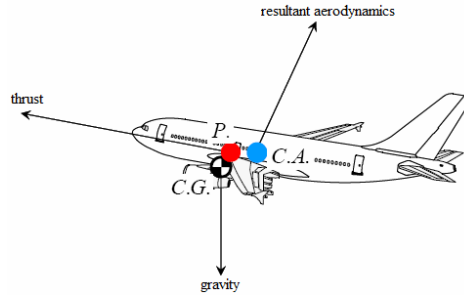


Figure A.3 External forces applied on the aircraft

Aerodynamic forces:

The aerodynamic force has three components: the drag D , lift L and lateral force Y which are expressed primarily in the aerodynamic frame. General expressions for aerodynamic forces can be written as:

$$\bar{A}_w = \begin{bmatrix} A_{xw} \\ A_{yw} \\ A_{zw} \end{bmatrix} = \begin{bmatrix} -D \\ Y \\ -L \end{bmatrix} = \frac{1}{2} \rho S V_a^2 \begin{bmatrix} -C_D \\ C_Y \\ -C_L \end{bmatrix} \quad (\text{A.4})$$

where ρ is the density of air, V_a is the air speed, S is the reference area of wing, and C_D , C_Y and C_L are the non-dimensional aerodynamic coefficients. The term $1/2 \rho V_a^2$ is the dynamic pressure, and is often noted as Q .

By a rotation matrix operation using (A.1), aerodynamic forces in the body-fixed frame can be expressed such as:

$$\bar{A}_B = L_{W \rightarrow B} \cdot \bar{A}_w \quad (\text{A.5})$$

with

$$\bar{A}_B = \begin{bmatrix} A_{xB} \\ A_{yB} \\ A_{zB} \end{bmatrix} = \begin{bmatrix} -D \cos \alpha \cos \beta - Y \cos \alpha \sin \beta + L \sin \alpha \\ -D \sin \beta + Y \cos \beta \\ -D \sin \alpha \cos \beta - Y \sin \alpha \sin \beta - L \cos \alpha \end{bmatrix} \quad (\text{A.6})$$

Gravity:

The gravity is expressed in the Earth frame by:

$$\bar{G}_E = m \begin{bmatrix} 0 \\ 0 \\ g(z) \end{bmatrix} \quad (\text{A.7})$$

By a rotation operation using (A.2), the gravity will be expressed in the body-fixed frame:

$$\bar{G}_B = \begin{bmatrix} G_{XB} \\ G_{YB} \\ G_{ZB} \end{bmatrix} = mg(z) \begin{bmatrix} -\sin \theta \\ \sin \phi \cos \theta \\ \cos \phi \cos \theta \end{bmatrix} \quad (\text{A.8})$$

Engine thrust:

$$\bar{T}_B = \begin{bmatrix} T_{XB} \\ T_{YB} \\ T_{ZB} \end{bmatrix} \approx \begin{bmatrix} T_{XB} \\ 0 \\ 0 \end{bmatrix} \quad (\text{A.9})$$

Summing up (A.6), (A.8) and (A.9), the resultant external forces are written:

$$\bar{F}_B = \begin{bmatrix} F_{XB} \\ F_{YB} \\ F_{ZB} \end{bmatrix} = \begin{bmatrix} A_{XB} + G_{XB} + T_{XB} \\ A_{YB} + G_{YB} + T_{YB} \\ A_{ZB} + G_{ZB} + T_{ZB} \end{bmatrix} \quad (\text{A.10})$$

Aerodynamic moments:

The aerodynamic moment generating from the different actuators is generally defined with respect to the aerodynamic center.

It can be divided into three components in the aerodynamics frame:

$$\bar{M}_W^A = \begin{bmatrix} M_{XW}^A \\ M_{YW}^A \\ M_{ZW}^A \end{bmatrix} = \begin{bmatrix} L \\ M \\ N \end{bmatrix} = \frac{1}{2} \rho V_a^2 S \begin{bmatrix} b \cdot C_l \\ \bar{c} \cdot C_m \\ b \cdot C_n \end{bmatrix} \quad (\text{A.11})$$

where b and \bar{c} are reference lengths. In general, b is the wing span and \bar{c} is the mean chord length. C_l , C_m , and C_n are the dimensionless moment coefficients.

The aerodynamic moments in the body-fixed frame can be expressed by the following expression considering the contributions from aerodynamic forces and moments:

$$\bar{M}_B^A = (\bar{r}_{CP} - \bar{r}_{CG}) \times \bar{A}_W + \bar{M}_W^A \quad (\text{A.12})$$

where $(\bar{r}_{CP} - \bar{r}_{CG})$ represents the position of the aerodynamic center with respect to the center of gravity.

The moment created by the engine thrust:

The moment of thrust comes from the torque effects caused by asymmetric. Its expression in the body frame is given by:

$$\bar{M}_B^P = (\bar{r}_P - \bar{r}_{CG}) \times \bar{T}_P \quad (\text{A.13})$$

where $(\bar{r}_P - \bar{r}_{CG})$ represents the position of the thrust pressure center with respect to the center of gravity. \bar{T}_P denotes the asymmetric thrust.

The weight is totally applied to the center of gravity and creates no moment there. The resulting total moment is the sum of the aerodynamic moment and the thrust moment. It is given in the body-fixed frame by:

$$\bar{M}_B = \bar{M}_B^A + \bar{M}_B^P \quad (\text{A.14})$$

A.1.4 Equations of motion

At first, the equations about the translational motion will be built. According to Newton's second law, the relation between the translational accelerations and the external forces can be expressed as:

$$m(\dot{\underline{V}} + \underline{\Omega} \times \underline{V}) = \sum F_{ext} \quad (\text{A.15})$$

where $\underline{V} = [u \ v \ w]'$ is a velocity vector, and $\underline{\Omega} = [p \ q \ r]'$ is rotational angular rates. Both of them are expressed in the body-fixed frame. The external forces expressed in body-fixed frame can be found using (A.10). \times is a cross product operator.

The more detailed space representation of (A.15) is given by:

$$\begin{cases} \dot{u} = \frac{F_{XB}}{m} - (qw - rv) \\ \dot{v} = \frac{F_{YB}}{m} - (ru - pw) \\ \dot{w} = \frac{F_{ZB}}{m} - (pv - qu) \end{cases} \quad (\text{A.16})$$

The aerodynamic effects depend on the orientation of the air velocity relative to the body-fixed frame, which can be formulated as:

$$\vec{V}_a = \begin{bmatrix} u_a \\ v_a \\ w_a \end{bmatrix}_B = \begin{bmatrix} u - W_X \\ v - W_Y \\ w - W_Z \end{bmatrix}_B \quad (\text{A.17})$$

its module:

$$V_a = \sqrt{u_a^2 + v_a^2 + w_a^2} \quad (\text{A.18})$$

the expressions of the aerodynamic angles:

$$\begin{cases} \alpha = \tan^{-1}\left(\frac{w_a}{u_a}\right) \approx w_a/u_a \approx w_a/V_a \\ \beta = \sin^{-1}\left(\frac{v_a}{V_a}\right) \approx v_a/V_a \end{cases} \quad (\text{A.19})$$

In the same way as (A.15), the equations about rotational motion can be built. According to Newton's second law, the relation between the angular accelerations of the aircraft around its center of gravity and the external moments can be expressed as:

$$I_m \dot{\underline{\Omega}} + \underline{\Omega} \times (I_m \underline{\Omega}) = \sum M_{ext} \quad (\text{A.20})$$

where external moments expressed in body-fixed frame can be found using (A.14). The inertial matrix I_m is given by:

$$I_m = \begin{bmatrix} I_{xx} & -I_{xy} & -I_{xz} \\ -I_{xy} & I_{yy} & -I_{yz} \\ -I_{xz} & -I_{yz} & I_{zz} \end{bmatrix} = \begin{bmatrix} \int (y^2 + z^2) dm & -\int (xy) dm & -\int (xz) dm \\ -\int (xy) dm & \int (x^2 + z^2) dm & -\int (yz) dm \\ -\int (xz) dm & -\int (yz) dm & \int (x^2 + y^2) dm \end{bmatrix} \quad (\text{A.21})$$

here usually $I_{xy} = I_{yz} = 0$ because the transportation aircraft is symmetric about XZ plane.

A more detailed space representation of moment equation (A.20) where the moments caused by engine is neglected because of very small values is given by:

$$\begin{bmatrix} L \\ M \\ N \end{bmatrix} = \begin{bmatrix} I_{xx}\dot{p} - I_{xz}\dot{r} \\ I_{yy}\dot{q} \\ -I_{xz}\dot{p} + I_{zz}\dot{r} \end{bmatrix} + \begin{bmatrix} -I_{xz}pq + (I_{zz} - I_{yy})qr \\ (I_{xx} - I_{zz})pr + I_{xz}(p^2 - r^2) \\ (I_{yy} - I_{xx})pq + I_{xz}qr \end{bmatrix} \quad (\text{A.22})$$

or express in a form of angular rate accelerations:

$$\begin{bmatrix} \dot{p} \\ \dot{q} \\ \dot{r} \end{bmatrix} = \begin{bmatrix} \frac{I_{xz}(I_{xx} - I_{yy} + I_{zz})}{\Delta}pq + \frac{I_{zz}(I_{yy} - I_{zz}) - I_{xz}^2}{\Delta}qr \\ \frac{I_{zz} - I_{xx}}{I_{yy}}pr + \frac{I_{xz}}{I_{yy}}(r^2 - p^2) \\ \frac{I_{xx}(I_{xx} - I_{yy}) + I_{xz}^2}{\Delta}pq + \frac{I_{xz}(I_{yy} - I_{xx} - I_{zz})}{\Delta}qr \end{bmatrix} + \begin{bmatrix} \frac{I_{zz}}{\Delta} & 0 & \frac{I_{xz}}{\Delta} \\ 0 & \frac{1}{I_{yy}} & 0 \\ \frac{I_{xz}}{\Delta} & 0 & \frac{I_{xx}}{\Delta} \end{bmatrix} \begin{bmatrix} L \\ M \\ N \end{bmatrix} \quad (\text{A.23})$$

where $\Delta = I_{xx}I_{zz} - I_{xz}^2$

Associated Euler equations:

$$\begin{cases} \dot{\phi} = p + \tan \theta (q \sin \phi + r \cos \phi) \\ \dot{\theta} = q \cos \phi - r \sin \phi \\ \dot{\psi} = \frac{q \sin \phi + r \cos \phi}{\cos \theta} \end{cases} \quad (\text{A.24})$$

that relate the angular rates in the body-fixed frame to the variation rates of attitude angles (Euler angles).

The components of the inertial velocity of the aircraft in the Earth frame:

$$\begin{bmatrix} \dot{x} \\ \dot{y} \\ \dot{z} \end{bmatrix}_E = \begin{bmatrix} \cos \psi \cos \theta & \cos \psi \sin \theta \sin \phi - \sin \psi \cos \phi & \cos \psi \sin \theta \cos \phi + \sin \psi \sin \phi \\ \sin \psi \cos \theta & \sin \psi \sin \theta \sin \phi + \cos \psi \cos \phi & \sin \psi \sin \theta \cos \phi - \cos \psi \sin \phi \\ \sin \theta & -\cos \theta \sin \phi & -\cos \theta \cos \phi \end{bmatrix} \begin{bmatrix} u \\ v \\ w \end{bmatrix}_B \quad (\text{A.25})$$

ANNEX B

FAULT TOLERANT CONTROL

TECHNIQUES

B.1 Fault Tolerant Control

The field of fault-tolerant control has attracted increasing attention of many researchers who have proposed various solutions. For example, Stoustrup and Niemann [Stoustrup & Niemann, 2001] used the state feedback linearization and Ghosh and Paden [Ghosh & Paden, 2000] proposed the use of pseudo-inverse method. Adaptive control approaches using artificial neural networks have been introduced in the Aeronautics mainly by Idan [Idan et al., 2003] and Calise [Anthony J Calise et al., 2000]. Johnson [E. Johnson et al., 2002] also made important contributions to the model following control. Table B.1 displays some areas of application of fault tolerant control.

Table B.1 Examples of FTC applications

Application	References
Aviation	[Alwi, 2008; Blanke, 1999; Anthony J Calise et al., 1998, 2000; Anthony J. Calise et al., 2001; Yang & Blanke, 2000b]
Space	[Hodel & Callahan, 2002; E. N. Johnson et al., 2001; Tillerson et al., 2002]
Navy	[Fossen & Johansen, 2006; R. J. Patton, 1997]
Automobile	[Tøndel & Johansen, 2005]
Engine control	[Frank W. Burcham et al., 1997; Anthony J Calise et al., 1998, 2000]
Chemical process	[Polycarpou & Ioannou, 1991]
Robots	[Reich & Sklar, 2006]

The development of fault tolerant control laws is a multidisciplinary task including control theory, signal processing and human factors. Nowadays, there are still many challenges for the design of fault tolerant control [Y. Zhang & Jiang, 2008].

B.2 Passive and Active Approaches

Many fault-tolerant control (FTC) approaches have been developed and different classification

methods are possible. Here they are distinguished mainly by the nature of the mechanism at the presence of a fault. Following this principle, there are two main families of approaches for synthesizing fault tolerant control laws as Figure B.1 shows:

- The passive fault tolerant control (PFTC)
- And active fault tolerant control (AFTC)

The passive approaches (PFTC) control techniques are mainly robust control type which aims to certain types of structural failures that can be modeled by uncertainty regions around a nominal model. This type of approach can handle all faults that do not lead the system parameters outside the stability domain of the robust controller.

Usually a PFTC type control system has the following characteristics:

- Robust against expected defects, unable to face some failures that are not listed.
- Use of physical redundancy (multiple actuators and sensors).
- More conservative goals: essentially it is to ensure the operation stability.
- The faulty system maintain operation with the same regulator and the same control structure, objectives as the nominal system (remain unchanged)
- However, on-line failure information may be available but is not exploited.

The active approaches (AFTC), or reconfiguration methods, differ from passive approaches in that they explicitly take into account the information from the fault detection and identification and will not just hold a static nominal model. The reconfiguration control is still a very academic concept because even if a variety of methods were developed after several decades of research programs [Jones, 2005; Y. Zhang & Jiang, 2001b], but no control system based on these principles has been implemented operationally on commercial transport aircraft.

The general characteristics of AFTC type systems are:

- Using the analytical redundancy in addition to available hardware redundancy.

- Using techniques like FDI and reconfiguration techniques.
- Redefinition control objectives in the presence of failures (generally adopt limited control objectives).

The design of AFTC type systems is generally a complex multidisciplinary task that uses different areas knowledge: stochastic systems, applied statistics, risk analysis, reliability, filtering and signal processing, neural networks, control and dynamic modeling, etc.

For AFTC type systems, reconfiguration controller is considered necessary to offset the effects of failed components.

AFTC approaches differ from PFTC approaches by the principles outlined above such as the use of a FDI module, an online synthesis of the regulator, as proposed by Patton [R. J. Patton, 1997], Blanke [Yang & Blanke, 2000a], Maciejowski [Maciejowski & Jones, 2003], Petersen [Petersen & Bodson, 2005].

It is possible to classify the AFTC approaches according to a certain criteria such as:

- Active control based on off-line control laws (pre-computed) and the online selection of one of them.
- Active control based on the fault accommodation (for example, switching between failure patterns) and don't use FDI.
- Active control undoubtedly uses FDI.

In AFTC, the control system is automatically changed to reflect the occurrence of the failure. To accomplish its reconfiguration or restructuring, an active fault-tolerant system requires a priori knowledge of the expected failure types or a mechanism to detect and isolate unexpected faults. The proper functioning of the FDI module is essential. However, some types of active control are sometimes difficult to categorize and thus the following classification is not exhaustive, but it can identify some major trends. Thus, taking into account the choice of the controller online and methods of online calculating control signals, a classification of reconfiguration mechanisms can be done.

Two main approaches can be distinguished:

- Control laws linked with assumed failure conditions are calculated a priori in the design stage and select online based on real-time information from FDI.
- Control laws are synthesized on-line after the fault is detected.

The main fault-tolerant control mechanisms are classified in Figure B.1 according to the utilized design approaches.

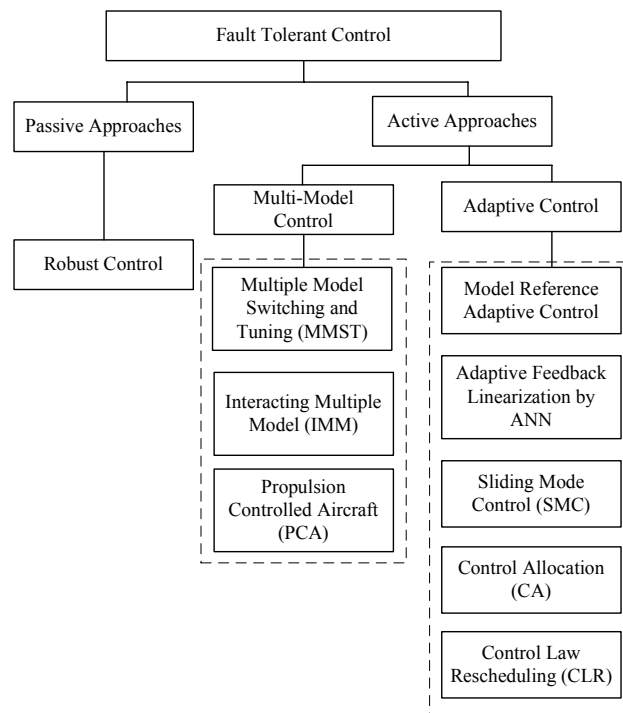


Figure B.1 Main approaches of fault tolerant control

B.3 Active Fault Tolerant Control Approaches

B.3.1 Multi-model control

A most studied general method for fault tolerant control is the multi-model control (MMC). It can be subdivided into:

- Transit and adapt between models (Multiple Model Switching and Tuning, MMST)

- Interact between multiple models (Interacting Multiple-Model, IMM).

For these two types of methods, all possible failure cases are described in principle with the failure mode and effects analysis (FMEA) and failure models are built to cover every situation. When a failure occurs, MMST changes the current control law to another pre-calculated control law which is supposed to correspond to the current failure situation. To obtain a model adapted to the current failure situation, IMM uses a model which is a convex combination of all pre-calculated models. Propulsion Controlled Aircraft method-PCA can be distinguished as a special case of MMST.

Multiple Model Switching and Tuning

Multiple Model Switching and Tuning (MMST) was developed by Maybeck [Maciejowski & Jones, 2003]. When a failure occurs, MMST strategy switches to a pre-calculated control law corresponding to the current situation. Each failure scenario is described by different models. These models are implemented in parallel and each corresponds to a different regulator.

For MMST, the problem is equivalent to define at every moment which pair (M, K) model and controller are the most appropriate for a particular situation. In the presence of a failure, the representation of the system is supposed to depart (in terms of distance parameter) from the nominal model (M_0) and adopt a failure model (M_f) . MMST method allows in principle to converge quickly to the model which better addresses the effects of failure and is therefore more efficient than a single model approach.

Interacting Multiple-Model

Interacting Multiple-Model (IMM) mitigates the limitations of the MMST by interaction of multiple models, whose models of failure are represented by a convex combination of a set of models. For IMM algorithm, Zhang and Jiang [Y. Zhang & Jiang, 2001a] associated each failure with a particular model while controlled system is described as a stochastic system.

By using a Kalman filter bank where each filter is associated with a different operation mode of the system, IMM control the system through interaction of multiple models. It is able to estimate the state of the system with reducing errors and without increasing calculation burden.

The estimate used at the beginning of every cycle is a combination of recent estimates, which allows the IMM to take into account the changing modes of the system. IMM will never implement a dramatic change in the controlled system. The probabilities associated with each model are calculated at every moment to decide if it should transit from the current model to a new model.

For all MMC algorithms, a common feature is that only a predetermined finite number of failures can be detected. Indeed, for most MMC methods studied, they consider that only a single failure may occur simultaneously in the system and therefore a single model should be chosen. If the model representing the system at the k moment is not fall in predefined models, then the associated control is likely to be ineffective because it corresponds to an inadequate weighting of several models. In this case the control may lead system to instable.

B.3.2 Adaptive control

Adaptive control is an approach that can best meet the expected characteristics of an AFTC. Indeed, it has the ability to automatically adjust the controller parameters according to the change of system detected from the performance achieved by the system. Therefore, it does not require the FDI module as is the case of other AFTC control approaches. Controlling parameters with Linear Parameter Varying (LPV) [Kanev & Verhaegen, 2000] dedicated to the FTC and other methods such as those developed by Huzmezan [Huzmezan & Maciejowski, 1997] and Calise [E. N. Johnson et al., 2001] are adaptive control techniques. However, these methods do not use an FDI module and without any supervision, convergence problems may occur when estimating the parameters.

Model reference adaptive control

Model Reference Adaptive Control (MRAC) was developed mainly by Calise [Anthony J Calise et al., 1998] for application in Aeronautics. It has been successfully evaluated by simulation on advanced fighter aircraft (TAFAs) [Frank W Burcham et al., 1994; Anthony J Calise et al., 2000] and the X-36 [Anthony J Calise et al., 2000]. In the case of controlling an aircraft, the approach considers the aircraft dynamics to consist of three SISO sub-systems and the control system includes a reference model, a module for developing control signals, a

mechanism for distributing control signals to the various aerodynamic actuators.

Adaptive state feedback linearization

State feedback linearization (Feedback Linearization) is a nonlinear control technique for online reconfiguration. It is based on an adaptive controller that modifies parameters of the algorithm by estimating them on line before calculating the control signal. Examples of such method are developed by Fravolini [Fravolini et al., 2001] and Polycarpou [Polycarpou & Ioannou, 1991] which are based on an adaptive approach that uses neural networks to estimate these parameters.

Linear regulators generally do not work properly for large variations of the variables around their nominal value. State feedback linearization or output feedback linearization can be used to offset the effects associated with nonlinearities. Faults are identified by estimating the parameters of the equations of motion of the aircraft by the recursive least squares method. The estimated parameters are then used to update the new controller gains. Since the dynamics of an aircraft involves many parameters, difficulty may arise during the identifying of these parameters.

Sliding mode control

Sliding Mode Control (SMC) was introduced by Slotine in the seventies and developed by Demircin [Demirci & Kerestecioglu, 2005] and Halim [Alwi, 2008] in the context of fault-tolerant control. The advantage of it for the reconfiguration control is twofold:

- A robust controller deals with structural failures, this leads to a change of overall system dynamics.
- It can handle partial loss of the actuator effectiveness, avoiding saturation by use of integrators, even if this reduces the accuracy of results.

Applicability conditions for this technique: The system must be square (that is to say have as many independent control inputs as controlled outputs), this assumes that a control surface is associated with a control variable, and no control surface can be totally lost. Thus, in [Demirci & Kerestecioglu, 2005] only faults that cause partial loss of the effectiveness of control surfaces were considered. Often this does not correspond to realistic failure scenarios, for example it is the

case when the actuator is locked at a fixed position.

Actuators allocation

With the existing functional redundancies between various actuators, if an actuator failure occurs, this control technique will use the remaining nearby actuators to achieve the desired forces or moments. Various techniques have been proposed in the literature to be applied to the flight control, but generally they do not consider a linearized model of flight dynamics, which considerably limits its scope. Thus, Johansen [T. A. Johansen et al., 2004] and Tondel [Tondel & Johansen, 2005] advocated techniques of linear programming, even linear quadratic programming. In principle, if there exists an actuators allocation algorithm whose control signals depending on the state of the actuators, a control law can be synthesized using a set of virtual actuators that produce desired forces and moments regardless of the failure state of system. Control allocation has attracted much attention in the literature of reconfigurable systems because it allows failures of actuators to be managed without the need to modify the control law.

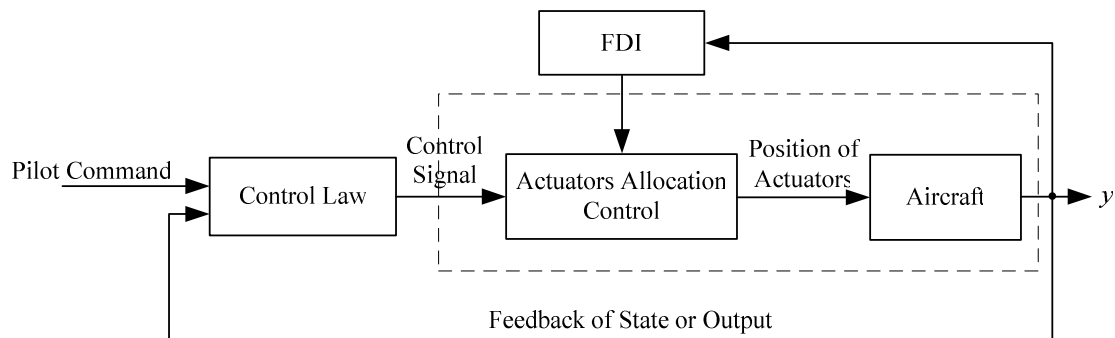


Figure B.2 Block diagram of actuator allocation system

However, there are two important limitations to this reconfiguration approach:

- The system will not surely obtain its rated performance even in the presence of a stabilizing control law, because the action actually applied to the controlled system is equal to that provided by the controller.
- Changes in the dynamics and limitations of the actuators after a failure are not considered in the control law. This means that the controller may send control signals to which the sensors will be unable to obey normally.

Control law rescheduling

A simple approach to design fault tolerant control laws is to store pre-computed gain parameters. This corresponds to the Control Law Rescheduling (CLR). This type of control is like gain scheduling that was considered as a solution for dealing with changes in flight aerodynamic coefficients with changes in flight parameters such as Mach number, altitude, and angle-of-attack. For this type of application, the CLR mechanism is triggered by the detection of differences between expected performance and actual performance. The implementation of such a technique requires:

- The use of FDI mechanisms.
- The estimation of the state to reconfigure the controller.
- The availability of pre-computed and recorded control laws.

B.4 Methods of Control Laws Synthesis

Here are examined only some of the latest methods of control laws synthesis that will be implemented at a given time to generate the control signals for actuators. Here no review about the conventional methods such as pole placement and linear quadratic regulator is provided.

Nonlinear inverse control (NLI) will be detailed in Annex E.

B.4.1 Model following control

In this approach, the controller gains are calculated on-line and finally the system imposes the desired trajectory by using the technique of model following or by minimizing the quadratic cost function differences between the actual values of states and those generated by the model. Figure B.3 shows the general structure of a system implementing this technique.

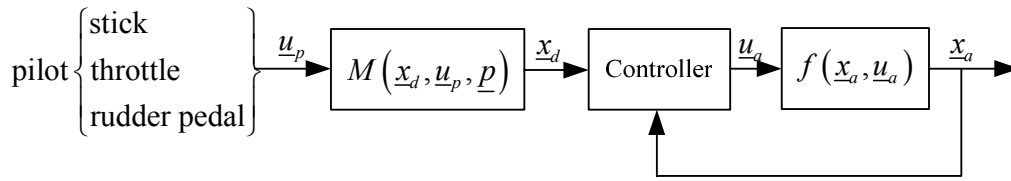


Figure B.3 Scheme of model following control

where $f(\underline{x}_a, \underline{u}_a)$ represents the aircraft failure or not, $\underline{x}_a \in R^n$ is the measured state vector of the aircraft, $M(\underline{x}_d, \underline{u}_p, \underline{p})$ is the reference model, $\underline{x}_d \in R^n$ is the desired state vector of the aircraft, $\underline{p} \in R^p$ is the performance parameters vector, $\underline{u}_p \in R^l$ is the pilot's command (through stick, throttle, rudder pedals) to the aircraft and then $\underline{u}_a \in R^m$ is the control signal of aerodynamic actuators.

One of the main drawbacks of this method is the difficulty to choose a reference model for system reconfiguration. An appropriate reference model should be chosen based on its performance, but also should take into account the difficulty for the system to be reconfigured to follow a nominal trajectory generated by the model.

B.4.2 Model predictive control

The synthesis of the model predictive control law was used in the context of fault-tolerant control by several authors including Huzmezean [Huzmezean & Maciejowski, 1997], Jones [Jones, 2005] and Maciejowsky [Maciejowski & Jones, 2003]. It has taken different forms over time such as: basic model predictive control, receding horizon control, generalized predictive control, dynamic matrix control and open loop sequential optimization.

This method differs from others because:

- An internal model is used to explicitly predict the behaviour of the system.
- The optimal control is calculated at every instant to maximize a performance measure on the horizon (the horizon is receding back at every time step).
- Only the initial part of the control signal calculated on the receding horizon is effectively

implemented and the next instant, the cycle of prediction and optimization is repeated.

The constraints related to input, output and state signals can be taken into account easily when using MPC. [Kale & Chipperfield, 2002, 2005] considered a reconfigurable control using MPC for a failure fighter aircraft at the same time guarantee the handling qualities. Using MPC as a model update way and dynamic inversion to linearize the nonlinear system to obtain a reconfigurable control method, Joosten [Joosten et al., 2008] and [Van Oort et al., 2006] combined both of them and applied respectively in the fault tolerant flight control of transport aircraft and fighter aircraft.

Some authors also used MPC to design command governor to maximum the tracking performance as well as satisfy the constraints related to actuators and states, see [Martino, 2008]. Also someone used MPC as a control allocation method under some actuators failures [Lafourcade et al., 2010]. [De Almeida, 2011; De Almeida & Leissing, 2009] proposed a feasible target tracking model predictive control which can modify the control to be feasible and redistribute actuators following an optimal way when some failures happen.

ANNEX C

RECCURENT NEURAL NETWORKS

FOR LQ PROBLEM

Refer to Chapter 5 for the meaning of some symbols used here.

Figure C.1 shows simplified block diagram of this neural network where two-layer structure displayed clearly. Activate functions of the first layer and the second layer are respectively piecewise-linear function and integrator.

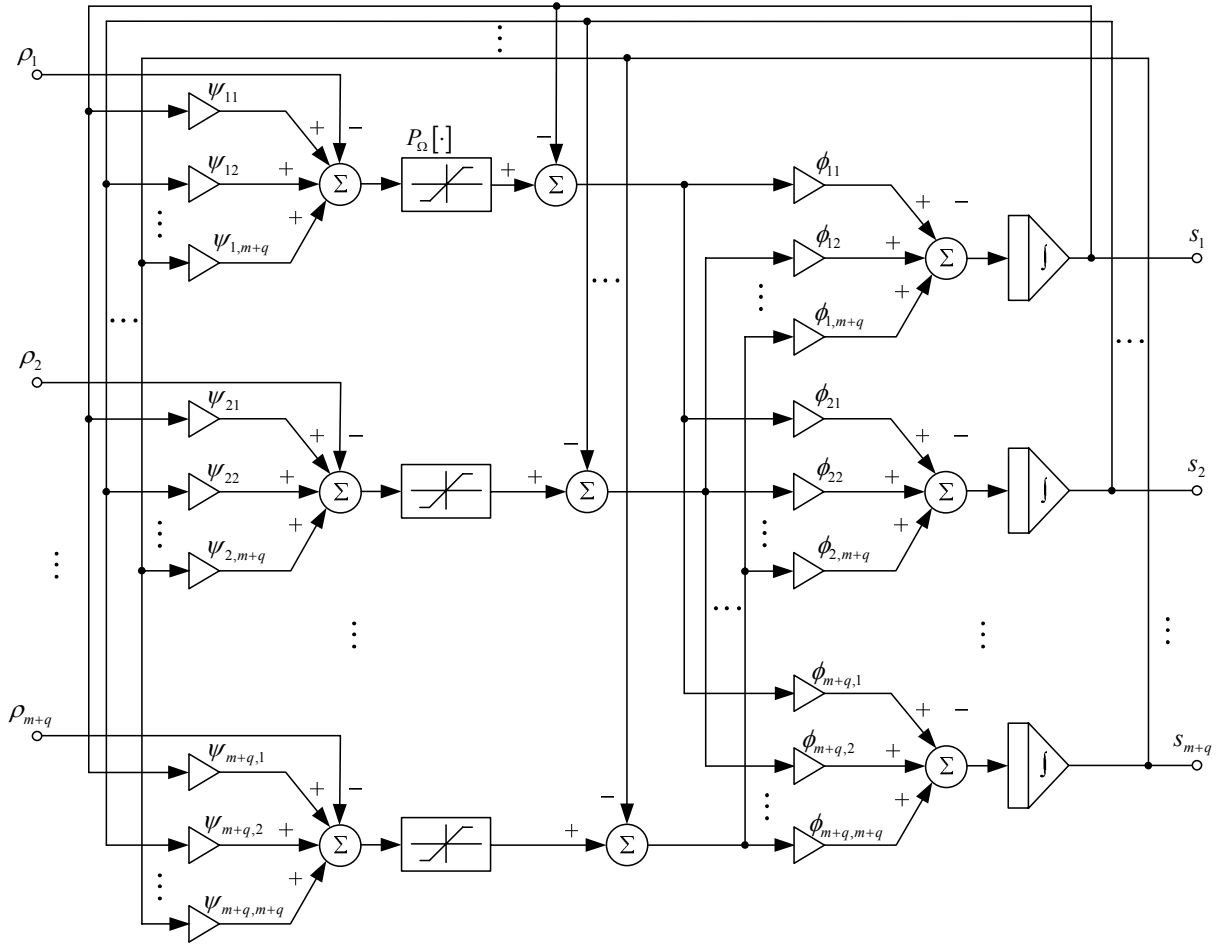


Figure C.1 Two-layer structure of the neural network model (source: [xia, 2000])

In Figure C.1, ψ_{ij} and ϕ_{ij} are respectively the elements of matrix $I_{d_3} - N$ and $I_{d_3} + N^T$.

According to the definition of convex set and closed set [Luenberger & Ye, 2008], it is easy to show that Ω defined by (5.30) is a closed convex set.

Lemma C.1 Let the projection of $\underline{s} \in R^{m+q}$ on the close convex set Ω is

$P_{\Omega}(\underline{s}) = \arg \min_{\underline{y} \in \Omega} (\|\underline{s} - \underline{y}\|^2)$, then the necessary and sufficient condition for the projection is:

$$(P_{\Omega}[\underline{s}] - \underline{s})^T (\underline{z} - P_{\Omega}[\underline{s}]) \geq 0, \quad \forall \underline{z} \in \Omega \quad (\text{C.1})$$

Proof: Since $\|\underline{s} - \underline{y}\|^2$ is a convex function and definition region Ω is a close convex set, so $\arg \min_{\underline{y} \in \Omega} (\|\underline{s} - \underline{y}\|^2)$ is a convex optimization problem. The gradient of objective function is $\nabla (\|\underline{s} - \underline{y}\|^2) = 2(\underline{y} - \underline{s})$, through the necessary and sufficient condition of convex optimization problem: $\nabla f(\underline{x}^*)^T (\underline{x} - \underline{x}^*) \geq 0$, substituting gradient into this relation, then (C.1) is obtained.

Theorem C.1 (equivalent of solution \underline{s}^* of (5.30) and equilibrium point of (5.33))

Proof: Suppose \underline{s}^* satisfy (5.30), i.e., $(\underline{s} - \underline{s}^*)^T (N\underline{s}^* + \underline{\rho}) \geq 0 \quad \forall \underline{s} \in \Omega$.

Adding $(\underline{s}^*)^T (\underline{s} - \underline{s}^*)$ to both side and rearrange the equation:

$$\left\{ \underline{s}^* - [\underline{s}^* - (N\underline{s}^* + \underline{\rho})] \right\}^T (\underline{s} - \underline{s}^*) \geq 0 \quad \forall \underline{s} \in \Omega \quad (\text{C.2})$$

According Lemma C.1, $\underline{s}^* = P_{\Omega}[\underline{s}^* - (N\underline{s}^* + \underline{\rho})]$ which is exactly the equilibrium point of (5.33). At the same time \underline{s}^* is the unique point which satisfies (5.30), so Theorem C.1 is proved.

Theorem C.2 (LVI-Based PDNN global convergence) No matter where the initial point is, the state vector $\underline{s}(t)$ of neural networks (5.33) will convergent to an equilibrium point \underline{s}^* , of which the first m elements constitute the optimal solution \underline{u}^* to the quadratic problem (5.7, 5.8) [Y. Zhang, 2005].

Proof: Substitute \underline{s} with $[\underline{s} - (N\underline{s} + \underline{\rho})]$ and \underline{z} with \underline{s}^* in relation (C.1), then:

$$\left\{ \underline{s} - (N\underline{s} + \underline{\rho}) - P_{\Omega}[\underline{s} - (N\underline{s} + \underline{\rho})] \right\}^T \left\{ P_{\Omega}[\underline{s} - (N\underline{s} + \underline{\rho})] - \underline{s}^* \right\} \geq 0, \quad \forall \underline{s} \in R^{m+q}, \underline{s}^* \in \Omega \quad (\text{C.3})$$

Substitute \underline{s} with $P_{\Omega}[\underline{s} - (N\underline{s} + \underline{\rho})]$ in relation (5.30), then:

$$\left\{ P_{\Omega}[\underline{s} - (N\underline{s} + \underline{\rho})] - \underline{s}^* \right\}^T (N\underline{s}^* + \underline{\rho}) \geq 0 \quad \forall \underline{s} \in R^{m+q} \quad (\text{C.4})$$

Add (C.3) and (C.4),

$$\left\{ P_{\Omega} \left[\underline{s} - (N\underline{s} + \underline{\rho}) \right] - \underline{s}^* \right\}^T \left\{ N(\underline{s}^* - \underline{s}) + \underline{s} - P_{\Omega} \left[\underline{s} - (N\underline{s} + \underline{\rho}) \right] \right\} \geq 0$$

which can be expressed in another form:

$$\left(P_{\Omega} \left[\underline{s} - (N\underline{s} + \underline{\rho}) \right] - \underline{s} + \underline{s} - \underline{s}^* \right)^T \left(N(\underline{s}^* - \underline{s}) + \underline{s} - P_{\Omega} \left[\underline{s} - (N\underline{s} + \underline{\rho}) \right] \right) \geq 0 \quad (\text{C.5})$$

Expand relation (C.5) and rearrange the equation:

$$\left(\underline{s} - \underline{s}^* \right)^T \left(I_{d_3} + N^T \right) \left\{ \underline{s} - P_{\Omega} \left[\underline{s} - (N\underline{s} + \underline{\rho}) \right] \right\} \geq \left\| \underline{s} - P_{\Omega} \left[\underline{s} - (N\underline{s} + \underline{\rho}) \right] \right\|^2 + \left(\underline{s} - \underline{s}^* \right)^T N \left(\underline{s} - \underline{s}^* \right) \quad (\text{C.6})$$

Through (5.32), it is easy to verify that N is positive semidefinite. So

$$\left(\underline{s} - \underline{s}^* \right)^T \left(I_{d_3} + N^T \right) \left\{ \underline{s} - P_{\Omega} \left[\underline{s} - (N\underline{s} + \underline{\rho}) \right] \right\} \geq 0 \quad (\text{C.7})$$

Define a Lyapunov function $V(\underline{s}) = \left\| \underline{s} - \underline{s}^* \right\|^2 / 2$, the first order derivative of the Lyapunov function can be deduced using (5.33):

$$\frac{dV(\underline{s})}{dt} = \left(\underline{s} - \underline{s}^* \right)^T \frac{d\underline{s}}{dt} = \eta \left(\underline{s} - \underline{s}^* \right)^T \left(I_{d_3} + N^T \right) \left\{ P_{\Omega} \left(\underline{s} - (N\underline{s} + \underline{\rho}) \right) - \underline{s} \right\} \leq 0 \quad (\text{C.8})$$

By Lyapunov theory, the state \underline{s} of dynamical system (5.33) is stable and globally convergent to an equilibrium point \underline{s}^* where $\dot{V}(\underline{s}^*) = 0$. Through Theorem C.1, \underline{s}^* is also the solution of LVI (5.30) and the first m elements are the solution to original linear quadratic problem.

Theorem C.3 (convergence speed of LVI-Based PDNN) An exponential convergence speed can be achieved for neural network (C.4) if there exists a constant $\delta > 0$ such that [Y. Zhang, 2005]:

$$\left\| \underline{s} - P_{\Omega} \left[\underline{s} - (N\underline{s} + \underline{\rho}) \right] \right\|^2 \geq \delta \left\| \underline{s} - \underline{s}^* \right\|^2 \quad (\text{C.9})$$

Proof: Substitute (C.6) into (C.8):

$$\frac{dV(\underline{s})}{dt} \leq -\eta \left[\left\| \underline{s} - P_{\Omega} \left[\underline{s} - (N\underline{s} + \underline{\rho}) \right] \right\|^2 - \left(\underline{s} - \underline{s}^* \right)^T N \left(\underline{s} - \underline{s}^* \right) \right] \leq 0 \quad (\text{C.10})$$

If (C.9) exists, according to N is a positive semidefinite matrix, then

$$\frac{dV(\underline{s})}{dt} \leq -\eta \left(\underline{s} - \underline{s}^* \right)^T \left(\delta \cdot I_{d_3} + N \right) \left(\underline{s} - \underline{s}^* \right) \leq -\eta \delta \left\| \underline{s} - \underline{s}^* \right\|^2 = -\eta \delta \cdot V(\underline{s}) \quad (\text{C.11})$$

where $\eta\delta > 0$ is the convergent rate. Therefore

$$\|\underline{s}(t) - \underline{s}^*\|^2 \leq \|\underline{s}(t_0) - \underline{s}^*\|^2 e^{-\eta\delta(t-t_0)} \quad (\text{C.12})$$

The exponential convergence speed is proved.

ANNEX D

PARAMETERS FOR THE MPC

PROBLEM

From relation (6.16c), the expression of the predicted values for $\underline{\delta}^p(k+i|k)$, $i=1$ to $K-1$ can be got:

$$\begin{bmatrix} \underline{\delta}^p(k+1|k) \\ \vdots \\ \underline{\delta}^p(k+K-1|k) \end{bmatrix} = \begin{bmatrix} (I_\delta - B_1) \\ \vdots \\ (I_\delta - B_1)^{K-1} \end{bmatrix} \cdot \underline{\delta}(k) + \begin{bmatrix} B_1 & \cdots & 0 \\ \vdots & \ddots & \vdots \\ (I_\delta - B_1)^{K-2} B_1 & \cdots & B_1 \end{bmatrix} \underline{\delta}_c(k) \quad (D.1)$$

where $B_1 = \Lambda T$.

Relation (D.1) can be written in a more compact form as:

$$\underline{\delta}^p(k) = \underline{C}_{\delta 1} \underline{\delta}(k) + H_{\delta 1} \underline{\delta}_c(k) \quad (D.2)$$

From relations (6.16b) and (D.1), the expression of the predicted values for $\underline{\omega}^p(k+i|k)$, $i=1$ to K can be got:

$$\begin{bmatrix} \underline{\omega}^p(k+1|k) \\ \underline{\omega}^p(k+2|k) \\ \vdots \\ \underline{\omega}^p(k+K|k) \end{bmatrix} = \begin{bmatrix} I_\omega \\ I_\omega \\ \vdots \\ I_\omega \end{bmatrix} \cdot \underline{\omega}(k) + \begin{bmatrix} I_\omega \\ 2I_\omega \\ \vdots \\ KI_\omega \end{bmatrix} \cdot C_0 + \begin{bmatrix} B_2 \\ B_2 \sum_{i=0}^1 (I_\delta - B_1)^i \\ \vdots \\ B_2 \sum_{i=0}^{K-1} (I_\delta - B_1)^i \end{bmatrix} \cdot \underline{\delta}(k) + \begin{bmatrix} 0 & 0 & \cdots & 0 \\ B_2 B_1 & 0 & \cdots & 0 \\ \vdots & \vdots & \ddots & \vdots \\ B_2 \left(\sum_{i=1}^{K-2} (I_\delta - B_1)^i \right) B_1 & \vdots & \cdots & B_2 B_1 \end{bmatrix} \underline{\delta}_c(k) \quad (D.3)$$

where $C_0 = I_m^{-1} T M^0$, $B_2 = I_m^{-1} T C$.

Relation (D.3) can be written in a more compact form as:

$$\underline{\omega}^p(k) = \underline{C}_\delta + H_\delta \underline{\delta}_c(k) \quad (D.4)$$

From relations (6.17a), (6.17b) and (6.17c), the expression of the reference values for $\underline{\tilde{\omega}}(k+i)$, $i=1$ to K can be written as:

$$\begin{bmatrix} \underline{\tilde{\omega}}(k+1) \\ \underline{\tilde{\omega}}(k+2) \\ \vdots \\ \underline{\tilde{\omega}}(k+K) \end{bmatrix} = \begin{bmatrix} B_5 B_4 \\ B_5 \left(\sum_{i=0}^1 B_3^i \right) B_4 \\ \vdots \\ B_5 \left(\sum_{i=0}^{K-1} B_3^i \right) B_4 \end{bmatrix} \cdot \underline{\tilde{\omega}}_c \quad (D.5)$$

$$\text{where } B_3 = \begin{bmatrix} I_\omega & TI_\omega \\ -TW_\omega^2 & (I_\omega - 2TZ_\omega W_\omega) \end{bmatrix}, B_4 = \begin{bmatrix} 0 \\ TW_\omega^2 \end{bmatrix}, B_5 = [I_\omega \quad 0].$$

Relation (D.5) can be written in a more compact form as:

$$\underline{\tilde{\omega}}(k) = H_\omega \underline{\tilde{\omega}}_c \quad (\text{D.6})$$

From expressions (6.18), (D.4) and (D.6), the following relations for the objective function (6.22) will be arrived:

$$R(k) = H_\delta^T H_\delta \quad \underline{s}(k) = 2H_\delta^T (\underline{C}_\delta - H_\omega \underline{\tilde{\omega}}_c) \quad (\text{D.7})$$

From relations (6.19a), (6.19b), (6.20) and (D.2), the expression for inequality constraints (6.23) can be written as:

$$A(k) = \begin{bmatrix} H_{\delta 1} \\ -H_{\delta 1} \\ D_\delta H_{\delta 1} \\ -D_\delta H_{\delta 1} \\ D_{Y_{j1}} H_{\delta 1} \\ D_{Y_{j2}} H_{\delta 1} \end{bmatrix}, \quad \underline{b}(k) = \begin{bmatrix} \underline{C}_{\delta 1} \underline{\delta}(k) - \underline{\delta}^{\max} \\ -\underline{C}_{\delta 1} \underline{\delta}(k) + \underline{\delta}^{\min} \\ D_\delta \underline{C}_{\delta 1} \underline{\delta}(k) - T \underline{\dot{\delta}}^{\max} \\ -D_\delta \underline{C}_{\delta 1} \underline{\delta}(k) + T \underline{\dot{\delta}}^{\min} \\ \underline{A}_{j1} + D_{Y_{j1}} \underline{C}_{\delta 1} \underline{\delta}(k) - \underline{M}_{j1}^{\max} \\ \underline{A}_{j2} + D_{Y_{j2}} \underline{C}_{\delta 1} \underline{\delta}(k) - \underline{M}_{j2}^{\max} \end{bmatrix} \quad (\text{D.8})$$

$$\text{where } D_\delta = \begin{bmatrix} -I_\delta & I_\delta & \cdots & 0 & 0 \\ \vdots & \vdots & \ddots & \vdots & \vdots \\ 0 & 0 & \cdots & -I_\delta & I_\delta \end{bmatrix}, \quad D_{Y_{j1}} = \begin{bmatrix} Y_{bend} & \cdots & 0 \\ \vdots & \ddots & \vdots \\ 0 & \cdots & Y_{bend} \end{bmatrix}, \quad D_{Y_{j2}} = \begin{bmatrix} Y_{tors} & \cdots & 0 \\ \vdots & \ddots & \vdots \\ 0 & \cdots & Y_{tors} \end{bmatrix},$$

$$\underline{\delta}^{\max} = \begin{bmatrix} \underline{\delta}^{\max} \\ \vdots \\ \underline{\delta}^{\max} \end{bmatrix}, \quad \underline{\delta}^{\min} = \begin{bmatrix} \underline{\delta}^{\min} \\ \vdots \\ \underline{\delta}^{\min} \end{bmatrix}, \quad \underline{\dot{\delta}}^{\max} = \begin{bmatrix} \underline{\dot{\delta}}^{\max} \\ \vdots \\ \underline{\dot{\delta}}^{\max} \end{bmatrix}, \quad \underline{\dot{\delta}}^{\min} = \begin{bmatrix} \underline{\dot{\delta}}^{\min} \\ \vdots \\ \underline{\dot{\delta}}^{\min} \end{bmatrix},$$

$$\underline{A}_{j1} = \begin{bmatrix} A_{bend} \\ \vdots \\ A_{bend} \end{bmatrix}, \quad \underline{A}_{j2} = \begin{bmatrix} A_{tors} \\ \vdots \\ A_{tors} \end{bmatrix}, \quad \underline{M}_{j1}^{\max} = \begin{bmatrix} M_{bend}^{\max} \\ \vdots \\ M_{bend}^{\max} \end{bmatrix}, \quad \underline{M}_{j2}^{\max} = \begin{bmatrix} M_{tors}^{\max} \\ \vdots \\ M_{tors}^{\max} \end{bmatrix}$$

ANNEX E

NONLINEAR INVERSE CONTROL

TECHNIQUE

E.1 Introduction

Nonlinear inverse control (NLI) was first developed in the context of solving control problems in robotics where it is necessary to master the major evolution of a system (robot arm, carriage, crane, etc.) apart from any balance situation. With the high nonlinearities which are present in general, this has led to the abandonment of linear control methods that will lead to chaotic behaviour associated with repeated saturation of the actuators. The nonlinear inverse control technique emerges directly from the physical laws of governing the system, so it can control the general trends of the system. Very quickly the research communities in Aeronautics and Space have become interested in this approach and have tried to use it in various applications ranging from stabilization of the natural oscillation modes to trajectory following. In this annex, after the nonlinear inverse control is introduced, its application in many control problems associated with the aircraft piloting is considered.

E.2 Affine nonlinear system

Many dynamical systems admit a state space representation termed *affine*:

$$\begin{cases} \dot{\underline{x}} = f(\underline{x}) + \sum_{j=1}^m g_j(\underline{x})u_j & \underline{x} \in R^n \\ \underline{y} = h(\underline{x}) & \underline{y} \in R^p \end{cases} \quad (\text{E.1})$$

where in general $f(\underline{x})$, $g_i(\underline{x})$ and $h(\underline{x})$ are smooth vector fields of \underline{x} .

A dynamical system which admits an affine state space model is termed as an affine system. The study of systems admitting a representation of affine state space form has grown significantly over the last twenty years and mainly for two reasons:

- This formalism can represent the natural nonlinear dynamics of many mechanical systems and other systems.
- It is possible to achieve an analytical synthesis of control laws for this type of nonlinear systems.

Considering the equations of flight dynamics presented in Annex A, the assumption of linearity of the aerodynamic coefficients towards the angular positions of different control surfaces, implies that the flight dynamics can be expressed in an affine state space model. It is the same for its components (longitudinal dynamics, lateral dynamics, piloting dynamics, guidance dynamics).

E.2.1 Relative degree

Recall that for a scalar function $\lambda(\underline{x})$ and a vector field $f(\underline{x})$, the Lie derivative is defined as follows:

$$\begin{cases} L_f \lambda(\underline{x}) = \langle d\lambda(\underline{x}), f(\underline{x}) \rangle = \frac{\partial \lambda}{\partial \underline{x}} f(\underline{x}) = \sum_{i=1}^n \frac{\partial \lambda}{\partial x_i} f_i(\underline{x}) \\ L_f^k \lambda(\underline{x}) = \frac{\partial (L_f^{k-1} \lambda)}{\partial \underline{x}} \lambda \quad \text{with} \quad L_f^0 \lambda(\underline{x}) = \lambda(\underline{x}) \end{cases} \quad (\text{E.2})$$

Definition: A nonlinear multivariable affine system has the form:

$$\begin{cases} \dot{\underline{x}} = f(\underline{x}) + \sum_{j=1}^m g_j(\underline{x}) u_j \\ \underline{y} = h_i(\underline{x}) \quad i = 1 \text{ to } p \end{cases} \quad (\text{E.3})$$

has a relative degree vector (r_1, r_2, \dots, r_p) defined on the neighbourhood U of an operating point \underline{x}_0 if:

$$L_{g_j} L_f^k h_i(\underline{x}) = 0 \quad 1 \leq j \leq m, 1 \leq i \leq p, k < r_i - 1$$

with

$$L_{g_j} L_f^{r_i-1} h_i(\underline{x}) \neq 0 \quad 1 \leq j \leq m, 1 \leq i \leq p$$

and the matrix $B(\underline{x})$ given by equation (E.4) is full rank at point :

$$B(\underline{x}) = \begin{bmatrix} L_{g_1} L_f^{r_1-1} h_1(\underline{x}) & \cdots & L_{g_m} L_f^{r_1-1} h_1(\underline{x}) \\ L_{g_1} L_f^{r_2-1} h_2(\underline{x}) & \cdots & L_{g_m} L_f^{r_2-1} h_2(\underline{x}) \\ \cdots & \cdots & \cdots \\ L_{g_1} L_f^{r_p-1} h_p(\underline{x}) & \cdots & L_{g_m} L_f^{r_p-1} h_p(\underline{x}) \end{bmatrix} \quad (\text{E.4})$$

Here the relative degree is the minimum order of derivative of the output for which at least one input appears explicitly in the analytical expression of these derivatives.

Especially the relation:

$$\sum_{i=1}^p r_i \leq n \quad (\text{E.5})$$

indicates that the sum of the relative degrees of outputs is less than or equal to the dimension of the system. If $\sum_{i=1}^p r_i < n$, the system presents, with respect to the chosen outputs, some internal dynamics.

E.2.2 Normal form

Isidori [Isidori, 1999] showed that an affine system satisfying the above conditions admits an equivalent affine state space model termed *normal form*:

$$\left\{ \begin{array}{l} \dot{\xi}_{i,1} = \xi_{i,2} \\ \vdots \\ \dot{\xi}_{i,r_i-1} = \xi_{i,r_i} \\ \dot{\xi}_{i,r_i} = A_i(\underline{\xi}, \underline{\eta}) + \sum_{j=1}^m B_{i,j}(\underline{\xi}, \underline{\eta}) u_j \\ i = 1 \text{ to } p \\ \dot{\underline{\eta}} = q(\underline{\xi}, \underline{\eta}, \underline{u}) \end{array} \right. \quad (\text{E.6})$$

where $\underline{\xi}_i = (\xi_{i,1}, \dots, \xi_{i,r_i})' = (y_i, y_i^{(1)}, \dots, y_i^{(r_i-1)})'$

Noting $\underline{\xi} = (\underline{\xi}_1', \dots, \underline{\xi}_p')'$ and $\underline{\eta} = (\eta_1, \dots, \eta_{n-r})'$ with $\dim(\underline{\xi}) + \dim(\underline{\eta}) = n$, the diffeomorphism associated with the transformation of state written:

$$(\underline{\xi}, \underline{\eta})^T = \Phi(\underline{x}) \quad (\text{E.7})$$

assume that $B_{i,j}(\underline{\xi}, \underline{\eta})$ are the coefficients of matrix $B(\underline{x})$ defined by equation (E.4),

$A_i(\underline{\xi}, \underline{\eta})$ are components of the vector $A(\underline{x}) = [L_f^1 h_1(\underline{x}), \dots, L_f^p h_p(\underline{x})]^T$ where \underline{x} is replaced

by $\Phi^{-1}(\underline{\xi}, \underline{\eta})$. (E.6) can be rewritten in a compact form:

$$\begin{aligned} \begin{pmatrix} \dot{\underline{\xi}}_1 \\ \vdots \\ \dot{\underline{\xi}}_p \end{pmatrix} &= A(\underline{\xi}, \underline{\eta}) + B(\underline{\xi}, \underline{\eta}) \underline{u} \\ \dot{\underline{\eta}} &= q(\underline{\xi}, \underline{\eta}, \underline{u}) \end{aligned} \quad (\text{E.8})$$

which shows two distinct dynamics: one of the output and one of other variables which are called internal dynamics. It is clear that if the inputs are dedicated exclusively to control the evolution of output and internal dynamics will develop freely.

The normal form of affine systems is the basis for several methods of synthesis of control laws for affine nonlinear systems. In most cases, the nonlinear control methods such as nonlinear inverse control, sliding mode control, the singular perturbation control and high-gain control, assume that the controlled system admits a representation that is actually a linearizable normal form.

The normal form is a representation in which the external part of the dynamics can be linearized by a static output feedback. Note that it is not a linearization approximation but an exact transformation applied to the state model of system.

E.3 Introduction to nonlinear inverse control

At first, the concepts and assumptions for nonlinear inverse control are presented. Note in particular that although this technique does not apply to all nonlinear dynamical systems, it still has a very wide range of applications.

Consider an affine nonlinear system such as:

$$\begin{cases} \dot{\underline{x}} = f(\underline{x}) + \sum_{j=1}^m g_j(\underline{x}) u_j & \underline{x} \in R^n \\ \underline{y} = h(\underline{x}) & \underline{y} \in R^p \end{cases} \quad (\text{E.9})$$

where relative degrees of outputs are (r_1, r_2, \dots, r_p) on the neighbourhood U of an operating point \underline{x}_0 , then these outputs obey following equations:

$$y_j^{(r_j)} = A_j(\underline{x}) + B_j(\underline{x})\underline{u}, \quad j = 1 \text{ to } p \quad (\text{E.10})$$

In the case where the matrix B^* given by:

$$B^*(\underline{x}) = \begin{bmatrix} B_1(\underline{x}) \\ \vdots \\ B_p(\underline{x}) \end{bmatrix} \quad (\text{E.11})$$

is invertible, it is possible to synthesize a control law that gives each output a predetermined dynamics. It will be for example:

$$\underline{u} = -\left(B^*(\underline{x})\right)^{-1} \left(\begin{bmatrix} \sum_{k=1}^{r_1-1} a_{1k} y_1^{(k)} + a_{10} (y_1 - y_{1c}) \\ \vdots \\ \sum_{k=1}^{r_p-1} a_{pk} y_p^{(k)} + a_{p0} (y_p - y_{pc}) \end{bmatrix} + \begin{bmatrix} A_1(\underline{x}) \\ \vdots \\ A_p(\underline{x}) \end{bmatrix} \right) \quad (\text{E.12})$$

here a linear dynamic around their desired values for each output is adopted. For example, the output j obeys the dynamics:

$$y_j^{(r_j)} + \sum_{k=1}^{r_j-1} a_{jk} y_j^{(k)} + a_{j0} (y_j - y_{jc}) = 0, \quad j = 1 \text{ to } p \quad (\text{E.13})$$

In general, the polynomials $s^{r_j} + \sum_{k=1}^{r_j-1} a_{jk} s^k + a_{j0}$ will be selected to obtain stable dynamics for output and thus converge to their desired values. The approach proposed as shown in (E.13) also leads to a theoretical decoupling of the dynamics of each output, which can also be a target of this approach in the specification of the control law. For example, regarding the lateral control of a transport aircraft, the sideslip angle (β) and the bank angle (ϕ) are preferred to be decoupled.

Regarding the trajectory following of the outputs of the system, it will be possible if the dynamics chosen for the outputs of the system are much faster than the dynamics of the reference trajectory.

However, it must satisfy several conditions before these objectives are actually achieved:

- The actuators must not be led by this law to saturation (in velocity or position), which will

lead to performance degradation.

- There is no internal dynamics ($\sum_{i=1}^p r_i = n$), or if there are internal dynamics ($\sum_{i=1}^p r_i < n$), they are stable; otherwise the survival of the system would be put at risk.
- The model used to perform the inversion is sufficiently representative of the dynamics that is claimed to invert, otherwise a shift will happen.

BIBLIOGRAPHY

- Airbus. (2000). A340-Flight deck and systems briefing for pilots.
- Alwi, H. (2008). *Fault Tolerant Sliding Mode Control Schemes with Aerospace Applications*.
- Andrei, Geanina. (2010). *Contribution à la commande tolérante aux pannes pour la conduite du vol*. (PhD), INSA.
- Antonious, Andreas, & Lu, Wusheng. (2007). *Practical Optimization Algorithms and Engineering Applications*: Springer.
- Australian Transport Safety Bureau. (2007). In-flight upset event 240 km north-west of Perth, WA Boeing Company 777-200, 9M-MRG 1 August 2005.
- Aviation Safety Network. (2013). ASN Aircraft Accident Airbus A300 Baghdad International Airport. <http://aviation-safety.net/database/record.php?id=20031122-0>
- Bajpai, G., Chang, B. C., & Kwatny, H. G. (2002). *Design of fault-tolerant systems for actuator failures in nonlinear systems*. Paper presented at the American Control Conference.
- Balasubramanian, R. (1989). *Continuous Time Controller Design*. Stevenage, UK: Peter Peregrinus Ltd.,.
- Belcastro, Christine M. (2011). *Aircraft Loss-of-Control: Analysis and Requirements for Future Safety-Critical Systems and their Validation*. Paper presented at the 8th Asian Control Conference.
- Belcastro, Christine M., & Foster, John V. (2010). *Aircraft Loss-of-Control Accident Analysis*. Paper presented at the AIAA Guidance, Navigation and Control Conference.
- Bertsekas, Dimitri P. (1982). *Constrained Optimization and Lagrange Multiplier Methods*. New York, USA: Academic Press.
- Billings, Charles E. (1997). *Aviation automation: The search for a human-centered approach*.
- Bjorck, Ake. (1996). *Numerical Methods for Least Squares Problems*: SIAM.
- Blanke, Mogens. (1999). *The robust control mixer module method for control reconfiguration*. Paper presented at the American Control Conference.
- Bodson, Marc. (2002). Evaluation of Optimization Methods for Control Allocation. *Journal of Guidance, Control, and Dynamics*, 25(4), 703-711.
- Boeing Commercial Airplanes. (2013). Statistical Summary of Commercial Jet Airplane Accidents Worldwide Operations 1959-2012.
- Boskovic, J. D., & Mehra, R. K. (1998). *A stable scheme for automatic control reconfiguration in the presence of actuator failures*. Paper presented at the American Control Conference, Philadelphia, Pennsylvania, USA.
- Boskovic, Jovan D., & Mehra, Raman K. (1999). *Stable multiple model adaptive flight control for accommodation of a large class of control effector failures*. Paper presented at the American Control Conference.
- Bouzerdoum, A., & Pattison, T. R. (1993). Neural Network for Quadratic Optimization with Bound Constraints. *IEEE transactions on neural networks*, 4(2), 293-304.
- Boyd, Stephen, & Vandenberghe, Lieven. (2004). *Convex Optimization*. New York, USA:

Cambridge University Press.

Briere, Dominique, Favre, Christian, & Traverse, Pascal. (2001). Electrical Flight Controls, From Airbus A320/330/340 to Future Military Transport Aircraft: A Family of Fault-Tolerant Systems.

Broyden, CG, & Attia, NF. (1988). Penalty functions, Newton's method, and quadratic programming. *Journal of optimization theory and applications*, 58(3), 377-385.

Buffington, James M. (1999). Modular Control Law Design for the Innovative Control Aircraft Configuration (pp. 154-154).

Buffington, James M., & Enns, Dale F. (1996). Lyapunov stability analysis of daisy chain control allocation. *Journal of Guidance, Control, and Dynamics*, 19(6), 1226-1230.

Burcham, Frank W, Burken, John, & Maine, Trindel A. (1994). *Flight testing a propulsion-controlled aircraft emergency flight control system on an F-15 airplane*: National Aeronautics and Space Administration, Office of Management, Scientific and Technical Information Program.

Burcham, Frank W., Burken, John J., Maine, Trindel A., & Fullerton, C. Gordon. (1997). Development and Flight Test of an Emergency Flight Control System Using Only Engine Thrust on an MD-11 Transport Airplane.

Bureau d'Enquetes et d'Analyses. (2012). Final report on the accident on 1st June 2009 to the Airbus A330-203 registered F-GZCP operated by Air France flight AF 447 Rio de Janeiro–Paris: Tech. rep., Bureau d'Enquêtes et d'Analyses pour la sécurité de l'aviation civile, 2012,(English Translation).

Burken, John J., Lu, Ping, Wu, Zhenglu, & Bahm, Cathy. (2001). Two Reconfigurable Flight-Control Design Methods: Robust Servomechanism and Control Allocation. *Journal of Guidance, Control, and Dynamics*, 24(3), 482-494.

Calise, Anthony J, Lee, Seungjae, & Sharma, Manu. (1998). *Direct adaptive reconfigurable control of a tailless fighter aircraft*. Paper presented at the Proceedings of the 1998 AIAA Guidance, Navigation and Control Conference.

Calise, Anthony J, Lee, Seungjae, & Sharma, Manu. (2000). *Development of a reconfigurable flight control law for the X-36 tailless fighter aircraft*. Paper presented at the AIAA Guidance, Navigation, and Control Conference.

Calise, Anthony J., Lee, Seungjae, & Sharma, Manu. (2001). Development of a Reconfigurable Flight Control Law for Tailless Aircraft. *Journal of Guidance, Control, and Dynamics*, 24(5), 896-902.

Chang, Bor-Chin, Kwatny, Harry G, Belcastro, Christine, & Belcastro, Celeste. (2008). *Aircraft Loss-of-Control Accident Prevention: Switching Control of the GTM Aircraft with Elevator Jam Failures*. Paper presented at the AIAA Guidance, Navigation and Control Conference and Exhibit.

Cichocki, A., & Unbehauen, R. (1993). Neural Networks for Optimization and Signal Processing. *Book*.

Civil Aviation Authority. (2013). Global Fatal Accident Review 2002 to 2011 *CAP 1036*.

- De Almeida, Fabio A. (2011). Reference Management for Fault-Tolerant Model Predictive Control. *Journal of Guidance, Control, and Dynamics*, 34(1), 44-56.
- De Almeida, Fabio A., & Leissling, Dirk. (2009). *Fault tolerant flight control system using model predictive control*.
- Demirci, Ufuk, & Kerestecioglu, Feza. (2005). Fault tolerant control with re-configuring sliding-mode schemes. *Turk J Elec Engin*, 13(1), 175-187.
- Dennis, J. E., & Schnabel, Robert B. (1996). *Numerical Methods for Unconstrained Optimization and Optimization and Nonlinear Equations*: SIAM.
- Durham, Wayne C. (1994). Attainable Moments for the Constrained Control Allocation Problem. *J. Guidance*, 17(6), 1371-1373.
- Edwards, C., Smaili, H., & Lombaerts, T. (2010). *Fault Tolerant Flight Control-A Benchmark Challenge*: Springer-Verlag.
- Etkin, Bernard, & Reid, Lloyd Duff. (1996). *Dynamics of Flight: Stability and Control*.
- European Aviation Safety Agency. (2007). Certification Specifications for Large Aeroplanes CS-25.
- Fliess, M, Levine, J, Martin, Ph, & Rouchon, Ph. (1992). On differentially flat nonlinear-systems. *COMPTEs RENDUS DE L ACADEMIE DES SCIENCES SERIE I-MATHEMATIQUE*, 315(5), 619-624.
- Fliess, Michel, Lévine, Jean, Martin, Philippe, & Rouchon, Pierre. (1995). Flatness and defect of non-linear systems: introductory theory and examples. *International journal of control*, 61(6), 1327-1361.
- Fossen, T. I., & Johansen, T. A. (2006). *A Survey of Control Allocation Methods for Ships and Underwater Vehicles*. Paper presented at the the 14th Mediterranean Conference on Control and Automation, Ancona, Italy.
- Frank, Paul M. (1991). *Enhancement of robustness in observer-based fault detection*. Paper presented at the IFAC, IMACS Safeprocess Symposium, Baden-Baden, Germany
- Fravolini, Mario L, Campa, Giampiero, & Napolitano, MR. (2001). *A Neural Network Based Tool for Aircraft SFDIA Modeling and Simulation*. Paper presented at the Proceedings of the IASTED Conference, Pittsburgh, PA.
- Gaulocher, S., Cumer, C., & Alazard, D. (2007). Aircraft load alleviation during maneuvers using optimal control surface combinations. *Journal of Guidance, Control, and Dynamics*, 30(2), 591-600.
- Gertler, Janos J. (1988). Survey of model-based failure detection and isolation in complex plants. *Control Systems Magazine, IEEE*, 8(6), 3-11.
- Ghasabi-Oskoei, H., & Mahdavi-Amiri, N. (2006). An Efficient Simplified Neural Network for Solving Linear and Quadratic Programming Problems. *Applied Mathematics and Computation*, 175(1), 452-464.
- Ghosh, Jayati, & Paden, Brad. (2000). *Pseudo-inverse based iterative learning control for plants with unmodelled dynamics*. Paper presented at the American Control Conference, 2000. Proceedings of the 2000.

- Gill, P.E., Gould, N.I.M., Murray, W., Saunders, M.A., & Wright, M.H. (1982). Range space methods for convex quadratic programming: Systems Optimization Laboratory, Department of Operations Research, Stanford University.
- Gill, Philip E., & Murray, Walter. (1978). Numerically Stable Methods for Quadratic Programming. *Mathematical Programming*, 14(1), 349-372.
- Gondzio, Jacek. (2012). Interior Point Methods 25 Years Later. *European Journal of Operational Research*, 218(3), 587-601.
- Gould, Nicholas I. M., Hribar, Mary E., & Nocedal, Jorge. (2001). On the Solution of Equality Constrained Quadratic Programming Problems Arising in Optimization. *SIAM Journal on Scientific Computing*, 23(4), 1376-1405.
- Goupil, Philippe. (2011). AIRBUS state of the art and practices on FDI and FTC in flight control system. *Control Engineering Practice*, 19(6), 524-539.
- Han, Y., Oh, S., Choi, B., Kwak, D., Kim, H. J., & Kim, Y. (2012). Fault detection and identification of aircraft control surface using adaptive observer and input bias estimator. *IET Control Theory & Applications*, 6(10), 1367-1387.
- Harkegard, O. (2002). *Efficient active set algorithms for solving constrained least squares problems in aircraft control allocation*. Paper presented at the the 41st IEEE Conference on Decision and Control.
- He, Bingsheng, & Hubland, Am. (1992). A Projection and Contraction Method for a Class of Linear Complementarity Problems and Its Application in Convex Quadratic Programming. *Applied Mathematics and Optimization*, 25(3), 247-262.
- Hindi, Haitham. (2006). *A tutorial on convex optimization II: duality and interior point methods*. Paper presented at the American Control Conference.
- Hodel, A. S., & Callahan, Ronnie. (2002). *Autonomous Reconfigurable Control Allocation (ARCA) for Reusable Launch Vehicles*. Paper presented at the AIAA Guidance, Navigation, and Control Conference and Exhibit, Monterey, California.
- HONEYWELL, & Lockheed Martin. (1996). Application of Multivariable Control Theory to Aircraft Control Laws _ Final Report: Multivariable Control Design Guidelines.
- Hunt, Valerio R, & Zellweger, Andres. (1987). The FAA's Advanced Automation System: strategies for future air traffic control systems. *Computer*, 20(2), 19-32.
- Huzmezan, Mihai, & Maciejowski, J. (1997). Reconfigurable flight control methods and related issues—a survey. *DERA Report No: ASF/3455*.
- Hwang, Inseok, Kim, Sungwan, Kim, Youdan, & Seah, Chze Eng. (2010). A Survey of Fault Detection, Isolation, and Reconfiguration Methods. *IEEE Transactions on Control Systems Technology*, 18(3), 636-653.
- ICAO. (2007). *ICAO Annex 10 Volume IV Surveillance and Collision Avoidance Systems*.
- Idan, Moshe, Calise, Anthony J, Kutai, All T, & Parekh, David E. (2003). Adaptive neural network based approach for active flow control. *COURSES AND LECTURES-INTERNATIONAL CENTRE FOR MECHANICAL SCIENCES*, 287-298.
- Isermann, R., & Balle, P. (1997). Trends in the application of model-based fault detection and

- diagnosis of technical processes. *Control Engineering Practice*, 5(5), 709-719.
- Isermann, Rolf. (2005). Model based fault detection and diagnosis - status and applications. *Annual Reviews in Control*, 29(1), 71-85.
- Isermann, Rolf. (2006). *Fault-Diagnosis Systems - an introduction from fault detection to fault tolerant*: Springer Verlag.
- Isidori, Alberto. (1983). *Nonlinear Control Systems: An Introduction*: Springer-Verlag.
- Isidori, Alberto. (1999). *Nonlinear Control Systems II*: Springer-Verlag.
- Jiang, Jin, & Yu, Xiang. (2012). Fault-tolerant control systems: A comparative study between active and passive approaches. *Annual Reviews in Control*, 36(1), 60-72.
- Jiang, Jin, & Zhao, Qing. (2000). Design of Reliable Control Systems Possessing Actuator Redundancies. *Journal of Guidance, Control, and Dynamics*, 23(4), 709-718.
- Johansen, T. A., Fossen, T. I., & Berge, S. P. (2004). Constrained Nonlinear Control Allocation With Singularity Avoidance Using Sequential Quadratic Programming. *IEEE Transactions on Control Systems Technology*, 12(1), 211-216.
- Johansen, Tor A., & Fossen, Thor I. (2013). Control Allocation - A Survey. *Automatica*, 49(5), 1087-1103.
- Johnson, E, Calise, Anthony, & Corban, J Eric. (2002). *A six degree-of-freedom adaptive flight control architecture for trajectory following*. Paper presented at the Proceedings of the AIAA Guidance, Navigation, and Control Conference.
- Johnson, Eric N, Calise, Anthony J, & Corban, J Eric. (2001). *Adaptive guidance and control for autonomous launch vehicles*. Paper presented at the Aerospace Conference, 2001, IEEE Proceedings.
- Jones, Colin N. (2005). Reconfigurable Flight Control First Year Report.
- Joosten, D. A., Boom, T. J. J. van den, & Lombaerts, T. J. J. (2008). *Fault-tolerant control using dynamic inversion and model-predictive control applied to an aerospace benchmark*. Paper presented at the the 17th World Congress of the International Federation of Automatic Control, Seoul, Korea.
- Kale, M. M., & Chipperfield, A. J. (2002). *Reconfigurable flight control strategies using model predictive control*.
- Kale, M. M., & Chipperfield, A. J. (2005). Stabilized MPC formulations for robust reconfigurable flight control. *Control Engineering Practice*, 13, 771-788.
- Kamel, Mohamed S., & Xia, Youshen. (2009). Cooperative recurrent modular neural networks for constrained optimization: a survey of models and applications. *Cognitive neurodynamics*, 3(1), 47-81.
- Kanev, S, & Verhaegen, M. (2000). *A bank of reconfigurable LQG controllers for linear systems subjected to failures*. Paper presented at the Decision and Control, 2000. Proceedings of the 39th IEEE Conference on.
- Kennedy, M. P., & Chua, L. O. (1988). Neural Networks for Nonlinear Programming. *IEEE Transactions on Circuits and Systems*, 35(5), 554-562.

- Kuhn, Harold W, & Tucker, Albert W. (1951). *Nonlinear programming*. Paper presented at the Proceedings of the second Berkeley symposium on mathematical statistics and probability.
- Lafourcade, L., Cumer, Ch, & Döll, C. (2010). *IMMUNE: Control Reallocation after Surface Failures Using Model Predictive Control*. Paper presented at the the 27th International Congress of the Aeronautical Sciences, Nice, France.
- Lambrechts, Paul, Bennani, Samir, Looye, Gertjan, & Moormann, Dieter. (1997). *The RCAM design challenge problem description*. Paper presented at the Robust Flight Control Lecture Notes in Control and Information Sciences.
- Lau, Mark S. K., Yue, S. P., Ling, K. V., & Maciejowski, J. M. (2009). *A Comparison of Interior Point and Active Set Methods for FPGA Implementation of Model Predictive Control*. Paper presented at the European Control Conference, Budapest, Hungary.
- Li, Hongbin, Zhao, Qing, & Yang, Zhenyu. (2007). Reliability Modeling of Fault Tolerant Control Systems. *International Journal of Applied Mathematics and Computer Science*, 17(4), 491-504.
- Liu, Qingshan, & Wang, Jun. (2008a). A One-Layer Recurrent Neural Network with a Discontinuous Activation Function for Linear Programming. *Neural Computation*, 20, 1366-1383.
- Liu, Qingshan, & Wang, Jun. (2008b). A one-layer recurrent neural network with a discontinuous hard-limiting activation function for quadratic programming. *IEEE transactions on neural networks*, 19(4), 558-570.
- Liu, Qingshan, & Wang, Jun. (2011). Finite-time convergent recurrent neural network with a hard-limiting activation function for constrained optimization with piecewise-linear objective functions. *IEEE transactions on neural networks*, 22(4), 601-613.
- Lombaerts, T. J. J., Chu, Q. P., Mulder, J. a, & Joosten, D. a. (2011). Modular Flight Control Reconfiguration Design and Simulation. *Control Engineering Practice*, 19(6), 540-554.
- Lu, W, Mora-Camino, F, & Achaibou, K. (2005). *Differential Flatness and Flight Guidance: A Neural Adaptive Approach*. Paper presented at the AIAA, Guidance Navigation and Control Conference, San Francisco, USA.
- Lu, Wenchi. (2005). *Contribution au Suivi Automatique de Trajectoire par un avion: Commande Plate et Réseaux de Neurones*. (PhD), Thèse doctorale, Université Toulouse II.
- Lu, Wenchi, Mora-Camino, Félix, de Coligny, M, & Achaibou, K. (2004). *Flight mechanics and differential flatness*. Paper presented at the Dynamics and Control Conference. Ilha Solteira, Brasil.
- Luenberger, David G., & Ye, Yinyu. (2008). *Linear and Nonlinear Programming*: Springer.
- Luo, Yu, Serrani, A., Yurkovich, S., Doman, David B., & Oppenheimer, Michael W. (2004). *Model Predictive Dynamic Control Allocation with Actuator Dynamics*. Paper presented at the American Control Conference.
- Maa, Chia-Yiu, & Shanblatt, Michael A. (1992). Linear and Quadratic Programming Neural Network Analysis. *IEEE transactions on neural networks*, 3(4), 580-594.
- Maciejowski, Jan M., & Jones, Colin N. (2003). *MPC fault-tolerant control case study: FLIGHT*

1862. Paper presented at the Proc. IFAC Safe Process Conf.
- Marcos, Andrés, Ganguli, Subhabrata, & Balas, Gary J. (2003). *New strategies for fault tolerant control and fault diagnostic*. Paper presented at the Fault Detection, Supervision and Safety of Technical Processes 2003 (SAFEPROCESS 2003): A Proceedings Volume from the 5th IFAC Symposium, Washington, DC, USA, 9-11 June 2003.
- Martino, Davide. (2008). *Flight Control with Amplitude and Rate Constraints: a Command Governor Approach*. Paper presented at the American Control Conference, Washington, USA.
- MathWorks. (2009). *Matlab User's Guide's Version 7.8*. USA.
- Mayne, D. Q., Rawlings, J. B., Rao, C. V., & Scokaert, P. O. M. (2000). Constrained model predictive control: Stability and optimality. *Automatica*, 36, 789-814.
- McLean, Donald. (1990). *Automatic Flight Control Systems*: Prentice-Hall.
- McMahan, Jack. (1978). Flight 1080. *Air Line Pilot*, 47(7), 6-11.
- Menon, Padmanabhan K, Sweriduk, Gregory D, & Bilimoria, Karl D. (2004). New approach for modeling, analysis, and control of air traffic flow. *Journal of Guidance, Control, and Dynamics*, 27(5), 737-744.
- Mora-Camino, F. (2013). *Lecture Notes on Flight Control Systems*: ENAC.
- National Transportation Safety Board. (2001). Aircraft Accident Report 01/01: United Airlines Flight 585.
- National Transportation Safety Board. (2004). Aircraft Accident Report 04/01: Air Midwest Flight 5481.
- Nichols, R. A., Reichert, R. T., & Rugh, W. J. (1993). Gain scheduling for H-infinity controllers: a flight control example. *IEEE Transactions on Control Systems Technology*, 1(2), 69-79.
- Nocedal, Jorge, & Wright, Stephen J. (1999). *Numerical Optimization*: Springer.
- O'Leary, Dianne Prost. (1980). A generalized conjugate gradient algorithm for solving a class of quadratic programming problems. *Linear Algebra and its Applications*, 34, 371-399.
- Oppenheimer, Michael W., Doman, David B., & Bolender, Michael A. (2006). Control Allocation for Over-actuated Systems. *the 14th Mediterranean Conference on Control and Automation*(2), 1-6.
- Pashilkar, A. A., Sundararajan, N., & Saratchandran, P. (2006). A Fault-Tolerant Neural Aided Controller for Aircraft Auto-Landing. *Aerospace Science and Technology*, 10, 49-61.
- Patton, R. (1997). *Where are we in fault tolerant control*. Paper presented at the Seminar notes, June.
- Patton, Ron J. (1997). *Fault-tolerant control systems: The 1997 situation*. Paper presented at the Proc. of IFAC Symp. on Fault Detection, Supervision and Safety for Technical Processes (SAFEPROCESS'97), Hull, UK.
- Petersen, J. A. M., & Bodson, Marc. (2005). Interior-point Algorithms for Control Allocation. *Journal of guidance, control, and dynamics*, 28(3), 471-480.
- Polycarpou, Marios M, & Ioannou, Petros A. (1991). *Identification and control of nonlinear*

systems using neural network models: Design and stability analysis: Citeseer.

Pratt, Roger W. (2000). *Flight Control Systems practical issues in design and implementation*: Institution of Engineering and Technology.

Pyne, I. B. (1956). Linear Programming on an Electronic Analogue Computer. *Transactions of the American Institute of Electrical Engineering*, 75, 139-139.

Reich, Joshua, & Sklar, Elizabeth. (2006). *Toward automatic reconfiguration of robot-sensor networks for urban search and rescue*. Paper presented at the Proceedings of the 1st International Workshop on Agent Technology for Disaster Management.

Roux, Élodie. (2006). *Modèle de Masse Voilure: Avions de transport civil*. Thesis PhD, 349-349.

Rugh, W. J. (1991). Analytical framework for gain scheduling. *IEEE Control Systems*, 11(1), 79-84.

Shamma, J. S., & Athans, M. (1992). Gain scheduling: potential hazards and possible remedies. *IEEE Control Systems*, 12(3), 101-107.

Shin, D., Moon, G., & Kim, Y. (2005). Design of Reconfigurable Flight Control System Using Adaptive Sliding Mode Control: Actuator Fault. *Proceedings of the Institution of Mechanical Engineers, Part G: Journal of Aerospace Engineering*, 219(4), 321-328.

Slotine, Jean-Jacques E., & Li, Weiping. (1991). *Applied Nonlinear Control*: Prentice-Hall.

Smaili, M. H., Breeman, J., Lombaerts, T. J. J., & Stroosma, O. (2008). *A Simulation Benchmark for Aircraft Survivability Assessment*. Paper presented at the the 26th International Congress of the Aeronautical Sciences.

Steinberg, Marc L. (2005). A Historical Overview of Research in Reconfigurable Flight Control. *Proceedings of the Institution of Mechanical Engineers, Part G: Journal of Aerospace Engineering*, 219(4), 263-275.

Stevens, Brian L., & Lewis, Frank L. (1992). *Aircraft Control and Simulation*: Wiley.

Stoustrup, Jakob, & Niemann, Henrik. (2001). *Fault tolerant feedback control using the youla parameterization*. Paper presented at the Proceedings of the 6th European Control Conference.

Tøndel, P., & Johansen, T. A. (2005). *Control allocation for yaw stabilization in automotive vehicles using multiparametric nonlinear programming*. Paper presented at the American Control Conference.

Tang, Xidong, Tao, Gang, & Joshi, Suresh M. (2007). Adaptive actuator failure compensation for nonlinear MIMO systems with an aircraft control application. *Automatica*, 43(11), 1869-1883.

Tank, David W., & Hopfield, J. J. (1986). Simple "Neural" Optimization Networks: An A/D Converter, Signal Decision Circuit, and a Linear Programming Circuit. *IEEE Transactions on Circuits and Systems*, 33(5), 533-541.

Tao, Qing, Cao, Jinde, Xue, Meisheng, & Qiao, Hong. (2001). A high performance neural network for solving nonlinear programming problems with hybrid constraints. *Physics Letters A*, 288(2), 88-94.

Tillerson, Michael, Inalhan, Gokhan, & How, Jonathan P. (2002). Co - ordination and control of

- distributed spacecraft systems using convex optimization techniques. *International Journal of robust and nonlinear control*, 12(2 - 3), 207-242.
- Tomlin, Claire, Pappas, George J., & Sastry, Shankar. (1998). Conflict resolution for air traffic management: A study in multiagent hybrid systems. *Automatic Control, IEEE Transactions on*, 43(4), 509-521.
- Tondel, P., & Johansen, T.A. (2005). *Control allocation for yaw stabilization in automotive vehicles using multiparametric nonlinear programming*. Paper presented at the Proceedings of the American Control Conference.
- Total, Joseph J. (1996). *Simulation evaluation of a neural-based flight controller*. Paper presented at the AIAA Flight Simulation Technologies Conference.
- Traverse, Pascal, Lacaze, Isabelle, & Souyris, Jean. (2006). *Airbus fly-by-wire: a process toward total dependability*. Paper presented at the ICAS.
- Van Oort, E. R., Chu, Q. P., Mulder, J. A., & van den Boom, T. J. J. (2006). *Robust Model Predictive Control of a Feedback Linearized Nonlinear F-16/MATV Aircraft Model*. Keystone, Colorado.
- Wang, Jun. (1993). Analysis and design of a recurrent neural network for linear programming. *IEEE Transactions on Circuits and Systems I: Fundamental Theory and Applications*, 40(9), 613-618.
- Wang, Qingguo. (2003). *Decoupling control* (Vol. 285): Springer.
- Wickens, Christopher D. (1998). *The future of air traffic control: Human operators and automation*: National Academies Press.
- Wong, Elizabeth. (2011). *Active-Set Methods for Quadratic Programming*.
- Wright, S. (1988). A fast algorithm for equality-constrained quadratic programming on the Alliant FX/8. *Annals of Operations Research*, 14(1), 225-243.
- Wright, Stephen J. (1997). *Primal-Dual Interior-Point Methods*: SIAM.
- Wu, Xin-Yu, Xia, Youshen, Li, Jianmin, & Chen, Wai-Kai. (1996). A high-performance neural network for solving linear and quadratic programming problems. *IEEE transactions on neural networks*, 7(3), 643-651.
- Xia, Youshen. (1996). A new neural network for solving linear and quadratic programming problems. *IEEE transactions on neural networks*, 7(6), 1544-1548.
- Xia, Youshen, & Wang, Jiasong. (1995). Neural Network for Solving Linear Programming Problems with Bounded Variables. *IEEE transactions on neural networks*, 6(2), 515-519.
- Xia, Youshen, & Wang, Jun. (2001). *Recurrent Neural Networks for Optimization: the State of the Art*: CRC Press.
- Yang, Zhenyu, & Blanke, Mogens. (2000a). Adaptive control mixer method for nonlinear control reconfiguration: A case study.
- Yang, Zhenyu, & Blanke, Mogens. (2000b). *The robust control mixer module method for control reconfiguration*. Paper presented at the American Control Conference, 2000. Proceedings of the 2000.

- Yang, Zhenyu, Shao, Huazhang, & Chen, Zongji. (1999). *The frequency-domain heterogeneous control mixer module method for control reconfiguration*. Paper presented at the IEEE International Conference on Control Applications.
- Yeh, Y. C. Bob. (1998). *Design Considerations in Boeing 777 Fly-By-Wire Computers Flight Systems*. Paper presented at the the 3rd IEEE International High-Assurance Systems Engineering Symposium.
- Zhang, Nan. (2010). *Détection et isolation de pannes basées sur la platitude différentielle: application aux engins atmosphériques*. (PhD), l'INSA de Toulouse.
- Zhang, Youmin, & Jiang, Jin. (2001a). Integrated active fault-tolerant control using IMM approach. *Aerospace and Electronic Systems, IEEE Transactions on*, 37(4), 1221-1235.
- Zhang, Youmin, & Jiang, Jin. (2001b). Integrated design of reconfigurable fault-tolerant control systems. *Journal of Guidance, control, and Dynamics*, 24(1), 133-136.
- Zhang, Youmin, & Jiang, Jin. (2008). Bibliographical Review on Reconfigurable Fault-Tolerant Control Systems. *Annual Reviews in Control*, 32(2), 229-252.
- Zhang, Yunong. (2005). *On the LVI-based Primal-Dual Neural Network for Solving Online Linear and Quadratic Programming Problems*. Paper presented at the American Control Conference, Portland, OR, USA.
- Zhang, Yunong, Ge, Shuzhi Sam, & Lee, Tong Heng. (2004). A Unified Quadratic-Programming-Based Dynamical System Approach to Joint Torque Optimization of Physically Constrained Redundant Manipulators. *IEEE Transactions on Systems, Man, and Cybernetics*, 34(5), 2126-2132.
- Zhang, Yunong, & Wang, Jun. (2002). A dual neural network for convex quadratic programming subject to linear equality and inequality constraints. *Physics Letters A*, 298(4), 271-278.
- Zhang, Yunong, Wang, Jun, & Xia, Youshen. (2003). A dual neural network for redundancy resolution of kinematically redundant manipulators subject to joint limits and joint velocity limits. *IEEE transactions on neural networks*, 14(3), 658-667.
- Zhong, Lunlong, & Mora-Camino, Félix. (2012). *Neural Networks Based Aircraft Fault Tolerant Control*. Paper presented at the 14th AIAA/ISSMO Multidisciplinary Analysis and Optimization Conference, Indiana, USA.
- Zhong, Lunlong, & Mora-Camino, Félix. (2013). *Aircraft Fault Tolerant Control Based on Active Set Method*. Paper presented at the 25th Chinese Control and Decision Conference, Guiyang, China.
- Zhong, Lunlong, & Mora-Camino, Félix. (2014). *MPC Based Handling Qualities Assessment for a Transportation Aircraft with Failed Actuators*. Paper presented at the AIAA Science and Technology Forum and Exposition 2014, National Harbor, Maryland, USA.
- Zhong, Lunlong, Wu, Hongying, Bouadi, Hakim, & Mora-Camino, Félix. (2011). *Management of control channels under actuator failure: An optimization approach*. Paper presented at the 30th AIAA/IEEE Digital Avionics Systems Conference, Seattle, WA, USA.

RÉSUMÉ

CONTRIBUTION À LA COMMANDE TOLERANTE AUX FAUTES POUR LA CONDUITE DU VOL AVEC PANNE D'ACTIONNEUR

INTRODUCTION GÉNÉRALE

L'automatisation des systèmes embarqués occupe une place de plus en plus importante pour assurer la sécurité des opérations aériennes. Aujourd'hui, deux principaux domaines de recherche se développent dans le domaine de la commande automatique appliquée au domaine aéronautique:

- Il s'agit d'abord d'un domaine de recherche qui concerne la conception de systèmes automatiques intégrés qui aident à maintenir la sécurité des vols face à l'occurrence de défaillances du système de conduite automatique du vol des avions de transport (défaillance des composants et sous-systèmes de circuits électriques ou hydrauliques, des chaînes de commande): menant à la conception de systèmes de commande tolérants aux pannes qui sont généralement adaptatifs et non linéaires afin d'aider à la gestion des situations de pannes critiques.

- L'autre domaine de recherche concerne la conception des systèmes automatiques embarqués qui contribuent à la gestion du trafic aérien. En effet, au cours des dernières décennies, il a été possible de gérer simplement la capacité limitée de l'espace aérien et de minimiser les risques de collision entre les aéronefs. Mais depuis, l'accroissement du trafic aérien a conduit à de nouveaux problèmes où la sécurité est en jeu et au développement de nouvelles fonctions de conduite automatique du vol. Aujourd'hui l'automatisation offre une contribution significative à l'efficacité du contrôle du trafic aérien.

Cette thèse porte sur le premier domaine de recherche et tente de contribuer à la sécurité des vols de l'aviation commerciale en développant de nouvelles techniques de contrôle automatique afin de mieux gérer les situations de pannes matérielles des chaînes de commande. Les statistiques montrent que la perte de contrôle (LOC) reste l'un des plus grands contributeurs aux accidents mortels dans le monde entier et la panne des systèmes critiques est le premier facteur contribuant à la LOC. Par l'utilisation "intelligente" des actionneurs restants pour contrôler, à l'aide des surfaces de contrôle et des moteurs ou d'une combinaison des deux, les mouvements de l'avion suivant ses trois axes, il est possible d'assurer la sécurité du vol.

L'objectif principal de ces stratégies de contrôle est de restaurer la stabilité et la manœuvrabilité

de l'avion face à une défaillance des actionneurs aérodynamiques qui est une panne critique pour les aéronefs. Grâce à la redondance des actionneurs, ce type de pannes peut être compensée en tenant compte de leurs effets sur la dynamique du vol. Pendant ce temps, l'intégrité structurelle doit être considérée en tenant compte de la possibilité d'apparition de charges excessives générées par les actionneurs en panne et les actionneurs restants plus fortement sollicités. Ainsi, cette situation peut être gérée de manière aussi sûre que possible avec la réaffectation des actionneurs restants afin d'effectuer la manœuvre désirée ou une autre manœuvre tout en maintenant l'intégrité structurelle de l'avion.

En fait, il est supposé dans cette thèse que les techniques de détection de défaut et d'identification (Fault Detection and Identification-FDI) permettent de détecter et d'identifier les défaillances d'actionneurs en temps réel afin que la reconfiguration immédiate puisse être mise en œuvre. De nombreuses études dans ces domaines ont déjà été produites, ce qui conduit à des méthodes efficaces de détection en ligne de pannes des actionneurs et de leur identification.

Dans cette thèse premièrement sont analysées dans le cas des avions de transport modernes, la structure de leurs chaînes de commande de vol et les modes de défaillance de leurs principaux composants. Les qualités de vol de l'avion de transport moderne sont revisitées tandis que les conséquences des défaillances des actionneurs sur elles sont également discutées. Alors les techniques générales de commande tolérante aux pannes sont considérées tandis que les solutions adoptées sur les avions de transport modernes sont présentées et discutées. Différents concepts utiles pour analyser la tolérance aux pannes sont présentés dans cette thèse, tels que: le degré de multiplicité des actionneurs, une redondance complète d'entrée, la redondance totale des entrées, les entrées virtuelles, les matrices de distribution et de mélange.

Quand une défaillance d'actionneur se produit, une reconfiguration immédiate devrait aboutir à la réaffectation des actionneurs restants opérationnels. Ce problème de réaffectation a été formulé comme un problème linéaire quadratique (LQ) où différents cas peuvent être distingués lors de l'examen de l'existence et de la multiplicité des solutions. Au cours de cette recherche, trois solveurs de programmation linéaire quadratique ont été étudiés, programmés et appliqués à différentes situations de pannes des actionneurs.

La première situation considérée est abordée en ligne et vise à caractériser les qualités de vol

restantes et les qualités de manœuvrabilité lorsque un scénario de défaillance des actionneurs particulier se produit. Ce problème a été abordé en adoptant une approche de type commande prédictive à base de modèle (Model Predictive Control-MPC), ce qui conduit effectivement à la résolution d'un problème LQ.

Dans l'autre cas considéré, où il est déjà connu que le cas de courant de panne ne devrait pas nuire à la réalisation d'une manœuvre particulière, la solution en ligne d'un problème LQ propose la réaffectation nécessaire des actionneurs opérationnels. Dans ce cas, les valeurs requises pour les entrées virtuelles pour exécuter la manœuvre envisagée sont calculées par inversion non linéaire de la dynamique de sortie.

Dans le chapitre 1, l'organisation des chaînes de commande des avions de transport modernes est affichée et analysée, tandis qu'un aperçu des types de défaillance des commandes de vol est présentée, montrant la diversité des situations de défaillance à 'être surmontées.

Dans le chapitre 2, sont examinés les effets des pannes d'actionneurs aérodynamiques sur les qualités de vol et sur les limites du domaine de vol en montrant la possibilité de respecter les performances minimales grâce à la tolérance aux pannes obtenue à l'aide de la redondance matérielle.

Dans le chapitre 3, l'utilisation de la redondance physique et analytique pour obtenir la tolérance aux pannes des systèmes dynamiques complexes est discutée de façon générale. Puis les solutions adoptées pour les chaînes de commande des avions de transport modernes sont analysées.

Dans le chapitre 4, une approche de commande en deux étapes pour faire face aux situations de pannes d'actionneurs est proposée où dans un premier pas les entrées virtuelles sont calculées à partir d'une loi de commande appropriée, puis la contribution des actionneurs restants opérationnels est établie par la solution d'un problème LQ. Cette approche a considéré que, en fonction de la configuration actuelle de l'aéronef, les conséquences des défaillances des actionneurs peuvent être assez différentes, permettant ou non le vol en toute sécurité.

Dans le chapitre 5, des méthodes de résolution rapide pour obtenir la solution d'un problème d'optimisation LQ sont étudiées. Il s'agit de la méthode des « active sets », de la méthode du point intérieur et d'une méthode de résolution basée sur les réseaux de neurones. Ces techniques

numériques sont utilisées plus loin dans cette thèse.

Dans le chapitre 6, on propose une méthode pour l'évaluation des qualités de vol résiduelles d'un aéronef après panne partielle des actionneurs. L'approche proposée conduit à faire usage d'une technique de type MPC résultant dans la formulation d'un problème d'optimisation LQ. Dans l'étude de cas considérée, la commande en vitesse angulaire, ce problème est résolu en utilisant un solveur de problèmes LQ à base de réseaux de neurones.

Dans le chapitre 7, on propose une méthode pour la réaffectation des actionneurs efficaces restant à effectuer une manœuvre prévue. On montre que dans le cas de la dynamique de vol, qui possède la propriété de platitude différentielle, l'approche à deux étapes proposée dans le chapitre 4 est applicable ici. L'étude de cas choisie se réfère à une manœuvre classique, le virage stabilisé. Il semble que les trois solveurs considérés pour traiter le problème LQ résultant, sont en mesure de fournir en ligne des solutions de réaffectation des actionneurs encore opérationnels.

Enfin, dans la conclusion, les principaux résultats de cette thèse sont réunis pour souligner son apport méthodologique, puis des perspectives de recherche sont discutées.

Cinq annexes sont également prévus pour donner plus de terrain aux différents concepts et les méthodes utilisées dans les chapitres précédents.

CHAPITRE 1

CHAÎNES DE COMMANDES DE VOL

Ce premier chapitre est consacré aux chaînes de commande de vol, on y est amené à faire une distinction entre les chaînes de commande lentes dédiées à corriger la configuration de l'avion et les chaînes de commande rapides dédiés à la stabilisation et aux de fonctions de pilotage. En ce qui concerne les chaînes de commande rapides, la solution technique actuelle, la commande de vol

électrique (Fly-by-Wire-FBW), est discutée. Ensuite, un aperçu des principaux types de défaillances pour les composants des chaînes des commandes de vol (capteurs, les processus et les actionneurs) est effectué.

Ce chapitre montre la complexité des chaînes de commande de vol pour les avions de transport modernes ainsi que la diversité des situations de panne. Ces situations de panne, lorsqu'elles ont des conséquences importantes (pannes catastrophiques) sur le vol doivent être rendues aussi improbables que possible en adoptant des solutions à sécurité maximale. Dans le prochain chapitre, les conséquences des pannes des actionneurs sur le domaine de vol et les qualités de vol d'un avion de transport moderne seront introduites.

CHAPITRE 2

QUALITÉS DE VOL DES AVIONS DE TRANSPORT

Dans ce chapitre, les caractéristiques classiques du domaine de vol et les qualités de vol d'un avion de transport sont introduits. Une approche moderne pour l'établissement et l'analyse des qualités de vol, basée sur une représentation de l'Etat, est adoptée (les équations décrivant la dynamique de vol d'un aéronef sont présentées à l'annexe A). Ensuite, les conséquences des défaillances des actionneurs sur le domaine de vol ainsi que sur les qualités de vol sont discutées. Dans le second cas différents scénarios de pannes sont considérés avec leurs conséquences dans le plan vertical et dans le plan horizontal de l'avion. De l'analyse qui précède, il apparaît que les qualités de vol naturelles doivent être renforcées par des systèmes d'augmentation de la stabilité. Ces systèmes génèrent des signaux de commande pour les actionneurs rapides lorsqu'une défaillance de l'un des actionneurs se produit et que les qualités de vol et de manœuvrabilité qui en résultent sont en cause. Pour éviter ces situations, différents systèmes tolérants aux pannes doivent être adoptés et un compromis difficile entre sécurité des vols et l'efficacité des vols doit être trouvé. La question de la commande tolérante aux pannes est introduite dans le chapitre suivant.

CHAPITRE 3

LA COMMANDE TOLÉRANTE AUX PANNES

Dans ce chapitre, un aperçu des techniques conduisant à un système de commande de vol tolérant aux pannes est effectué. Les redondances physiques et analytiques sont les principales bases de la détection des pannes et de leur identification. Bien que l'étude des techniques de FDI reste à un niveau général dans cette thèse, une grande importance a été accordée à la tolérance aux pannes basée sur la redondance physique. L'annexe B est consacrée à la conception de lois de commande tolérantes aux pannes. Dans ce chapitre, le cas des chaînes de commande de vol électriques est analysé, montrant la stratégie à deux niveaux adoptée par les avionneurs. De l'analyse qui précède, il apparaît que en ce qui concerne le domaine de la conduite du vol, malgré de nombreuses publications académiques, de nombreux résultats de simulation numérique et des tests effectués sur des prototypes réels, l'application de commande tolérante aux pannes est encore très limitée dans ce domaine. Ainsi les techniques de redondance physique continuent à jouer un rôle essentiel pour assurer la sécurité du vol. Cela a conduit à l'introduction de nouveaux concepts pour évaluer les conséquences des pannes physique, comme la redondance absolue d'entrée et la redondance totale d'entrée alors qu'une définition de la tolérance de panne par rapport à une défaillance, d'un système commandé est proposée. La stratégie à deux niveaux adoptée par les principaux avionneurs, selon l'importance des éléments défaillants dans les chaînes de commandes de vol, conduit à inhiber des fonctions de protection automatique pour des excursions hors du domaine de vol nominal. Une manière de limiter la dégradation de ces fonctions est de faire un usage optimisé des actionneurs opérationnels restants. Cette question est abordée dans le chapitre suivant où le problème de la réaffectation des actionneurs est présentée et analysée.

CHAPITRE 4

FORMULATION DU PROBLÈME DE RÉAFFECTATION DES ACTIONNEURS

Le but de ce chapitre est de formuler le problème de réaffectation des actionneurs (Actuator Reassignment Problem-ARP) qui devrait en général être résolu dans le cas d'une situation de panne d'actionneur's rapides. Puisque l'efficacité des actionneurs rapides est étroitement liée à la configuration actuelle aérodynamique de l'avion, une représentation d'état paramétrée par la configuration aérodynamique est proposée. Ensuite, les principales limitations des actionneurs rapides et lents sont considérées tandis que les contraintes de position et de vitesse sont introduites. Pour mieux formuler le problème ARP, la notion d'entrées virtuelles dont les valeurs sont liées à la manœuvre prévue par la loi de commande adoptée, est introduite. Ensuite, compte tenu de la multiplicité des contributions des actionneurs aux entrées virtuelles, le problème de l'affectation des actionneurs est formulé comme un programme de programmation mathématique linéaire quadratique (LQ problem). L'existence et l'unicité de solutions ainsi que de solutions approchées pour ce problème sont discutées. Dans ce chapitre, le problème d'affectation des actionneurs qui fait partie d'une approche de commande à deux étapes pour obtenir un certain degré de tolérance aux pannes a été formulé comme un problème général de type LQ et l'existence et l'unicité de la solution ont été discutées. Selon l'objectif de commande choisi, ce problème doit être résolu en ligne ou non. Certaines méthodes directes et plutôt intuitive ont été conçus pour résoudre ce problème. Cependant, puisque ces méthodes directes très souvent fournissent la solution exacte, les méthodes de solution exacte pour le problème LQ ont été étudiés et sont discutés dans le chapitre 5.

CHAPITRE 5

APPROCHES DE RÉOLUTION RAPIDE DU PROBLÈME LQ

Dans ce chapitre, le problème mathématique général qui doit être résolu pour réaliser la réaffectation des actionneurs est considéré. Les conditions nécessaires d'optimalité particulières pour ce problème sont introduites (conditions de KKT), celles-ci sont également suffisantes pour un problème convexe comme l'ARP dans la formulation adopté. Parmi les nombreuses méthodes de résolution et les algorithmes permettant de résoudre ce problème, ou de manière équivalente (dans le cas LQ) les conditions KKT, trois approches de solutions ont été étudiées avec plus de

précision. Deux de ces méthodes (les méthodes de points intérieurs et les méthodes des «active sets») ont été choisies compte tenu du grand nombre de contraintes et de la nécessité d'avoir à portée de main à chaque itération une solution réalisable. La méthode des «active sets» est également réputée pour son efficacité pour faire face aux contraintes de niveaux minimum et maximum. Une méthode de résolution directe par les réseaux de neurones des conditions d'optimalité, a été aussi introduite. Dans ce cas, les conditions d'optimalité sont atteintes à l'état d'équilibre du système dynamique qui en résulte. La convergence de ce processus est décrit à l'annexe C. De l'analyse effectuée, ainsi que des applications numériques qui sont affichées dans les chapitres suivants, il semble que les trois types d'algorithmes peuvent être considérés comme de bons candidats pour résoudre le problème LQ résultant du problème de réaffectation des actionneurs. Il sera démontré que ces techniques de résolution numérique peuvent être soit utilisées pour résoudre hors ligne ou en ligne des problèmes LQ dans un système de commande tolérante aux pannes.

CHAPITRE 6

ÉVALUATION DE LA MANOEUVRABILITÉ APRÈS PANNE D'ACTIONNEURS

L'objectif de ce chapitre est de contribuer à l'évaluation de la maniabilité résiduelle d'un avion de transport dans la situation dans laquelle certains actionneurs aérodynamiques sont en panne tandis que la gestion de la redondance de l'actionneur est efficace. L'approche de la solution adoptée ici est d'effectuer d'abord une étude hors ligne en utilisant un modèle de simulation de vol réaliste de l'avion pour concevoir un contrôleur pour le débattement des actionneurs restants avec l'objectif d'effectuer des manœuvres de référence d'une manière nominale. Lors de l'examen d'une manœuvre particulière qui ne peut être plus effectué nominalement, l'adoption de cette approche de commande rendra possible d'évaluer les manœuvres dégradées réalisables. La démarche de conception hors ligne de la commande qui est adoptée lors de cette étape de l'étude avec l'objectif ci-dessus et qui est décrite dans ce chapitre suit les principales étapes de la commande de type MPC

classique en utilisant comme banc d'essai un modèle de simulation de vol réaliste de l'avion considéré. Cette approche conduit à la formulation d'un problème linéaire quadratique à résoudre hors ligne. Puis, en effectuant une génération systématique de scénarios possibles de pannes des actionneurs où une certaine efficacité sur chaque axe reste possible, un panorama complet des qualités de vol d'un avion avec des possibilités de réaffectation des actionneurs peut être construit et structuré comme une base de connaissances. La question de la maniabilité ici se concentre sur la commande des trois rotations le long des axes principaux d'un avion de transport, car ils sont à la base de la stabilisation, de la commande d'attitude et des autres manœuvres. Ces rotations sont principalement le résultat des moments aérodynamiques créées par la déviation des actionneurs aérodynamiques primaires et secondaires. Depuis il est considéré que dans des conditions libres de pannes, les valeurs cibles pour les vitesses angulaires doivent être atteints suivant des dynamiques linéaires nominales. La question est de savoir si ceci sera encore possible, ou si ces valeurs cibles seront atteintes avec un retard supplémentaire ou si ces valeurs cibles resteront hors de portée. Dans ce chapitre, l'approche proposée pour évaluer les qualités de vol restantes d'un avion de transport en cas de pannes d'actionneurs aérodynamiques a été basée sur la résolution hors ligne d'un problème de suivi de modèle de type MPC couplé à un solveur de réseau neuronal dynamique pour obtenir une solution au problème LQ associé. L'approche proposée peut être appliquée à d'autres manœuvres ainsi que pour d'autres types d'actionneurs que ceux considérés dans cette étude, spécialement les moteurs. Cela fournit un nouvel outil pour prédire les qualités de manœuvrabilité dégradées résultant d'une panne d'actionneurs et permet ensuite de construire une base de connaissances exhaustive qui devrait être utile pour la surveillance d'un système de commande de vol tolérant aux pannes efficace.

CHAPITRE 7

RÉAFFECTATION EN LIGNE DES ACTIONNEURS D'UN AVION MANOEUVRANT

Dans ce chapitre, on considère le cas où la réaffectation des actionneurs est nécessaire afin de

continuer à effectuer une manœuvre connu comme possible même avec certains actionneurs en panne. Compte tenu de la propriété de la platitude différentielle de la dynamique du vol, il est alors montré que l'approche proposée en deux étapes (voir chapitre 4) peut être adoptée lors du calcul des entrées virtuelles associées aux trois moments principaux ainsi que éventuellement à la poussée. Pour illustrer la faisabilité de cette approche, le cas d'une manœuvre latérale dans laquelle l'avion doit effectuer en palier un virage stabilisé est traitée. Les valeurs des entrées virtuelles correspondantes sont calculées grâce à une technique de contrôle non linéaire inverse alors que le problème de la réaffectation de l'actionneur est formulé comme un problème LQ qui doit être résolu en ligne. Dans ce chapitre, un cadre général, basé sur la propriété de platitude différentielle de la dynamique de vol des aéronefs, a ainsi été mis en place. Cela donne une base théorique à l'approche à deux étapes proposée pour faire face aux défaillances partielles d'actionneurs d'aéronefs. Lors de l'examen d'une manœuvre classique réalisée par des avions de transport, la transition entre le vol rectiligne et le virage stabilisé, il a été montré que le problème de LQ résultant peut être résolu en ligne par l'une des trois méthodes numériques étudiées précédemment (la méthode du point intérieur, la méthodes des «active sets» et les réseaux de neurones). Cela prouve l'efficacité de la méthode proposée. La structure de commande tolérante aux pannes obtenue est présentée.

CHAPITRE 8

CONCLUSION GÉNÉRALE

L'objectif principal de cette recherche a été de contribuer à la conception de commandes de vol tolérantes aux pannes d'actionneurs pour les avions de transport de transport en optimisant l'utilisation d'actionneurs redondants. Mais le long du chemin vers cet objectif, différents concepts classiques ont été revisités tandis que de nouveaux concepts, utiles pour effectuer l'analyse requise, ont été introduits. Il a été particulièrement important de faire la distinction entre les actionneurs lents et rapides, ce qui a permis une définition plus précise des différents niveaux de redondance ainsi que de la tolérance aux pannes. Cela a également conduit à proposer une nouvelle vision de la

dynamique de vol pour les avions de transport où les changements de configuration associées aux actionneurs lents a des conséquences sur l'efficacité des actionneurs rapides dans une situation de défaillance partielle de ceux-ci. De la même manière, lorsque l'on considère les performances des aéronefs en vertu d'une panne partielle des actionneurs, l'analyse effectuée a distingué les effets sur les qualités de vol et les effets sur les limites du domaine de vol. Aussi, pour atteindre cet objectif, différentes méthodes et techniques ont été étudiées et lorsque cela est jugé utile, développées et appliquées. C'est le cas avec les différentes techniques de conception de commande de vol avancées telles que le Model Predictive Control (MPC) et la commande non linéaire inverse (NLI). C'est le cas avec les différentes méthodes pour résoudre un problème LQ associé au problème de la réaffectation des actionneurs: méthode de points intérieurs, méthodes des «active sets», les réseaux neuronaux dédiés. L'approche proposée pour aborder de la meilleure façon la redondance des actionneurs et les situations de pannes partielles est composé de deux étapes:

- une étape où, selon la manœuvre envisagée, les niveaux des entrées virtuelles, telles que définies dans cette thèse, sont établis selon une méthode de synthèse de loi de commande adéquate.
- une étape où, la réaffectation des actionneurs opérationnels restants est effectuée pour produire les niveaux requis pour les entrées virtuelles.

Dans le cas de la dynamique de vol, il a été démontré, que, compte tenu de sa propriété de platitude différentielle qui peut être abordée soit au niveau du guidage, soit au niveau du pilotage, des entrées virtuelles naturelles apparaissent. Dans cette thèse, le problème de la réaffectation des actionneurs a été formulé comme un problème LQ, et des situations différentes, des scénarios de panne et des objectifs de commande ont été traités. Des méthodes de résolution efficaces à ce problème ont été développées et comparées, montrant leur capacité à traiter ce problème en ligne, nécessitant alors une convergence très rapide vers la solution.

L'approche proposée a été appliquée avec deux objectifs différents mais complémentaires:

- D'un côté, elle a permis d'étudier les qualités de vol restantes dans un scénario de panne partielle des actionneurs et par la formulation d'un problème de suivi de trajectoire de référence, résolu hors ligne en utilisant l'approche MPC qui a conduit à la solution d'un

problème LQ. Comme dit dans le chapitre 6, cela fournit un outil permettant de prévoir, pour une situation de panne donnée, identifiée par l'utilisation de certaines techniques de FDI, les qualités de vol résiduelles qui en résultent.

- De l'autre côté, l'approche proposée a permis de concevoir une structure de commande tolérante aux pannes pour réaliser, lorsque cela est encore possible, des manœuvres standard associées soit à un plan de vol ou à des directives de l'ATC. L'étude de cas considérée correspond à une manœuvre classique pour les avions de transport. Il y est fait usage de la technique de commande NLI pour générer les valeurs de référence en ligne pour les entrées virtuelles correspondantes et de solveurs spécialisés pour obtenir une solution en ligne du problème résultant LQ du problème de la réaffectation des actionneurs.

A ce stade de la recherche, de nombreux points restent encore être étudiés, analysés et développés.

Certains d'entre eux peut être encore abordés dans le domaine académique, ce sont des points plus théoriques, tels que:

- La commande des systèmes non linéaires complexes via des contrôleurs lents et rapides avec ou sans panne des actionneurs.
- L'introduction des entrées virtuelles pour élaborer une loi de commande par platitude différentielle ou par d'autres propriétés mathématiques de la dynamique de vol.
- L'intégration de la fonction FDI avec la fonction de gestion des actionneurs pour développer des structures tolérantes aux pannes plus efficaces pour la conduite du vol.

Quelques autres points devraient être abordés dans le domaine de l'industrie, ce sont des points plus pratiques tels que:

- La construction une liste exhaustive des scénarios de pannes d'actionneurs et de l'évaluation des qualités de vol et de manœuvrabilité de l'appareil qui en résulte.
- La construction d'un système de supervision qui, basé sur les résultats d'une FDI pour les chaînes de commande de vol, effectuera le diagnostic et autorisera ou non certaines

manœuvres, limitera ou non certaines d'entre elles et de fournira aux pilotes une vue claire de la capacité résiduelle de l'avion.

L'amélioration de la sécurité du transport aérien est une tâche sans fin et il est à espérer que cette thèse contribuera avec un petit pas vers cet objectif.